THE UNIVERSITY
of EDINBURGH

Axon-glia interactions during central nervous system myelination

Rafael Almeida

PhD

The University of Edinburgh

2014

I have read and understood The University of Edinburgh guidelines on plagiarism and declare that this thesis is the result of my own work except where indicated by references. This thesis has been submitted to The University of Edinburgh for the degree of Doctor of Philosophy only.

Rafael Almeida

Abstract

Myelination drastically speeds up action potential propagation along axons, which is fundamental for the correct function of neuronal circuits. However, axon-oligodendrocyte interactions regulating the onset of myelin formation remain unclear. I sought to determine how reticulospinal axons control myelination, as they are the first myelinated in the zebrafish spinal cord. I genetically manipulated zebrafish in order to either remove such axons from a region of the spinal cord, or to increase their number, and characterized oligodendrocyte-lineage cells following this axonal loss- or gain-of-function.

In kinesin-binding protein (*kbp*) mutants, reticulospinal hindbrain neurons start axonogenesis but axons fail to grow along the entire spinal cord as in wildtype, providing an axon-deficient posterior spinal cord and an intact anterior region. I found that early stages of oligodendrocyte development, such as the specification of oligodendrocyte precursors, their distribution and migration were not affected in the posterior spinal cord of these mutants. However, both the proliferation and the survival of late precursors were impaired, resulting in a significant reduction of mature oligodendrocytes in the posterior region of mutants at the onset of myelination. Since the anterior spinal cord of mutants is indistinguishable from wildtype, these results demonstrate that reticulospinal axons provide a mitogenic and a survival signal to a subset of developing OPCs, enabling their differentiation and lineage progression.

I then found that the absence of reticulospinal axons did not affect the timing of oligodendrocyte differentiation, which matured on time, suggesting that this follows an intrinsic timer, as previous studies suggested. Oligodendrocytes also did not myelinate incorrect axonal targets, but instead adapted to the reduced axonal surface by elaborating fewer myelin sheaths. Additionally, oligodendrocytes made shorter sheaths, and also incorrectly ensheathed neuron somas in the mutant spinal cord, suggesting that either *kbp* function or a precise amount of axonal surface are required

to prevent ectopic myelination of somas and to promote the longitudinal growth of myelin sheaths.

In wildtype animals, the two reticulospinal Mauthner axons are the very first myelinated in the spinal cord. In animals where Notch1a function is temporarily abrogated or *hoxb1* genes are temporarily upregulated, supernumerary Mauthner neurons are generated. I found that these extra axons are robustly myelinated, with no impairment of myelination of adjacent axons. Surprisingly, the number of oligodendrocytes was not altered, but I found that each individual oligodendrocyte elaborated more myelin sheaths, whose total length was also longer than in wildtypes. Additionally, dorsal oligodendrocytes, which normally myelinate only small-calibre dorsal axons, readily extended processes ventrally to myelinate the supernumerary large-calibre Mauthner axons, in addition to small-calibre axons. These results suggest that oligodendrocytes are plastic and are not destined to myelinate a particular type of axon, and conversely, that axonal signals that induce myelination are similar for different axons. The long-standing observation that oligodendrocytes tend to myelinate either few large axons or many small axons thus reflects local interactions of oligodendrocyte processes with the nearby axons, rather than different subtypes of oligodendrocytes specified by an intrinsic programme of differentiation.

Collectively, this work shows that axons extensively influence both oligodendrocyte lineage progression and oligodendrocyte myelinating potential in vivo.

Acknowledgements

This work would not have been possible without Dave's supervision. Thank you for providing a good analogy of local regulation of potential and giving me the guidance that I needed, when I needed. Thanks for letting me pursue questions that sometimes led nowhere, but that made me want to keep on doing this. If it ever amounts to anything, you have been instrumental in it.

Thanks are also due to members of the Becker and Brophy labs for materials, reagents and expertise.

This work would have been utterly boring and likely unfeasible if it weren't for the awesome group that is the Lyons lab and its honorary members, past and present: your scientific input was always appreciated; your cake fortifying, and your cheerfulness required. Thanks for blurring (in fact, shattering) the line between colleagues and friends.

Thanks to my other friends, near and far, who kept me sane, arguably, through the ebbs and flows: Leonor, Tânia and Vicente; Telma and Cátia. Thanks to Inês, Ricardo e Rita for assorted geekiness, gossip and vagabondage. Thanks to Cristina, James and the rest of the Edinburgh crew (Ale, Vanessa, Pedro, Elisa): if science doesn't always rule, you guys do.

Thanks to Gordon, who, by coming into the picture at the final stages of writing this thesis, efficiently sped up the process.

Finally, a special thanks to my family. To my brothers Rodrigo and Francisco, who sometimes put up with me more than I deserve. To my parents, for their enduring support, and their reminders to live a bit, occasionally. À tia Mena, e ao avô Marcelino.

Table of contents

1. Introduction

Escaping a predator, swinging a baseball bat or writing a PhD thesis all require very fast and concerted nerve impulse propagation, despite the protracted duration of some of these activities (Davis and Parker 1997). During evolution, vertebrates accomplished this fast propagation by forming myelin sheaths around the axons of nerve cells. Myelin sheaths are a specialized extension of the plasma membrane of glial cells, which concentrically wrap around the axon, insulating them (Sherman and Brophy 2005). In the central nervous system (CNS), after generating neurons, neural progenitor cells switch to originate cells of the oligodendrocyte (OL) lineage, which are responsible for CNS myelination, the culminating event in CNS maturation (Rowitch 2004). Many CNS axons become myelinated, hinting at the importance of myelination. In fact, disruption to myelin sheaths results in devastating diseases such as multiple sclerosis or leukodystrophies (Gustavsson, Svensson et al. 2011). In mammals, myelination starts from birth, and continues into adulthood (Wang and Young 2014), and recent work has shown that myelination in adulthood may underlie novel forms of neural plasticity, and that oligodendrocytes may provide more than just text-book insulation. These underappreciated roles may contribute to the underlying pathology of a range of neurodegenerative or neuropsychiatric diseases, not traditionally thought to be related to myelin dysfunction.

The myelin sheath structure is a remarkable example of communication and collaboration between two very different cells. Despite its importance, our understanding of how it comes to be formed during development in an intact organism is limited, especially compared with inter-neuronal interactions. We may know exactly what makes an axon growth cone turn left or right (Colak, Ji et al. 2013), or the precise splice isoforms that guide the matching of that axon with its dendritic target, amidst a very complex milieu (Takeichi 2007, Hong, Mosca et al. 2012). Yet, we don't know of a single molecule displayed on CNS axons that is absolutely required for myelination (Emery 2010), and we are only now starting to glimpse the cellular interactions that drive the initial wrapping of oligodendrocyte membrane around a target axon in vivo (Snaidero, Mobius et al. 2014). In this thesis, I will explore the developmental interactions between two cell types, neurons and oligodendrocytes, which result in the appropriate myelination of a complex region of the vertebrate CNS: the spinal cord. By live imaging of the zebrafish spinal cord, I

identified that a number of steps of oligodendrocyte-lineage cell development can be regulated by axons: proliferation and survival. Furthermore, during myelination, axons can also locally regulate the extension of myelin sheaths at the level of individual oligodendrocytes, unambiguously demonstrating the plasticity of these cells in vivo. Hopefully, further elucidation of the fundamental cellular and molecular mechanisms of developmental myelination will open new avenues for myelin repair in pathological conditions.

In this introduction, I will briefly summarize the known functions of myelin and the consequences of its dysfunction, and how oligodendrocyte-lineage cells develop and elaborate myelin sheaths.

1.1 Function of Myelin

Myelin has classically been described as a lipid-rich membrane that repeatedly wraps around axon, 'insulating' them and permitting fast, 'saltatory' conduction of action potentials. How does the formation of such a structure speed up the propagation of electrical impulses?

The axonal membrane (axolemma) separates charges, and strongly maintains a positive extracellular side and a negative intracellular surface. In unmyelinated axons, voltage-gated sodium channels are distributed throughout the axonal membrane. When sodium channels open, sodium cations flow into the negative cytoplasmic surface and depolarize the membrane in that region. The voltage change induces a conformational change in nearby channels, opening them. More sodium ions flow in through these channels, which will in turn depolarize the membrane a little further down. The depolarization wave will continue down the axon, where it will eventually arrive at synaptic terminals and culminate in neurotransmitter vesicle release into another neuron. In unmyelinated axons, given the diffuse distribution of channels, the propagation of the action potential occurs in a continuous, slow manner down the axon (Hartline and Colman 2007).

In myelinated axons (Figure 1.1), long stretches of the axolemma are covered by myelin (internodes). The myelin sheath insulates the axon along the internode and prevents charges from accumulating near the membrane, that is, prevents the axolemma from depolarizing. Internodes are interrupted only at short (~1μm) unmyelinated gaps, thought to be regularly spaced, the nodes of Ranvier, in which voltage-gated sodium channels accumulate (Salzer 2003). Since they are unmyelinated, nodes are the only regions along the axolemma that can be depolarized. When this happens, sodium ions can flow through the channels. The myelin sheath along the internode also increases the membrane resistance to leakage of the ionic current (Bakiri, Karadottir et al. 2011), which is carried down the cytoplasm and is sufficient to depolarize the next node. This in turn opens its sodium channels, allowing more sodium ions to flow in, which regenerates the action potential. Thus, in myelinated axons, the depolarizing wave of the action potential does not slowly propagate along the membrane in the internodal segment. Instead it 'hops' from node to node, in what is known as saltatory conduction (from the Latin *saltare*, to leap).

Saltatory conduction results in several advantages at the level of individual axons, and of the whole organism (Hartline and Colman 2007). It is much faster than continuous propagation (tenfold faster for axons larger than 1μm in diameter). It is more energetically efficient, since the active transport of ions back across the membrane to restore the resting potential only occurs at nodes. Finally, it economizes space: the alternative solution for faster propagation is an increase in axonal diameter, but to achieve the same ten-fold improvement in conduction speed, axons would need to be a hundred times thicker.

Thus, myelin and saltatory conduction increase the conduction velocity of electrical impulses, which decreases reaction times to external stimuli such as a predator, for instance, but also improves temporal precision and potential synchronization of impulses. In sum, it allowed for the evolution of nervous systems with much higher information processing capacity.

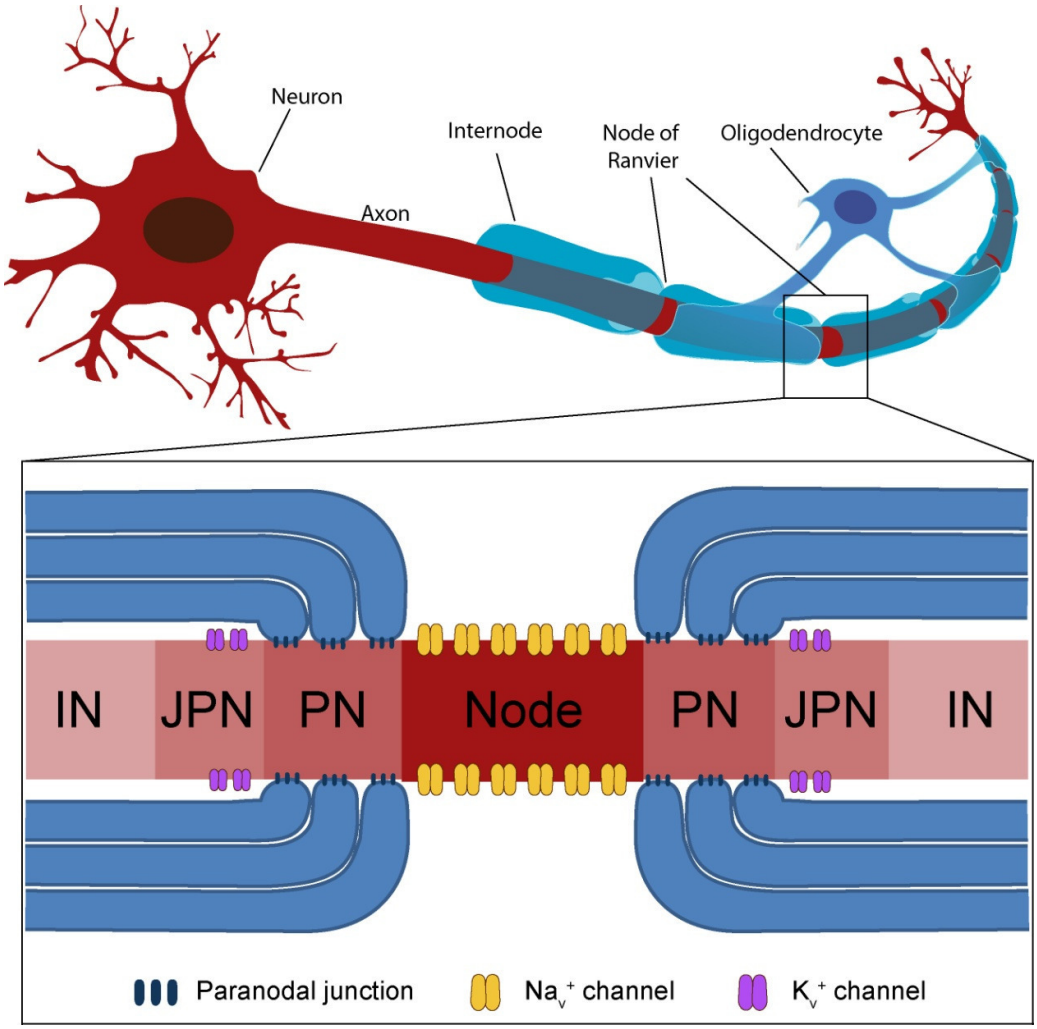

Figure 1.1 – Axonal domains in myelinated axons.

The unmyelinated axolemma at the node of Ranvier is highly concentrated in voltage-gated sodium channels. It is flanked by paranodes (PN) on each side, where the myelin is anchored to the axon by an axoglial adhesion complex. Next to it are the juxtaparanodes (JPN), which contain voltage-gated potassium channels. The internode (IN) comprises most of the space under the myelin sheath.

CNS myelin sheaths in vertebrates vary in their thickness and length. Myelin thickness has long been predicted to influence conduction speed: for a given axonal diameter, there is an optimal myelin sheath thickness that maximizes conduction speed (Rushton 1951, Waxman 1980, Ritchie 1982). A number of researchers have predicted that the g-ratio (quotient between axon diameter and the diameter of the axon with its myelin sheath) that maximizes conduction speed falls between 0.6-0.7

(Waxman 1980, Chomiak and Hu 2009). Strikingly, most myelinated axons in the CNS of any vertebrate have g-ratios that fall between those values (Hildebrand and Hahn 1978, Sherman and Brophy 2005). This means that smaller axons have thinner sheaths, and larger axons have thicker sheaths, with more wraps or lamellae around them. Thus, the thickness of the myelin sheath seems to be perfectly adapted to the particular axon it wraps.

Myelin sheath length determines the distance between nodes of Ranvier, which must not be too short (Court, Sherman et al. 2004) or too far (Wu, Williams et al. 2012) to allow the action potential to regenerate and permit saltatory conduction. It is remarkable that in some instances the internodal length seems optimized not to maximize conduction speed, but to ensure the temporal accuracy of impulse propagation. One interesting example is the auditory pathway, where the distance between nodes of Ranvier is adjusted in different neurons of the cochlear nucleus to ensure synchronicity of arrival of auditory information, effectively delaying the conduction in some axons. This and other examples are reviewed in (Waxman 1997, Seidl 2014).

These observations suggest that axons can locally regulate some parameters of myelin sheath formation, such as the number of wraps, or the length of myelin sheaths. This implies that axons and oligodendrocytes must communicate intimately during development. Interestingly, recent work has revealed that the fine structure of myelin is not fixed, and is probably refined throughout life, implying a continued communication between these cells. Refinement in white matter tracts (where most myelinated axons are located) could occur in response to neuronal activity itself. This is reviewed in (Boulanger and Messier 2014, O'Rourke, Gasperini et al. 2014, Wang and Young 2014), and I will mention some of this work in more detail in Chapters 3 and 4. Briefly, white matter changes are increasingly being reported to occur in the normal, mature CNS, which may be due to addition of new internodes to myelinated axons (for instance, reflecting myelin turnover), or de novo myelination of unmyelinated axons. A recent study demonstrated that individual adult cortical neurons are intermittently myelinated along their length (Tomassy, Berger et al. 2014), suggesting that addition of internodes may occur in partially myelinated axons

as well. At the level of a single axon, small alterations in internodal length or myelin thickness may have a small effect on the axon's conduction speed. However, even small variations in conduction velocity can have pronounced effects on the functional output of the entire neuronal network, by affecting synchronicity and oscillation patterns, for instance (Pajevic, Basser et al. 2014). Thus, higher-order functions of the nervous system and its information processing capacity may be actively influenced by myelination, which may be allowing more than a faster escape from a predator.

The importance of myelin in permitting efficient saltatory conduction is underscored by those conditions where it is disrupted. The most prevalent of demyelinating diseases in young adults is multiple sclerosis, in which inflammatory insults destroy the myelin sheath, leading to neurodegeneration, and severe functional impairment. Primary demyelination of axons is associated with impaired conduction speed (McDonald and Sears 1970, Rasminsky and Sears 1972, Waxman 2003). Demyelinated axons also present with an increased number of mitochondria, which is thought to be an adaptation to the energetically inefficient redistribution of the ion channels that occurs in the demyelinated axolemma (Mutsaers and Carroll 1998, Mahad, Lassmann et al. 2008, Campbell and Mahad 2011). This observation further hints at one of the benefits of myelin and saltatory conduction: that of energetic savings.

Interestingly, remyelination often occurs, whereby nearby adult OPCs are mobilized to the demyelinating lesion, induced to proliferate and differentiate and remyelinate the denuded axon. These new myelin sheaths associated with remyelination are thinner than normal myelin sheaths, and shorter, but seem enough to restore function (Blakemore 1974, Smith, Blakemore et al. 1979, Ludwin and Maitland 1984, Franklin and Ffrench-Constant 2008). However, in multiple sclerosis, remyelination eventually fails, and the chronically demyelinated axons undergo degeneration, causing neuronal damage and death – which is associated with the severe clinical decline of later stages of the disease (De Stefano, Matthews et al. 1998). Are thinner sheaths not able to support function in the long-term? OPCs migrate into lesioned areas, but why do they fail to differentiate and remyelinate chronic lesions? The

molecular mechanisms behind the failure to remyelinate are not fully understood and the extent to which developmental myelination is recapitulated in during remyelination is also under debate (Franklin and Ffrench-Constant 2008, Fancy, Chan et al. 2011).

A range of neuropsychiatric diseases have recently been associated with alterations in white matter integrity, which could result from disruption to the molecular organization of myelinated axons. These include schizophrenia, autism, bipolar disorder, among others, reviewed in (Bernstein, Steiner et al. 2009, Faivre-Sarrailh and Devaux 2013, Amlien and Fjell 2014, Arancibia-Carcamo and Attwell 2014). It could be that these conditions reflect impairment in the refinement of myelin sheaths in mature axons in the adult CNS, which could affect higher-order functions in the nervous system, as I mentioned previously.

The view presented so far suggests that oligodendrocytes respond to axon-derived signalling and modulate the structure of myelin sheaths to maximize the function of axons. However, the picture is more complex, and oligodendrocytes do more for axons than permit saltatory conduction to occur. For instance, mice which completely lack the oligodendrocyte-specific *proteolipid protein* (*plp*) gene, which encodes a protein found in CNS myelin, still form compact myelin and develop fully myelinated axons (Klugmann, Schwab et al. 1997). Strikingly, despite the mostly normal myelin, these mice develop a very late onset, slowly progressing primary neurodegeneration (Griffiths, Klugmann et al. 1998). Another example is that of mice deficient for 2',3'-cyclic nucleotide 3'-phosphodiesterase (gene *cnp1*), an enzyme found in myelin: mice develop normally early on and form myelinated axons, but present with a primary axonal degeneration later on (Lappe-Siefke, Goebbels et al. 2003), despite the formation of compact myelin around the axons. This strongly suggests that oligodendrocytes support the axons and preserve their function in ways that are independent of their myelinating role (Nave and Trapp 2008). It may well be that such a support function emerged during evolution precisely because the development of the insulating myelin sheath physically prevent access of axons to nutrients and trophic factors.

Strikingly, recent studies confirmed that oligodendrocytes do in fact directly provide metabolic support to the axons they myelinate (Figure 1.2) (Morrison, Lee et al. 2013, Saab, Tzvetanova et al. 2013). Specifically, oligodendrocytes are thought to export lactate through transporter MCT1 to the internodal space, which is taken up by axons, where it can be used as an alternative energy source to glucose (Funfschilling, Supplie et al. 2012). Disruption of MCT1 in oligodendrocytes caused axon degeneration and motor neuron death in vitro as well as in vivo. Furthermore, (Lee, Morrison et al. 2012) found that expression of MCT1 was decreased in tissue from patients with amyotrophic lateral sclerosis as well as in a mouse model of the disease. These observations suggest that the loss of oligodendrocyte-mediated metabolic support may directly contribute to the pathology of this disease, and highlight that communication and interaction between neurons and glia is bidirectional, and sustained support between the two is crucial for the maintenance of a healthy CNS.

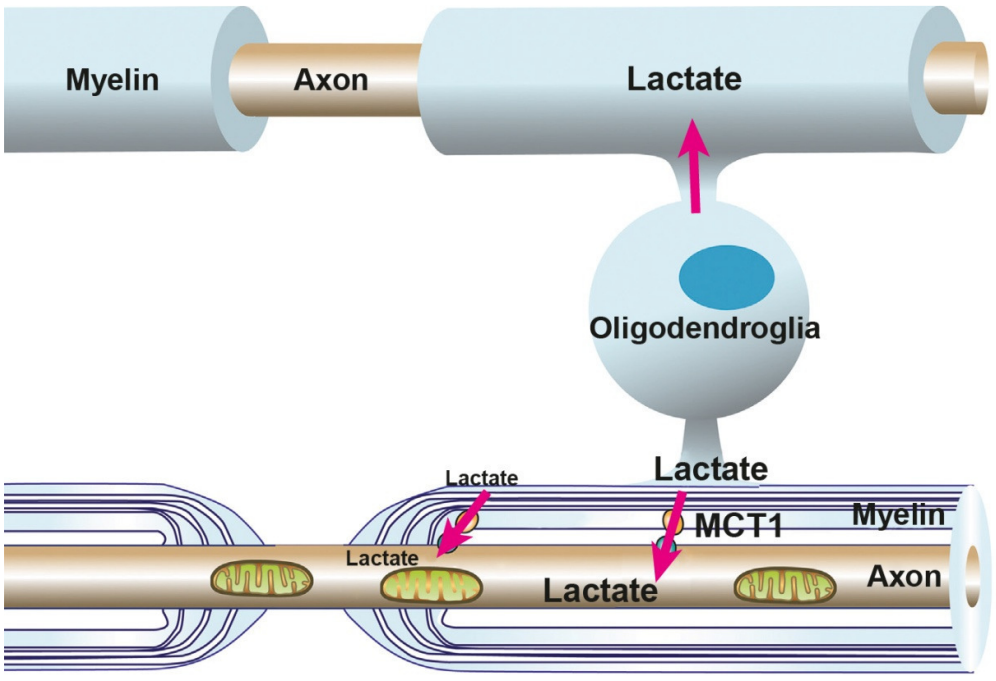

Figure 1.2 – Oligodendroglia provide metabolic support to axons.

Oligodendrocytes are thought to export lactate through the MCT1 transporter along the internode, which can be taken up by axons and provide a substrate for glycolysis and ATP production. Image adapted from (Morrison, Lee et al. 2013).

Furthermore, it implies that we must re-evaluate the role of oligodendrocyte loss in neurodegenerative diseases. Especially in 'primarily demyelinating' diseases, such as multiple sclerosis, it may be that much of the axonal and neuronal loss observed later in the disease is due to the chronic loss of metabolic support from oligodendrocytes.

Despite the clear importance of oligodendrocytes and myelin for the function of the nervous system, our understanding of how myelination occurs during development is incomplete. The factors that mediate communication and interaction between neurons and oligodendrocytes and that control the onset of CNS myelination in vivo, during development, remain incompletely understood, although we now have a notion of some intrinsic factors that regulate the initial stage of oligodendrocyte specification and differentiation. I will briefly outline how oligodendrocytes develop in the CNS next.

1.2 Oligodendrocyte development

Oligodendrocyte-lineage cells first arise from a discrete domain in the ventral spinal cord, the pMN domain (Figure 1.3) (Richardson, Kessaris et al. 2006). These domains in the embryonic neural tube are patterned along the dorsal-ventral axis by a gradient of morphogens. For instance, Sonic hedgehog (Shh) is secreted ventrally from the notochord and floor plate; and Bone morphogenetic proteins are secreted dorsally from the dorsal roof plate. At each dorsal-ventral level, their particular concentrations induce the expression of specific transcription factors in multipotent neural progenitor cells (Mitew, Hay et al. 2014). The unique combination of transcription factors in each domain specifies the identity of the neural progenitors, and ultimately defines the cellular subtypes produced in that region (Rowitch 2004). In the pMN domain, Shh induces expression of Olig2, a basic helix-loop-helix transcription factor that is required for the generation of all pMN offspring – motor

neurons and oligodendrocyte-lineage cells (Ligon, Fancy et al. 2006, Meijer, Kane et al. 2012). During embryonic development, Olig2+ pMN progenitors first give rise to motor neurons, and subsequently switch to generate oligodendrocyte-precursor cells (Colognato and ffrench-Constant 2004, Rowitch and Kriegstein 2010). For instance, in the mouse neural tube, motor neurons are born in the pMN domain at embryonic days E9-E10.5, and OPCs at E12.5 (Rowitch 2004). In zebrafish, most Olig2+ motor neurons are born between 24-51hpf (Reimer, Norris et al. 2013); and Olig2+ OPC specification in the spinal cord starts around 36hpf (Kirby, Takada et al. 2006). Interestingly, post-translational modifications of Olig2 within pMN progenitors can regulate the switch of motor neuron production to OPC generation (Li, de Faria et al. 2011). Olig2 expression persists throughout the developmental stages of OPC, from specification through to myelination, and has recently been shown to also regulate later aspects of oligodendrocyte development (Mei, Wang et al. 2013).

After their specification in the pMN domain, OPCs migrate, proliferate and distribute throughout the grey and white matter. They extend dynamic filopodia-like processes into their vicinity. An OPC will retract its processes upon contact with another OPC, and OPCs often migrate away subsequently. Following death of an OPC, neighbouring OPCs proliferate and invade the region. These OPC-OPC interactions seem to resemble a tiling mechanism that ensures their uniform distribution, in preparation for myelination, both in the developing zebrafish spinal cord (Kirby, Takada et al. 2006) and in adult rodent grey matter (Hughes, Kang et al. 2013). OPC processes may also survey the territory for potential axonal targets, and it is thought that the selection of axons that become myelinated occurs at this stage (Almeida and Lyons 2013, Czopka, Ffrench-Constant et al. 2013). Some molecules that regulate long-range OPC migration have been identified (de Castro, Bribian et al. 2013), including some axonal regulators (Akiyama, Hasegawa et al. 2014). However, the molecular mechanisms that regulate either the repulsive OPC-OPC interactions or recognition and selection of potential axonal targets remain unknown.

In Chapter 3, I will investigate the role of axons in these earlier steps in the development of oligodendrocyte-lineage cells.

Later in embryonic development, closer to the postnatal period, several intrinsic and extrinsic factors regulate OPC differentiation and maturation, thoroughly reviewed in (Li, He et al. 2009, Emery 2010, He and Lu 2013). Oligodendrocyte processes contacting axonal targets extend and loosely ensheath the axon and myelin genes start to be expressed. Transcription factors such as Olig1 and Sox10 are intrinsic regulators of OPC development and are important for the final differentiation and production of myelin structural components. For instance, Olig1 regulates transcription of myelin components such as Myelin basic protein (Mbp) and Proteolipid protein (Plp), and may also serve to suppress alternative astrocyte fates. In Olig1-null mice, OPC generation is not affected, but these cells fail to fully differentiate and to form compact myelin (Xin, Yue et al. 2005). Sox10 physically interacts with Olig1/2 and directly activates the promoter of *mbp* in mammals, although interestingly, in zebrafish, Sox10 only interacts with Olig1 (Li, Lu et al. 2007, Kuspert, Hammer et al. 2011). Similarly to *olig1*-null mice, *sox10*-null mice generate OPCs, but their terminal differentiation is disrupted (Stolt, Rehberg et al. 2002). Sox10 may also be required to promote oligodendrocyte survival following axonal ensheathment, as *sox10* mutant zebrafish generate OPCs that die following ensheathment (Takada, Kucenas et al. 2010). Later, Nkx2.2, an homeodomain transcription factor, is also required from the OPC stage to promote differentiation of a subset of myelinating oligodendrocyte-lineage cells (Zhou, Choi et al. 2001, Liu, Hu et al. 2007, Kucenas, Snell et al. 2008). These transcription factors can be used as markers for the oligodendrocyte-lineage from the OPC stage. Their presence, sequential order of expression and presumed function are remarkably well conserved in zebrafish (Figure 1.3).

Subsequently, these cells must initiate a timely differentiation program that elicits biochemical and biophysical mechanisms capable of synthesizing, transporting, assembling and compacting a specialized lipid membrane (Baumann and Pham-Dinh 2001). Unlike the myelinating Schwann cell in the peripheral nervous system, which only associates with one segment of one axon, oligodendrocytes can associate with numerous segments on different axons, therefore they must be able to support myelin biosynthesis at the end of several processes. As they exit the cell cycle, these premyelinating oligodendrocytes express a particularly specific transcription factor

required for this program of differentiation, *My*elin *R*egulatory *F*actor (Emery, Agalliu et al. 2009). Together with Sox10, MyRF stimulates expression of myelin components, such as Mbp and Plp (Bujalka, Koenning et al. 2013, Hornig, Frob et al. 2013). Expression of myelin structural proteins can be used a marker for the oligodendrocyte stage. Continued MyRF expression is required for the maintenance of myelin and of a differentiated oligodendrocyte phenotype in adults (Koenning, Jackson et al. 2012).

Interestingly, not all OPCs differentiate into myelinating oligodendrocytes (Richardson, Young et al. 2011). Some OPCs remain undifferentiated into adulthood, even if less proliferative than developmental OPCs (Psachoulia, Jamen et al. 2009, Young, Psachoulia et al. 2013). These adult OPCs can differentiate into oligodendrocytes in pathological or demyelinating conditions, for instance (Rivers, Young et al. 2008, Zhu, Bergles et al. 2008, Zhu, Hill et al. 2008, Kang, Fukaya et al. 2010, Tripathi, Rivers et al. 2010). Adult OPCs represent around 5% of all cells in the adult brain, but their full range of functions remains unknown (Trotter, Karram et al. 2010, Boda and Buffo 2014). They may orchestrate de novo myelination, myelin turnover or remodelling, which is now thought to occur under normal conditions in the mature CNS (Young, Psachoulia et al. 2013), as I will briefly discuss later.

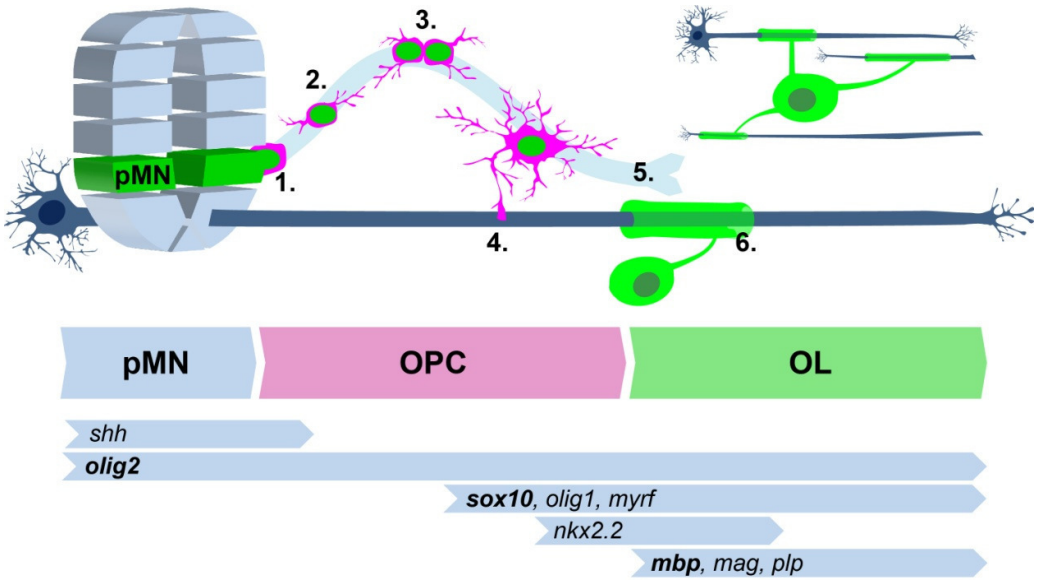

Figure 1.3 – Overview of oligodendrocyte-lineage cell development and markers.

OPCs are specified in the pMN domain in the ventral spinal cord (1). Subsequently, OPCs migrate (2) and proliferate (3) to populate the spinal cord. OPC processes contact target axons (4), which potentially promotes their survival and differentiation (5), after which oligodendrocytes form myelin sheaths around their targets (6). Developmentally regulated genes that regulate myelination are indicated below, in bold are those of particular interest (see main text for details).

1.3 Myelin sheath formation and structure

Oligodendrocyte-lineage cells undergo a remarkable morphological transformation as myelination occurs: OPCs initially extend multiple branching processes, and this arborisation decreases when OPCs mature into oligodendrocytes, which have fewer processes, supporting a myelin sheath at their end (Hardy and Friedrich 1996). A number of factors regulating the initial protrusion of processes and the cytoskeletal remodelling that must accompany these changes have been identified (Simons and Trotter 2007, Richter-Landsberg 2008, Bauer, Richter-Landsberg et al. 2009). These dynamic processes likely explore and sense their environment. Cell bodies or dendrites are not myelinated, therefore, axon-OPC contacts must be preferentially formed or stabilized, and transport of myelin components must be targeted to these contacts preferentially (Simons and Trotter 2007). Additionally, only contact with those axons that are competent for myelination should be stabilized. Recent work identified that spinal cord oligodendrocytes will elaborate all of their myelin sheaths within 5 hours, and 75% will remain stable, with only 25% of retractions within 2 days (Figure 1.4) (Czopka, Ffrench-Constant et al. 2013). In a milieu where over 90% of the axons are unmyelinated, this means that OPCs and oligodendrocytes are remarkably accurate when the time comes to form myelin sheaths, implying that oligodendrocytes do not select axons at random, and that selection of axonal targets occurred prior to actual myelination. The molecular regulators of this axonal selection in the CNS remain to be fully elucidated, particularly those that promote or stabilize the interaction between axon and OPC process (some inhibitory signals have been identified and are discussed in the literature referenced in section 1.2).

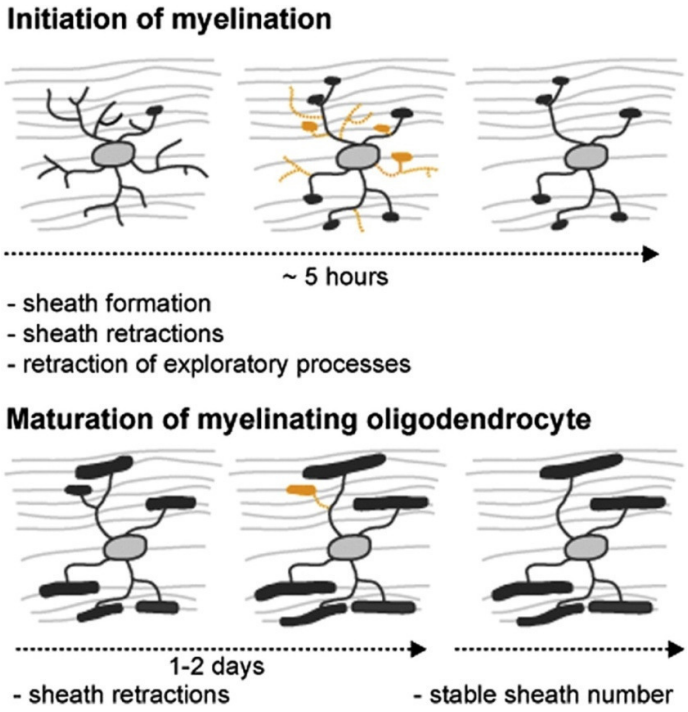

Figure 1.4 – Onset of oligodendrocyte myelination.

Following the formation of their first myelin sheath, zebrafish spinal cord oligodendrocytes quickly form all of their myelin sheaths in a short period (~5 hours), after which point they may occasionally retract a sheath; but from two days after the onset of myelination, the number of sheaths per oligodendrocyte is stable. Image taken from (Czopka, Ffrench-Constant et al. 2013).

When myelination ensues, the axon-OPC contact must be converted into a myelin sheath. In the case of the PNS, where each Schwann cell wraps only a segment of one axon, it is generally accepted that the Schwann cell first extends its membrane along the full length of what will become that myelin sheath, then it curves around the axon, and the myelin sheath tip grows under the previously generated membrane layer, in what is known as the "carpet crawler" or "jelly roll" model (Bunge, Bunge et al. 1989). This model does not seem to represent the principal mode of CNS myelin sheath formation, since the number of wraps can vary along the length of a myelin sheath in the CNS (Knobler, Stempak et al. 1976). A recent study followed CNS myelin ensheathment at high resolution in vivo (Snaidero, Mobius et al. 2014) and determined that initially, the oligodendrocyte process flattens upon axonal contact, but oligodendrocyte membrane does not fully extend before curving around

the axon. The short inner tongue 'crawls' around the axon and grows under the already existing oligodendrocyte membrane. This inner edge of the sheath is smaller longitudinally than the outer layers; if the growing myelin sheath were unfurled, it would look like a spade (Figure 1.5). The myelin sheath is then formed by growth of the inner tongue under the deposited membranes, and by the longitudinal, lateral growth of the membranes until they reach their full extent along the axon. A network of cytoplasmic channels appears to exist in compact myelin, containing microtubules and vesicular carriers, which can provide a route for transport of materials to the inner tongue, where radial growth of the myelin sheath occurs. Additionally, in the lateral edges of each wrap are cytoplasmic pockets which remain in contact with the axon even as the sheath grows longitudinally. Delivery of membrane components to these cytoplasmic pockets permits the longitudinal, lateral growth of the myelin sheath. Interestingly, unlike the channels that lead to the inner tongue which close when myelination is finished, these lateral pockets will remain open even in mature, myelinated fibers, possibly for adjustment and refinement of myelin sheath length (Snaidero and Simons 2014).

Which components must be delivered to the growing myelin sheath? Early biochemical studies identified the gross molecular composition of myelin, and determined that myelin has a very high lipid content (about 75% of its dry weight) in comparison to other eukaryotic plasma membranes. It has unusually high levels of cholesterol, glycosphingolipids (such as galactosylceramyde, GalC, which can be used as a marker for immature oligodendrocytes), and plasmalogens (Jahn, Tenzer et al. 2009, Aggarwal, Yurlova et al. 2011). The remainder of myelin's dry weight are proteins which are embedded or attached to the lipid bilayer. These include Proteolipid protein (Plp) and Myelin basic protein (Mbp), which together may form a quarter of all myelin protein (Jahn, Tenzer et al. 2009). Other examples include Myelin associated glycoprotein (MAG), Myelin/oligodendrocyte protein (MOG), or 2′-3′-cyclic nucleotide-3′-phosphodiesterase (CNP), which has catalytic functions important in the formation of the sheath (Snaidero, Mobius et al. 2014).

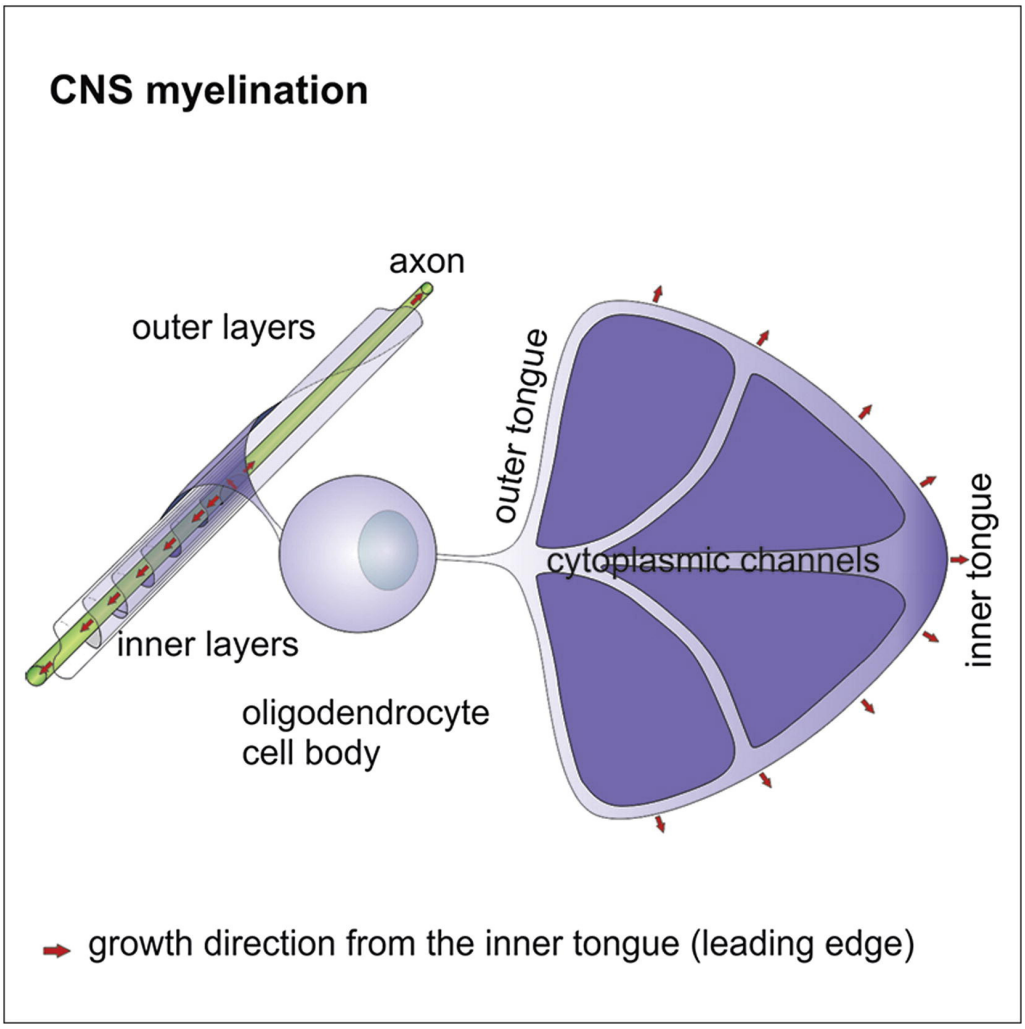

Figure 1.5 – Model of axonal ensheathment and myelin biogenesis in the CNS.

Myelin sheaths grow when the leading edge of the inner tongue wraps around the axon, and by the lateral extension of the layers of myelin towards what will become the nodes (left). Unwrapped growing myelin sheath on the right shows cytoplasmic channels, which provide a path for trafficking of myelin components to the region of active growth, the inner tongue. Compaction then proceeds from the outer towards the inner layers. Taken from (Snaidero, Mobius et al. 2014).

One other myelin protein, P0, an evolutionarily old immunoglobulin (Hartline and Colman 2007), is present in CNS myelin in zebrafish but only in PNS myelin in mammals (Brosamle and Halpern 2002, Schweitzer, Becker et al. 2003, Bai, Sun et al. 2011). Zebrafish express an array of growth-promoting molecules following a lesion, including P0 (Schweitzer, Becker et al. 2003), which may explain the

different regenerative capabilities of vertebrates: zebrafish are capable of regenerating axons (Becker and Becker 2007) and full-thickness myelin sheaths following an optic nerve lesion (Munzel, Becker et al. 2014). In mammals, Schwann cells which express P0 are highly regenerative, in contrast to oligodendrocytes in the CNS.

Oligodendrocytes appear to synthesize myelin components in a regulated sequence: for instance, glycosphingolipids specific to oligodendrocytes such as GalC are produced before major protein components such as Plp and Mbp. These components will then be delivered to the area of myelin sheath growth, the inner tongue, where they may self-assemble into myelin (Aggarwal, Yurlova et al. 2011). Synthesis and transport of myelin lipids starts in the endoplasmic reticulum, and proceeds through the secretory pathway, during which some myelin lipids may preassemble in lipid rafts. Some proteins, such as Plp (which interacts with cholesterol), may also associate with myelin lipids before they reach their destination. Vesicular and non-vesicular transport mechanisms may then exist in parallel for the final delivery of these components to the myelin membrane (Simons and Trotter 2007). Interestingly, *mbp* mRNA is transported in granules, on microtubules, to the myelinating process, where it is locally translated in response to a stimulus (possibly, neuronal activity (Wake, Lee et al. 2011)). This delivery as mRNA is likely related to its function. Mbp is a highly positively charged molecule, which upon translation quickly adheres to the negatively charged cytoplasmic membrane surfaces, bringing the two cytoplasmic membrane surfaces in close apposition. This also prevents diffusion of proteins with large cytoplasmic domains into myelin (Aggarwal, Yurlova et al. 2011), facilitating compaction of the several wraps of the myelin sheath. When targeting of *mbp* mRNA to oligodendrocyte processes is impaired by disruption of its transporter Kif1b, cytoplasmic translation of *mbp* mRNA results in ectopic myelin-like membrane close to the cell body (Lyons, Naylor et al. 2009). In a growing myelin sheath, Mbp translation seems to occur at the inner tongue, but the compaction of cytoplasmic membranes may be actively delayed by other myelin components (such as CNP) to prevent premature compaction of the growing zone (Snaidero and Simons 2014).

Following the growth of myelin sheaths, a mature, myelinated axon has distinct functional domains (Figure 1.1). The unmyelinated nodes of Ranvier, where voltage-gated sodium channels accumulate on the axon, are the site of action potential propagation. Flanking each node are paranodes, where the myelin membrane forms paranodal loops that are tightly anchored to the underlying axon by septate-like junctions. The lateral cytoplasmic pockets of each layer in a growing sheath move towards the ends of the myelin sheath, where they align and form these paranodal loops. Three cell adhesion molecules are the main known components of these axoglial junctions: on the axonal side, Contactin and Contactin-associate protein (Caspr); on the glial side, Neurofascin 155 (Nfasc155). Interestingly, disruption of this complex slows down the migration of the lateral edges of a growing myelin sheath (Zonta, Tait et al. 2008, Susuki, Chang et al. 2013), indicating that this axoglial junction is required for the longitudinal growth of myelin. This longitudinal migration of the axoglial junction may help form the nodes of Ranvier, by 'pushing' sodium channels along the axon, until two adjacent sodium channel clusters fuse into a single node of Ranvier (Zonta, Tait et al. 2008). Just next to the innermost paranodal loop, under the myelin sheath, lies the juxtaparanode, a short region where potassium channels accumulate in the axolemma, which are thought to regulate axonal excitability. Finally, the internode extends between juxtaparanodes and comprises most of length under the myelin sheath. The molecular composition and modes of assembly of these domains are reviewed in (Poliak and Peles 2003, Salzer 2003, Buttermore, Thaxton et al. 2013).

1.4 Axonal signals regulating oligodendrocyte-lineage cell development

Which signals underlie axon-oligodendrocyte communication and the development of such an intricate structure? Drawing on in vitro evidence and knowledge of peripheral nervous system myelination, a number of extrinsic signals have been identified that regulate oligodendrocyte-lineage cell development; I will briefly refer some examples presently.

Platelet-derived growth factor (PDGF)

PDGF was the first major secreted mitogen for OPCs identified in vitro, and confirmed in vivo: PDGF-A global knockout mice have greatly reduced numbers of OPCs, oligodendrocytes and myelin in their spinal cords and several brain regions; while overexpressing PDGF-A in neurons results in excess proliferation of OPCs and excess oligodendrocytes early on. (Calver, Hall et al. 1998, Fruttiger, Karlsson et al. 1999). Delivery of exogenous PDGF to the optic nerve reduces the normal levels of developmental oligodendrocyte apoptosis in control animals (Barres, Hart et al. 1992). PDGF is known to be produced by retinal ganglion cells (RGCs), which project axons to the optic nerve (Yeh, Ruit et al. 1991, Mudhar, Pollock et al. 1993). However, it is also well established that astrocytes produce the relevant form of PDGF. In fact, given that PDGF secretion by RGCs is restricted to their somas and not axons (Fruttiger, Calver et al. 2000), it seems more likely that this particular pathway is involved in a paracrine interaction between astrocytes and OPCs in the optic nerve. In other regions such as the spinal cord, where neuronal cell bodies exist in the vicinity of OPCs, it remains to be determined to what extent the endogenous neuronal production of PDGF contributes to the levels of this mitogen in the milieu.

Neuregulin1(Nrg1)-ErbB signaling

Nrg1 is a member of the epidermal growth factor family of proteins that function as extracellular ligands for the ErbB family of receptor tyrosine kinases. The *nrg1* gene generates numerous alternatively spliced isoforms of Nrg1, including secreted (e.g., type I) and transmembrane isoforms (e.g., type III) (Mei and Xiong 2008). In the peripheral nervous system, it is well established that Nrg1 expressed on axons activate ErbB receptors in Schwann cells, where they can regulate proliferation, survival, differentiation and even the thickness of the myelin sheath (Michailov, Sereda et al. 2004). In the CNS, early in vitro work established that oligodendrocyte-lineage cells are responsive to Nrg1 treatment (Vartanian, Corfas et al. 1994, Canoll,

Musacchio et al. 1996, Raabe, Suy et al. 1997, Shi, Marinovich et al. 1998, Canoll, Kraemer et al. 1999, Flores, Mallon et al. 2000, Calaora, Rogister et al. 2001). For instance, addition of Nrg1 prevents normal apoptosis of newly-differentiated oligodendrocytes in culture (Fernandez, Tang et al. 2000). Embryonic spinal cord explants from Nrg1 knockout mice specifically fail to generate mature oligodendrocytes; but the origin of these ligands was not clearly addressed (Vartanian, Fischbach et al. 1999). An axonal origin of Nrg1 was hinted by co-culture studies with dorsal root ganglia neurons - this alone was sufficient to prevent oligodendrocyte apoptosis. If direct contact was blocked at ligand or receptor level with anti- Nrg1 antibodies or antagonistic ErbB4 immunoglobulins, the survival induced by axons was mostly inhibited (Fernandez, Tang et al. 2000). Thus, oligodendrocyte survival seems to be mediated at least in part by axonal Nrg1 and to involve axonal contact.

In vivo, early expression of Nrg1 (and Shh) in the growing RGCs in the optic nerve induces the specification of primordial OPCs from the optic stalk, which subsequently migrate and colonize the nerve (Gao and Miller 2006). At later stages, normal oligodendrocyte developmental apoptosis in the optic nerve is increased with delivery of ErbB4 immunoglobulin, and decreased with exogenous Nrg1, without affecting OPC proliferation. Nrg1 also decreases the apoptosis that is induced by optic nerve transection during the period of active myelination (Fernandez, Tang et al. 2000). Collectively, these results poised Nrg1 to be a main axonal regulator of oligodendrocyte development, including their specification and their survival.

However, a more recent study showed normal myelination following conditional neuronal ablation of Nrg1 in specific CNS regions, from embryonic or postnatal stages. It was also normal following conditional Nrg1 knockout from all neuronal *and* glial lineages in a particular region of the forebrain. Conditional Nrg1 ablation from the entire developing CNS did not hamper myelination at birth in the earliest myelinated tracts, including generation of a normal density of Olig2+ and MBP+ cells in spinal cord and forebrain (Brinkmann, Agarwal et al. 2008). Long-term co-cultures of wildtype oligodendrocytes with Nrg1-null dorsal root ganglia neurons readily formed myelinated axons, suggesting that continued axonal Nrg1 expression

is dispensable for CNS myelination, unlike the PNS. In agreement with these results, conditional ablation of ErbB signaling in oligodendrocytes also did not prevent normal myelination of CNS tracts (Brinkmann, Agarwal et al. 2008). It may be that axonal NRG1 acts in redundancy with additional factors in the CNS that can also promote survival of oligodendrocytes and regulate myelination in vivo. It is conceivable, for instance, that survival of oligodendrocyte lineage cells may also be promoted by astrocyte-derived factors, for instance. If this is the case, in vivo, these can compensate for the lack of Nrg1, but in vitro, in the simpler co-culture studies, such additional factors may be absent, and Nrg1 signaling would seem to play a more important role.

Consistent with a role in myelination, though, animals that overexpress Nrg1 type I or III in neurons have hypermyelinated axons with many additional wraps. Additionally, more myelinated axons (particularly of smaller diameter) were found in the cortex of over-expressing animals, and in the optic nerve at P6, indicating that oligodendrocytes prematurely initiated myelination of Nrg1 expressing RGCs (Brinkmann, Agarwal et al. 2008). Since the number of oligodendrocytes was not altered, it is likely that the myelinating capacity of each individual oligodendrocyte was increased. Interestingly, socially isolated mice show an hypomyelinating phenotype in the prefrontal cortex, which is at least partly explained by a reduction in the myelinating capacity of individual oligodendrocytes, concomitantly with reduced Nrg1 expression (Makinodan, Rosen et al. 2012). The phenotype can be phenocopied in otherwise normal mice by loss of oligodendrocyte ErbB3 receptors.

Thus, in vivo, Nrg1 seems capable of regulating later aspects of myelination, including oligodendrocyte myelinating potential at the level of the single process/myelin sheath. This is agreement with the multiple functions of Nrg1 signaling in PNS myelination.

Notch ligands

Notch1 is a transmembrane receptor whose signaling pathway may play multiple roles during oligodendrocyte lineage progression. Genetic ablation of Notch1 ligands DeltaA/D or of the requisite enzyme for the signaling pathway, Mindbomb, resulted in excess neuron production and decreased OPCs in the zebrafish spinal cord. The Notch1 pathway may thus be required early on to maintain a pool of proliferative precursors that later gives rise to OPCs, subsequent to neuron production (Park and Appel 2003). Conversely, a mutation in *fbxw7* (encoding F-box/WD repeat-containing protein 7), which normally targets Notch1 for degradation, increases Notch1 function and resulted in excess production of OPCs from neural precursors (Snyder, Kearns et al. 2012).

Manipulation later on during development suggested that Notch1 also regulates the OPC-oligodendrocyte transition: in vitro, activation of the Notch1 pathway prevented differentiation of purified optic nerve OPCs into oligodendrocytes and maturation of newly differentiated oligodendrocytes, with no effect on OPC proliferation (Wang, Sdrulla et al. 1998). In vivo, constitutively active Notch1 also prevented maturation of OPCs into oligodendrocytes in the zebrafish spinal cord (Park and Appel 2003), resulting in excess OPCs. In the rodent spinal cord and forebrain, conditional ablation of Notch1 from OPCs caused premature differentiation of oligodendrocytes, without affecting OPC proliferation (Genoud, Lappe-Siefke et al. 2002). Similarly, mice heterozygous for a *notch1* null mutation show premature myelination of brain and optic nerve, and additionally show ectopic myelination of incorrect axons in the cerebellum, that normally never get myelinated (Givogri, Costa et al. 2002).

However, the identity of the cells that present Notch1 ligands is debatable. In the optic nerve, retinal ganglion cells (RGCs) express the ligand Jagged1, but so do oligodendrocytes. Thus, in this region, contact between mature oligodendrocytes and OPCs may result in an intra-lineage regulation of oligodendrocyte differentiation, as in vitro studies suggested previously (Zhang and Miller 1996, Yang, Lewis et al. 2011). Additionally, an in vitro study proposed that an axonal molecule present at the paranodal junction, Contactin, may itself serve as a ligand for the Notch1 pathway,

but seemed to act in the opposite way: Contactin-mediated activation of Notch1 promoted OPC differentiation and myelination (Hu, Ang et al. 2003).

Thus, the role of the Notch1 signaling pathway during the differentiation of oligodendrocyte is not fully elucidated, and it particularly remains unclear which ligands bind to the Notch1 receptor in vivo, and whether they have an axonal origin.

Integrin signaling

The laminin family of basal-lamina glycoproteins, which has been shown to promote survival in several cell types, can also regulate oligodendrocyte-lineage cell development through the signaling pathway downstream of the transmembrane receptor integrin. Co-culture studies using integrin-blocking antibodies (Frost, Buttery et al. 1999) show increased oligodendrocyte apoptosis, and a role for β1-integrin signaling in promoting oligodendrocyte survival and myelination was confirmed in vivo, using integrin receptor knock-out mice (Colognato, Baron et al. 2002, Benninger, Colognato et al. 2006, Barros, Nguyen et al. 2009) or mice expressing a dominant-negative β1-integrin transgene in oligodendrocytes (Lee, de Repentigny et al. 2006, Camara, Wang et al. 2009). In these mice, some degree of hypomyelination and reduction in oligodendrocyte number is found in specific CNS tracts, although this is variable between experimental paradigms.

A number of molecules have been identified as ligands for integrin signaling. Expression studies pointed to axonal laminin-2 (Colognato, Baron et al. 2002), and in fact, laminin-2 deficient mice present reduced oligodendrocyte number and hypomyelination or dysmyelination of some CNS axonal tracts (Chun, Rasband et al. 2003, Relucio, Tzvetanova et al. 2009), as do laminin-2 deficient human patients, which present alterations in CNS white matter tracts (Jones, Morgan et al. 2001). However, a direct interaction between axonal laminin-2 and oligodendroglial β1-integrin has not yet been unambiguously demonstrated in vivo, and at least in vitro, astrocytes may also promote oligodendrocyte survival via laminin-2-β1-integrin interactions (Corley, Ladiwala et al. 2001). Contactin, a molecule that is expressed

both by neurons and oligodendrocyte-lineage cells, may also mediate oligodendrocyte survival and promote myelination via α6β1- integrin (Laursen, Chan et al. 2009).

Additionally, integrin signaling may also be required in later aspects of oligodendrocyte development: laminin-2 promoted cell spreading and myelin sheath formation in vitro, an effect blocked by using anti-β1 integrin antibodies (Buttery and ffrench-Constant 1999, Relvas, Setzu et al. 2001). β1-integrin-null oligodendrocytes extend smaller myelin membrane sheaths when plated in vitro (Barros, Nguyen et al. 2009). In vivo, a dominant-negative form of β1-integrin receptor decreased the elaboration of myelin sheaths following a demyelinating lesion (Relvas, Setzu et al. 2001). In addition to disruption to a number of intracellular signaling cascades, these phenotypes may also be due to the ability of β1-integrin to directly promote local translation from the *mbp* mRNA in the processes of oligodendrocytes (Laursen, Chan et al. 2011). Collectively, these may explain some of the dysmyelination phenotypes observed in laminin-2 null mice, but the relevant oligodendroglial receptor remains to be determined – recently, the non-integrin receptor Dystroglycan has been found to mediate at least part of the laminin signaling in oligodendrocytes and promote myelination (Colognato, Galvin et al. 2007).

In sum, the exact molecules and the developmental stage at which they act remain to be fully clarified and it is possible that combinations of factors act at multiple stages to exert their functions in vivo. Other extracellular matrix components, namely Tenascin-C, also regulate myelination: the transient developmental expression of Tenascin-C seems to prevent *mbp* expression; interestingly, it requires interaction with Contactin, but is thought to act via α5 integrins (Czopka, von Holst et al. 2010). While laminins are secreted proteins present in the extracellular matrix, Contactin is membrane-anchored, which would act in a juxtacrine fashion.

Like Nrg1-ErbB signaling, integrin or dystroglycan signaling is also pleiotropic in oligodendrocyte development. Interestingly, the integrin signaling pathway may actually modulate oligodendrocyte-lineage cells' responsiveness to Nrg1 signaling and switch its effect from anti-differentiation to pro-differentiation and pro-survival (Colognato, Baron et al. 2002), explaining its pleiotropy.

Electrical activity

A number of observations have long suggested that neuronal electrical activity may influence myelination in vitro and in vivo (these have been reviewed in (Zalc and Fields 2000, Fields 2005, Fields 2010)). For instance, sensory and motor experience seem to drive myelination in vivo: myelination is accelerated with premature eye opening in rabbits (Tauber, Waehneldt et al. 1980); professional pianists with long-term training have increased white matter volume in specific tracts relating to fine finger movements (Bengtsson, Nagy et al. 2005, Han, Yang et al. 2009). However, conflicting reports exist for much of this indirect evidence (Fields 2004). Direct testing of this hypothesis using highly specific neurotoxins in vivo also yielded conflicting results. Intravitreous injection of tetrodotoxin at the onset of myelination (postnatal day P4) in rats did not change the number of Mbp+ oligodendrocytes at P6, but greatly reduced the proportion of those that form myelin sheaths, and the rare myelin sheaths formed were loose and uncompacted. However, P5 injection had no effect (Demerens, Stankoff et al. 1996). Another group reported using intraocular injections from P0-P9; at P9, rats had normal numbers of myelinated axons in the optic nerve (Colello, Devey et al. 1995).

The recent observation that unmyelinated axons in many regions of the CNS make bona-fide synapses with OPCs provided further support to this notion, as it provides an anatomical and cellular correlate that may underlie the seemingly activity-driven myelination. Such synapses are both anatomically, ultrastructurally and electrophysiologically similar to classical neuron-neuron synapses, though their exact role in myelination, if any, remains unclear (Almeida and Lyons 2013). A recent elaborate in vitro study proposed that glutamatergic signaling at such axon-OPC synapses may directly regulate local translation of mbp mRNA (Wake, Lee et al. 2011). However, NMDA receptor-based glutamatergic signaling is dispensable for myelination in vivo (De Biase, Kang et al. 2011), and the exact molecular mechanisms underlying such synaptic communication remain unclear.

In addition to glutamate-based synaptic vesicle release, a number of other pathways have been proposed to mediate the influence that electrical activity has on

myelination. For instance, purinergic signaling may indirectly stimulate astrocytes to enhance myelination (Fields and Burnstock 2006). Another study reported that NRG1 type I expression was shown to be dynamically regulated by electrical activity in axons (Liu, Bates et al. 2011); axonal overexpression of this particular isoform of Nrg1 caused hypermyelination (Brinkmann, Agarwal et al. 2008). As mentioned before, mice grown in social isolation exhibit reduced levels of Nrg1 and a hypomyelinating phenotype, which was phenocopied by inhibition of ErbB3 (Makinodan, Rosen et al. 2012). Thus, the Nrg-ErbB pathway seems to be downstream of an experience-driven, neuronal activity-driven stimulus for myelination.

Thus, the exact aspect of myelination that may be modulated by electrical activity is not clear, and it may be that electrical activity directly or indirectly influences multiple steps of oligodendrocyte development and myelination.

In sum, many factors can influence the same developmental stage of myelination and potentially compensate for the absence of any single factor. Individual molecules can play multiple roles at different stages. Additionally, extrinsic factors likely exert their regulation over an intrinsic developmental program. Why is such complex regulation necessary? It may have emerged during evolution to adapt the properties of myelin to each specific axon, optimizing the functional output of the circuit, as mentioned before.

1.5 Diversity of myelinated fibers

Complex regulatory signals, including those derived from axons, may be responsible for generating the immense diversity of oligodendrocytes and myelinated fibers observed among vertebrates and within one animal's nervous system, for which I will briefly provide examples.

Timing of oligodendrocyte differentiation and myelination

Within the same species, the variation in the timing of oligodendrocyte differentiation and myelination is considerable. In the rodent CNS, analysis of the expression of myelin genes such as *mbp* revealed that the first oligodendrocytes appear just before birth in the ventral spinal cord, and differentiation ensues in the caudal direction in the following days (Foran and Peterson 1992). Myelination, as determined by electron microscopy, quickly follows the pattern of differentiation. Axonal ensheathment in the ventral spinal cord is observed in late embryonic stages and compact myelin is observed at birth (Bjartmar, Hildebrand et al. 1994). In the forebrain, differentiation of oligodendrocytes and myelination of the corpus callosum only occur later in the third postnatal week (Foran and Peterson 1992). The general pattern of myelination is replicated in other vertebrates (Remahl and Hildebrand 1982, Hildebrand, Remahl et al. 1993). As previously mentioned, myelination continues to occur until adulthood, although at later stages it remains to be fully elucidated whether this represents de novo myelination or myelin turnover, for instance.

One striking example concerns the corticospinal tract in the dorsal spinal cord. This tract only exhibits mature oligodendrocytes (Schwab and Schnell 1989) and compact myelin (Matthews and Duncan 1971) on postnatal day 11, in contrast with the adjacent cuneate and gracile tracts, which are myelinated on the day of birth. The late myelination of the rat corticopinal tract illustrates the highly local regulation of differentiation and myelination even in the same region of the dorsal spinal cord.

Interestingly, some CNS regions show a different timing between oligodendrocyte differentiation and myelination. OPCs migrate into the rat optic nerve at late embryonic stages (Small, Riddle et al. 1987); the first differentiated oligodendrocytes (expressing myelin transcripts and proteins) are detected from P4 closer to the brain, and differentiation proceeds towards the retina (Colello, Devey et al. 1995). Surprisingly, the formation of compact myelin occurs in the opposite direction, starting at the retina and proceeding towards the brain. Thus, within the same animal, some oligodendrocytes clearly form myelin sheaths immediately upon differentiation, regardless of when that differentiation happens, but other

oligodendrocytes (such as optic nerve oligodendrocytes closer to the brain) experience a significant delay between the expression of myelin genes and the actual elaboration of myelin sheaths. This suggests that some oligodendrocytes may be subject to external, regional signaling that regulates the timing of their myelination.

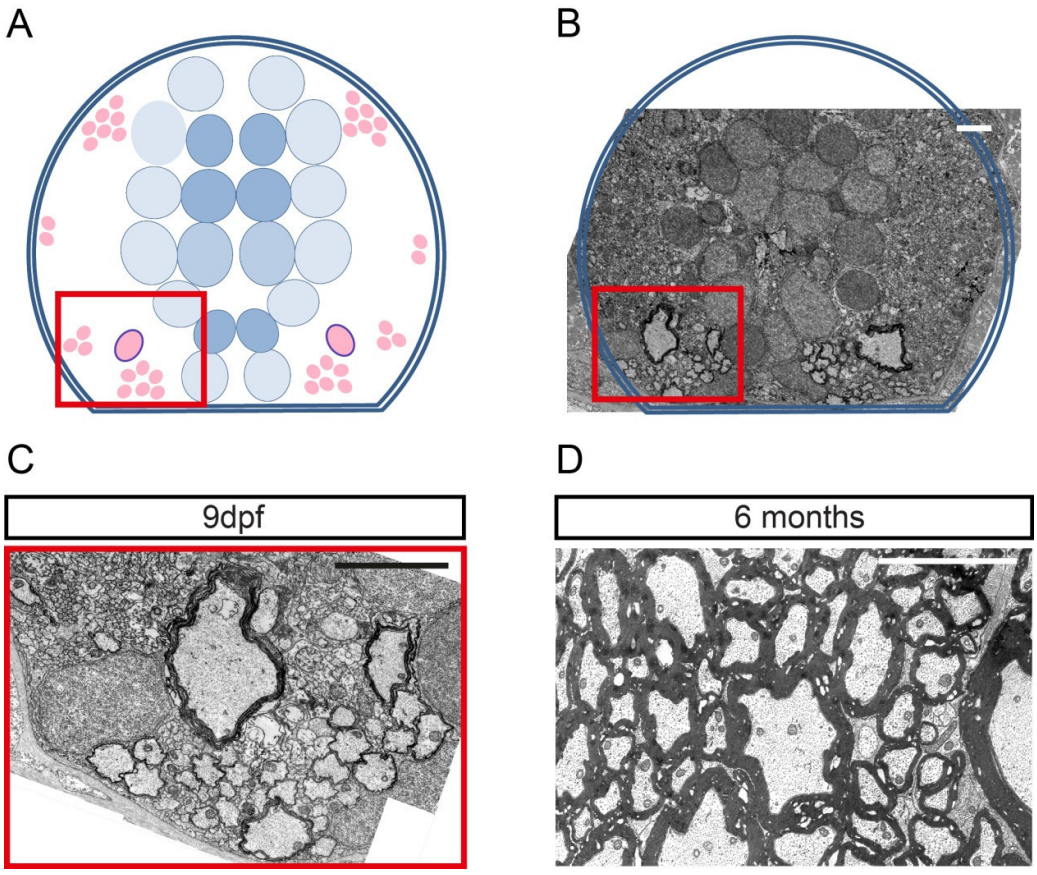

Figure 1.6 – 9dpf versus 6 month old zebrafish spinal cord

(**A, B**) 9dpf spinal cord: neuronal somas lie in the centre, flanked by clusters of axons, some myelinated. The large myelinated axon in the centre of the box is the Mauthner axon.
(**C**) Close up of the box in B; note it contains all myelinated axons in that hemi-spinal cord.
(**D**) An area similar in size to C in an adult zebrafish contains many more myelinated axons, and the spinal cord is orders of magnitude larger. Scalebars: 3 µm.

In the zebrafish CNS, expression of myelin genes (P0, DM20 and MBP) is first detected in the hindbrain at 2 days postfertilization (dpf). Oligodendrocytes rapidly increase in number and distribute through the midbrain and spinal cord by 4dpf

(Brosamle and Halpern 2002). In the optic nerve, the first oligodendrocytes only appear later, by 4dpf. The formation of compact myelin sheaths follows the same spatial pattern. Compact myelin is first detected in the ventral hindbrain and anterior spinal cord at 4dpf, and later in the optic nerve. After the emergence of oligodendrocytes and first myelinated axons, myelination proceeds at a rapid pace during larval development. The number of myelinated axons in the ventral spinal cord of adult animals is much larger compared to larvae (Figure 1.6), which indicates that as in mammals, myelination is an ongoing process that persists for a significant part of their development. Thus, the large regional variation in the timing of the onset of myelination is replicated in zebrafish, while the same general pattern is maintained.

Oligodendrocyte morphology

The first descriptions of oligodendroglia by Pio del Rio Hortega already highlighted the diversity of oligodendrocyte morphologies (Río-Hortega 1928). The number of processes and myelin sheaths and their spatial orientation varies greatly from oligodendrocyte to oligodendrocyte and from CNS region to CNS region. In the spinal cord, some oligodendrocytes extend just one large myelin sheath (resembling a Schwann cell) (Remahl and Hilderbrand 1990), whereas in the cerebral cortex, oligodendrocytes can maintain 60 smaller-calibre sheaths (Chong, Rosenberg et al. 2012), for instance. Hortega classified such diversity in four morphological subtypes (see examples in Figure 1.7). In the almost 100 years since, this morphological heterogeneity has been confirmed in all animal models studied, as reviewed in (Hildebrand, Remahl et al. 1993), and exemplified in (Almeida, Czopka et al. 2011, Chong, Rosenberg et al. 2012).

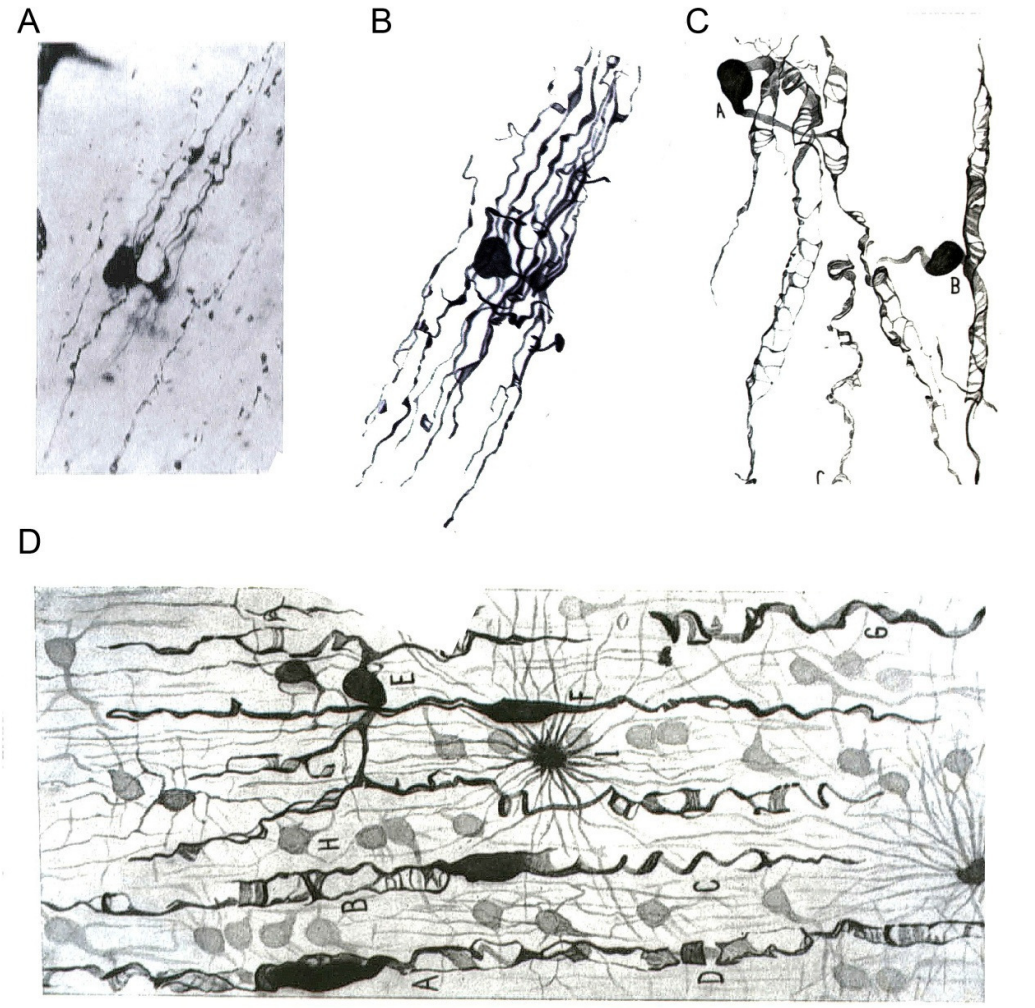

Figure 1.7 – Original silver impregnation microphotographs and illustrations by Pio del Rio Hortega

(**A, B**) Carbonate silver impregnation of brain tissue and drawing showing a type 2 oligodendrocyte, which extends many aligned small calibre myelin sheaths.
(**C**) Type 3 oligodendrocytes extend fewer and thicker sheaths.
(**D**) Type 3 (cell E at the top) and 4 (cells A-D at the bottom) oligodendrocytes; type 4 extend just one large sheath resembling a Schwann cell. All taken from (Río-Hortega 1928)

Strikingly, a particular tendency has been consistently observed amongst all this diversity: oligodendrocytes myelinating many axons tend to myelinate small-calibre axons, compared to those myelinating large axons, which extend fewer processes. For instance, at the onset of myelination in the rat CNS, spinal cord oligodendrocytes myelinate 3 axons on average, with a diameter of about 1μm, while oligodendrocytes in the corpus callosum myelinate 15 axons, with an average of about 0.5 μm

diameter; and this general pattern is confirmed in several CNS regions by several studies (Bjartmar, Hildebrand et al. 1994, Berry, Ibrahim et al. 1995, Weruaga-Prieto, Eggli et al. 1996). This relationship is also observed in the toad, chicken and cat, for instance (Hildebrand, Remahl et al. 1993). Interestingly, some reports describe a molecular correlate for this heterogeneity, whereby some antibodies recognize specifically either oligodendrocytes that associate with few large-diameter fibers (Anderson, Bjartmar et al. 1999) or oligodendrocytes that associate with many small diameter axons (Butt, Ibrahim et al. 1995). This indicates that the morphological classification is not purely artificial but indeed reflects different biochemical properties of subsets of oligodendrocytes. Could these different morphologies reflect intrinsically different subtypes of OPCs?

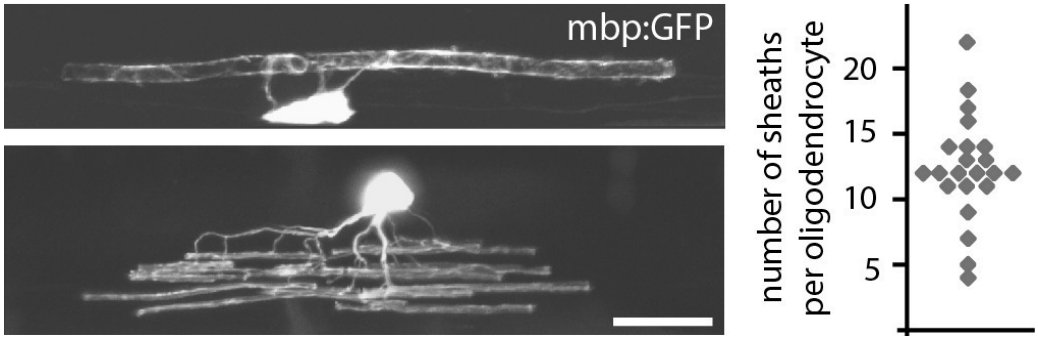

Figure 1.8 – Live imaging of mosaically labelled oligodendrocytes in the developing zebrafish spinal cord recapitulate diversity of oligodendrocyte morphologies

Two different oligodendrocyte morphologies, resembling a type 4 oligodendrocyte in Hortega's morphological classification (top) and a type 2 oligodendrocyte (bottom). On the right, graph illustrating the diversity of the number of sheaths that individual oligodendrocytes form in the larval zebrafish spinal cord. Taken from (Almeida, Czopka et al. 2011)

It is of particular interest to observe CNS regions such as the spinal cord, which contain many different axons. In our own studies of the zebrafish spinal cord, we have been able to directly analyze the morphology of living oligodendrocytes in vivo by genetically targeting the expression of fluorescent reporters such as GFP in individual cells (Figure 1.8). This is difficult to achieve in any other models of

myelination at the same single-sheath resolution. We have recapitulated the findings of Hortega: some oligodendrocytes extend only one, very large myelin sheath around the very large diameter Mauthner axon; but other oligodendrocytes can extend more than 20 sheaths, all on smaller axons (Almeida, Czopka et al. 2011). Interestingly, we also find that the vast majority of oligodendrocytes tend to fall into one of those categories. These oligodendrocytes coexist in very close proximity, and thus have access to the exact same complement of targets. What makes them choose only one particular type of axons?

In sum, there is a large variation in oligodendrocyte morphologies – both between different regions of the CNS and within the same region. This heterogeneity is conserved in all individuals of the same species, and the general patterns of myelination are conserved across vertebrate species, which suggests that rather than occurring stochastically, these parameters of myelination are adapted to optimize the function of axons and of the emerging neuronal circuits. How do such differing morphologies emerge during development? It is tempting to speculate that axons regulate some aspects of the morphological development of oligodendrocytes, given that the final morphology seems adapted to the axons, and the recent evidence that experience-driven neuronal activity can lead to changes in white matter. However, no in vivo study unambiguously or convincingly demonstrated that axons directly regulate the morphology of oligodendrocytes, at the level of the individual cells. The alternative hypothesis remains possible, that distinct oligodendrocyte morphologies reflect inherently distinct, 'fixed' subtypes of oligodendrocytes. I will explore this issue in Chapter 4.

1.6 **Aims**

My general aim in this thesis is to explore which aspects of oligodendrocyte development and myelination can be regulated by their target axons, and which aspects follow an intrinsic programme of development. This will address whether the diversity of oligodendrocytes observed reflects such axonal regulation, or intrinsically different subtypes of oligodendrocytes. Specifically, I will:

a) Investigate the requirement of axons for early oligodendrocyte lineage cell development, by analysing the specification and early behaviour of OPCs in the absence of the initial axonal targets for myelination (Chapter 3)

b) Address the requirement of axons for later aspects of oligodendrocyte lineage cell maturation, such as the timing of differentiation, the extent of myelination and the location of myelin sheaths, in the absence of the same axonal targets (Chapter 4)

c) Address whether the myelinating capacity of oligodendrocyte-lineage cells is plastic and responsive to the axonal environment, by challenging these cells with an excess of axonal targets (Chapter 4)

2. Experimental Procedures

2.1 Fish husbandry and lines used

Zebrafish were kept and raised in the Queen's Medical Research Institute animal facility under standard conditions (Nüsslein-Volhard and Dahm 2002, Westerfield 2007) and in accordance with UK Home Office guidelines. Adult animals were kept at 26.5°C at a 14 hours light and 10 hours dark cycle. Embryos were kept at 28.5°C in embryo medium[1] or conditioned aquarium water with methylene blue. Embryos were staged according to (Kimmel, Ballard et al. 1995). In addition to WT strains (WIK, AB and *golden*), the following transgenic or mutant lines were used:

Line name	***Use***	***Origin***
kbp$^{st23/+}$	Remove reticulospinal axons partially	(Lyons, Naylor et al. 2008)
sox10:mRFP	Visualize OPCs and oligodendrocyte membrane	(Kirby, Takada et al. 2006)
olig2:GFP	Visualize pMN progenitors and OPCs	(Shin, Park et al. 2003)
mbp:EGFP	Visualize oligodendrocytes	(Almeida, Czopka et al. 2011)
mbp:EGFP-CAAX	Visualize oligodendrocytes and myelin sheaths	
sox10:KalTA4	Sparsely label OPCs and oligodendrocytes	*this study*
mbp:Gal4	Sparsely label oligodendrocytes	*unpublished*
UAS:kaede	Visualize sparsely labelled cells	(Scott, Mason et al. 2007)
pax2a:GFP	Visualize a subset of spinal interneurons	(Picker, Scholpp et al. 2002)
glyt2:GFP		(McLean, Fan et al. 2007)

[1] 10mM HEPES-buffered E3 Embryo medium (500µM NaCl, 170 KCl µM, 330 µM $CaCl_2$, 330 µM $MgSO_4$).

In Figures and figure legends, 'Tg' before the line name means that a stable, germ-line inserted transgenic line was used, with transgene expression in all relevant cells. Otherwise, a transgene name designates injection of a plasmid which results in sparse, mosaic expression.

2.2 *kbp*^{st23} genotyping

Animals were genotyped for *kbp*^{st23} in at least one of three manners:

a) According to (Lyons, Naylor et al. 2008): genomic DNA was extracted by standard protocols (Nüsslein-Volhard and Dahm 2002), from which a 250bp long PCR product was amplified using primers

5′-AAAACGACCAACTGTGCCTA-3′
5′-ACAGTCAAACACCAGATCGAAAGTCA-3′,

and digested with restriction enzyme MaeIII (Roche). The WT PCR product is cleaved into 228bp + 22bp fragments, whereas the mutant PCR product is not cleaved; these were visualized by routine electrophoresis on a 4% agarose gel containing ethidium bromide. See example in Figure 4.13C.

b) When crossed with transgenic lines sox10:mRFP or mbp:EGFP-CAAX, myelin sheaths along the posterior lateral line and ventral spinal cord were easily visualized in a standard fluorescence microscope. The mutant phenotype was clearly identified, as sheaths do not extend past the urogenital opening, whereas in WT or heterozygous animals they extend the full length of the animal at all ages analysed.

c) When immunostained with 3A10 antibody, axons in the posterior lateral line and ventral spinal cord were easily visualized in a standard fluorescence microscope. The mutant phenotype was clearly identified, as axons do not extend past the urogenital opening, whereas in WT or heterozygous animals they extend the full length of the animal at all ages analysed.

2.3 sox10:KalTA4 Plasmid construction

The middle entry vector pME-KalTA4GI was generated by PCR-amplifying the coding sequence for KalTA4GI, an optimized version of Gal4, from plasmid pCSKalTA4GI (Distel, Wullimann et al. 2009), using attB site-containing primers

5'-GGGACAAGTTTGTACAAAAAAGCAGGCTGCCGCCACCATGAAACT
GCTCTCATCCATCG-3'
5'-GGGGACCACTTTGTACAAGAAAGCTGGGTTACGATCCGTCGAGGA
ATTAATTCTTTGC-3'

The PCR product was recombined with pDONR221 using BP clonase (Life technologies) to generate the ME element clone pME-KalTA4GI.

A previously described Gateway plasmid containing the 7.2kbp fragment of the sox10 promoter, p5E_sox10 (Czopka, Ffrench-Constant et al. 2013), was recombined in a LR Gateway reaction with pME-KalTA4GI, and plasmids p3E-polyA and pDestTol2CG2 from the Tol2kit (Kwan, Fujimoto et al. 2007) using LR clonase II Plus (Life technologies), to generate sox10:KalTA4GI, which contains a cmlc2:egfp transgenesis marker for EGFP expression in the heart.

2.4 GFP-2A-KBP plasmids construction

To generate WT *kbp* transgenic ("rescue") constructs, full-length *kbp* was initially amplified from complementary DNA (cDNA) of the AB strain and cloned in pCR2.1-Topo (Life technologies), using primers

5'-ATGGCTGCCAACAACAGTATCGAGTGG-3'
5'-TCACTTGGAGGAGGCCAGAGTGG-3'

generating pCR2.1-kbp. Subsequently, a GFP-encoding fragment was PCR-amplified from pME-EGFP (from the Tol2kit) and a WT *kbp*-encoding fragment from pCR2.1-kbp, using the following primers:

GFP:
5'-CGCTCTATCGATGCCACCATGGTGAGCAAGGG-3'
5'-GTCTCCTGCTTGCTTTAACAGAGAGAAGTTCGTGGCTCCGGATCCCT
TGTACAGCTCGTCCATGCCG-3'

kbp:
5’-GCCACGAACTTCTCTCTGTTAAAGCAAGCAGGAGACGTGGAAGAA
AACCCCGGTCCTATGGCTGCCAACAACAGTATCGAG-3’
5’-CCGACACTCGAGTCACTTGGAGGAGGCCAGAGTGG-3’

These primers include sequences for attaching a porcine teschovirus-1 2A (‘2A’) sequence, which is a short peptide that induces a strand break during messenger RNA translation to obtain two separate proteins from a single open reading frame. According to (Szymczak-Workman, Vignali et al. 2012, Szymczak-Workman, Vignali et al. 2012), standard recombinant PCR was then used to ligate the two fragments and generate GFP-2A-KBP, which was cloned into the expression vector pCS2+ (producing pCS2-GFP-2A-KBP) and Sanger-sequenced to verify that the correct sequence was generated.

The GFP-2A-KBP sequence was then PCR-amplified from this vector using attB-containing primers

5’-GGGGACAAGTTTGTACAAAAAAGCAGGCTGCCACCATGGTGAGCA
AGGG-3’
5’-GGGGACCACTTTGTACAAGAAAGCTGGGTTCACTTGGAGGAGGCCA
GAGTGG-3’

The PCR product was recombined with pDONR221 using BP clonase to generate the ME element clone pME-GFP-2A-KBP.

Finally, p5E_sox10, p5E_HuC[2], pME-GFP-2A-KBP, p3E-polyA and pDestTol2pA2 from the Tol2kit were recombined in a LR Gateway reaction using LR clonase II Plus to generate HuC:GFP-2A-KBP and sox10:GFP-2A-KBP.

2.5 DNA microinjections

Fertilised eggs were injected with 1 nL of a solution containing 5-10 ng/µL plasmid DNA and 25-50 ng/µL tol2 transposase mRNA. Injected fish were analysed as

[2] unpublished, generated by Dr. T. Czopka by recombining a 3kbp HuC promoter fragment from a huC:Gal4 plasmid (a kind gift from Dr. M. Meyer), into a pDONRP4-P1R vector in a standard Gateway BP reaction.

mosaics or grown to adulthood to raise stable transgenic lines. For the generation of the stable transgenic line Tg(sox10:KalTA4), plasmid DNA encoding sox10:KalTA4 and transposase mRNA were injected as described in 1-cell stage AB fertilized eggs. Successful integration of sox10:KalTA4 into the genome was detected by cmcl2:EGFP expression in the heart. GFP+ potential founders were individually outcrossed to AB wildtype, and screening for green hearts in the offspring identified founders with germ-line transmission of sox10:KalTA4; this F2 generation was also raised and screened for stable sox10:KalTA4 genome integration.

2.6 *notch1a* morpholino injection

Fertilized eggs (between1-8 cell stage) were injected with 500pg of a morpholino directed against a *notch1a*-specific splice junction (Ma and Jiang 2007) (Gene Tools, LLC) to temporarily abrogate embryonic notch1a expression.

2.7 *hoxb1* mRNA injection

Fertilized eggs (between1-8 cell stage) were injected with 50pg of *hoxb1b* mRNA. The majority of *hoxb1b* mRNA-injected animals were morphologically normal and typically had two Mauthner axons on one side of the CNS and one on the contralateral side. A subset of *hoxb1b* mRNA-injected animals had morphological abnormalities as have been previously described (Hale, Kheirbek et al. 2004) and were therefore excluded from further study.

2.8 *notch1a* RT-PCR

To assay *notch1a* mRNA expression levels, total RNA was extracted from pools of 10-20 10hpf embryos or 72hpf larvae and cDNA was synthesized using a poly-d(T) primer, according to standard protocols (Nüsslein-Volhard and Dahm 2002). Following normalization of total cDNA levels, specific *notch1a* cDNA levels were assessed by PCR amplification using primers

5′-CTTCTGCACTTTCTGGAGATTTAAA GAAG-3′ (Ma and Jiang 2007)
5′-CACACGTCTGACCTGTGAAGC-3′;

in parallel with amplification of a ubiquitously expressed control transcript EF1α, using primers

5′-AGGACATCCGTCGTGGTAAT-3′
5′-AGAGATCTGACCAGGGTGGTT-3′

2.9 Acridine Orange treatment

Dechorionated larvae were incubated for 30minutes in the dark in embryo medium containing 2µg/ml acridine orange (Sigma), followed by two quick 5-minute washes in embryo medium, and immediately live-imaged after.

2.10 Transmission electron microscopy

Transmission electron microscopy was performed as described in (Almeida, Czopka et al. 2011, Czopka and Lyons 2011). Briefly, zebrafish were terminally anaesthetised in tricaine (4.2mg/mL 3-amino benzoic acid ethyl ester, Sigma) and immersed immediately in primary fixative (4% paraformaldehyde and 2% Glutaraldehyde in 0.1M sodium cacodylate buffer) microwave-stimulated (using a Panasonic microwave with `Inverter' technology), and incubated for 2 hours at room temperature. Alternatively, a small number of adult animals (Figure 1.6) were perfused with the same primary fixative solution under the careful (and generous) guidance of Dr. T. Becker, and the spinal cords were dissected after primary fixation. Samples were transferred to a secondary fixative (2% osmium tetroxide in 0.1M sodium cacodylate and 0.1M imidazole buffer) at room temperature for 3 hours with microwave stimulation. Samples were subsequently stained *en bloc* with an aqueous saturated uranyl acetate solution (~8% w/v), and subsequently dehydrated in an ethanol gradient solution series (50%, 75%, 95% and 100%. Ethanol), followed by acetone dehydration. Samples were then pre-infiltrated with an EMbed-812 resin (Electron Microscopy Sciences)/acetone solution, which was then replaced by 100%

EMbed. The EMbed infiltrated tissue samples were then aligned in silicon moulds and solidified at 65°C for at least 24hours.

Blocks were then trimmed in the shape of a trapezoid around the embedded fish, and the regions of interest in the spinal cord were cut into 80nm thick sections on an ultramicrotome (Reichert Jung Ultracut Microtome, Leica). Blocks were visualized under a dissection microscope to ensure sections were cut on comparable somite levels. Sections were chloroform-stretched, captured and allowed to dry on electron microscopy grids with hexagonal grid pattern (PELCO 300 Mesh Grids, Ted Pellar Inc.). Sections on grids were further stained with a solution of saturated uranyl acetate and absolute ethanol, washed, dried, and subsequently incubated in Sato lead stain (Czopka and Lyons 2011) for 5minutes. Grids were then washed, dried and stored until imaging. TEM images were taken at magnifications between 520x-6500x on a Phillips CM120 Biotwin transmission electron microscope at the Electron Microscope Facility, Daniel Rutherford Building, University of Edinburgh.

2.11 Immunohistochemistry

Whole-mount antibody labelling was carried out using standard protocols (Nüsslein-Volhard and Dahm 2002). Briefly, zebrafish were terminally anaesthetised in tricaine and immersed immediately in primary fixative (2% paraformaldehyde and 1% Trichloroacetic acid, or alternatively 4%PFA, in PBS). Samples were then permeabilized (by incubation in either acetone at -20ºC or 10µg/ml proteinase K in PBS at room temperature), blocked in normal goat serum ('NGS', 10% in PBS), and incubated with primary antibodies over two nights at 4ºC, followed by secondary antibodies over one night at 4ºC. Samples were extensively washed in between steps (with PBS containing 1% Triton X-100). Primary antibodies used were 3A10 antibody (1:200, Developmental Studies Hybridoma Bank), HB9 (MNR2, 1:400, Developmental Studies Hybridoma Bank), phosphorilated-histone 3 (PH3 Ser10, 1:200, Cell Signalling #9701), at indicated dilutions in 5% NGS in PBS. Secondary antibodies were all used at 1:2000 dilution in 2%NGS in PBS, conjugated with Alexa fluor dyes - Al488, Al568 or Al633 (from Molecular Probes, Life Technologies).

Samples were then equilibrated in a graded glycerol series (30%, 50%, 70%, 95% in PBS).

Antibody labelling of 5dpf dissected brains was performed as above, but after fixation, the tissue around the brain was carefully dissected using dissection forceps, and permeabilization was abbreviated, with all other steps remaining equal. Alternatively, some animals were immunostained in whole-mount, and dissection was performed after secondary antibody incubation.

2.12 Mounting for imaging

Live embryonic and larval zebrafish were embedded in 1.5% low melting point agarose (Sigma) in embryo medium with tricaine (168µg/mL 3-amino benzoic acid ethyl ester, Sigma). Animals were placed laterally on their sides and carefully pressed against the coverslip along the length of their trunk to ensure they were as flat as possible.

For imaging of immunostained samples, samples were placed in a drop of 95% glycerol in PBS between a coverslip and a glass slide, in some cases with three small drops of vacuum grease to support the coverslip and prevent flattening and disruption of the tissue.

2.13 Image acquisition

Most imaging was performed with a Zeiss LSM710 confocal microscope except for the following: mature oligodendrocytes in 4dpf and 8dpf WT and *kbp* mutants (Figure 3.4C and Figure 4.4A); oligodendrocyte-lineage cells in 48hpf and 60hpf WT and *kbp* mutants (Figure 3.7), and acridine orange labelled apoptotic cells in 72hpf WT and *kbp* mutants (Figure 3.15). These experiments were imaged in a Zeiss Imager Z1 equipped with an Apotome2 structured illumination unit.

For all imaging of WT versus *kbp* mutants in Chapter 3, the anterior region of the spinal cord was acquired in all animals by aligning the edge of the visual field in the eyepiece to the urogenital opening somite; and the posterior region by aligning the

edge of the visual field to the very last somite in the spinal cord, using a 20X objective (Zeiss Plan-Apochromat 20x dry, NA=0.8, Carl Zeiss Microscopy), zoom 1x. This resulted in a 425µm long image in the Zeiss LSM710 confocal microscope and in a 488µm long image in the Zeiss Imager Z1. The only exception was imaging the posterior region of 72hpf and 96hpf oligodendrocyte-lineage cells in double transgenic Tg(olig2:GFP; sox10:mRFP) (Figure 3.8B), which were imaged using a 63x objective (Zeiss C-Apochromat 63x, water immersion, NA=1.2, Carl Zeiss Microscopy), zoom 1x, aligning the visual field (~2 somites) to 7 somites posterior to the urogenital opening, and tiling two lengths of the visual field. This resulted in a 270 µm long image in the Zeiss LSM710 confocal microscope. In all cases, Z-stacks were acquired of the entire depth of the spinal cord, with a Z-interval 2 µm.

For time-lapse imaging in the Zeiss LSM710 confocal microscope, animals were kept in a heated stage adjusted to approximate 28.5ºC in the preparation. Z-stacks of the entire depth of the spinal cord were acquired every 14 minutes, with a Z-interval of 2.1 µm. The posterior spinal cord was imaged overnight and larvae were checked in the morning for circulation and general health.

For all imaging of WT versus *kbp* mutants in Chapter 4, anterior and posterior spinal cord regions were defined as for Chapter 3. All images were acquired using a 20X objective, zoom 1x, Z-step of 2 µm, except for oligodendrocyte myelinating capacity (Figure 4.3), which were acquired using a 63x objective, and Z-step of 1.5 µm. For some time-coursed mosaically labelled oligodendrocyte-lineage cells (Figure 4.1), the posterior spinal cord of Tg(UAS:kaede animals) was illuminated briefly (~1 minute) with an UV light immediately after 60hpf or 72hpf imaging to achieve kaede photoconversion and facilitate identification of individual cells in the field of view at later time points.

Imaging of WT and animals with supernumerary Mauthner axons in Chapter 4 was as follows: 3A10 immunostained brains (Figure 4.5) were imaged using a 63X objective and a 1 µm Z-step; ensheathment of axons (Figure 4.6) was imaged using a 40x objective and a 1 µm Z-step; mature oligodendrocytes (Figure 4.9) were imaged using a 20x objective and a 1.5 µm Z-step; single oligodendrocyte morphology (Figure 4.10-4.12) was imaged using a 40x or 63x objective and a 0.7-2 µm Z-step.

All fluorescent spinal cord images represent a lateral view, anterior to the left and dorsal on top.

2.14 Image processing

For most imaging, processing was kept to a minimum and included only global change of brightness and contrast; most processing and analysis was done in Fiji software (a distribution of ImageJ). Figure panels were produced using Fiji and Adobe Illustrator CS8. For figures, maximum-intensity projections of Z-stacks were made, and a representative x-y area was cropped. Some images display only one channel in grayscale and were inverted (dark foreground on white background) for ease of visualization.

Electron micrograph tiles were aligned automatically using the automated photo-merge tool in Adobe Photoshop CS3.

Each time lapse movie was processed in Fiji as follows: for each time point, Z-stack slices encompassing the spinal cord were projected in a maximum intensity projection using the Image5D plugin. Projections were then registered in the x-y position between time points using the olig2:GFP channel as reference, using the 'Register virtual stack slices' plugin; subsequently the same registration was applied to the sox10:mRFP channel by using the 'Transform virtual stack slices' plugin. Global brightness and contrast were adjusted.

2.15 Image analysis

Cell counts

Oligodendrocyte number was counted in z-stacks of a lateral view of Tg(mbp:EGFP) larvae, in which GFP is expressed in the cytoplasm of oligodendrocytes, which facilitates the quantification of all oligodendrocyte cell bodies. OPC number was counted in z-stacks of a lateral view of Tg(olig2:GFP; sox10:mRFP) larvae, in which oligodendrocyte-lineage cells express both cytoplasmic GFP and membrane-tethered

mRFP; both channels were simultaneously visualized while counting. A grid was superimposed on the image and all cell bodies were counted throughout the z-stack using the cell counter plugin in Fiji. An approach based on unbiased stereological methods was used to ensure that each oligodendrocyte was only counted once (briefly, consecutive optical sections in the z-stacks should sample each cell body more than once, and each cell body was counted only in the first optical section it appears).

For counts in PH3 immunostained Tg(olig2:GFP) larvae (Figure 3.5), counting was performed blinded to the genotype.

sox10:mRFP debris analysis

For the numbers presented in section 3.3.8 relating to Figure 3.13B, the presence of at least a cluster of mRFP debris (not associated with clear oligodendrocyte-lineage cell processes) was determined in all images from experiments that included the Tg(sox10:mRFP) transgenic line imaged with a 20X objective (this included images acquired with a Zeiss LSM710 microscope and with a Zeiss Imager Z1 microscope).

Electron Micrographs

TEM images were processed as described above. Axons in the spinal cord were traced using the lasso tool in Adobe Photoshop CS3. Axons were included if they were located in the white matter region of the spinal cord; if they were transversal to the section (i.e. extending longitudinally in the spinal cord) and presented a (roughly) circular profile; and if they contained cross sectional profiles of neurofilaments (10 nm) and microtubules (24 nm), which are readily identifiable given their characteristic calibre and distribution (Czopka and Lyons 2011). The perimeter and area of traced axons were measured using the measuring tool in Adobe Photoshop, from which the diameter was calculated. Subsequently, the number and perimeter of all axons (for 9dpf electron micrographs) or of those above 0.5μm (for 3dpf electron

micrographs) in diameter was quantified. Colour code was added to the TEM images using the lasso and pain bucket tools in Adobe Photoshop CS3.

Time-lapses

A composite view of both GFP and mRFP channels of each time lapse was first analysed to detect a) the timing and number of mitotic and apoptotic events, b) the timing of the first dorsal migration of an olig2:GFP+ cell and c) the timing of first myelin sheath formation. In some time lapse movies, the specimen shifted slowly within the agarose in the z axis and drifted outside of the captured z-stack. Subsequently to this first analysis, only the subset of the movie that included the entire depth of the spinal cord was considered. In all animals imaged, every mitotic or apoptotic event and the start of myelination occurred after the dorsal migration of the first OPC; therefore, only the period of each movie after the onset of dorsal migration was considered, for comparison purposes (in Tables 3.2 and 3.3).

To analyse the dynamics of dorsal migration, the time at which the first dorsal OPC migrated above olig2:GFP+ band of neuronal somas was considered to be time point 0 (x=0; y=1 in graph in Figure 3.9B). The time at which any further olig2:GFP+ cell migrated dorsally was annotated, even if the cell returned a ventral position later. The number of dorsally-migrated OPCs (y axis) was plotted against time (x-axis) for each larva using Graphpad Prism 6, and standard regression with least-squares method was used to fit a line to the data of each larva. This line was forced to go through point x=0; y=1 (point at which the first OPC migrates dorsally). R^2 values varied between 0.82-0.98 for WT larvae and 0.78-0.97 for mutant larvae, showing that a straight line models this phase of the dorsal migratory dynamics well. An average regression line was then determined within all WT and within all mutant data, and used to fit those movies which already started with dorsal OPCs (Figure 3.9B).

To analyse the migratory properties of OPCs (Figure 3.10-3.11), dorsal or ventral OPCs that could be reasonably distinguished within the olig2:GFP+ band (prior to, or retrospectively, the onset of sox10:mRFP expression) were tracked using a semi-automated tracking Fiji plugin, Trackmate. Briefly, the annotation of each cell in

each frame is manual, and Trackmate automates the linking between annotated cells across time points. The plugin displays the tracks and provides a number of statistics for each tracked cell, including number of splits (i.e. mitoses), migrated distance, average speed and maximum speed.

Single oligodendrocytes

For analysis of single OPCs and oligodendrocytes at low magnification (Figure 4.1-4.2), individual cells were followed at three time points (60, 72, 96hpf) and were identified across time points based on the morphology of the cell body, morphology of the processes, location in the spinal cord (in the z-axis), relative location to sox10+ expressing radial glial or floor plate cells, and photoconverted kaede fluorescence from previous time points. At each time point the presence of tubular structures at the end of processes (myelin sheaths) was assessed. The target axonal track (dorsal, medial, ventral and motor) was assessed, as well as the presence of ensheathed cell bodies.

For analysis of the myelinating capacity of single mbp:EGFP-CAAX+ oligodendrocytes at high magnification (Figures 4.3 and 4.10-4.12) at 4, 5 or 9dpf, the length and number of individual internodes were measured throughout the z-stack using the measuring tool of either Fiji or Zen Software 2010 (Carl Zeiss Microscopy).

2.16 **Statistical analysis**

All statistical analysis was performed on Graphpad Prism 6. All data were averaged per biological replicate (larva), so in every case N represents number of larvae. All data was tested for normality using D'Agostino & Pearson omnibus test, Shapiro-Wilk test and Kolmogorov-Smirnov test. Direct experimental comparisons of control and manipulated group were subjected both to a parametric, unpaired, two-tailed Student's t-test, and a non-parametric Mann-Whitney test. P-values <0.05 were considered significant and are represented by an asterisk * in Figures. The particular

test displayed in individual figure legends was the t-test if the compared data passed at least two normality tests and the Mann-Whitney test it failed more than one normality test. In most cases, a significant result in a t-test was significant in the Mann-Whitney test, as was the case with non-significant results. For the occasional result which varied according to the statistical test, P-values from both tests are reported. Throughout the thesis and figures, error bars illustrated mean ± standard deviation (SD).

3. Axons regulate proliferation and survival of oligodendrocyte-lineage cells

3.1 Introduction

The sequence of events that results in the emergence of a successfully myelinated axon from a neural precursor and a glial precursor is extremely complex. In addition to the neuron's own differentiation, oligodendrocyte precursor cells (OPCs) must be generated at the appropriate time and location. OPCs first emerge during embryogenesis from a discrete ventral domain in the spinal cord, the pMN domain (Rowitch 2004, Rowitch and Kriegstein 2010). This domain is established by the concerted action of morphogens (such as sonic hedgehog and bone morphogenetic proteins), which distribute in gradients along the dorsal-ventral axis of the developing neural tube. The particular concentrations of the morphogen cocktail in a domain establishes it identity. In the case of the pMN domain, morphogen signalling induces the downstream expression of Olig transcription factors, which are required for the generation of pMN progenitors and their offspring (including OPCs), and can be used as marker of pMN identity (Meijer, Kane et al. 2012). Olig2+ pMN progenitors first generate motor neurons, and later on, switch to OPC generation.

Subsequently, OPCs must migrate and proliferate in a manner that leads to the population of the entire central nervous system. The number and distribution of OPCs and oligodendrocytes must be adequate, at each point, to ensheath and myelinate the required axonal targets. OPCs then extend ramified processes that interact with their local environment. After contacting the target axons, OPCs must ensheath them and kick-start a program of terminal differentiation into oligodendrocytes, which results in myelin biosynthesis and sheath formation. Notably, individual oligodendrocytes can myelinate numerous axons, and the thickness and length of each myelin sheath is often precisely adjusted to each axon. This suggests that the amount of myelin that must be synthesized at the end of each process varies and is locally regulated; further highlighting the complexity of the myelination process (I will address this in Chapter 4).

Regulation of this sequence of events can happen at different levels: from entire cell populations (for instance, proliferation, migration or survival of precursors, which

can be modulated by secreted signals acting at a distance), to the level of single cells (for instance, axonogenesis, or the elaboration of myelin sheaths – more likely regulated by localized, contact-dependent cues). In this chapter, I will address how the initial stages of a complex developmental process such as oligodendrocyte development may be regulated by a different cell type, neurons and their axons, which are intimately associated with the developing myelinating cell. I will focus specifically on whether axons can affect aspects such as specification, migration, proliferation, and survival of OPCs; which must be precisely regulated to lead to the successful colonization of the CNS prior to actual myelin sheath formation. In the next chapter, I will then address whether axons can regulate the later stages of oligodendrocyte development and myelination.

On the face of the complexity of developmental steps outlined above, and the sheer regional diversity of myelinated axons and their structure in the CNS (referred to in Chapter 1), axonal regulation of oligodendrocyte development would be a parsimonious way to explain the ontogenic and the evolutionary emergence of myelination. If neurons in living animals possess the signalling capabilities to effectively communicate and modulate oligodendrocyte development and myelination, then the diversity of myelinated fibers could be just a by-product of the axon-driven oligodendrocyte regulation. A less parsimonious alternative is that the diversity of myelinated fibers is also biologically encoded on the myelinating glia side: the location and timing of oligodendrocyte differentiation and the formation of every myelin sheath would also be genetically predetermined during development. It is possible that this alternative holds true for those particular regions of the CNS that exhibit a stereotyped, fixed structure in every individual. However, the first hypothesis, that axons regulate oligodendrocyte development and myelination, has gathered strong support from the study of CNS regions that exhibit experience-dependent structural plasticity, which I will mention below.

In humans, myelination is an ongoing process lasting well into the third decade of life (Fuster 2002). Recent work has revealed that myelin and oligodendrocyte-lineage cells in adult animals, like neurons, also respond to environmental change or an individual's experience. For instance, optogenetic stimulation of the premotor cortex

in mouse stimulates OPC proliferation and differentiation, which seems to result in some degree of increased myelination in the premotor cortex and subcortical white matter, with accompanying motor function improvements (Gibson, Purger et al. 2014). Similarly, stimulating the medullary pyramid in the rat brainstem promoted proliferation of OPCs in the corticospinal tract throughout the spinal cord (Li, Brus-Ramer et al. 2010). Other examples are reviewed elsewhere (Fields 2008, Zatorre, Fields et al. 2012, Wang and Young 2014). Thus, *de novo* myelin formation in response to neuronal-driven experience during adulthood may underlie aspects of cognition and complex behaviours in a way never before realized. The cellular and molecular mechanisms that underlie this regulation in adulthood are only now beginning to be queried (Wang and Young 2014). Understanding the fundamental mechanisms of neuronal regulation of oligodendrocyte development and myelin formation during development may also shed light on the basis of such myelin plasticity in adulthood, and contribute to understanding the cellular basis of complex behaviours and other aspects of cognition, or their dysfunction, in adults.

Moreover, in cases of demyelinating injury, such as in multiple sclerosis, OPCs remain present throughout the brain, but become surprisingly incapable of differentiating and remyelinating a lesioned area, leading to neuronal degeneration and disability progression (Franklin 2002, Franklin and Ffrench-Constant 2008). Why does remyelination eventually fail in this context, when de novo myelination can occur in other contexts in the adult CNS? Neurons and axons are present in the environment, but may differ substantially from their developmental stages, or from a healthy adult environment. The elucidation of the mechanisms that regulate developmental myelination and how they relate to those in a pathological context can provide new avenues for seeking potential therapies.

3.1.1 Some aspects of oligodendrocyte development are intrinsic and independent of neurons

Over thirty years ago, it was found that oligodendrocyte-lineage cells dissociated from brain (Abney, Bartlett et al. 1981) or optic nerve cultures (Raff, Abney et al. 1985) had the remarkable capacity to differentiate on schedule, replicating their in

vivo timing of differentiation – regardless of the age at which the tissue was dissociated, and even in culture without neurons (Zeller, Behar et al. 1985). This showed that positional information was not necessarily required for the timely emergence of cells of the oligodendrocyte lineage; but did not address whether external factors (for instance, derived from astrocytes, neurons or microglia that might be present in these cultures) might be required for oligodendrocyte development. Further work demonstrated that without astrocytes or their conditioned media, OPCs did not proliferate, and instead differentiated prematurely (Noble and Murray 1984). Platelet-derived growth factor (PDGF) was identified as this astrocyte-secreted mitogen (Noble, Murray et al. 1988, Raff, Lillien et al. 1988, Richardson, Pringle et al. 1988), and PDGF's role in promoting proliferation was confirmed in vivo. As long as astrocytes or PDGF were present in culture, an intrinsic program of development seemed to act within the OPCs that timely regulated their final differentiation: for instance, the offspring of an individual OPC divide the same number of times and differentiated simultaneously, even when two daughter cells were plated in separate microwells (Temple and Raff 1986).

Purification of OPCs to homogeneity and culture in serum-free media allowed researchers to more specifically define the factors required for oligodendrocyte development: with PDGF added to the medium, purified OPCs proliferated, but did so indefinitely and failed to differentiate. Thyroid hormone was identified as an additional factor required to induce their exit from the cell cycle, and was also shown to be sufficient to initiate differentiation (Gao, Apperly et al. 1998), a role confirmed in vivo (Barres, Lazar et al. 1994, Ibarrola, Mayer-Proschel et al. 1996, Ahlgren, Wallace et al. 1997, Baas, Legrand et al. 2002).

Thus, two external but non-neuronal factors were identified that regulated OPC proliferation and cell cycle exit in a paracrine (PDGF) or endocrine manner (thyroid hormone). Providing these two factors is enough for purified perinatal OPCs to develop in a petri dish: they are able to proliferate, and, like OPCs in vivo, progressively mature in morphology and antigenic phenotype (Gao and Raff 1997, Tang, Tokumoto et al. 2000). They timely stop proliferating and exit the cell cycle, and initiate a program of differentiation. Their morphology changes as they extend

many ramified processes (Kachar, Behar et al. 1986, Barres, Lazar et al. 1994), and they start expressing myelin structural proteins and glycolipids (Zeller, Behar et al. 1985, Dubois-Dalcq, Behar et al. 1986). Eventually, the cells even produce myelin sheaths (Bradel and Prince 1983, Rome, Bullock et al. 1986, Szuchet, Polak et al. 1986), either flat in the dish or around inert nano-fibers (Howe 2006, Lee, Leach et al. 2012, Li, Ceylan et al. 2014) or formaldehyde-fixed axons (Rosenberg, Kelland et al. 2008). All of these occur in the absence of neuronal influences and of live axonal contact, suggesting that oligodendrocyte-lineage cells have an intrinsic program of development, independent of the axons that these cells ensheath and myelinate.

3.1.2 Axons can influence oligodendrocyte development and myelination, even in vitro

Notwithstanding these observations that oligodendrocyte-lineage cells do not absolutely require axons for much of their developmental progression, and retain a certain capacity to differentiate by default, it quickly became clear that even in vitro, axons can drastically influence some steps of oligodendrocyte development. Under specific culture conditions, axons of dorsal root ganglia can promote proliferation of adult-isolated oligodendrocyte lineage cells (Wood and Bunge 1986). Co-culture of primary rat oligodendrocytes with chick spinal cord neurons is enough to raise the expression level of MBP and PLP mRNAs fourfold (Macklin, Weill et al. 1986). Additionally, oligodendrocytes will only wrap axons and not dendrites of co-cultured neurons, suggesting that neurons regulate oligodendrocyte adhesion or recognition of axonal versus non-axonal compartments (Lubetzki, Demerens et al. 1993).

What, then, is the role of axons during developmental myelination in the context of a living animal? Nervous systems display immense regional variation and complexity, including many types of neurons, with different myelination requirements – no myelin at all, thin or thicker myelin, early or later myelination, all of which are presumably fine-tuned to optimize neural circuit function (Waxman 1997). It is conceivable that myelinating glia have a default intrinsic program of development, which does not absolutely require axons for its essential stages, but that is plastic and responsive to axonal influence. Individual axons could then locally modulate specific

aspects of oligodendrocyte-lineage development and myelination. For instance, regulating local synthesis of myelin proteins at the tip of the oligodendrocyte process may ensure the correct timing of sheath compaction, or the correct thickness of sheaths: this would ensure optimal functional output for each neuron, and in turn for the whole circuit, and would explain the regional complexity and variation that is observed in vivo.

3.1.3 Which aspects of oligodendrocyte development and myelination can axons influence in vivo?

Which precise aspects of oligodendrocyte development are modulated by axonal contact, axonal activity or axon-secreted signals in vivo, and which are cell-autonomous or at least neuronal-independent? Addressing these questions requires a model where an identifiable subset or the totality of the axonal compartment can be consistently and robustly removed. What is the fate of oligodendrocyte-lineage cells when the axonal influence is removed? Are they generated in the first place? Can they successfully populate the nervous system? Can they progress through their differentiation program? Are they permanently arrested at a particular developmental stage, or is such a latent cell not sustainable for long and does it initiate a self-destruction program? Can axonal signals be compensated for by other cells? Do oligodendrocyte-lineage cells proceed with their differentiation program but adapt to their new environment and become changed? Analysis of all the stages of oligodendrocyte lineage development would address these questions.

3.1.4 The optic nerve as a model to assess axonal influence on glia

The rodent optic nerve provides an excellent model for addressing the issue of axonal influence on developing glial cells:

i) It has a simple composition: the sole neural component are the axons of retinal ganglion cells (RGCs), whose somas reside externally in the retina and project long axons towards the brain, relaying the entirety of visual

information. The only somas found within the optic nerve are those of astrocytes, OPCs and oligodendrocytes.

ii) Most axons become myelinated, and myelination occurs only postnatally, which facilitates experimental manipulation and analysis.

iii) The retina and RGC somas are accessible to pharmacological treatment (via eye injection) and to surgical manipulation: transection behind the retina or eye removal (enucleation) essentially removes the axonal component of the nerve within a few days (enucleation, for instance, causes a quick, drastic degradation of viable axons in the optic nerve within 48h).

iv) Such manipulations can be unilateral, allowing the contralateral nerve to serve as an internal control.

RGC axons develop from embryonic stages in rodents: in rats, at E17, RGCs are already electrically active (Galli and Maffei 1988). The number of axons peaks at birth and then, by developmental apoptosis of a subset of RGCs, decreases until P5 (Sefton and Lam 1984). OPCs migrate from the brain into the optic nerve, in the opposite direction of axon growth, around E17 (Small, Riddle et al. 1987); interestingly, the specification of these OPCs depends on signaling from growing RGC axons in chicken embryos (Gao and Miller 2006). OPCs then proliferate, greatly increasing their numbers and populating the entirety of the nerve by the end of the first postnatal week. From P4 onwards, differentiated oligodendrocytes (expressing myelin transcripts and proteins) are detected, first closer to the brain, and differentiation proceeds towards the retina, replicating the pattern of OPC migration. Surprisingly, however, ensheathment and formation of compact myelin occurs in the opposite direction, starting at the retinal end and proceeding towards the brain (Colello, Devey et al. 1995). This suggests that while differentiation and production of myelin proteins may follow an intrinsic schedule within the OPC, actual myelination may require additional signaling, stronger in the region closer to the eye. Interestingly, RGC axons have a much larger diameter closer to the eye than the brain (Colello, Devey et al. 1995). While the actual molecular mechanism remains to be determined, this further hints at a role of axons in regulating aspects of myelination.

Could it be that earlier aspects of oligodendrocyte development (for example, migration or proliferation of precursors) are autonomously determined, while later aspects such as sheath formation are modulated by axons?

To address this, a number of studies used neonatal or early postnatal enucleation of the retina or transection of the nerve behind the retina to remove the axonal influence on the glial cells of the optic nerve (reviewed in Table 3.1). Interestingly, the influence this has on the development of oligodendrocyte-lineage cells seems to depend crucially on the time of the operation, as I will outline below.

3.1.5 Effect of optic nerve transection on oligodendrocytes depends on stage of development

Prior to myelination

When nerves are operated early on (P0-P2, studies 1-4 in Table 3.1), prior to myelination, the most common finding is that appearance of differentiated oligodendrocyte is impaired – drastically fewer oligodendrocytes develop, and with a delay. No myelin sheaths are detected even at late juvenile stages. These findings suggest that the development of a significant proportion of OPCs or their terminal differentiation into oligodendrocytes requires axons. Given that a few oligodendrocytes do differentiate in the virtual absence of axons in some of these studies (studies 1, 2 and 4); and that OPCs retain some capacity for differentiation in the absence of axons in vitro, as mentioned previously, it seems likely that transecting axons affects development of normal numbers of OPCs (discussed later); rather than solely impede oligodendrocyte differentiation.

At the onset of myelination

Transecting nerves at the onset of oligodendrocyte differentiation allows OPCs time to migrate, proliferate and populate the entire nerve. Transection at P4 (study 5), when some OPCs are about to differentiate and produce myelin proteins, did not

affect the appearance or distribution of the initial MBP+ oligodendrocytes, which might have already entered their final program of differentiation at the time of transection. However, there was a significant, if transient, decrease in MBP+ oligodendrocyte density at P5, accompanied by a transient increase in apoptotic cells; both of these recovered to control levels at P6 and P7 (Ueda, Levine et al. 1999). Additionally, oligodendrocytes in transected nerves form no myelin, appeared more immature and had fewer and shorter processes. Thus, many oligodendrocytes are able to differentiate and produce myelin proteins without axons, as had been predicted before (Colello, Devey et al. 1995). The transient reduction in oligodendrocytes may indicate a role of neurons in providing a survival signal for a subset of OPCs-oligodendrocytes. Axons also seem to regulate later aspects of myelination such as the organization of the processes and the morphology of oligodendrocytes (Ueda, Levine et al. 1999).

An earlier study appears at variance with this. In optic nerves enucleated at P5, by morphological identification of cells, (Valat, Fulcrand et al. 1978) similarly found that the first oligodendrocytes appear without delay, and, by P7, represent 20% of all glial cells in the nerve, as in control animals. However, they then decrease to represent around 5% of glial cells, unlike control nerves, in which half the cells are oligodendrocytes. Enucleation at any developmental stage results in a decrease in the total number of cells (Fulcrand and Privat 1977, Valat, Fulcrand et al. 1978), so this report seems to indicate a much more significant effect of axons on oligodendrocyte development.

However, the two studies shouldn't be compared directly, since (Valat, Fulcrand et al. 1978) presented the oligodendrocyte *proportion* of total cell in transversal sections, while (Ueda, Levine et al. 1999) presented *absolute* numbers of MBP+ oligodendrocytes in longitudinal sections. In fact, up to P7, even (Valat, Fulcrand et al. 1978) reported similar proportions to the control levels; only later were the results different, time points which (Ueda, Levine et al. 1999) did not analyse. Additionally, enucleation is a more severe procedure than transection, even in the hands of the same investigators (Ueda, Levine et al. 1999), so the results may represent real differences in paradigms. Finally, criteria used to identify oligodendroglia in the

earlier were purely morphological (Valat, Fulcrand et al. 1978), compared to the more recent study, which used the more reliable immunocytochemical detection of MBP (Ueda, Levine et al. 1999).

Collectively, these studies strongly suggest a role for axons in promoting survival of a subset of OPCs or oligodendrocytes, and in regulating the morphology of individual oligodendrocytes at the later stages of myelination.

During active myelination

Operating on nerves during active myelination confirmed a role of axons in promoting oligodendrocyte survival. Using immunocytochemical detection with the RIP antibody (which detects a phosphodiesterase, CNP, present in myelin protein (Watanabe, Sakurai et al. 2006)), studies 7 and 8 found that P8-transection resulted in a drastic reduction in oligodendrocytes at P18 compared to control nerves (>95%) and compared to the normal number of oligodendrocytes at the age of transection (90%). This indicates that the survival of already differentiated oligodendrocytes must be compromised. In agreement with this, more pyknotic nuclei than normal were detected at P16 following P12-transection, most of which were RIP+. The more protracted period of apoptosis detected in this study, compared to P4-transected nerves (study 5), may be due to the increased number of oligodendrocytes at this later age of transection. Thus, newly-born oligodendrocytes require axons to promote their survival. Interestingly, P12-transected *Wld*^{S} ('Wallerian degeneration slow') mice, in which axons do not degenerate immediately, exhibited no increased cell death – suggesting that contact with the axonal surface is sufficient to promote survival and that physiological activity is dispensable.

After myelination

In stark contrast, when nerves are transected in late juveniles or adult animals (P20-onwards, studies 9-13), most oligodendrocytes persist for many weeks after transection, although myelin sheaths deteriorate and myelin debris abounds. This indicates that mature oligodendrocytes in the mature optic nerve lose their requirement for axons for survival. These studies will not be considered further as

late enucleations and consequent degeneration of already myelinated axons would obscure careful assessment of the developmental interactions between axons and OPCs.

In sum, although the timing of differentiation seems to be independent of axons, the mature morphology of individual oligodendrocytes may be regulated by axons. Moreover, axons seem to provide a vital survival signal for late OPCs or newly-differentiated oligodendrocytes; they then lose this requirement when they get older. The extent to which axons regulate oligodendrocyte differentiation *per se* remains unclear, since the number of OPCs may be reduced to start with, if their proliferation or survival is also affected. This begs the question as to precisely which aspects of OPC development are altered when the optic nerve is transected.

	Reference	*Age at operation*	*Age at analysis*	*oligodendrocyte ID criteria*	*Outcome in operated nerve (differences from control nerves)*	*Other outcomes (oligodendrocyte-related)*
1	(Ueda, Levine et al. 1999)	P0 (E)	P7	MBP+ cells in longitudinal sections	50% reduction in MBP+ cell density No myelin sheaths	Normal distribution along nerve
2	(David, Miller et al. 1984)	P1 (T)	P15, P60	GalC+ cells in suspensions IHC in cross sections	>20-fold reduction in GalC+ cells in suspensions Likely >8-fold reduction in situ	Few identifiable oligodendrocytes at P60 by EM
3	(Greenwood and Butt 2003)	P1 (E)	P16	CAII+ cells in longitudinal sections MBP+ cells (in situ and in western blot)	No CAII+ cells form Near complete loss of MBP labelling	No MBP reactivity in WB (P8-P15)
4	(Fulcrand and Privat 1977)	P2 (E)	P3-P38	Ultrastructural criteria in cross sections	OLs appear at P10, <5% of all cells (controls: appear P5, 50% of all cells at P20)	
5	(Ueda, Levine et al. 1999)	P4 (T)	P5-P7	MBP+ cells in longitudinal sections	No myelin 50% reduction in MBP+ cell density, normal P6-P7 Increased caspase3+ cells in P5, normal P6-P7	Normal distribution along nerve Immature morphology; shorter and fewer processes
6	(Fulcrand and Privat 1977)	P5 (E)	P6-P42	Ultrastructural criteria in cross sections	OLs appear P6, 20% of all cells at P7, decrease to 5-10% later	
7	(Barres, Jacobson et al. 1993)	P8 (T)	P18	RIP+ cells in cross sections	>90% fewer RIP+ cells than P8 or P18 controls increase in global cell death	Less apoptosis in transected *Wld*^{S} mice CNTF or IGF-1 rescue apoptosis
8	(Fulcrand and Privat 1977)	P8 (E)	P9-P210	Ultrastructural criteria in cross sections	Degeneration of myelin sheaths reduction in %	
9	(Fulcrand and Privat 1977)	P20 (E)	P21-P215	Ultrastructural criteria in cross sections	Degeneration of myelin sheaths reduction in %	
10	(Greenwood and Butt 2003)	P21 (T)	P36	MBP+ and CAII+ cells in longitudinal sections	Same number of CAII+ cells as control; myelin sheaths are lost	
11	(Butt and Kirvell 1996)	P21 (T)	P42	CAII+, MBP+ and MOG+ cells in longitudinal sections	Same number of CAII+ cells as control; MBP and MOG+ myelin sheaths become debris	
12	(Kidd, Hauer et al. 1990)	P21 (T)	P26-P61	CNP+ cells in cross sections	No difference	Decreased MBP and PLP mRNA levels
13	(McPhilemy, Mitchell et al. 1990)	P17, P35 (T)	P31-P63	MBP+ immunohistochemistry PLP mRNA in situ hybridization	No difference in MBP reactivity or PLP+ cell number	Decreased MBP, and PLP mRNA levels
14	(Ludwin 1990)	3-4 mo (E)	25 months	CAII+ cells in cross sections	Loss of myelin but not of oligodendrocytes	

Table 3.1 – Review of studies performing enucleation (E) or transection (T) of the optic nerve.

3.1.6 Does optic nerve transection affect oligodendrocyte precursor cell development?

The effect that removing axons early on has in depleting the oligodendrocyte population could be attributed to decreased migration or proliferation of OPCs, decreased survival of OPCs, decreased differentiation of OPCs into oligodendrocytes, or decreased survival of early born oligodendrocytes. A combination of these is more likely – for instance, a simple defect in OPC migration does not explain the normal distribution of those oligodendrocytes that differentiate when nerves are enucleated at P0 (Ueda, Levine et al. 1999). A defect only in OPC proliferation does not explain the reduced survival of early-born oligodendrocytes following P8 or P12 transection (Barres, Jacobson et al. 1993, Ueda, Levine et al. 1999). If there was only an impairment in differentiation when axons are removed, but development of OPCs was not affected, we might expect an accumulation of OPCs above control levels – however, that is not observed (Ueda, Levine et al. 1999). Several of the studies in Table 1 and additional studies directly addressed the fate of OPCs upon operation by direct labeling of this cell population. Earlier studies based on morphological identification of glial cell types report a decrease in the proportion of 'glioblasts', an umbrella term that designates mitotic immature cells that can differentiate into astrocytes, oligodendrocytes or microglia; these will not be considered. The advent of immunocytochemical methods and clarification of glial lineages allowed reliable identification of oligodendrocyte precursors in the developing optic nerve, and more recent studies take advantage of this.

Migration and proliferation

(Ueda, Levine et al. 1999) showed that neonatal transection does not change the distribution or density of OPCs (which express the neural/glial antigen 2 proteoglican marker, NG2) from P1 to P4. Since their numbers normally increase over this period, OPCs must still have proliferated in the absence of viable axons; and indeed a pulse of BrdU within two days of transection labels the same proportion of OPCs as control nerves of the same age. These OPCs extended fewer and shorter processes in the absence of axons, prefiguring the altered morphology that oligodendrocytes also show in the same paradigm. Enucleation at the same age also did not impede

colonization of the nerve by OPCs. An independent study confirmed that NG2+ glia were still abundant 3 and 15 days after enucleation at P1 or P5 (Greenwood and Butt 2003). Additionally, tritiated thymidine given six days after neonatal transection was incorporated by the same proportion of glial progenitors (as identified by immunoreactivity with the A2B5 antibody marker, and non-reactivity with more mature marker GalC and astrocytic Glial fibrilary acidic protein) as in control nerves.

These studies suggest that OPCs can autonomously migrate and colonize the optic nerve, and further, that live axons or electrical activity are dispensable for OPC proliferation.

However, a conflicting report indicated that P8-transection reduced the number of mitotic figures at P12 to 10% of control nerves (Barres and Raff 1993), but the authors did not determine the identity of the mitotic figures. P8 operation greatly increases microglial proliferation compared to earlier enucleations (Privat, Valat et al. 1981). Since the total number of cells is decreased in operated nerves (Valat, Fulcrand et al. 1978), it is unclear the extent to which the specific proliferation of OPCs was (proportionally) affected. Transection of P12 *Wld*^{S} mice, whose axons do not degenerate for some time, also reduced the number of mitotic figures, suggesting that this effect depends on physiological activity of the axons. In agreement with this, P15 eye-injection of tetrodotoxin, which abrogates action potentials, led to a significant decrease of mitotic figures two days later, although it is unclear, again, whether the total number of cells was changed. The authors assume these must be OPCs, since the decrease was specific in A2B5+ cells that incorporated BrdU one hour before sacrifice (however, A2B5 also labels presumptive astrocytes at this stage, and it is unclear whether they would be affected by ocular injection of the toxin).

In this regard, recent work in P35 juvenile mice has shown that optogenetic stimulation of layer-V neurons in the premotor cortex at physiological rates for 30 minutes was sufficient to induce an acute burst of OPC proliferation in the premotor cortex and subcortical white matter. It is unclear the extent to which the simultaneous proliferation of neural progenitor cells and microglia mediated the effect on OPCs (Gibson, Purger et al. 2014). Another recent report suggested the opposite effect:

sensorimotor deprivation from birth increased NG2 cell proliferation in the barrel cortex at P4-P6, although the effect was subtle (Mangin, Li et al. 2012).

In sum, there is conflicting evidence on whether axons regulate proliferation of OPCs in vivo. It is possible that OPCs proliferate at a basal rate but additionally are responsive to axonal signaling that modulates their proliferative rate; and that the magnitude or direction of their response depends on regional and temporal differences.

Survival

In control, wildtype mammals, many CNS regions exhibit developmental apoptosis of oligodendrocyte-lineage cells, including the optic nerve (Barres, Hart et al. 1992), brain cortex (Trapp, Nishiyama et al. 1997), and spinal cord (De Louw, Van De Berg et al. 2002); which are thought to be newly-generated oligodendrocytes, rather than OPCs. Potentially, competition for neuron-derived neurotrophic factors of these cells is the strategy that matches the amount of target axonal surface to the number of oligodendrocytes (Barres and Raff 1999). In agreement with this, no apoptotic NG2+ cells were detected in either control or P0-transected nerves (Ueda, Levine et al. 1999), suggesting that OPCs, before becoming oligodendrocytes, survive independently of axonal influences. It is only when transection is performed at the onset of myelination or after that there is some detectable apoptosis of oligodendrocytes, as mentioned previously.

One other study addressed the role of RGC axons on early oligodendrocyte-lineage cell development in the optic nerve by increasing their number. (Burne, Staple et al. 1996) investigated myelination in a transgenic mouse line where the promoter sequence of Neuron-Specific Enolase (NSE) drives expression of the human *bcl-2* (B-cell lymphoma 2) gene, which inhibits apoptosis, in several cells, including RGCs. Developmental apoptosis of RGCs was reduced, and the number of axons and the area of optic nerves were essentially doubled. Interestingly, the supernumerary axons were normally myelinated, which was due to increase in oligodendrocyte

number. This seemed caused by increased OPC survival, as well as proliferation. However, oligodendrocyte-lineage cells also spuriously expressed the apoptotic inhibitor transgene, and their increased survival may have been artifactual and unrelated to the increased number of axons. Additionally, doubling RGC number essentially doubled the number of astrocytes in transgenic animals, which are thought to be the source the main OPC mitogen (PDGF) within the optic nerve, rather than RGC axons (Fruttiger, Calver et al. 2000); therefore, the increase in OPC number may have been due to an indirect effect via astrocytes.

In sum, axon-derived signals may influence early OPC proliferation, but seem to have no major effect on migration or survival. As these cells progressively differentiate into oligodendrocytes, axon-derived signals promote their survival, and as discussed earlier, seem to regulate their morphology and the elaboration of processes and myelin sheaths. This would suggest that axon-derived signals are also necessary for the final maturation into oligodendrocytes, but such a direct requirement for differentiation is hard to extricate from the effects on proliferation and survival at this stage.

A number of specific axonal signals have been discussed in Chapter 1 that can be responsible for the effects outlined above. Axonal molecules such as Notch or integrin ligands can play a role in regulating the final differentiation of OPCs into oligodendrocytes (by regulating mbp mRNA translation and the elaboration of myelin sheaths, for instance), a role that the optic nerve studies suggested. The analysis and manipulation of specific neuronal molecules, especially using conditional neuron-specific genetic ablation paradigms, provided definitive evidence for the fundamental principle that neuronal and axonal signals can regulate oligodendrocyte development and myelin formation to a certain extent.

3.1.7 Shortcomings of axonal transection studies in the optic nerve

Although the enucleation and transection paradigms in the optic nerve have shed light on the complex axonal regulation of oligodendrocyte development, they have a

number of shortcomings. These are fairly invasive procedures with consequences that may confound interpretation of the effects observed during OPC and oligodendrocyte development. For instance:

a) byproducts of the degeneration of transected axons may actively influence behaviour of glial cell populations;
b) enucleation or transection at any age causes a significant decrease in cross-sectional area of the optic nerve (Valat, Fulcrand et al. 1978, Trimmer and Wunderlich 1990); this shrinkage could, for instance, impede OPC proliferation purely due to physical constraints. In fact, in vitro, OPC density and their spatial constraints can regulate differentiation into oligodendrocytes (Rosenberg, Kelland et al. 2008).
c) whereas normally blood vessel irrigation decreases with postnatal development, in transected nerves vessels are much increased proportionally in the glial scar formed (Trimmer and Wunderlich 1990), and it has recently been shown that signaling from blood vessels can affect oligodendrocyte development (Yuen, Silbereis et al. 2014).
d) even when performed early on, these operations cause changes not just in the number but also in the activation state of astrocytes, macrophages and microglia (Fulcrand and Privat 1977); and different functional phenotypes of microglia have been shown to differentially modulate OPC differentiation in vitro, and following remyelination in vivo (Miron, Boyd et al. 2013).
e) neonatal transection of the optic nerve seems to cause a small transient degeneration of a subset of axons in the contralateral nerve, at least in albino rats. P4 and P5 contralateral nerves after neonatal transection are fine, and myelination is 1 day delayed (Sefton and Lam 1984). Another report indicates that following P21-transection, the intact contralateral nerve shows significantly increased myelin structural protein transcripts 10 days post-operation (Kidd, Hauer et al. 1990).

One additional shortcoming relates to the generalization of lessons learnt from optic nerve oligodendrocytes: these oligodendrocytes may have specific properties not shared by other oligodendrocytes. For instance, purified optic nerve oligodendrocytes

proliferate in response to the neurotrophin NT-3 in vitro but spinal cord oligodendrocytes do not (Miller 2002). Xenopus optic nerve oligodendrocytes are permissive for neurite growth, but spinal cord oligodendrocytes are not (Lang, Rubin et al. 1995), highlighting the possibly different biochemical composition of their myelin. Additionally, in the optic nerve, oligodendrocytes face the task of myelinating a relatively homogenous array of axons (over 90% become myelinated), which may not directly translate to the analysis of oligodendrocyte behaviour in areas such as the brain or spinal cord, where they have to face more complex axonal environments.

3.1.8 Another model to look at axonal regulation of myelination in vivo

Zebrafish larvae have recently emerged as an ideal model to study myelination in vivo (Monk and Talbot 2009, Czopka and Lyons 2011): they are amenable to live imaging at single cell resolution of axons, OPCs and oligodendrocytes; myelination starts soon after fertilization (approximately 3 days), which allows following the same individual neuron from its undifferentiated state to its fully myelinated state with compact myelin; and a number of transgenic and genetic tools exist that allow us not only to visualize but also manipulate myelination, or the neuronal/axonal compartment (Almeida, Czopka et al. 2011, Czopka, Ffrench-Constant et al. 2013). Given the short time frame in which developmental myelination occurs, we can probe through time lapse imaging the real-time behaviour and dynamics of neurons and glia, and directly investigate aspects such as migration, proliferation and apoptosis *in vivo* without recourse to more indirect measures (such as the thymidine-analogue incorporation for proliferation rate measurements, for instance).

Like the optic nerve, zebrafish offer one additional crucial advantage – the manipulation of unambiguously identifiable subsets of axons fated for myelination, such as the axons belonging to reticulospinal neurons. The possibility, described below, of consistent and robust removal of a substantial number of reticulospinal axons from the spinal cord allows us to re-examine the effect of axons on myelination, in a context that circumvents many of the shortcomings of the optic nerve system, as I will outline now.

In the zebrafish CNS, reticulospinal neurons are a set of dozens of identifiable interneurons, most of which reside in the hindbrain and project a large-diameter axon along the length of the spinal cord, in one of three major spinal tracts, including the medial longitudinal fasciculus (mlf), which runs along the ventral spinal cord (Kimmel, Powell et al. 1982). Of note, one pair of such reticulospinal neurons, the Mauthner neurons, are among the earliest born in the zebrafish, around 10 hpf (Mendelson 1986). Their somas reside in the fourth rhombomere, one on each side of the midline, and each neuron projects a very large-diameter axon contralaterally (Mendelson 1986, Metcalfe, Mendelson et al. 1986). The Mauthner axons are the largest in the whole animal; due to their stereotyped position and caliber, several fold larger than the next largest axon, they are unambiguously identifiable in the zebrafish spinal cord (Bernhardt, Chitnis et al. 1990). Reticulospinal neurons are responsible for activating locomotor responses - the Mauthner axon, for instance, synapses directly with motor neurons (Celio, Gray et al. 1979, Fetcho and Faber 1988, Jontes, Buchanan et al. 2000).

Crucially, using a fluorescent transgenic reporter for myelin, mbp:EGFP-CAAX, we have previously demonstrated that reticulospinal axons are the first to be myelinated in the zebrafish spinal cord, in an anterior to posterior gradient. The very first myelin sheath detected in every animal is always on one of the two Mauthner axons, around 55 hpf (Almeida, Czopka et al. 2011).

If the outgrowth of such axons could be specifically manipulated, either negatively or positively, the role of axons on myelination could be formally assessed in vivo, in a non-invasive manner.

A number of zebrafish mutants have been identified where the normal development of a subset of neurons is affected – such is the case of the zebrafish mutant for *kif1-binding protein* (*kbp*). The function of the KBP protein remains largely unknown. In humans, homozygous mutations in the *KIAA1279/KBP* gene cause Goldberg–Shprintzen syndrome, a rare condition characterized by polymicrogyria, microcephaly, mental retardation, as well as defects to the enteric nervous system (Brooks, Bertoli-Avella et al. 2005). The KBP protein contains two tetratricopeptide repeats, which mediate protein-protein interactions (Blatch and Lassle 1999). In

vitro, KBP binds to the motor domain of Kinesin motor proteins, most notably Kif1 (Wozniak, Melzer et al. 2005), and interacts with a range of proteins implicated in microtubule transport and dynamics, such as the Stathmin family of proteins (Alves, Burzynski et al. 2010). More recently, it has also been shown to interact with filamentous actin (Drevillon, Megarbane et al. 2013). Interestingly, in a neuroblastoma-cell line, KBP knockdown reduced the length of dendritic spines as well as neurite length, whereas overexpression of KBP increased both (Drevillon, Megarbane et al. 2013), suggesting that a role of KBP in neuronal development may underlie the defects observed in Goldberg–Shprintzen patients.

In fact, in zebrafish where the *kbp* gene contains a splice-disrupting mutation, some neurons show destabilized and disorganized microtubules along their axons, as well as mislocalized mitochondria. These axons grow at reduced speeds, and many degenerate (Lyons, Naylor et al. 2008). This culminates in an axon outgrowth defect that does not affect all neurons similarly in the global *kbp* knockout mutant: in the CNS, reticulospinal axons are most affected and fail to extend along the entire spinal cord. In transversal electron micrographs, the number of large-diameter axons in the ventral spinal cord, mostly reticulospinal axons, is greatly reduced, but other tracts in the spinal cord, such as the dorsal tract, seem relatively unaffected by the loss of *kbp*, and the distribution and number of neuronal cell bodies is also unaffected (Lyons, Naylor et al. 2008*)*. As no single-cell resolution expression studies are available, it remains unclear whether the specificity of this phenotype in a global knockout reflects variegated expression from the *kbp* gene, which could normally be absent from other subpopulations of neurons. Alternatively, it could reflect a differential requirement of this protein in neurons containing very long axons, such as the reticulospinal neurons (however, other tracts containing very long axons seem unaffected, such as the dorsal tract). Since wildtype reticulospinal neurons transplanted into *kbp* mutants grow their axons normally, the role of *kbp* in promoting and maintaining axon outgrowth is neuron-autonomous, and is not due to the influence of other cell types.

Thus, this mutant provides us with a posterior region of the spinal cord (roughly a third to a half of its length) where the majority of the axons that are the first targets

for myelination are absent. In spite of a localized degeneration within one or two somites of *kbp* mutant axon growth cones, for the remainder of the spinal cord, reticulospinal axons simply never grow into this region. This is in contrast to the optic nerve transection studies where axons were potentially in contact with OPCs before subsequently degenerating, possibly triggering confounding effects. Additionally, this axon outgrowth failure allows study of even earlier events of OPC development, which are not so easy to address in the optic nerve, as such events occur prenatally. I will be able to examine whether reticulospinal axons are required for OPC specification. If OPCs are generated, they will exist in a drastically altered axonal environment, in the virtual absence of their first target axons, for the remainder of their development. Moreover, both the general morphology and the spinal cord structure of *kbp* mutants are similar to wildtype larvae, so there are no confounding effects of a drastic reduction in size. Finally, the initial period of axonogenesis occurs normally in *kbp* mutants; and the more rostral region of the spinal cord does contain reticulospinal axons. This should provide, in the same animal, an anterior region that could serve as an internal control for any effect observed in the region where axons are absent. This is especially important since this is a global *kbp* knockout mutant.

Therefore, once characterized in more detail, this system should allow me not only to determine the influence that growing axons have on oligodendrocyte-lineage development in zebrafish, but additionally will do so in a manner that overcomes many of the shortcomings of the previous paradigms using optic nerve operation.

3.2 **Aims**

My aim is to determine whether the axonal targets for myelination can regulate early aspects of oligodendrocyte development and myelination. I address this in the zebrafish spinal cord, by chronologically analysing oligodendrocyte-lineage cell progression into myelination in larvae which lack reticulospinal axons, the very first axons that become myelinated.

Specifically, I aim to further characterize the axonal outgrowth phenotype of *kbp* mutants, which should provide both a region where an identifiable subset of axons is absent, and an internal control region with a normal complement of axons. This should overcome many shortcomings of the optic nerve model, as mentioned above. Since reticulospinal axons are the first major initial targets for myelination, I expect that their absence represents a drastic alteration in the axonal environment. In this chapter, I will investigate whether specification, migration, proliferation, and survival of oligodendrocyte-lineage cells are affected. In the next chapter, I will address how later aspects of the development of oligodendrocyte-lineage cells, such as the timing of oligodendrocyte differentiation and the formation of myelin sheaths, could be regulated by reticulospinal axons.

3.3 Results

3.3.1 Reticulospinal axon outgrowth is specifically disrupted in *kbp*^{st23} mutant zebrafish

I sought to better characterize the timing of the axonal outgrowth defect in *kbp* mutants along the anterior-posterior axis of the spinal cord. The onset of myelination occurs in an anterior to posterior gradient in the spinal cord, having reached the posterior end of the spinal cord by 4dpf. I performed whole-mount immunohistochemistry on larvae with 3A10 antibody, which recognizes a neurofilament-associated epitope and labels most large-caliber, neurofilament-bearing axons, from 36 hpf until 4 dpf. In the majority of WT larvae at 36 hpf, and in their entirety at 48hpf (Figure 3.1 B), growing reticulospinal axons (most prominently, the Mauthner axons) have reached the caudal end of the spinal cord. In the same posterior region (about somites 20-24), in the *kbp* mutant, reticulospinal axons failed to do so, and are clearly absent from the ventral spinal cord (Figure 3.1 B). Other axons, including dorsal axons, those of Rohon-Beard neurons, medial axons and motor axons all remain present in the mutant in this region. In contrast, in an anterior region of the spinal cord (about somites 9-13), all axonal tracts are similar between wildtype and mutant (Figure 3.1 B), including the ventral tract where reticulospinal axons grow. This specific absence of reticulospinal axons in the posterior region of the *kbp* mutant spinal cord persisted at least through to 4dpf, when myelination is underway (Figure 3.1 C).

I confirmed these results in electron micrographs of transversal sections of the posterior spinal cord of 3 dpf larvae. At this stage, neuron somas occupy the central region of the spinal cord (grey matter), and lateral regions contain clusters of longitudinal axons (white matter), which will later form tracts such as the mlf in the ventral region (Figure 3.2 A). Similar numbers of large-diameter axons (with a diameter larger than 0.5 μm) are present in the dorsal region of the white matter of both WT and mutant spinal cords, but fewer large-diameter axons are present in the ventral region of mutant larvae (Figure 3.2 B-C). The perimeter of these cross-sectional axonal profiles reflects the axonal surface available for potential

interactions with oligodendrocyte-lineage cells. The combined perimeter of all large-diameter axons is specifically reduced in the ventral spinal cord: 34±16 μm/half-spinal cord in WT vs 7±4 μm in mutants (100 axons from N=5 WT larvae; 30 axons from N=5 mutants; p=0.0074 in t-test). In the dorsal spinal cord, the total perimeter is similar between WT and mutant animals: 31±7 μm in WT vs 26±5 μm in mutants (109 axons from N=5 WT larvae; 103 axons from N=5 mutants; p=0.2740 in t-test)

Thus, within the same mutant animal, the anterior region contains an apparently normal complement of axons, serving as an internal control for analysis of the posterior region, where the initial target axons for myelination are absent from an early age. In this region, the total axonal surface is greatly decreased (to ~ 20%) in the ventral spinal cord.

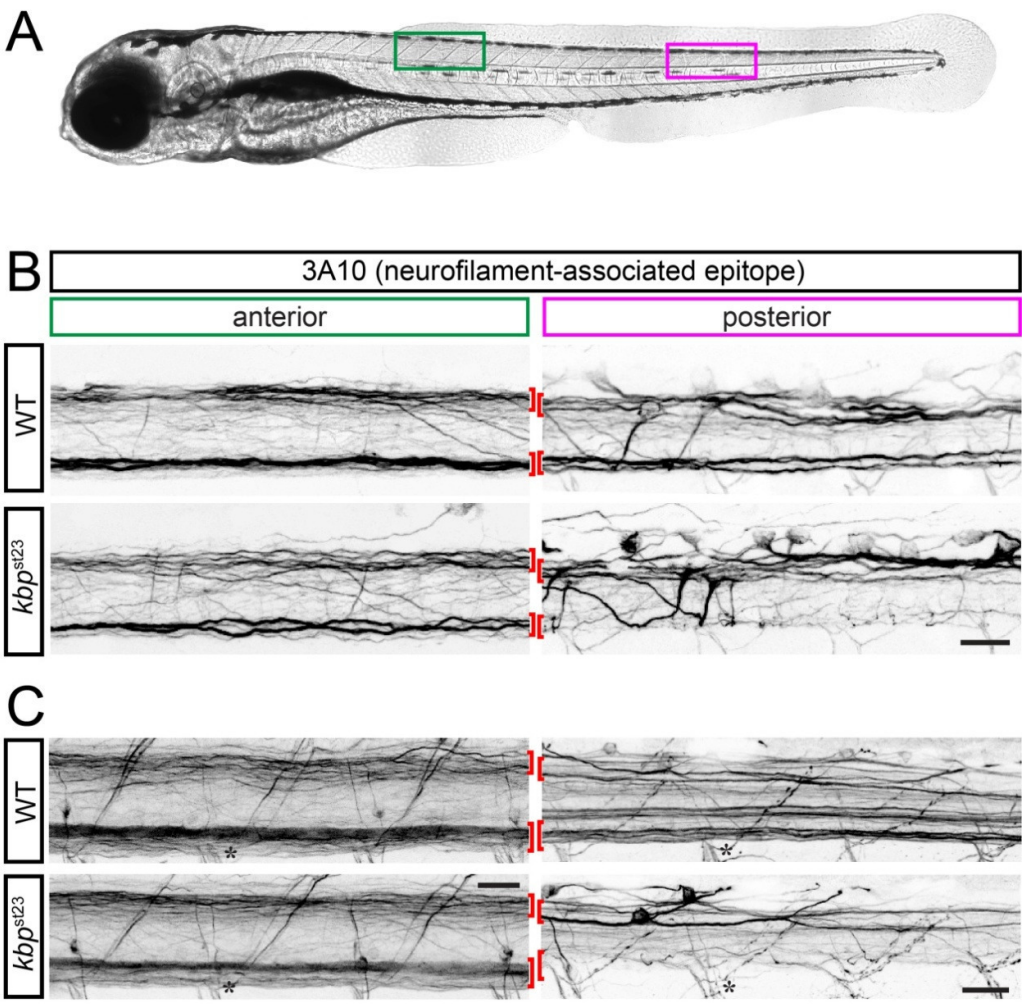

Figure 3.1 – *kbp*^{st23} mutants specifically lack the first axonal targets for myelination, only in the posterior spinal cord.

(**A**) Lateral view of a 4 days post fertilization (dpf) zebrafish larvae. Green and magenta boxes indicate anterior and posterior regions, respectively. In all figures, anterior is left and posterior is right; dorsal is up and ventral is down.
(**B**) Lateral views of 48 hpf larvae immunostained with 3A10 antibody. In *kbp*^{st23} mutant larvae (bottom), the ventral axonal tract (mostly reticulospinal axons) is absent in the posterior region. Brackets indicate dorsal and ventral tracts. Scalebar: 25 µm.
(**C**) Lateral views of 4dpf larvae immunostained with 3A10 antibody. Brackets indicate dorsal and ventral tracts; asterisks point to examples of ventral roots, where motor axons exit the spinal cord in each somite. Scalebar: 25 µm.
Brightfield image in (A) kindly provided by Jason Early.

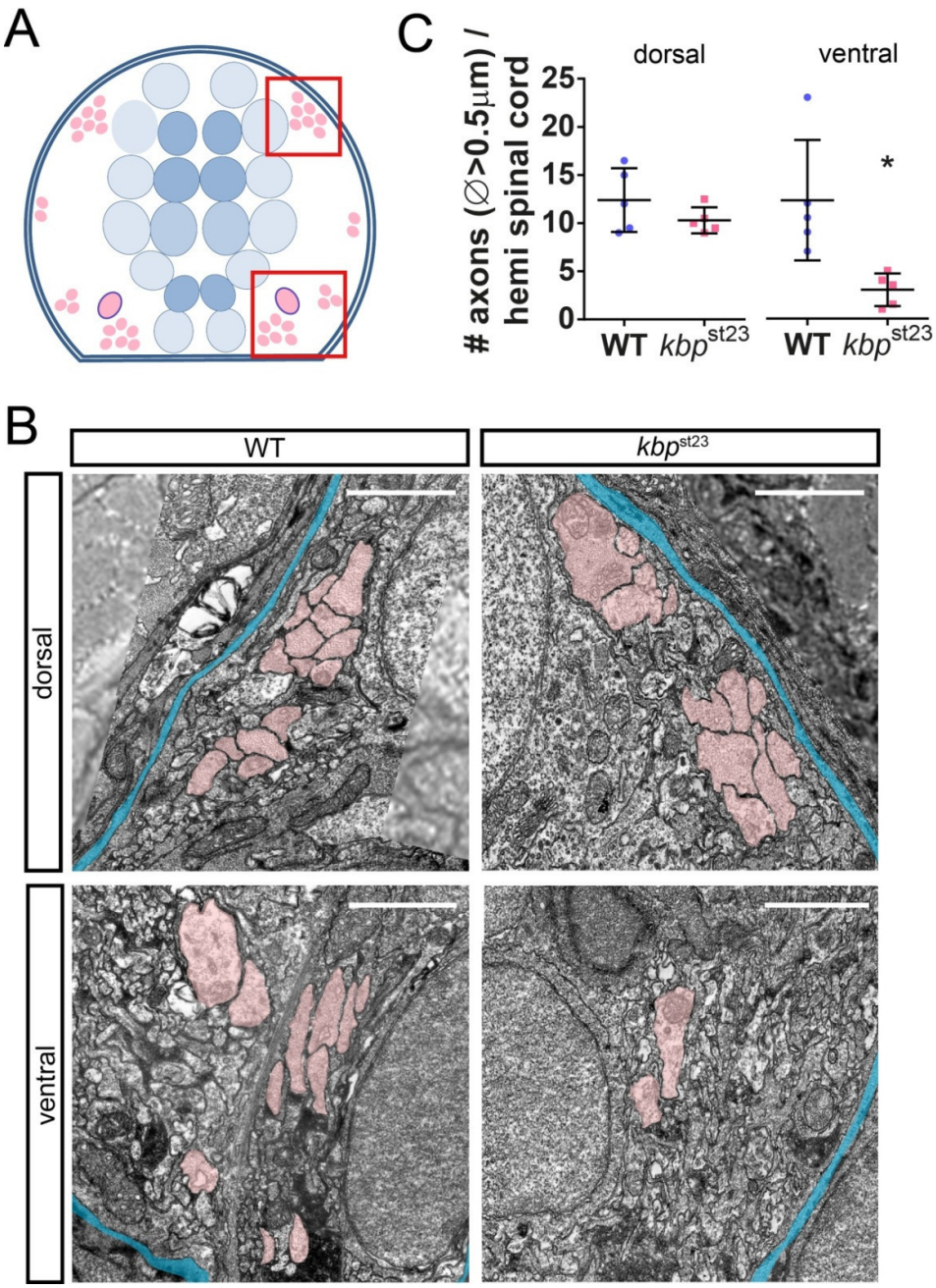

Figure 3.2 – *kbp*^{st23} mutants lack the first myelinated axons in the posterior spinal cord.

(**A**) Diagram of the zebrafish spinal cord. Neuron somas occupy the centre (blue circles), flanked by clusters of longitudinal axons (pink circles). Double blue line is the pia mater, which delimits the spinal cord. Boxes indicate regions captured in (B). (**B**) Representative dorsal and ventral regions showing longitudinal axons (pink); pia mater is shaded in blue. Scalebar: 2 µm. (**C**) Average number (±standard deviation) of large-diameter (>0.5 µm) axons in the posterior spinal cord.

Dorsal: 12±3 (N=5 WT) vs 10±1 axons (N=5 mutants), p=0.5159 in Mann-Whitney test

Ventral: 12±6 (N=5 WT) vs 3±2 axons (N=5 mutants), p=0.0079 in Mann-Whitney test

3.3.2 Reticulospinal myelin sheaths are specifically absent in the posterior spinal cord of mutants

I then examined myelin sheaths in *kbp*^{st23} mutants by live-imaging of a Tg(mbp:EGFP-CAAX) reporter, where membrane-tethered GFP is expressed in myelinating oligodendrocytes (Almeida, Czopka et al. 2011). At 4 dpf the onset of myelination has reached the posterior region of the spinal cord. In WTs, the reticulospinal axons possess myelin sheaths easily identifiable in the ventral tract of the spinal cord (Figure 3.3 A, brackets); and some medial, dorsal and motor myelin sheaths have also formed. In the mutant, I observed a drastic reduction of ventral myelin sheaths ensheathing reticulospinal axons, but other medial, motor and dorsal sheaths formed normally. No obvious difference in myelination was evident in the anterior region between WT and mutants (Figure 3.3 A). Thus, the pattern of myelination is partially disrupted, and specifically so in the region corresponding to the absence of reticulospinal axonal targets.

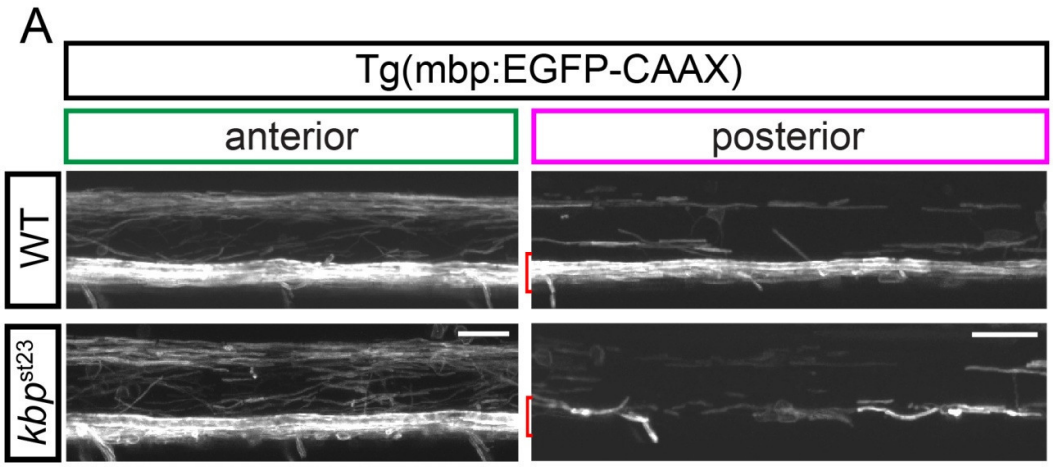

Figure 3.3 – *kbp*^{st23} mutants specifically lack reticulospinal myelin sheaths, only in the posterior spinal cord.

(**A**) Lateral view of live Tg(mbp:EGFP-CAAX) larvae at 4dpf. Myelin sheaths in the anterior region (left) are identical in WT and mutant larvae. In the posterior region (right), reticulospinal myelin sheaths are specifically absent in the ventral spinal cord (brackets). Myelin in the dorsal, medial and ventral (non-reticulospinal) tracts of the spinal cord, and on motor axons forms normally. Scalebar: 25 µm.

3.3.3 Absence of RS axons correlates with reduced number of ventral oligodendrocytes

I wondered whether this disruption in myelination represented a reduction in the myelinating capacity of oligodendrocytes, or simply a reduction in the number of oligodendrocytes. To address this, I imaged the transgenic line mbp:EGFP, in which cytoplasmic GFP expressed in mature oligodendrocytes labels their somas (Figure 3.4A), enabling counting and analysis of their dorsal-ventral distribution (Figure 3.4B). At 4 dpf, in the anterior spinal cord, where reticulospinal axons are present, there is no difference in the total number of mbp:EGFP+ oligodendrocytes, or in the ventral subset. In the posterior region, where reticulospinal axons are absent, the total number of oligodendrocytes is significantly reduced (30±6 oligodendrocytes in WT vs 22±5 in mutants, $p=0.0004$ in t-test). The reduction is especially significant in the subset of ventral oligodendrocytes (grey bars in Figure 3.4B, 21±4 oligodendrocytes in WT vs 16±3 in mutants, $p<0.0001$ in Mann-Whitney test).

In an independent experiment, I imaged the double transgenic line mbp:EGFP; mbp:EGFP-CAAX in a slightly more caudal region of the spinal cord. The reduction in oligodendrocyte number in the posterior spinal cord was confirmed: 22±4 oligodendrocytes in WT vs 11±4 in mutants (N=10 WT, 11 mutants; $p<0.0001$ in t-test); whereas the number of anterior oligodendrocytes remained similar between WT and mutant (49±4 oligodendrocytes in WT vs 48±4 in mutants, N=11 for both, $p=0.54$ in t-test). Additionally, at 8 dpf, the number of ventral oligodendrocytes remains significantly reduced in the posterior spinal cord of mutants: 26±5 oligodendrocytes in WT vs 14±2 in mutants (N=10 WT, 11 mutants; $p<0.0001$ in t-test). At the caudal end of the spinal cord, the presence of oligodendrocytes along the anterior-posterior axis terminates earlier in mutants compared to WTs (Figure 3.4C, note arrowheads). This second experiment may have overestimated the decrease in oligodendrocyte density in mutants by including this more caudal region that is devoid of oligodendrocytes.

The oligodendrocyte number phenotype in the posterior spinal cord was somewhat variable between individual mutant larvae. Such variability may exist in the

underlying axonal phenotype, which may reflect the nature of the *kbp*^{st23} genetic lesion. Rather than a complete loss of function, *kbp*^{st23} disrupts a splice donor site which generates a number of spurious transcripts that coexist in mutant cells – at least one of which is described to encode an in frame insertion that retains wildtype *kbp* function (Lyons, Naylor et al. 2008). The severity of the loss of *kbp* function may vary according to relative level of transcripts at any time in each neuron. While my analysis indicated a consistent and drastic axonal phenotype in reticulospinal neurons, there may be subtler and variable outgrowth defects in other axons of the spinal cord (including the anterior region) that escaped my analysis. It would require an exhaustive cataloguing of all neuronal subtypes to completely elucidate the extent and variability of the *kbp* (axonal) phenotype.

However, in the absence of ventral reticulospinal axons, there is consistently a correlating reduction in the number of mature ventral oligodendrocytes. This reduction strongly suggests a disruption in the developmental progression of oligodendrocyte-lineage cells – potentially affecting only those oligodendrocytes that normally myelinate reticulospinal axons. I therefore proceeded to investigate which aspect of oligodendrocyte development was affected in the absence of axonal targets.

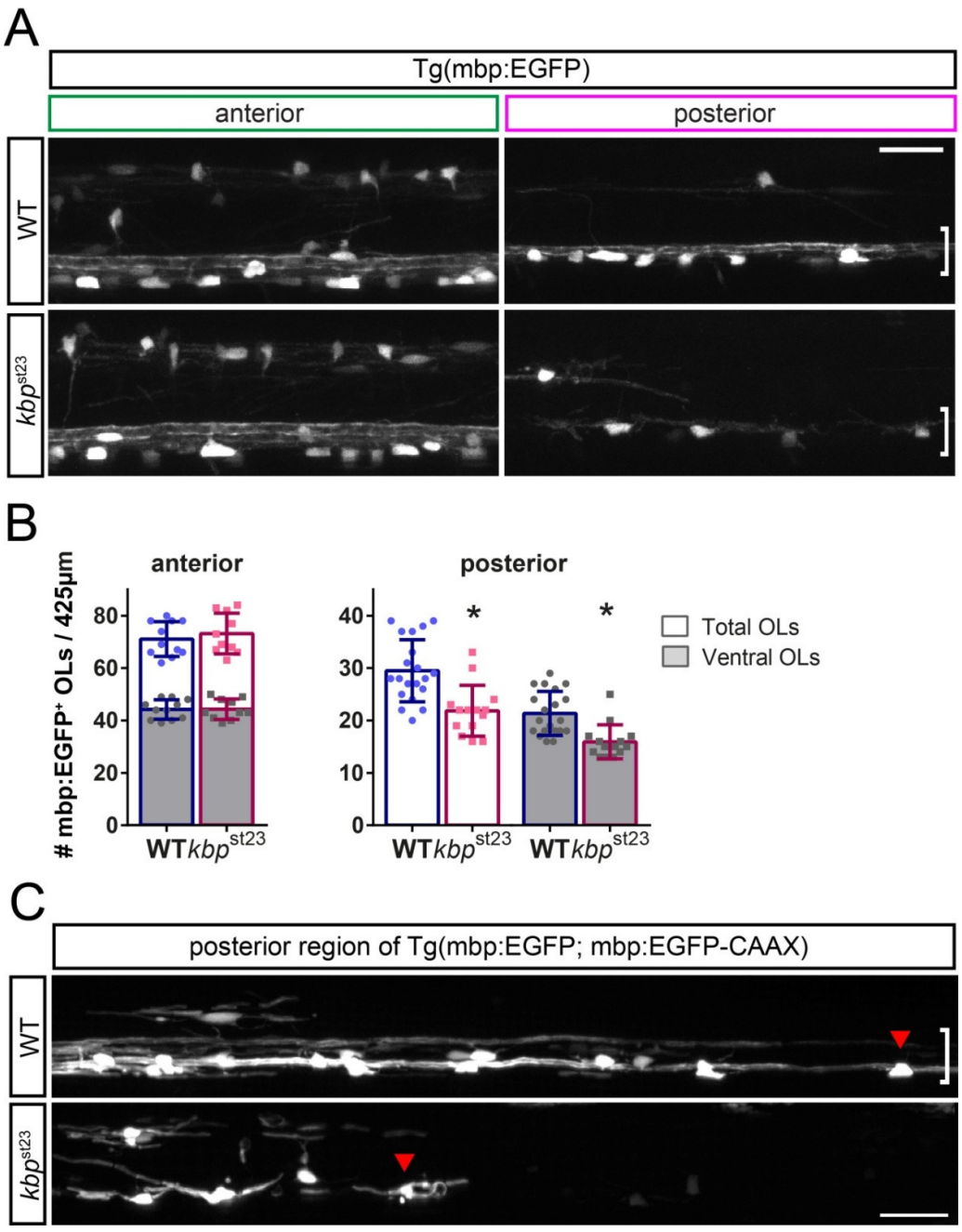
A
Tg(mbp:EGFP)
anterior
posterior
WT
kbp^st23
B
anterior
posterior
mbp:EGFP+ OLs / 425µm
80
60
40
20
0
40
30
20
10
0
*
*
WTkbp^st23
WTkbp^st23
WTkbp^st23
Total OLs
Ventral OLs
C
posterior region of Tg(mbp:EGFP; mbp:EGFP-CAAX)
WT
kbp^st23

Figure 3.4 – *kbp*^{st23} mutants have a reduced number of mature oligodendrocytes in the posterior spinal cord

(**A**) Lateral views of the spinal cord of 4dpf Tg(mbp:EGFP) larvae. oligodendrocyte somas are visible in the spinal cord; some ventral oligodendrocytes associate with the Mauthner myelin sheaths (brackets), except in the posterior region of mutants, which also has fewer oligodendrocytes. Scalebar: 25 µm.

(**B**) Quantification of mbp:EGFP+ cell number per 425 µm length of tissue (~5 somites), in 4dpf larvae. Grey bars (ventral subset of oligodendrocytes) in posterior region are displayed to the side for ease of visualization. Error bars represent standard deviation.

Anterior:

Total oligodendrocytes: 71±7 (N=11 WT) vs 73±8 oligodendrocytes (N=10 mutants), p=0.5097 in t-test

Ventral oligodendrocytes: 44±4 (N=11 WT) vs 44±4 oligodendrocytes (N=10 mutants), p=0.9443 in t-test

Posterior:

Total oligodendrocytes: 30±6 (N=20 WT) vs 22±5 oligodendrocytes (N=14 mutants), p=0.0004 in t-test

Ventral: 21±4 (N=20 WT) vs 16±3 oligodendrocytes (N=14 mutants), p<0.0001 in Mann-Whitney test

(**C**) Lateral views of a more posterior region of the spinal cord of 4dpf Tg(mbp:EGFP; mbp:EGFP-CAAX) larvae. Brackets indicate the ventral tract where the Mauthner axons are located. Mutants have fewer oligodendrocytes in the same region, and oligodendrocytes terminate earlier (arrowheads). Scalebar: 25 µm.

3.3.4 Absence of reticulospinal axons does not affect the balance of motor neuron – OPC production from the pMN domain

Oligodendrocyte-lineage cells arise from the pMN domain, a population of proliferative Olig2+ precursor cells that initially generates motor neurons (until ~55hpf) and later switches to production of OPCs. A recent study showed that dopamine release from the axons of non-reticulospinal, diencephalic projection neurons can promote the proliferation of pMN precursors and generation of motor neurons from the pMN domain (Reimer, Norris et al. 2013). This study sets a precedent for projection neurons from the brain and their axons regulating spinal cord neurogenesis. Therefore, I wondered if the absence of reticulospinal axons could alter the balance of motor neuron and OPC production from the pMN domain.

I first investigated the number of mitotic olig2+ pMN precursors immunoreactive for phosphorylated histone 3 (PH3). At 36hpf (when reticulospinal axons have just extended along the entire spinal cord in most WT larvae), and later at 48-50hpf, I found a similar number of olig2:GFP+ PH3+ cells in both the anterior and posterior regions of WT and mutant larvae (Figure 3.5). Furthermore, the number of total PH3+ mitotic cells in the spinal cord also did not reach statistically significant differences at either time point.

I then investigated the number of HB9+ motor neurons produced in the absence of reticulospinal axons. At 48 hpf, when most motor neurons have been born, there was no difference in the number of HB9+ motor neurons between WT and mutant larvae in either the anterior or posterior spinal cords (Figure 3.6)

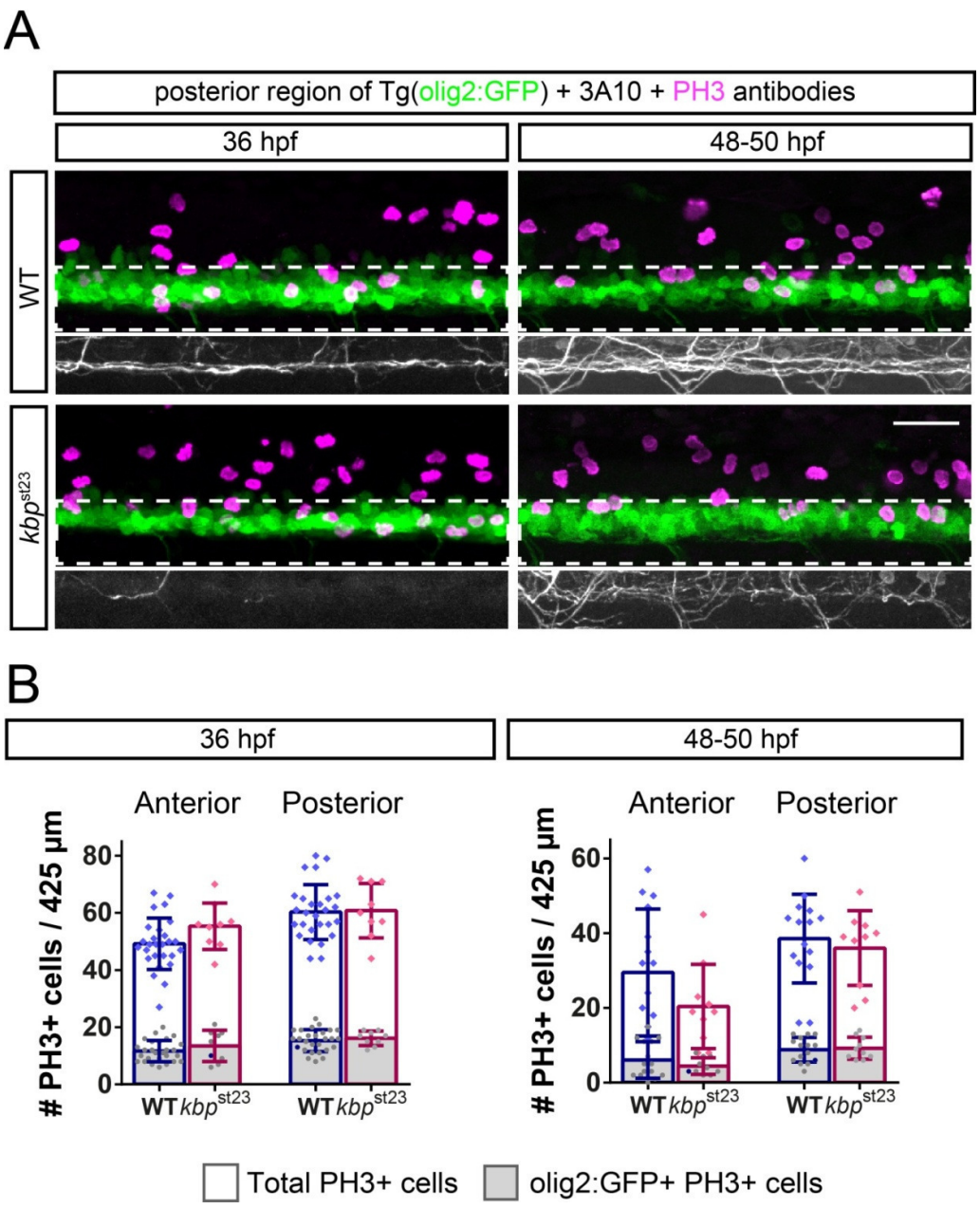
A
posterior region of Tg(olig2:GFP) + 3A10 + PH3 antibodies
36 hpf
48-50 hpf
WT
kbp^st23
B
36 hpf
48-50 hpf
Anterior
Posterior
PH3+ cells / 425 µm
0
20
40
60
80
WT
kbp^st23
Total PH3+ cells
olig2:GFP+ PH3+ cells

Figure 3.5 – Mitotic pMN precursor number is not altered in *kbp*^{st23} mutants.

(**A**) Lateral view of the posterior region of 36hpf and 48-50 hpf Tg(olig2:GFP) larvae immunostained for anti-GFP (green), 3A10 (grey, inset) and PH3 (magenta), a marker of mitosis. The dotted box indicates the region displayed under each panel, in the 3A10 channel. Note the absence of ventral Mauthner axons already at 36hpf. Panels denote the same individual larvae at the anterior and posterior region. Scalebar: 25 μm.
(**B**) Quantification of total PH3+ and olig2:GFP+ PH3+ subset of cells per 425 μm length of tissue (~5 somites). Error bars represent standard deviation.

36 hpf, Anterior:
Total PH3+ cells: 49±9 (N=27 WT) vs 55±8 cells (N=9 mutant), p=0.0786 in t-test
GFP+ PH3+ cells: 12±4 (N=27 WT) vs 13±6 cells in (N=9 mutant), p=0.2698 in t-test

36 hpf, Posterior:
Total PH3+ cells: 60±10 (N=27 WT) vs 61±10 cells (N=9 mutant), p=0.8968 in t-test
GFP+ PH3+ cells: 15±4 (N=27 WT) vs 16±3 cells in (N=9 mutant), p=0.5603 in t-test

48-50 hpf, Anterior:
Total PH3+ cells: 29±17 (N=15 WT) vs 20±11 cells (N=10 mutant), p=0.1528 in t-test
GFP+ PH3+ cells: 6±5 (N=27 WT) vs 4±2 cells in (N=9 mutant), p=0.3240 in t-test

48-50hpf, Posterior:
Total PH3+ cells: 39±12 (N=15 WT) vs 36±10 cells (N=10 mutant), p=0.5839 in t-test
GFP+ PH3+ cells: 9±3 (N=15 WT) vs 9±3 cells in (N=10 mutant), p=0.7605 in t-test

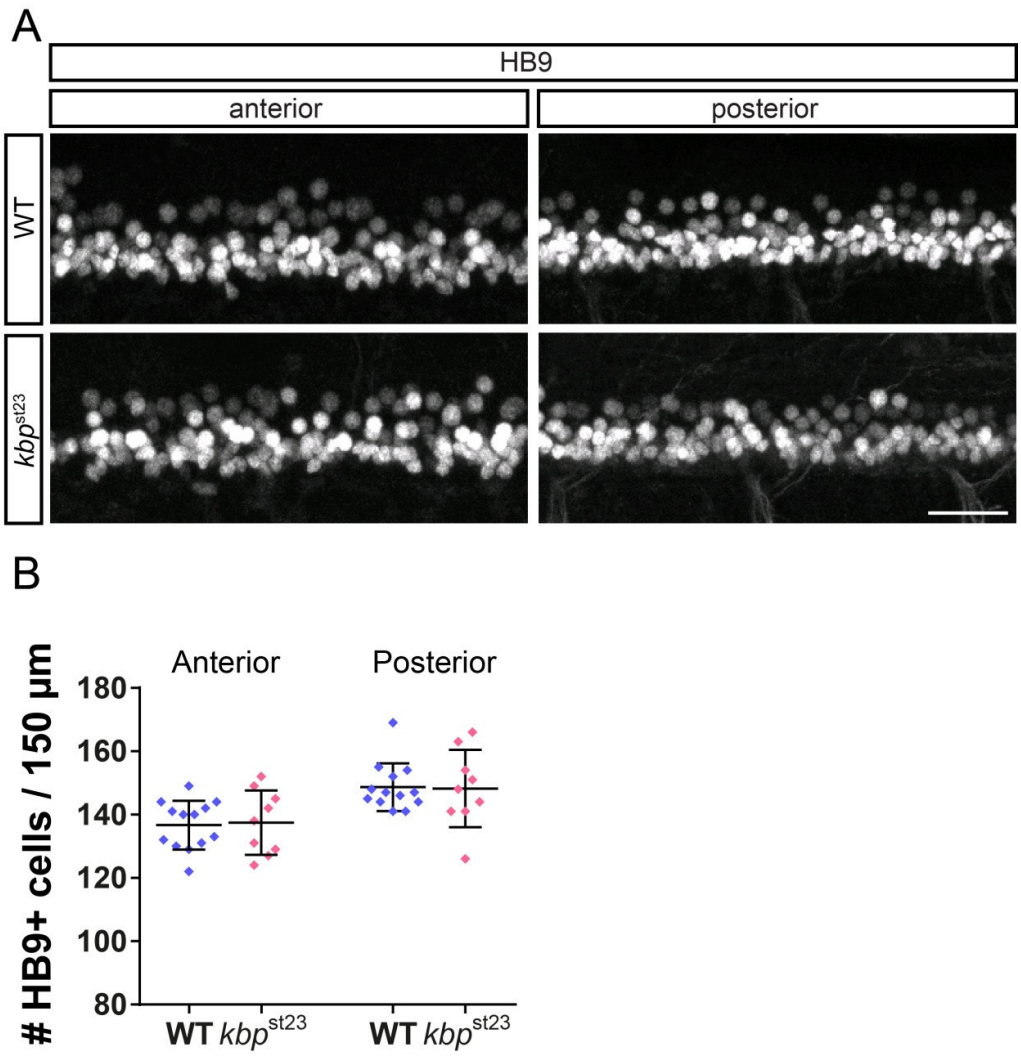

Figure 3.6 – Number of mature motor neurons is not altered in *kbp*^{st23} mutants.

(**A**) Lateral view of 48 hpf larvae immunostained for HB9, a marker of post-mitotic motor neurons. Scalebar: 25 µm.

(**B**) Quantification of HB9+ cells per 150 µm length of tissue (2 somites). Error bars are standard deviation.

Anterior: 137±8 (N=13 WT) vs 137±10 cells (N=9 mutants), p=0.8454 in t-test;

Posterior: 149±8 (N=13 WT) vs 148±12 cells (N=9 mutants), p=0.9341 in Mann-Whitney test.

Finally, to investigate the specification of OPCs, I imaged the double transgenic line olig2:GFP; sox10:mRFP at 48hpf. Either transgene alone labels several subpopulations of cell types in the spinal cord: olig2 is expressed by pMN precursors, motor neurons and oligodendrocyte-lineage cells, and sox10 is expressed by oligodendrocyte-lineage cells and also a population of dorsal olig2$^-$ neurons. However, the combination of both transgenes specifically marks only oligodendrocyte-lineage cells in the spinal cord (Figure 3.7A).

The number of initial OPCs at 48hpf, although variable, is not significantly different between WT and mutant larvae in either the anterior or posterior spinal cord (Figure 3.7B). At 60 hpf, more OPCs have been specified, and a subset of OPCs starts to migrate dorsally in the posterior spinal cord (Figure 3.7A, right, dorsal arrowheads). The number of OPCs also did not reach a statistically significant difference, although a non-significant trend towards a decrease in OPCs in mutant animals was observed. Note that the variability of total OPC number at this time point is large, which severely reduced the power of this particular analysis (about 50% power to detect the difference between observed means). As discussed earlier, this variability may reflect the nature of the *kbp* genetic lesion. It would require a very large number of animals to make it a highly powered analysis to observe that difference (for instance, about 40 animals per group to reach 80% power).

Thus, I cannot exclude the possibility that the absence of reticulospinal axons affects the number of oligodendrocyte-lineage cells soon after their generation; but the appearance of the very first OPCs does not seem to be affected. Therefore, the reduced number of mature oligodendrocytes later on is most likely due to an effect on a later aspect of oligodendrocyte-lineage cell development than their specification.

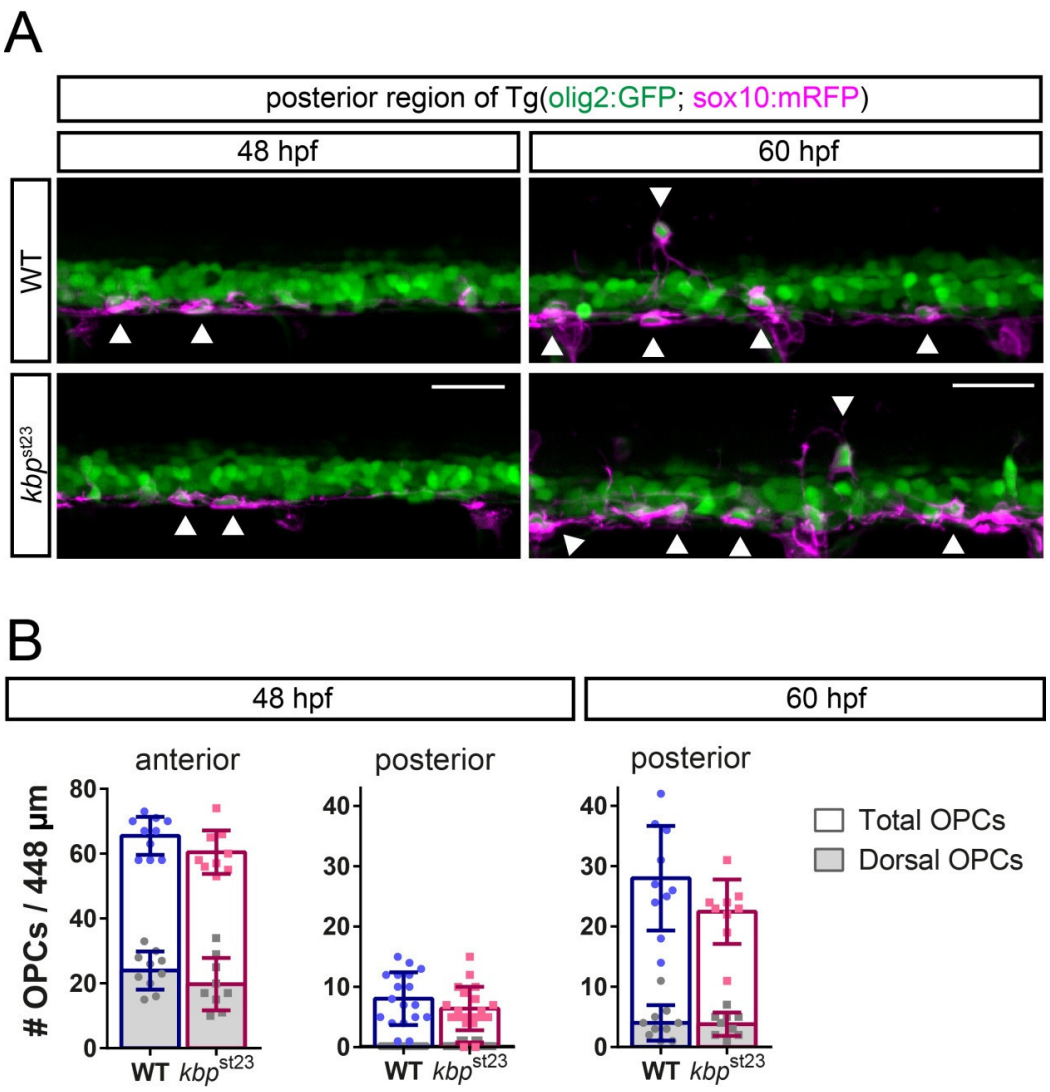

Figure 3.7 – The initial number of OPCs is not altered in *kbp*^{st23} mutants.

(**A**) Lateral view of the posterior region of 48-60hpf Tg(olig2:GFP; sox10:mRFP) larvae (arrowheads point to double-labelled cells, OPCs). No difference in OPC number is apparent at either time point. Scalebar: 25 µm. (**B**) Quantification of olig2:GFP+ sox10:mRFP+ cells per 448 µm length of tissue (6 somites). Error bars are standard deviation:

48hpf, anterior:

Total OPCs: 66±6 (N=10 WT) vs 60±7 cells (N=9 mutants), p=0.0965 in t-test

Dorsal OPCs: 24±6 (N=10 WT) vs 20±8 cells (N=9 mutants), p=0.2079 in t-test

48hpf, posterior:

Total OPCs: 8±4 (N=18 WT) vs 6±4 cells (N=20 mutants), p=0.2092 in t-test

Dorsal OPCs: 0±0 (N=18 WT) vs 0±0 cells (N=20 mutants), p=0.1071 in Mann-Whitney test

60hpf, posterior:

Total OPCs: 28±8 (N=10 WT) vs 22±5 cells (N=9 mutants), p=0.1157 in t-test

Dorsal OPCs: 4±3 (N=10 WT) vs 4±2 cells (N=9 mutants), p=0.8498 in t-test

3.3.5 Dorsal distribution of OPCs is normal in the absence of target axons

A subset of OPCs starts migrating dorsally at 60 hpf in a stereotyped anterior to posterior gradient. By 72hpf, several OPCs have accumulated in the dorsal spinal cord, above the olig2:GFP band where motor neurons reside (delimited by red dotted line in Figure 3.8A). Since reticulospinal axons run along the ventral spinal cord, I wondered whether more OPCs might migrate dorsally in mutants when reticulospinal axons are absent, perhaps in search of other targets for myelination. As I have just shown, at 60hpf, the number of the very first dorsal OPCs is similar in the posterior spinal cord of WT and mutants (Figure 3.7B, grey bars). I investigated the number of dorsal olig:GFP+ sox10:mRFP+ OPCs later, at 72and 96 hpf. At these time points, a subset of GFP+ mRFP+ cells has matured into oligodendrocytes but retains expression of both markers; therefore I will refer to them as 'oligodendrocyte-lineage cells', rather than 'OPCs'.

At 72hpf and 96hpf, the total number of oligodendrocyte-lineage cells is already reduced in the posterior spinal cord of mutant larvae (Figure 3.8 B). However, the number of dorsal cells is not significantly different between WT and mutant. This suggests that the subset of OPCs that migrate dorsally in the spinal cord does so independently of the presence of reticulospinal axons. Additionally, it suggests that the disruption to (ventral) oligodendrocyte-lineage cell development must start occurring between 60-72hpf.

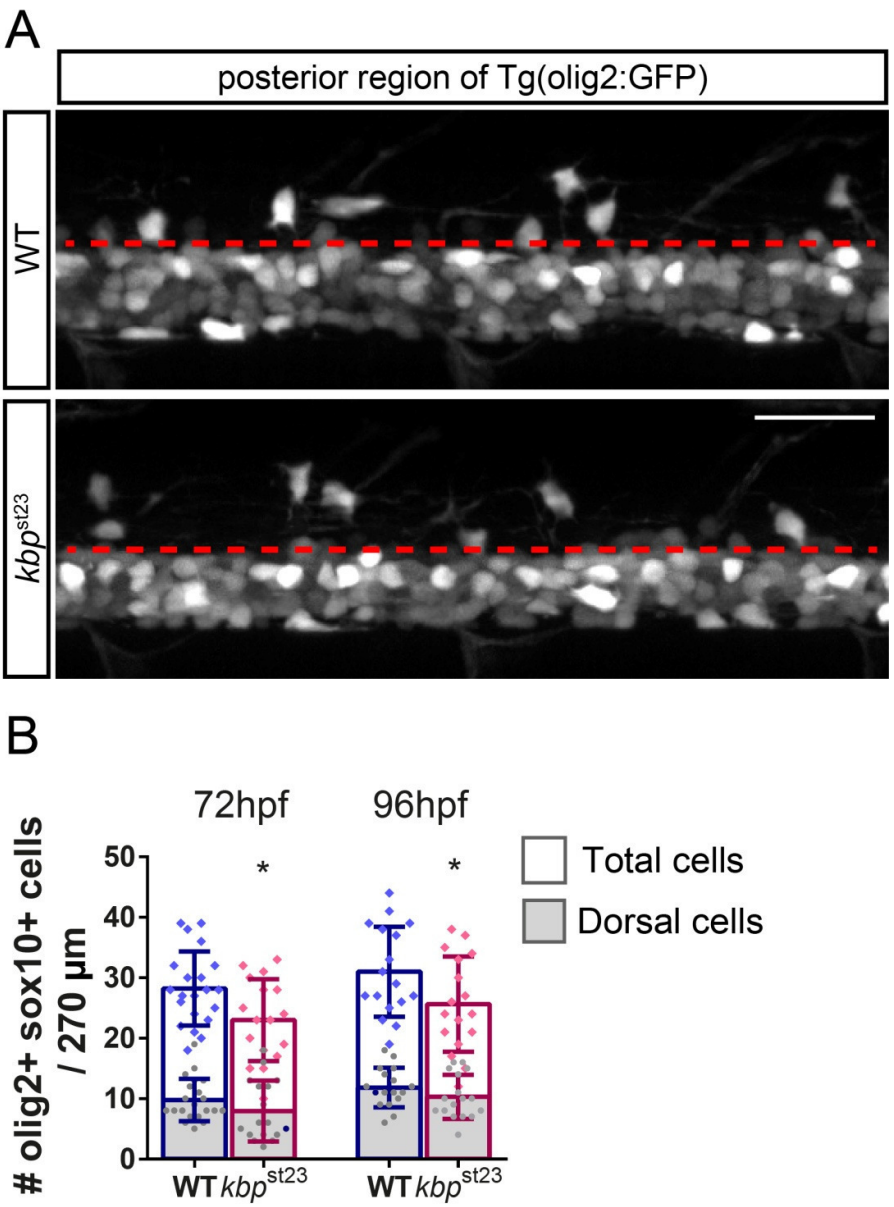

Figure 3.8 – The dorsal distribution of a subset of oligodendrocyte-lineage cells is not affected in *kbp*^{st23} mutants.

(**A**) 72hpf posterior spinal cord of Tg(olig2:GFP) larvae, which labels oligodendrocyte-lineage cells, motor neurons and pMN progenitors. Cells above dotted line are dorsally migrated OPCs. Scalebar: 25 µm.

(**B**) Quantification of oligodendrocyte-lineage cells in the posterior region of the spinal cord.

72hpf, posterior:

Total cells: 28±6 (N=21 WT) vs 23±7 cells (N=17 mutants), p=0.0170 in t-test

Dorsal cells: 10±3 (N=18 WT) vs 8±5 cells (N=17 mutants), p=0.0947 in Mann-Whitney test

96hpf, posterior:

Total cells: 31±7 (N=17 WT) vs 26±8 cells (N=17 mutants), p=0.0499 in t-test

Dorsal cells: 12±3 (N=17 WT) vs 10±4 cells (N=17 mutants), p=0.2073 in t-test

I additionally performed time lapse-imaging of the posterior spinal cord of the same reporter line starting approximately at 60 hpf, imaging the entire depth of the spinal cord every 14 minutes. OPCs move towards the dorsal spinal cord frequently in both WT and mutant larvae, starting a few hours after the emergence of the first olig2:GFP+, sox10:mRFP+ cells in each somite (Figure 3.10A, arrowheads). OPCs kept accumulating dorsally for the duration of the imaging period (longest time lapse is 17 hours long), occasionally dividing (Figure 3.10A, asterisk). To analyze the dynamics of the dorsal migration, I normalized the time in all movies by setting time point 0 when the first olig2:GFP+ OPC migrated above the olig2:GFP+ band (Figure 3.10B). I found a relatively large range of migration dynamics within the WT larvae, with OPCs accumulating dorsally at rates ranging from 0.5 to 3 OPCs per hour per animal; this, however, was not significantly different from mutant larvae (mean ± standard deviation: 1.164 ±0.73 OPCs/hour in N=17 WT larvae versus 1.077±0.48 OPCs/hour in N=19 mutant larvae).

Collectively, these results indicate that the distribution of a subset of oligodendrocyte-lineage cells to the dorsal spinal cord is a feature independent of ventral, reticulospinal axons, and suggests that these OPCs are not “searching” for targets for myelination when they migrate dorsally.

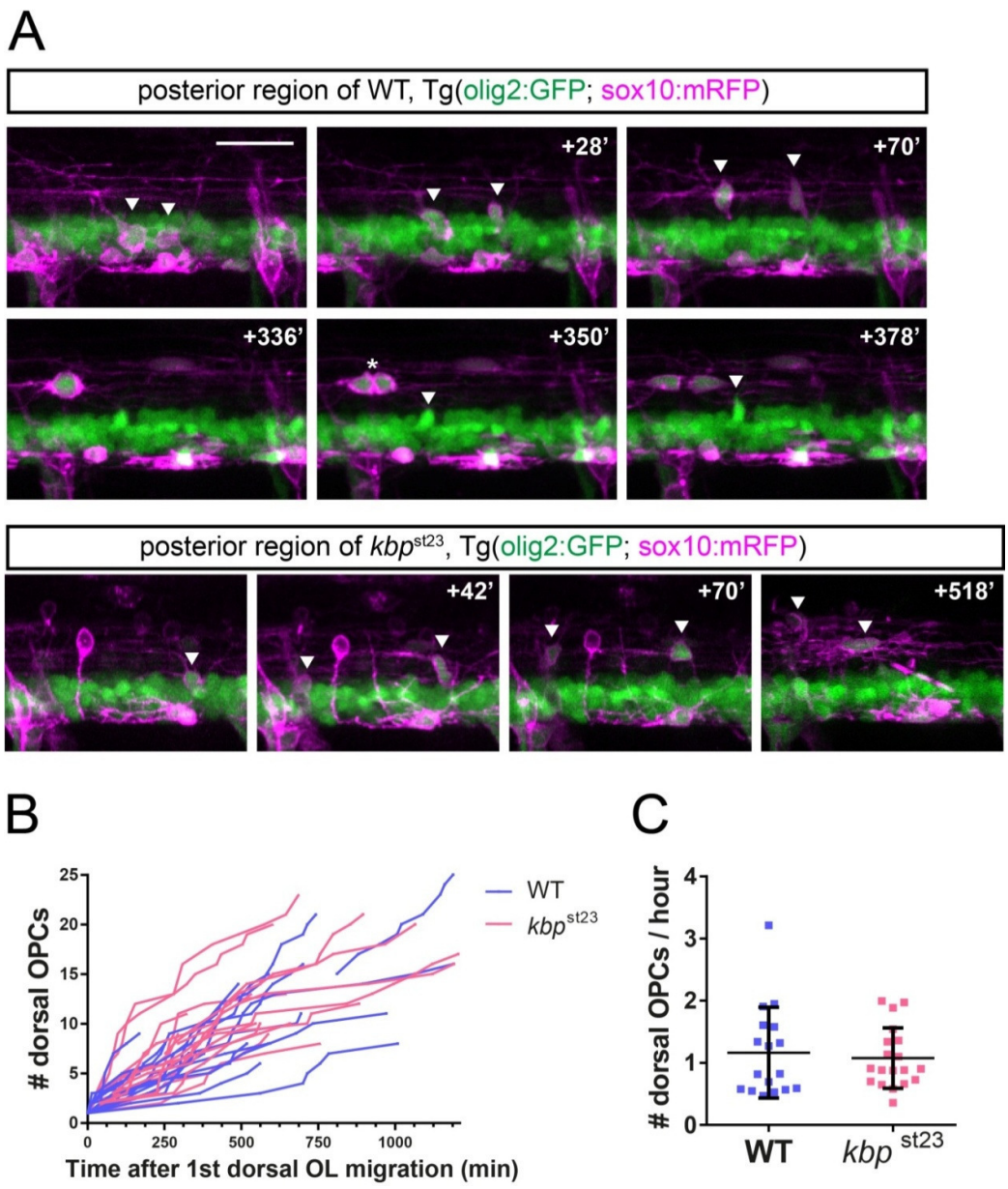

Figure 3.9 – Dorsal OPCs migrate at a similar rate in WT and *kbp*^{st23} mutants.

(**A**) Time-lapse movies of Tg(olig2:GFP; sox10:mRFP) larvae. A subset of OPCs migrates dorsally in both WT and mutants (arrowheads), occasionally dividing (asterisk), over a protracted period of time that overlaps with the onset of myelination (note myelin sheaths on last panels). Scalebar: 25 μm.

(**B**) Dorsal migration dynamics of OPCs. The number of accumulated dorsal OPCs is plotted against time (minutes); x=0 is the point at which the first OPC migrates dorsally. Blue traces, WT; Pink traces, mutant.

(**C**) Number of OPCs that migrated dorsally divided by the duration of the imaging period, per larvae. Each dot represents one larva. Error bars are standard deviation: 1.164±0.731 (N=17 WT) vs 1.077±0.484 OPCs/hour (N=19 mutants), p=0.6670 in Mann-Whitney test.

3.3.6 OPC migration is subtly affected in the absence of axon targets

I then wondered if the migratory capacity of OPCs is affected by the lack of reticulospinal axons. OPCs express several receptors that could respond to a number of secreted or adhesion molecules expressed on the surface of axons (Tsai and Miller 2002, de Castro and Zalc 2013). Migration of OPCs seems directed and not an random in the zebrafish spinal cord (Kirby, Takada et al. 2006, Mathews, Mawdsley et al. 2014), in the chicken or rodent brain, or during remyelination (de Castro and Zalc 2013). In vitro, the motility of OPCs seems responsive to factors such as the neurotransmitter glutamate (Gudz, Komuro et al. 2006) or to extracellular matrix molecules (Milner, Edwards et al. 1996), suggesting that specific signaling from axons, or at least the physical environment in which they exist, may regulate OPC migration. Although optic nerve OPCs still seemed to distribute throughout the nerve following nerve transection (Ueda, Levine et al. 1999), this broad analysis may not have uncovered subtler defects in the migratory properties of OPCs. To address this, I tracked individual OPCs in my time lapses in WT and mutant larvae; parsing out between dorsal OPCs and those that remain in the ventral spinal cord.

Dorsal OPCs

I tracked 172 dorsal OPCs from 17 WT larvae and 215 dorsal OPCs from 19 mutant larvae, varying from 1-18 hours per cell, and 5-23 cells per larvae. My "dorsal" analysis refers to all OPCs that rose above the olig2:GFP band at any point during the imaging period. As previously described (Kirby, Takada et al. 2006, Lee, Padmanabhan et al. 2010), OPCs move intermittently and frequently change their trajectories, and some OPCs returned to more ventral positions after migrating dorsally. Examples of dorsal OPC trajectories (of those OPCs with the largest tracked distances) are represented in Figure 3.11 A (WT) and B (mutant).

In agreement with previous studies (Kirby, Takada et al. 2006), the total distance covered by each OPC varied greatly, with a range of 6-216 μm in WT and 9-191 μm

in mutant larvae. Representative examples of OPC distances tracked in three WT and three mutant larvae are shown in Figure 3.11C. The average distance tracked per OPC per animal is not significantly different between WT and mutants (Figure 3.11 D).

The average speed at which OPCs migrated also varied greatly. Interestingly, the average OPC speed per larvae is slightly reduced in *kbp* mutants (Figure 3.11 E). A histogram of the frequency distribution of speeds of all OPCs tracked further suggested that a larger proportion of mutant OPCs migrate at slower rates (<6 μm/hour) than WTs (Figure 3.11 F). Since OPCs frequently pause in their trajectories, a decreased average speed may mean that OPCs paused more often while migrating, or that OPCs migrate at an actual lower velocity. The maximum speed that dorsal OPCs attained between individual time points was not significantly different between WT and mutants (Figure 3.11G), therefore, mutant dorsal OPCs may simply have paused more.

As I exemplified in Figure 3.11 C, the variability in these parameters in-between OPCs and between each individual larvae is high. This somewhat reduced the power of my statistical analysis to detect the small differences in the observed means, despite the high number of cells and animals imaged. However, it is very hard to determine the biological relevance of the slight reductions in the average values of these parameters. Considering that the range of speeds and distances covered is similar between WT and mutant, as is the maximum speed attained, the migratory parameters of mutant dorsal OPCs are mostly similar to WT dorsal OPCs. This suggests that reticulospinal axons do not strongly or specifically influence dorsal OPC migration.

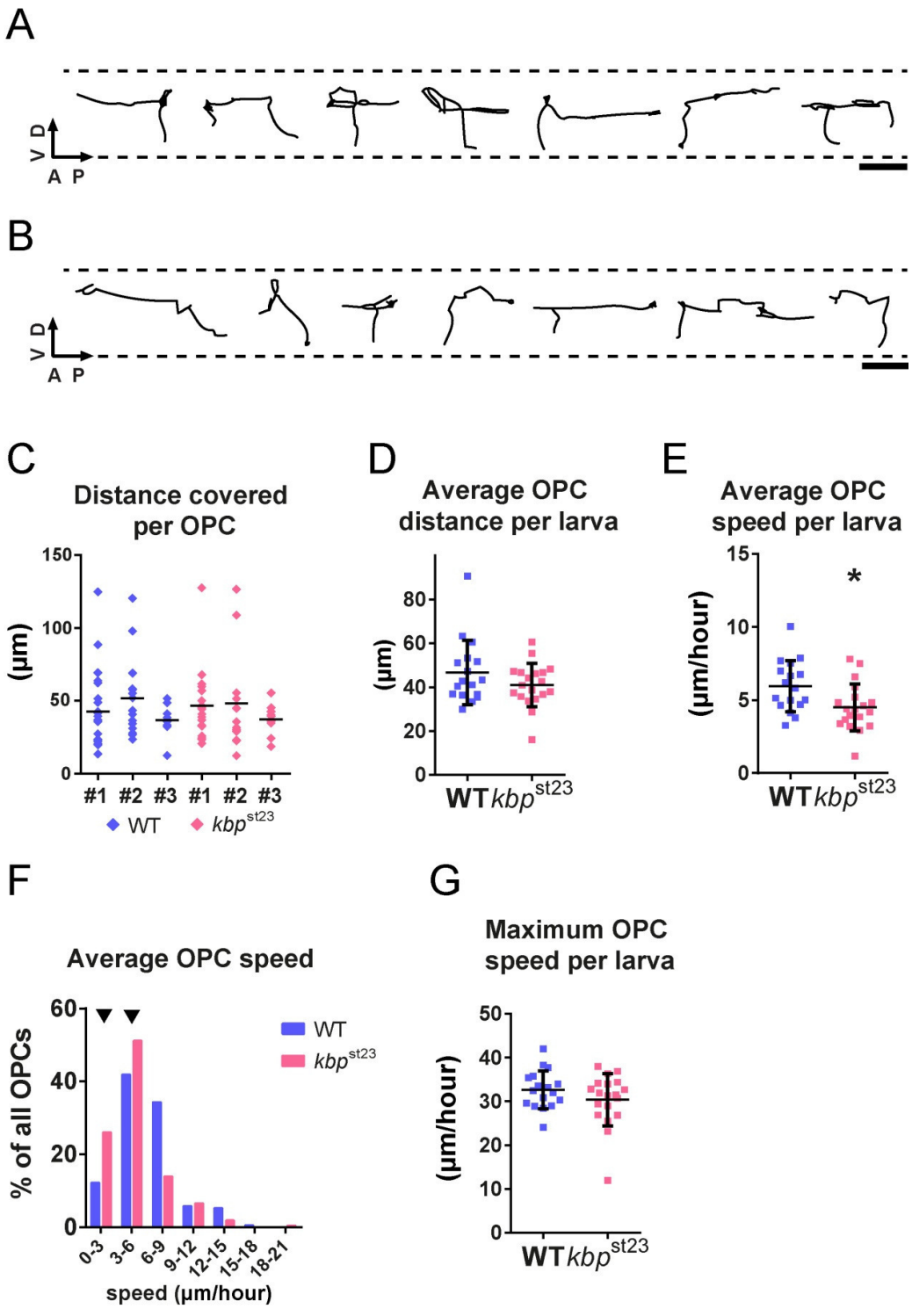
A
V D
A P
B
V D
A P
C
Distance covered per OPC
(µm)
150
100
50
0
#1 #2 #3 #1 #2 #3
WT
kbp^st23
D
Average OPC distance per larva
(µm)
80
60
40
20
0
WT kbp^st23
E
Average OPC speed per larva
(µm/hour)
15
10
5
0
*
WT kbp^st23
F
Average OPC speed
% of all OPCs
60
40
20
0
WT
kbp^st23
0-3 3-6 6-9 9-12 12-15 15-18 18-21
speed (µm/hour)
G
Maximum OPC speed per larva
(µm/hour)
50
40
30
20
10
0
WT kbp^st23

Figure 3.10 – Migratory parameters of dorsal OPCs are mostly unaffected in the posterior spinal cord of *kbp*^{st23} mutants.

(**A, B**) Tracing of the migratory paths of seven WT (A) and seven mutant (B) dorsal OPCs which covered the largest distances. All traces are oriented so that anterior is left and dorsal is up. Note that some paths finish ventrally. Dashed lines delineate direction of spinal cord. Scalebar: 25 μm.

(**C**) Examples of distances covered for all tracked dorsal OPCs in three representative WT and mutant larvae. Each dot represents the distance covered by one OPC.

(**D**) Quantification of the average dorsal OPC distance covered per larvae. Bars represent standard deviation: 47±15 (N=17 WT) vs 41±10 μm/cell (N=19 mutants), p=0.3764 in Mann-Whitney test

(**E**) Quantification of the average dorsal OPC speed per larvae. Bars represent standard deviation: 5.95±1.75 (N=17 WT) vs 4.50±1.61 μm/hour (N=19 mutants), p=0.0142 in t-test

(**F**) Histogram of the frequency of speeds of all dorsal OPCs tracked (172 WT OPCs and 215 mutant OPCs). Speeds are split into 3 μm/hour bins, and the percentage of all OPCs tracked in each bin is plotted on the *y* axis. More mutant OPCs are present in the lower-speed bins (arrowheads): 12% WT OPCs vs 26% mutant OPCs average 0-3 μm/hour; 42% WT OPCs vs 51% mutant OPCs average 3-6 μm/hour.

(**G**) Quantification of the maximum dorsal OPC speed per larvae. Bars represent standard deviation: 32.67±4.35 (N=17 WT) vs 30.40±5.94 μm/hour (N=19 mutants), p=0.4113 in Mann-Whitney test

Ventral OPCs

The combination of transgenes that I used permitted me to similarly analyse the migratory parameters of ventral OPCs, that is, of OPCs that never migrate above the olig2:GFP band. These include those OPCs that will myelinate reticulospinal axons, and are thus more likely to be affected by their absence.

I tracked 213 ventral OPCs from 18 WT larvae and 241 ventral OPCs from 19 mutant larvae, varying from 3-18 hours per cell, and 7-19 cells per larvae. As expected, the trajectories of ventral OPCs are more aligned along the anterior-posterior axis, rather than presenting a net dorsal movement as dorsal OPCs do. Examples of ventral OPC trajectories (of those OPCs with the largest tracked distances) are represented in Figure 3.12 A (WT) and B (mutant).

The total distance covered by each OPC varied from 5-142 μm in WT and 0-94 μm in mutant larvae. This reduced maximal distance covered by mutant OPCs was in fact accompanied by a significant reduction in the average distance tracked per OPC per larva in mutants (Figure 3.12 C). Additionally, the average OPC speed per larvae is significantly reduced in *kbp* mutants (Figure 3.12 D). A histogram of the frequency distribution of speeds of all OPCs tracked confirmed that a larger proportion of mutant OPCs migrate at slower rates (<2 μm/hour) than WTs (Figure 3.12 E). Furthermore, the maximal speed that ventral OPCs attained between individual time points was also significantly reduced in mutants (Figure 3.12F).

Thus, in the absence of reticulospinal axons, ventral OPCs seem to migrate less than WT OPCs, and at slower speeds. This is in contrast with dorsal OPCs, which seem comparatively less affected. It is important to remember that especially these ventral OPCs migrate in a drastically altered axonal environment, which makes is very hard to extricate an effect of the absence of specific signalling provided by the missing axons.

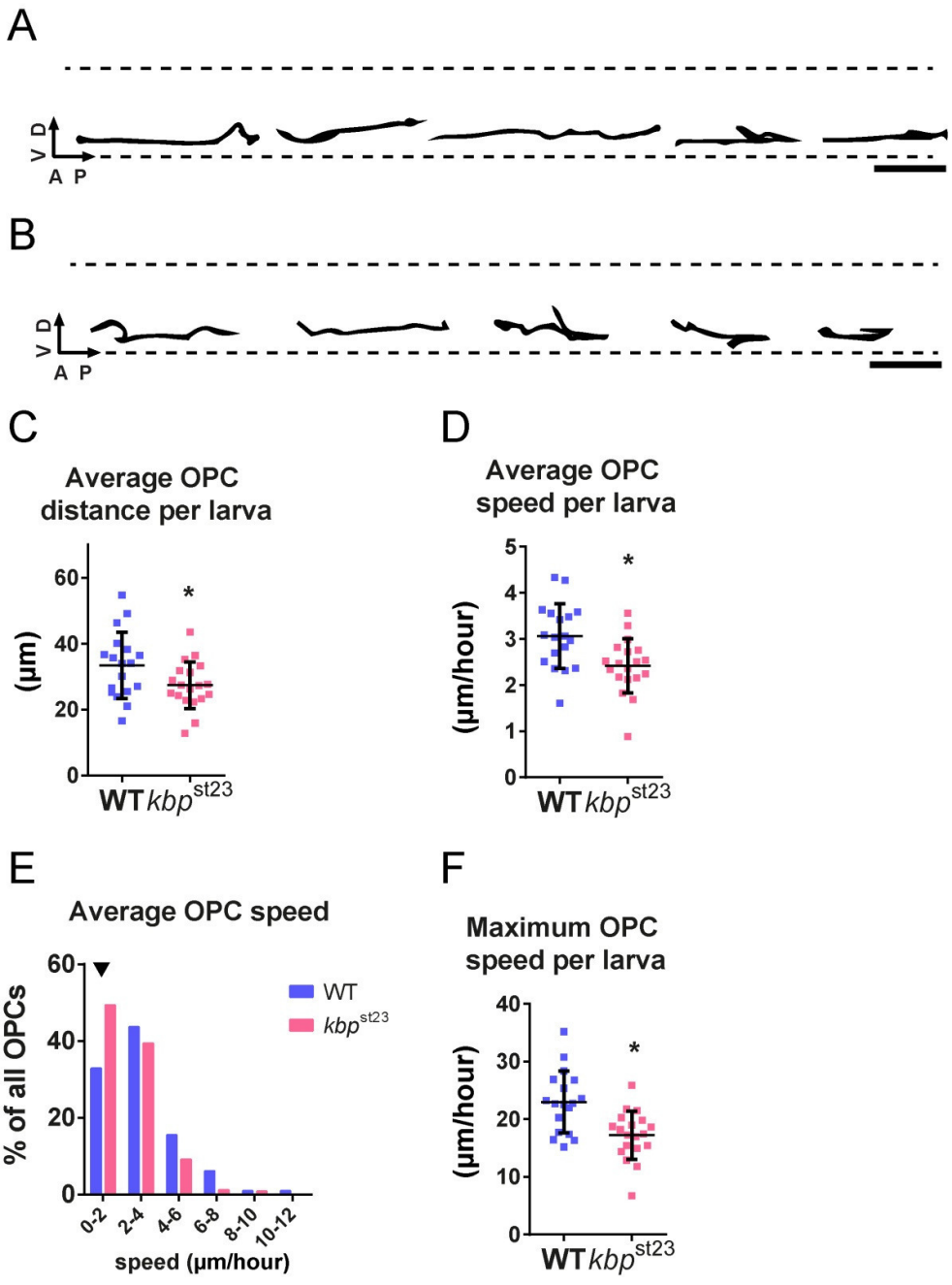
A
V D
A P
B
V D
A P
C
Average OPC
distance per larva
(µm)
60
40
20
0
*
WT
kbp st23
D
Average OPC
speed per larva
(µm/hour)
5
4
3
2
1
0
*
WT
kbp st23
E
Average OPC speed
% of all OPCs
60
40
20
0
WT
kbp st23
0-2
2-4
4-6
6-8
8-10
10-12
speed (µm/hour)
F
Maximum OPC
speed per larva
(µm/hour)
40
30
20
10
0
*
WT
kbp st23

Figure 3.11 – Ventral OPCs migrate slightly less and slower in the posterior spinal cord of *kbp*^{st23} mutants.

(**A, B**) Tracing of the migratory paths of five WT (A) and five mutant (B) ventral OPCs which covered the largest distances. All traces are oriented so that anterior is left and dorsal is up. Dashed lines delineate direction of spinal cord. Scalebar: 25 μm.
(**C**) Quantification of the average ventral OPC distance covered per larvae. Bars represent standard deviation: 33±10 (N=18 WT) vs 27±7 μm/cell (N=19 mutants), p=0.0404 in t-test
(**D**) Quantification of the average ventral OPC speed per larvae. Bars represent standard deviation: 3.06±0.70 (N=18 WT) vs 2.42±0.59 μm/hour (N=19 mutants), p=0.0047 in t-test
(**E**) Histogram of the frequency of speeds of all ventral OPCs tracked (213 WT OPCs and 241 mutant OPCs). Speeds are split into 2 μm/hour bins, and the percentage of all OPCs tracked in each bin is plotted on the *y* axis. More mutant OPCs are present in the lower-speed bins (arrowhead): 33% WT OPCs vs 49% mutant OPCs average 0-2 μm/hour.
(**F**) Quantification of the maximum ventral OPC speed per larvae. Bars represent standard deviation: 22.98±5.36 (N=18 WT) vs 17.22±4.20 μm/hour (N=19 mutants), p=0.0008 in t-test

3.3.7 OPCs divide fewer times in the posterior spinal cord of mutants

A reduction in oligodendrocyte-lineage cell number is already evident by 72hpf (Figure 3.8). My time-lapse imaging of OPCs in the posterior spinal cord starting from 60hpf allowed me to monitor the period during which this disruption to the development of oligodendrocyte-lineage cells starts occurring. After specification from pMN progenitors (whose mitotic rate was not affected by the absence of reticulospinal axons, Figure 3.5), OPCs are committed to the oligodendrocyte lineage, but still proliferate. I wondered if a reduction in OPC proliferation could contribute to the reduction in mature oligodendrocyte numbers later.

I found that my time-lapses allowed me to directly visualize OPC mitotic events. Occasionally, the mRFP+ processes of an OPC seemed to partially retract. mRFP+ membrane accumulated in the center of the cell, resembling a cleavage furrow, which split in two, followed by separation of GFP+ cytoplasm in two portions (within 14-42 min; see example in Figure 3.9 A, asterisk). Table 3.2 summarizes the total number of mitotic events I observed in dorsal and in ventral OPCs in all animals imaged. The total number OPC mitotic events observed in all mutant larvae is halved compared to WTs, even though more cells were tracked, more animals were imaged, and for a longer total amount of time.

Table 3.2 – Total OPC mitoses in the posterior spinal cord (60-72hpf)

	# mitotic events			*# cells tracked**			*time imaged** (hours)*	*# larvae*
	dorsal	*ventral*	*total*	*dorsal*	*ventral*	*total*		
WT	10	9	19	172	213	385	176	18
mutant	4	6	10	215	241	456	218	21

* Does not include OPCs already dorsal when imaging starts and OPCs that migrated away or into the field of view (including in the z-axis). However, mitotic events were counted in some of these subsets.
** Includes only the length of time after the onset of dorsal migration (See Chapter 2)

In individual larvae, between the 60-72hpf periods, OPC mitoses were not frequent in the 425 μm-stretch of posterior spinal cord imaged. No OPC mitoses were

observed in 9/18 WT larvae and in 13/21 mutant larvae. In one WT larva (the longest imaged), 4 mitotic events occurred; but in most animals only one mitosis occurred.

Based on my previous imaging of the same reporter line (Figures 3.7 and 3.8), the number of oligodendrocyte-lineage cells should rise from about 27 at 60hpf to 44 at 72hpf in WT larvae in the length of tissue imaged in my time-lapses. In mutants, it should rise from 21 to 36 cells at 96hpf. Therefore, one or two mitoses per larvae in this region may represent up to about 5% of all oligodendrocyte-lineage cells. This is roughly similar to the global analysis of total mitotic events: 19/385 cells underwent mitosis in WT (5%) versus 10/456 in mutants (2%).

The majority of mitotic events I observed occurred in the second half of the imaging period, suggesting that the rate of mitosis is just starting to increase. If this mitotic rate persists or increases for the next 24 hours of development, then an apparent halving of total mitotic events in the absence of reticulospinal axons may contribute significantly towards the reduced number of mature oligodendrocytes observed at 96hpf.

Interestingly, both dorsal and ventral OPC mitoses were affected in the mutants, despite the fact that target axonal surface is only reduced in the ventral spinal cord. This suggests that the signals underlying this effect on OPC proliferation act at a distance, and could be secreted, rather than acting juxtacrinally and requiring contact.

3.3.8 Axons regulate survival of OPCs

When imaging the reporter line sox10:mRFP, I noticed the presence of mRFP+ debris in the posterior region of mutant larvae (Figure 3.13A). Since RFP is membrane-tethered in this line, this suggests that there is loss or shedding of the processes of sox10+ cells, or even loss of cellular integrity and death. I rarely observed this in WT larvae, where all mRFP fluorescence belongs to OPC processes and to oligodendrocyte myelin sheaths. The extent of debris present was variable between individual larvae. I quantified the number of animals that presented at least a cluster of mRFP+ debris not associated with a clear OPC process or oligodendrocyte myelin sheath (Figure 3.13B). At 48hpf, debris was rare: 1/19 WT and 1/20 mutants presented debris in the anterior region and 1/19 WT and 2/20 mutants had debris in the posterior region. At 60hpf, 0/22 WT and 2/18 mutants presented debris anterior and 1/22 WT and 1/17 mutants had debris in the posterior region. From then on, many more mutant animals presented debris than WTs. At 72hpf, 6/44 WT and 11/36 mutants presented debris anterior compared to 3/54 WT and 37/47 mutants in the posterior spinal cord. Finally, at 96hpf, 0/11 WT and 0/8 mutants presented debris anterior, and 6/28 WT and 21/25 mutants presented debris in the posterior spinal cord.

These results showed that loss of cellular integrity of oligodendrocyte-lineage cells starts potentially from 60hpf. My time-lapse analysis of olig2:GFP; sox10:mRFP larvae at 60hpf showed that in mutant animals, starting between 6-14 hours after the onset of dorsal migration, a subset of ventral oligodendrocyte-lineage cells undergoes cell death: mRFP+ membrane disintegrates, resulting in disappearance of cellular processes and soma membrane and appearance of mRFP+ debris. Additionally, cell death is also inferred by the disappearance of olig2:GFP+ cytoplasm. On one occasion, an oligodendrocyte-lineage cell very transiently (~2 hours) formed a myelin sheath before it died (Figure 3.14A), but in the majority of cell death events no such structures were observed. Neighbouring OPCs in the same region of a dying cell behave normally, differentiating and forming myelin sheaths (Figure 3.14). The total number of cell death events I observed is summarized in Table 3.3.

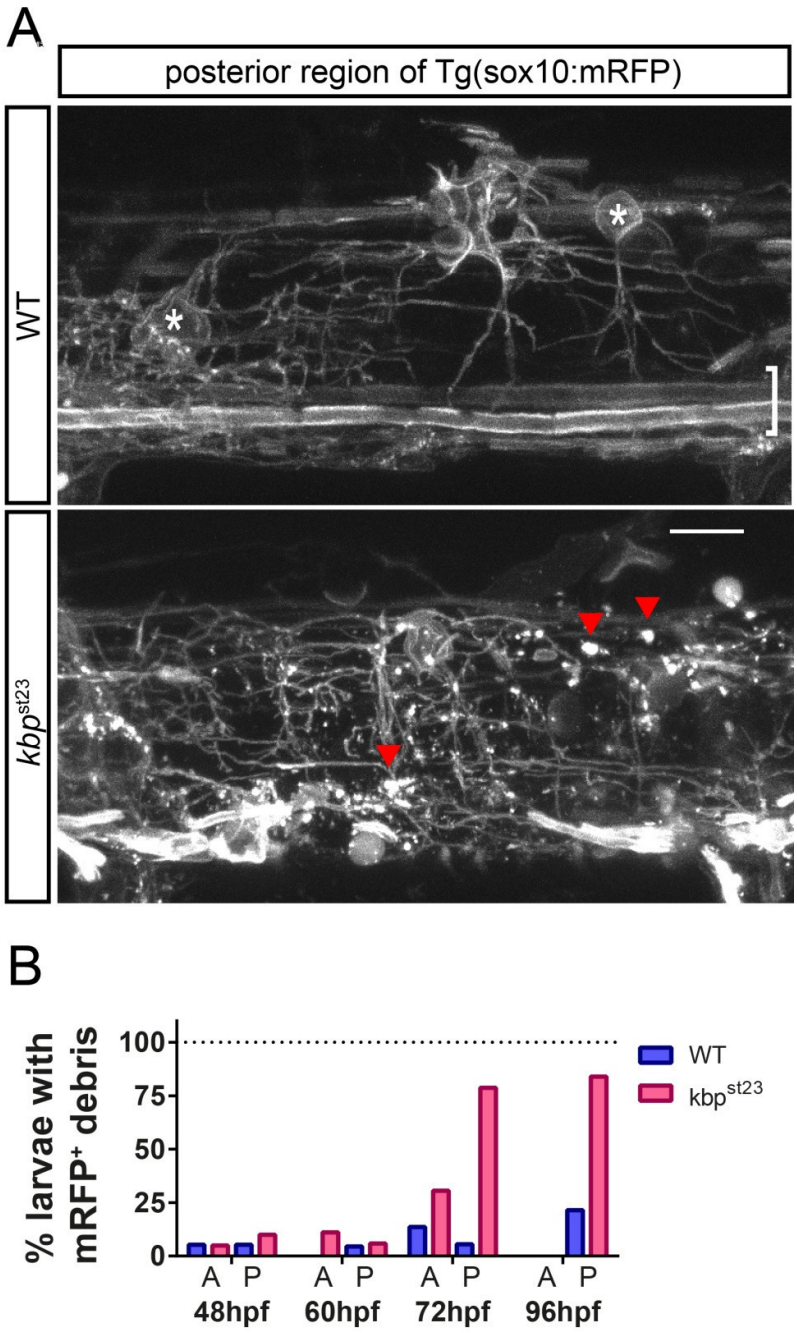

Figure 3.13 –sox10:mRFP+ debris in the posterior spinal cord of *kbp*^{st23} mutants.

(**A**) High-magnification view of the posterior region of 72hpf Tg(sox10:mRFP) larvae. In WT, mRFP labels OPC processes (asterisks), and myelin sheaths (brackets). In mutants, mRFP+ debris is readily apparent (arrowheads). Scalebar: 10 µm.
(**B**) Percentage of larvae with mRFP+ debris in the anterior (A) and posterior (P) spinal cord. From 60hpf onwards, debris was ubiquitous in mutant posterior spinal cord (see text for details).

Table 3.3 – Total OPC cell death events in the posterior spinal cord (60-72hpf)

	# cell death events			*Length of time imaged (hours; all larvae combined)*	*# larvae*
	dorsal	*ventral*	*total*		
WT	0	0	0	176	18
mutant	1	12	13	218	21

I never observed oligodendrocyte-lineage cells undergoing cell death in WT larvae, whereas cell death events occurred in 11/21 mutant larvae imaged at similar stages of development. Typically, I observed only one such event in each individual larva; only two mutant larva displayed two cell death events. Like the mitotic rate of OPCs in the previous section, in the context of a single animal, this represent the death of a small (<5%) subset of cells in the region analyzed; but this effect may accumulate at even higher rates during the next 24 hours of development and contribute significantly towards the decrease in mature oligodendrocyte number in mutants at 96hpf.

These results indicate that developmental apoptosis of OPCs does not occur early on in the spinal cord of WT larvae, and suggest that in the absence of reticulospinal axons, a subset of ventral oligodendrocyte-lineage cells undergoes cell death. Since such events occurred only ventrally and in a restricted number of cells, the underlying signal that would usually promote survival probably does so in a contact-dependent manner, unlike the mitotic signal described in the previous section.

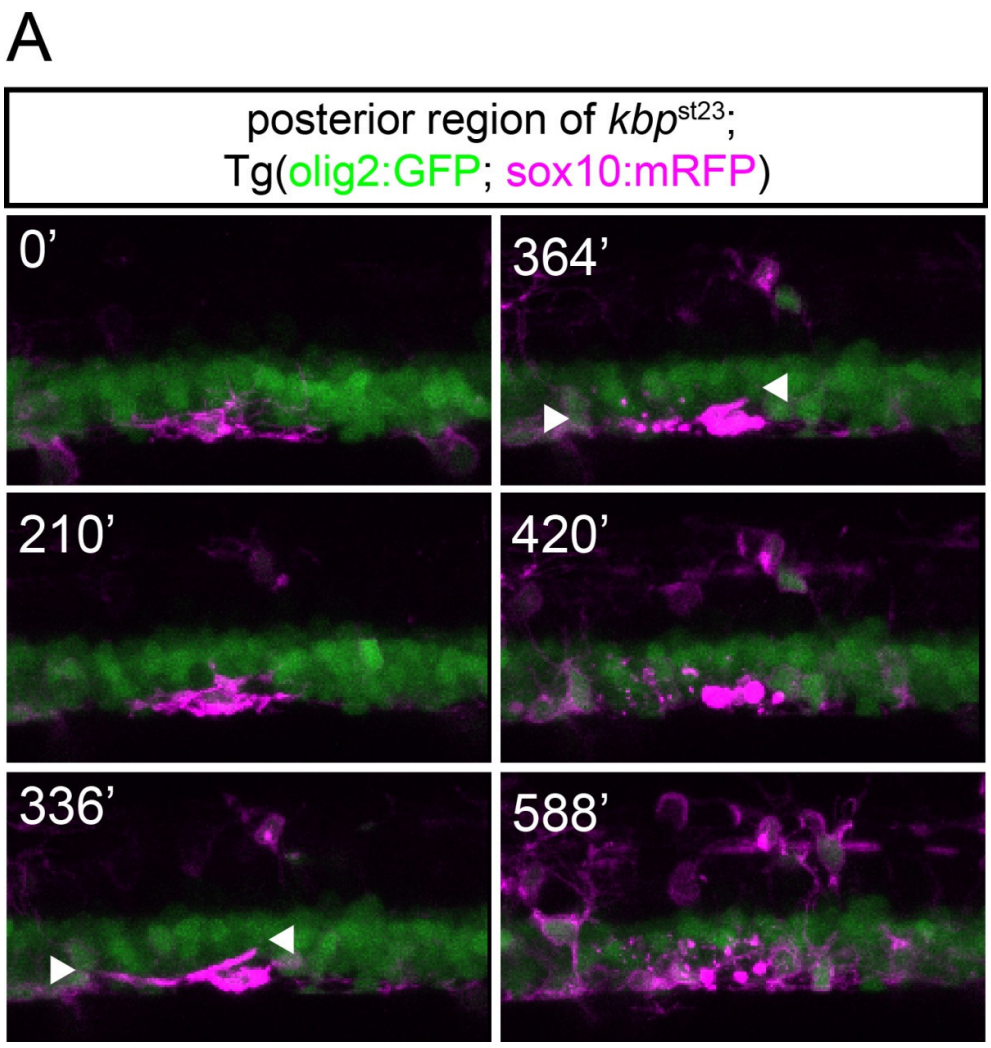

Figure 3.14 –A subset of oligodendrocyte-lineage cells dies in the posterior spinal cord of *kbp*^{st23} mutants.

(**A**) Lateral view of the posterior region of a mutant Tg(olig2:GFP; sox10:mRFP) larva, imaged from 60 hpf. Timing indicates minutes. A single visible OPC differentiates and forms a myelin sheath at 336’ (arrowheads). At 364’ the myelin sheath is degraded into RFP+ debris, and other processes are gone by 420’; by 588’ the cell has died, resulting in a cluster of mRFP+ cell debris. Note other OPCs differentiating nearby.

Finally, I further confirmed that I was observing cell death by treating sox10:mRFP animals with Acridine Orange (AO). AO is a fluorescent, cationic, vital dye that intercalates DNA and facilitates visualization of dying cells (with compromised nuclear integrity and fragmented DNA), and which has been used to label dying cells in zebrafish larvae (Hammerschmidt, Pelegri et al. 1996, Paquet, Bhat et al. 2009). A 30-minute treatment was enough to brightly label some foci in the posterior region of 72hpf larvae. These AO+ foci were readily apparent in mutants, often in the ventral region and surrounded by mRFP+ debris (Figure 3.15A). Quantification of total AO+ foci showed that mutant larvae have significantly more AO+ foci in the posterior region of the spinal cord, whereas the number of these foci in the anterior region was just borderline significantly different between WT and mutant larvae, according to the statistical test used (see Figure 3.15B legend for details).

Additionally, the number of AO+ foci specifically surrounded by mRFP+ debris is significantly increased only in the posterior region of mutants (Figure 3.15B), but not in the anterior region. Moreover, in an alternative, independent binning of the same data, the number of AO+ foci specifically localized in the ventral spinal cord is also significantly increased only in the posterior region of mutants, but not in the anterior region (Figure 3.15 C).

Collectively, my results indicate that the absence of reticulospinal axons and the severe reduction in target axonal surface correlate a) with a drastic ~50% reduction in the proliferation rate of all spinal cord OPCs, and b) with the cell death of a subset of ventral oligodendrocyte-lineage cells. The absence of these target axons did not affect the initial number of OPCs specified or their migration pattern and dorsal distribution. At a later stage, the number of mature oligodendrocytes is also reduced, especially in the ventral spinal cord. These data strongly suggest that the initial target axons for myelination promote proliferation and survival of oligodendrocyte lineage cells, regulating the number of mature oligodendrocytes later on.

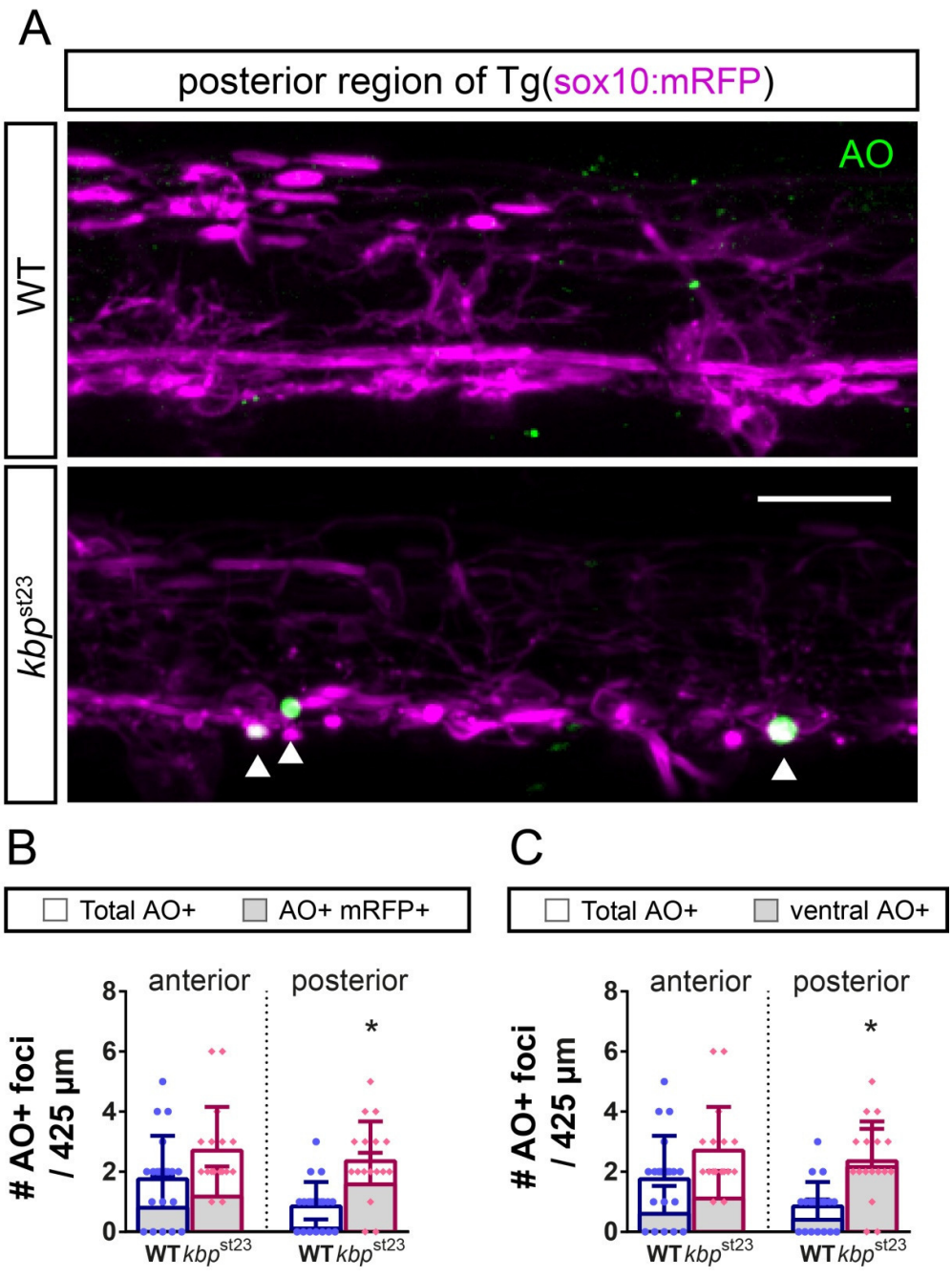
A
posterior region of Tg(sox10:mRFP)
WT
kbp^st23
AO
B
Total AO+
AO+ mRFP+
anterior
posterior
AO+ foci / 425 µm
WT
kbp^st23
C
Total AO+
ventral AO+

Figure 3.15 – A subset of ventral oligodendrocyte-lineage cells dies in the posterior spinal cord of *kbp*^{st23} mutants.

(**A**) Lateral view of the posterior region of Tg(sox10:mRFP) larvae at 72hpf, incubated for 30 minutes with the vital dye Acridine Orange (AO), which stains apoptotic cells in green. In mutants, green apoptotic foci are apparent (arrowhead), often in the ventral region and surrounded by mRFP+ debris. Scalebar: 20 μm.

(**B**) Quantification of total AO+ foci and AO+ foci surrounded by mRFP+ debris (grey bars). Error bars represent standard deviation.

Anterior:

Total AO+ foci: 1.75±1.45 (N=20 WT) vs 2.7±1.45 foci (N=17 mutant), p=0.0530 in t-test, p=0.0441 in Mann-Whitney test

AO+ mRFP+ foci: 0.8±1.06 (N=20 WT) vs 1.18±1.02 foci in (N=17 mutant), p=0.1762 in Mann-Whitney test

Posterior:

Total AO+ foci: 0.85±0.81 (N=20 WT) vs 2.35±1.32 foci (N=17 mutant), p=0.0002 in Mann-Whitney test

AO+ mRFP+ foci: 0.10±0.31 (N=20 WT) vs 1.59±1.06 foci in (N=17 mutant), p<0.0001 in Mann-Whitney test

(**C**) Quantification of total AO+ foci and AO+ foci specifically localized in the ventral spinal cord (grey bars). Independent binning of same dataset in (B), see (B) for total AO+ foci descriptive statistics. Error bars represent standard deviation.

Anterior, ventral AO+ foci:

0.60±0.94 (N=20 WT) vs 1.12±0.93 foci in (N=17 mutant), p=0.0687 in Mann-Whitney test

Posterior, ventral AO+ foci:

0.40±0.68 (N=20 WT) vs 2.18±1.29 foci in (N=17 mutant), p<0.0001 in Mann-Whitney test

3.4 Discussion

My analysis of the *kbp* mutant provided insight into the development of oligodendrocyte-lineage cells in the absence of their first major axonal targets, and therefore into their requirement for OPC and oligodendrocyte development. My main finding was that early developmental aspects such as OPC specification and population of the spinal cord were not drastically affected in the absence of axons; however, later aspects were affected: proliferation was reduced and survival impaired. These effects were observed by non-invasive time lapse imaging, which provides the most unambiguous, direct measure of proliferation and cell death in vivo.

Crucially, these were all determined in a physiological milieu, without recourse to an invasive manipulation to remove axons, and therefore are less likely to represent confounding effects of such manipulations, as indicated in the introduction to this chapter.

This indicates that axons promote the proliferation and survival of oligodendrocyte-lineage cells, in vivo, in what may represent a mechanism to match the numbers of oligodendrocyte lineage cells to the axonal surface competent for myelination.

3.4.1 OPC Specification

I found that the emergence of the very first OPCs is similar in control animals and in animals lacking reticulospinal axons (Figure 3.7). This indicates that the specification of OPCs in the spinal cord is independent of contact with axons. As mentioned previously, Shh induces the generation of the pMN domain. In the spinal cord, sonic hedgehog is secreted by the notochord and floor plate cells, both of which are unaffected in the *kbp* mutant; it is unsurprising then that OPCs formed normally. Interestingly, in apparent contrast, in the chicken optic nerve, RGC axons seem in fact indispensable for inducing OPC specification at the base of the optic nerve. However, RGC axons themselves deliver sonic hedgehog, as well as neuregulin

signalling (Gao and Miller 2006), highlighting the role of the sonic hedgehog pathway in OPC specification throughout the CNS. It would be interesting to determine whether the outgrowth of RGC axons is affected in the *kbp* mutant, and whether this impacts OPC development in that region of the CNS.

A recent study implicated diencephalic dopaminergic neurons, which project their axons from the brain to the ventral spinal cord, in the specification of motor neurons from the pMN progenitor domain. (Reimer, Norris et al. 2013) showed that during zebrafish embryonic development, dopamine release from these axons stimulates the sonic hedgehog pathway in pMN progenitors, promoting their proliferation. Dopamine gain-of-function manipulations significantly expand the pMN progenitor population and the number of motor neurons formed during development and regeneration. This study sets a precedent for projection neurons and their axons regulating spinal cord neurogenesis. The target spinal cord neural progenitors happen to be pMN progenitors, which subsequently specify OPCs, so it is conceivable that later, gliogenesis from the same domain may also be modulated by disruption of projection axons. The authors did not determine whether the OPC population was increased, as was the motor neuron population, following dopamine gain-of-function. In *kbp* mutants, the number of mitotic olig2+ pMN progenitors and of HB9+ motor neurons in the posterior spinal cord was similar to WT (Figure 3.5 and 3.6), so it is unlikely that axon outgrowth of dopaminergic projection neurons is disrupted as is the outgrowth of reticulospinal axons. Additionally, commitment to the oligodendrocyte lineage may be regulated by distinct mechanisms that would compensate for an increase in the number of pMN progenitors.

3.4.2 OPC migration and distribution

After specification, OPCs migrate away to colonize the entire CNS. In the zebrafish embryonic spinal cord, a subset of OPCs migrates dorsally. (Kirby, Takada et al. 2006) previously time-lapse imaged these dorsal OPCs and showed that they often associate with axons running along a dorsal tract, the dlf, whose axons I have observed to become myelinated typically by dorsal oligodendrocytes (see Chapter 4). OPCs in the dorsal spinal cord extend numerous filopodia-like processes; when they

contact neighbouring OPC processes, they retract and often migrate away. Ablation of single OPCs is often followed by colonization of that space by neighbouring OPCs. These OPC process interactions may thus ensure their uniform distribution during embryonic spinal cord development in zebrafish, in preparation for myelination. Additionally, a similar repulsive behaviour was observed between OPCs residing in adult rodent brain (Hughes, Kang et al. 2013), implying that this mechanism is retained throughout life. The molecular mechanisms underlying these repulsive interactions remain unknown, but analogies with dendrite outgrowth and axon-dendrite targeting may be drawn, and families of molecules such as DSCAM and protocadherins could be a potential avenue for starting that investigation (Almeida and Lyons 2013). Neither the study on embryonic zebrafish spinal cord, nor the study on adult rodent brain addressed whether neurons or axons played any role in regulating this behaviour.

If the migratory capacity of OPCs really serves to distribute them through the nervous system to adequately myelinate axons, axons may actively regulate OPC motility or, at a population level, the pattern of migration of many OPCs. For instance, immature axons not ready for myelination could promote OPC migration, whereas axons competent for myelination could provide a stop signal and arrest it, to increase the probability of the OPC differentiating locally and myelinating it. One might have predicted that in the absence of a subset of those target axons, OPCs would keep migrating for longer, or specifically migrate elsewhere, attracted by other myelination targets.

However, I showed that the absence of the ventral reticulospinal axons does not affect the number of dorsal OPCs (Figure 3.7 and 3.8), or the rate of migration of a subset of OPCs that migrates towards the dorsal spinal cord (Figure 3.9). This strongly indicates that the induction of a subset of OPCs to migrate dorsally is independent of ventral axonal influences. The molecular mechanisms underlying this induction of dorsal migration are entirely unknown. Interestingly, mutant zebrafish where the pMN domain generates an excess of OPCs have increased numbers of dorsal OPCs (Fbxw7 mutant) (Snyder, Kearns et al. 2012), whereas mutants where the pMN domain generates fewer total OPCs have fewer dorsal OPCs (pescadillo

mutant (Simmons and Appel 2012), or swap70 morphants (Takada and Appel 2011)). This suggests that such induction of dorsal migration is purely due to the size of the initial OPC population, possibly by a ventral density-dependent mechanism. This further suggests that mechanisms regulating dorsal migration are OPC-autonomous and axon-independent.

After a subset of OPC in induced to migrate dorsally, how do they recognize their targets and stop migrating? Dorsal axons in the dlf are suitably located to provide a stop signal and limit the extent of dorsal OPC migration, but this remains unverified. A recent study showed that isoprenylation activity was required within OPCs to recognize whatever their dorsal targets may be and arrest migration: (Mathews, Mawdsley et al. 2014) found that OPCs often ectopically migrated dorsally too much in a mutant in the isoprenoid and cholesterol biosynthetic pathway, hmgcs1. The authors suggest that the target for this isoprenylation may be a G-protein γ subunit of Cxcr2, a GPCR that binds the ligand Cxcl1, and whose disruption in rodents causes a similar migratory OPC phenotype. The origin of Cxcl1, even if it is the relevant ligand, remains speculative, although it is known to be secreted by astrocytes. In fact, most previous studies have identified factors capable of regulating OPC migration that are not produced by axons – these include, for instance, PDGF (Frost, Zhou et al. 2009), the floor-plate derived Netrin-1 (Jarjour, Manitt et al. 2003), and secreted ECM components acting partly through the α5β1 integrin pathway (Frost, Kiernan et al. 1996, Milner, Edwards et al. 1996). It will be interesting to determine if any of these signals plays a role in limiting dorsal migration in zebrafish, and if so, what their origin is; interestingly, classical astrocytes are not present in zebrafish.

Unlike (Kirby, Takada et al. 2006), who used a particular transgenic reporter line that prevented clear OPC visualization of the ventral spinal cord, I was also able to monitor the migration of ventral OPCs, which myelinate most reticulospinal axons in WT larvae. I found that in the absence of reticulospinal axons, a number of migratory parameters of ventral OPCs are slightly reduced – average distance covered and average speed; and dorsal OPCs were comparatively even less affected (Figure 3.10 and 3.11). It remains possible that this effect is due to the lack of *kbp* function in OPCs, which may itself be required for transducing migratory signals. Imaging the

anterior spinal cord, where reticulospinal axons are present but *kbp* function is not, will help answer this question. If this phenotype really is specific to the posterior spinal cord of mutants, it remains to be determined what the biological relevance of these subtle reductions may be. It is hard to determine whether they are due to the lack of specific reticulospinal-derived axonal signalling, or instead due to the altered environment. The dying oligodendrocyte-lineage cells present in the mutant could be releasing molecules to the milieu which perturb these migratory parameters. Additionally, in a normal situation, axons may subtly facilitate migration purely by providing a physical substrate for OPCs, even if their signals don't play a major role in regulating OPC migration.

Collectively, my results provide the first direct demonstration in a living organism that the general directedness and motility of many OPCs is mostly normal in the absence of a substantial number of their axonal targets. This supports the idea that the distribution and tiling of OPCs is independent of axons.

3.4.3 OPC proliferation

I showed that the number of mitotic pMN olig2+ progenitors was unchanged in the absence of reticulospinal axons through the onset of OPC specification (Figure 3.5). This indicates that reticulospinal axons do not regulate the proliferation of pMN progenitors, unlike dopaminergic axons, which do regulate proliferation of pMN progenitors at similar stages. Later on, OPCs specified from these progenitors are committed to the oligodendrocyte lineage, but are still proliferative, and are identifiable by the sox10:mRFP marker in my time-lapse imaging of double transgenic larvae Tg(olig2:EGFP; sox10:mRFP). This allowed me to directly count the number of mitoses in the posterior spinal cord (Figure 3.9 and Table 3.2). The total number of mitotic events was halved in the mutants, an effect that became apparent when the absolute frequencies for all larvae were combined. Strikingly, both ventral mitoses and dorsal mitoses are reduced in the absence of (ventral) reticulospinal axons. This suggests that the missing signal can act at some distance, and thus may more likely be a secreted mitogen, rather than a contact-dependent cue.

If it were a contact-dependent signal, many other axons in the dorsal spinal cord could presumably provide such a signal.

What might this mitogenic signal be? Neuronal activity has recently been demonstrated to regulate OPC proliferation in vivo (Mangin, Li et al. 2012, Gibson, Purger et al. 2014), as had been predicted before (Barres and Raff 1993). It remains to be determined if this regulation occurs directly between axons and OPCs, for instance, mediated by axonal factors secreted in an activity-dependent manner, such as neurotransmitters. Axonal neurotransmitters could communicate with OPCs at axon-OPC synapses, which occur ubiquitously in vivo (Almeida and Lyons 2013), or be secreted into the milieu along the axon. OPCs express many neurotransmitter receptors (Karadottir and Attwell 2007), but the end result of the activation of these receptors, in vivo, remains obscure. Alternatively, it remains possible that the observed effect on OPC proliferation upon neuronal stimulation may be indirect, via neural precursor or microglial activation, since these cells were also affected by the stimulus (Gibson, Purger et al. 2014).

More traditionally, some secreted, long-range acting signals are thought to regulate OPC proliferation. Known mitogens for OPCs include integrin ligands (Blaschuk, Frost et al. 2000), neurotrophin-3 (Barres, Raff et al. 1994), or the main mitogen PDGF (see Introduction). It is interesting to note that the source of these molecules in mammals is thought to be astrocytic. Directly analogous cells with stellate astrocyte morphology are notably absent from zebrafish, although GFAP+ radial glia exist in the spinal cord and share many of the roles of astrocytes (Lyons and Talbot 2014, in press). To date, no studies exist on the expression or role of PDGF and its receptor in the development of the zebrafish spinal cord. Is it expressed in the appropriate time and place to serve as a mitogen for OPCs? Do radial glial cells produce it, if there are no astrocytes? A comparative study showed that the zebrafish orthologue of PDGF-A diverges extensively from the mouse and human orthologues in the signal peptide region and C-terminus of the mature peptide (Liu, Korzh et al. 2002). Does it serve the exact same function as in mammals, given its divergence? Could it be that zebrafish PDGF is not mitogenic for OPCs? Are zebrafish OPCs responsive to PDGF, i.e., do they express the relevant receptor? Are there other mitogens specific

to the zebrafish spinal cord? It is noteworthy that at the stages included in my time-lapse analysis, I did not observe extensive OPC proliferation. Although it cannot be excluded that OPC proliferation ramps up later on, it is possible that extensive OPC proliferation simply does not occur in zebrafish. Could this relate to the absence of astrocytes, and possibly of PDGF, in the zebrafish spinal cord? In the mammal spinal cord, OPCs must populate and myelinate an immensely larger volume, several orders of magnitude larger than the zebrafish embryonic spinal cord. It is thought that the evolution of the larger volume of the mammal spinal cord required, or led to the evolutionary emergence of a secondary, dorsal source of OPCs (Richardson, Kessaris et al. 2006). In contrast, during embryonic and larval development, a single oligodendrocyte can extend processes that span the entire height of the zebrafish spinal cord.

In sum, my results suggest that axons promote OPC proliferation. To formally rule out a role of *kbp* itself in proliferation, I would need to investigate the anterior spinal cord of *kbp* mutants, where reticulospinal axons are present, and where OPC proliferation should not be affected. Still, my results suggest that axons provide a long-range acting mitotic signal during OPC development in vivo, contributing to the regulation of mature oligodendrocyte number later on.

3.4.4 OPC/oligodendrocyte survival

I also found that the survival of a subset of OPCs was impaired in the absence of reticulospinal axons. My live imaging indicates that several hours after the onset of dorsal migration, a small subset of ventral OPCs dies in the posterior spinal cord (Figure 3.13 and 3.14). My time-lapse analyses were focused on the 60hpf-72hpf hour period, and all cell death events occurred towards the end of this period, implying that whatever triggered cell death had just started its effect, and suggesting that the rate of cell death for the next 24 hour period may increase further.

What was the stage of development of the dying cells? Both olig2 and sox10 endogenous expression, and GFP and mRFP protein levels, persist in zebrafish OPCs when they terminally differentiate into oligodendrocytes. This means that the dying

double labelled cells could be an OPC or an oligodendrocyte. Since mRFP is membrane bound, I could visualise the morphology of these cells at a moderate resolution. During terminal differentiation, OPCs retract many of their ramified processes and elaborate myelin sheaths with a characteristic tubular profile. Using this morphological criterion, I could identify one cell that formed a clear myelin sheath and maintained it for approximately 2 hours, before undergoing cell death (Figure 3.14). Although this one cell could be defined as an 'early' oligodendrocyte when it died, the majority of dying cells do not clearly form myelin sheaths prior to the sudden appearance of mRFP+ debris. However, the onset of the terminal differentiation may occur slightly before the morphological specialization that the formation of a myelin sheath represents, so the cells might already have been oligodendrocytes. Similarly, the point of no return in terminal differentiation may occur slightly before endogenous expression of mbp and of the reporter transgene mbp:EGFP-CAAX (which labels the membrane of oligodendrocytes). Thus, although no GFP-CAAX+ debris is apparent in the posterior spinal cord of *kbp* mutants, reporter protein might simply not have accumulated to detectable levels before death ensues.

Therefore, as such cells may have already entered a terminal differentiation program when they died, the requirement for an axonal-derived survival signal in the zebrafish spinal cord may also be only from the oligodendrocyte stage, as previous studies would suggest (Ueda, Levine et al. 1999).

Time-lapse analyses at a higher spatial and temporal resolution would allow me to investigate the fine morphology and dynamics of oligodendrocyte-lineage cell processes prior to their death in the absence of reticulospinal axons. This would provide a better indication as to the stage of morphological development of these cells. I would also be able to better assess whether the dying cells ever manage to ensheath any axons. Interestingly, in zebrafish larvae where Sox10 (a transcription factor required to induce myelin gene expression in OPCs(Li, Lu et al. 2007)) is genetically disrupted, OPCs are generated normally and clearly ensheath axons, forming what resembles a myelin sheath like the one I observed in one mutant cell (Figure 3.14). They then undergo apoptosis (Takada, Kucenas et al. 2010). Sox10

could be promoting survival of oligodendrocytes downstream of a pro-survival pathway induced by an axonal signal; it would be interesting to determine if this could be the same survival signal that is missing when reticulospinal axons are absent. Sox10 mutant oligodendrocytes may be surviving slightly longer since the required axonal signal is not disrupted, and they have a bit more time to elaborate myelin sheaths before the apoptotic program is triggered; whereas in the posterior spinal cord of *kbp* mutants, the absence of an upstream reticulospinal axon-derived signal triggers cell death earlier. In this scenario, most oligodendrocytes would not even have time to form myelin sheaths before disintegrating. It would be interesting to determine if the activity of Sox10 or expression of its target genes is altered in the dying OPCs. However, it would be hard to assess this at single cell resolution, which would be required given that only a small subset of oligodendrocyte-lineage cells die in my experiments.

What determines whether a particular cell dies or survives in the absence of reticulospinal axons? In other contexts, precociously-differentiated oligodendrocytes in the conditional Notch1 mutant (Genoud, Lappe-Siefke et al. 2002), or ectopically-located oligodendrocytes in the grey matter of animals overexpressing PDGF (Calver, Hall et al. 1998), also could not survive in the long-term and resulted in increased apoptosis. In these cases, it is thought that oligodendrocytes died because they missed out on the right time or place for survival cues. In *kbp* mutants, dying cells were in their normal locations within the spinal cord and in close vicinity (within the same one somite) to cells that survived. Some of these were already producing myelin sheaths at the time of cell death, suggesting that the dying cells were not differentiating prematurely. Thus, rather than the wrong place or time, the dying cells might have be lacking the right amount of signal. In WT larvae, there may normally be a limiting amount of survival signals; just enough to prevent an inherent apoptosis program in the majority of oligodendrocyte-lineage cells. Possibly, when the axonal environment is disrupted, a localized, transient oscillation on the combined level of pro-survival signals may be enough to tip the cell over the edge and trigger an irrevocable programme of apoptosis.

Given that OPC cell death in the absence of reticulospinal axons occurred only in the ventral spinal cord, in a localized and sparse manner, I would expect that this signal acts in a contact-dependent manner. This could potentially include physiological activity-derived cues, such as synaptic and extra-synaptic vesicle release along axons, or signals exposed on the surface of axons such as classical juxtacrine signalling pathways - for instance, NRG1. Although shown to promote survival in vitro, an absolute requirement of NRG1 for CNS myelination in vivo was not found (Brinkmann, Agarwal et al. 2008, Perlin, Lush et al. 2011). This could be due to redundancy with other pathways, which could compensate for its absence, so I cannot exclude that NRG1 exposed on the surface of axons promotes oligodendrocyte survival in vivo.

It is remarkable that I observed little or no OPC developmental apoptosis in the spinal cord of WT, control animals. As mentioned previously, most CNS regions in mammals exhibit a significant proportion of dying OPCs, including up to 50% of all oligodendrocytes in the optic nerve (Barres, Hart et al. 1992). This species-difference is not limited to OPCs: developmental cell death of motor neurons also does not occur naturally in zebrafish (Lewis and Eisen 2003). In the case of OPCs, it could be related to the aforementioned observation that widespread OPC proliferation may simply not occur in zebrafish. Zebrafish OPCs may proliferate at a low, basal rate which may be enough to populate the zebrafish spinal cord. Thus, in WTs, there is no large excess of OPCs that needs to be trimmed down to match the available axonal area, and no significant apoptosis ensues. A survival cue from axons is still needed for the number of oligodendrocytes that do mature; a requirement which may simply be a feature of oligodendrocytes in all species.

3.4.5 Multiple mechanisms match OPC population size to available axonal surface

In an individual WT larva, I determined that over 12 hours, from 60-72hpf, 1-2 OPCs divide in 425μm of the posterior spinal cord of WT (corresponding to ~5% of all

OPCs in that region). If this rate persists through the next 24h, and based only on the 72hpf absolute numbers, I would expect that by 96hpf, ~6 OPCs are generated through OPC divisions. In mutants, OPC proliferation is roughly halved. Thus, by 96hpf, I would expect this proliferation defect to contribute with a reduction in ~3 OPCs compared to WT numbers.

I additionally observed that a subset of ventral oligodendrocyte-lineage cells die in the mutants, whereas developmental apoptosis was never observed in WTs. In an individual larva, I mostly observed only one such event over the same 12-hour period. If this rate persists for the next 24h, I would expect 3 OPCs to have died due to a missing survival signal at 96hpf.

Adding both effects, I would expect a reduction in ~6 oligodendrocyte-lineage cells in mutants compared to WT in a 425µm stretch of the posterior spinal cord. In fact, this is roughly the reduction I found when counting mature oligodendrocytes at 96hpf in a similar stretch of the spinal cord (Figure 3.4): I counted 30±6 total oligodendrocytes in WT versus 22±5 in mutant; and 21±4 ventral oligodendrocytes in WT versus 16±3 in mutants. Thus, the combination of both factors accounts for the reduction of mature oligodendrocyte number. This suggests that axons can regulate both OPC proliferation and survival to a certain extent, in what may be a mechanism to attempt to match OPCs to the existing axonal surface.

It remains formally possible that axons only actually regulate one of these aspects, and the second effect is a consequence of the first. For instance, it could be that reticulospinal axons only provide a survival signal, and not a mitogenic signal. When these axons are absent, a subset of oligodendrocyte-lineage cells dies, and the debris and cell death byproducts that are released into the milieu are inhibitory to the proliferation of other OPCs, which could occur autonomously. In the future, to address this possibility, it will be interesting to attempt to specifically block the apoptosis of oligodendrocyte-lineage cells in the *kbp* mutant. For instance, caspase-inhibiting peptides or p53 morpholinos (antisense oligonucleotides that interfere with expression of the target gene) have both been used in zebrafish to prevent the apoptotic signaling cascade (Williams, Barrios et al. 2000, Robu, Larson et al. 2007).

This would allow me to dissociate the proliferation phenotype from the survival phenotype.

Interestingly, in other contexts, when excessive numbers of OPC are generated in a cell-autonomous manner (for instance, in the spinal cord of PDGF-overexpressing mice (Calver, Hall et al. 1998), and of Neurofibromatosis type-1 mutant zebrafish (Lee, Padmanabhan et al. 2010, Shin, Padmanabhan et al. 2012)), the final number of mature oligodendrocytes is normal, as the number of OPCs is trimmed down through apoptosis. These findings support the fundamental model that axons can regulate the size the OPC population that matures into oligodendrocytes. It would be interesting to determine if the trimming down of numbers in these contexts is also due to competition for limited amounts of proliferative and survival signals derived from axons. If this is the case, then a prediction is that artificially increasing the axonal surface and axon-derived signals in these animals (for instance, in NF1 mutant zebrafish), would rescue some of apoptosis observed. In the next chapter, I will describe a strategy for increasing the axonal surface in zebrafish, which could be used to test this prediction.

It remains to be determined whether the reduced oligodendrocyte number in *kbp* mutants is actually matched to the remaining axonal surface. Note that specification of OPCs was not drastically affected, and in fact I observed in my time-lapse analysis that the emergence of most olig2+ sox10+ OPCs is due to *de novo* specification from olig2+ pMN progenitors, rather than proliferation of OPCs. Therefore, a core number of OPCs might still develop, but does their differentiation into oligodendrocytes occur normally, and is their myelination perfectly adequate to the axonal surface that remains? There was a drastic 80% reduction in the ventral axonal surface that is the initial target for myelination. Yet, at 4dpf, oligodendrocytes were reduced only in ~25%. Are they actually matched? If there is still a surplus of oligodendrocyte-lineage cells, how is their differentiation affected, if at all? I will address these questions in the next chapter.

In sum, my aim was to address whether previous in vitro and indirect in vivo findings that axon-derived signals can regulate aspects of oligodendrocyte-lineage development held true in the context of a living animal, in a physiological context that could be attributable to a direct effect of axons on OPCs. I demonstrated that reticulospinal axons do not regulate the proliferation of pMN progenitors, the generation of motor neurons, the specification of oligodendrocyte-lineage cells or their early migration patterns. Therefore these aspects of oligodendrocyte development are likely to follow an axon-independent programme. I then demonstrated that both proliferation and survival of OPCs are regulated by reticulospinal axons, the very first targets for myelination. They may represent both sides of the same coin in a mechanism that matches the size of the OPC population to the amount of axonal surface to be myelinated.

My work also highlighted some species differences to oligodendrocyte-lineage development in mammals. I did not observe widespread OPC proliferation or apoptosis in control, WT animals; whereas both of these occur extensively in several regions of the mammal CNS. It may be that the emergence of larger CNSs required, or followed, the evolution of mechanisms for expansion of the OPC population (such as PDGF-dependent proliferation, and secondary sources of OPCs), concomitantly with a mechanism for trimming down excess OPCs (based on competition for limited axonal signals that suppress an endogenous apoptotic programme). The primordial, primitive features of this mechanism may already be present in the teleost lineage that includes zebrafish, and may simply have been scaled up by evolution. Such scaling may even have been driven by axons – which could secrete novel factors or express more signals in mammals.

What happens subsequently? Can axons also regulate later aspects of oligodendrocyte development, such as the actual formation of myelin sheaths, or their maintenance, in vivo? Many oligodendrocyte-lineage cells survive in the posterior spinal cord of *kbp* mutants and differentiate into oligodendrocytes. They do so in an altered axonal environment. Can they form their myelin sheaths normally in this environment? In the next chapter, I will address these questions by determining

the fate of the surviving oligodendrocytes, and investigate whether their myelinating capacity is affected. I will also address these questions by adopting a "gain-of-function" strategy in which I will increase the axonal surface that is the initial target for myelination in the zebrafish spinal cord.

4. Axons regulate the myelinating capacity of individual oligodendrocytes

4.1 Introduction

The sequence of events that results in the emergence of a successfully myelinated axon from a neural precursor and a glial precursor is extremely complex. In Chapter 3, I demonstrated that the emergence of the first OPCs and their initial migration occur independently of axons, but that soon after, axons regulate proliferation and survival of oligodendrocyte-lineage cells in vivo. This likely constitutes a mechanism that contributes to match the size of the OPC population to the amount of axonal surface that will require ensheathment and myelination. This matching and migration into their target areas leads to population of the entire CNS by OPCs, a prerequisite for actual myelination. As each OPC ceases migrating and reaches its target area, it must sustain a programme of very dynamic extension and retraction of cellular processes (Fox, Afshari et al. 2006), presumably to sample potential targets and other structures not destined for myelination; such remodelling must be responsive to local signalling derived from contact with its milieu. The cell also likely centrally regulates its core level of process arborisation. As myelination approaches, oligodendrocyte-lineage cells remodel their plasma membrane, become less ramified, and maintain only those processes along which they will generate myelin sheaths (Hardy and Friedrich 1996). To start elaborating myelin sheaths, the cell must coordinate synthesis and delivery of many different structural components to the end of each process, and each component must be delivered at the appropriate time, rather than all simultaneously (Aggarwal, Yurlova et al. 2011). It shuttles specific proteins along those processes, but also specific messenger RNAs. Myelin basic protein, for instance, which is required for membrane compaction, is locally translated where myelin sheaths are being formed (Colman, Kreibich et al. 1982, Ainger, Avossa et al. 1993, Snaidero and Simons 2014). When myelination ensues, the cell must regulate the timing of synthesis and transport of each structural protein, but also regulate the timing and level of translation from those mRNAs localized to myelinating processes. This is in addition to the vast amounts of the specialized cellular membrane that it must synthesize – one rough estimation puts it at 1000 times the area of the soma membrane (Brady 2012). Another estimation is that during active myelination, the myelin surface area in each cell expands between

5000-50000 μm^2 each day, compared with the soma's surface area of about 300 μm^2 (Baron and Hoekstra 2010, Snaidero and Simons 2014). Individual oligodendrocytes can form up to 60 myelin internodes in adult mice, ranging from 20-200μm in length (Chong, Rosenberg et al. 2012). How does a single cell coordinate the complex events outlined above in all of its processes? Does every process belonging to the same oligodendrocyte receive the same myelin synthesis toolkit, and make identical myelin sheaths, as per the cell's central commands? If so, one would expect a single oligodendrocyte to make similar amounts of myelin and similar sheaths at the tip of all of its processes. Alternatively, the amount of myelin that is synthesized at the end of each process of an individual oligodendrocyte could be locally regulated by interaction with its target axon. Contact-dependent cues would regulate the extension, thickness and longitudinal growth of each particular sheath, and each oligodendrocyte should be able to generate different myelin sheaths on vastly different axons. In line with this, in global ultrastructural analyses of myelination in many CNS regions, the thickness and length of each myelin sheath is often precisely adjusted to each axon, suggesting local regulation. However, local regulation of myelin biogenesis in a process-specific manner remains to be unambiguously demonstrated in vivo. To address which hypothesis represents the fundamental mode of myelin formation, one must carefully observe an individual oligodendrocytes' formation of its full complement of myelin sheaths.

Since Pio del Rio Hortega's original descriptions of oligodendroglia almost 100 years ago (Río-Hortega 1928), the same types of oligodendrocyte morphologies are repeatedly found: oligodendrocytes tend to either elaborate many myelin sheaths on small-caliber axons or very few sheaths on large-calibre axons (Remahl and Hilderbrand 1990, Bjartmar, Hildebrand et al. 1994). Reports have described a molecular correlate of this heterogeneity – for instance, carbonic anhydrase II staining labels only those oligodendrocytes making many small-caliber myelin sheaths (Butt, Ibrahim et al. 1995).

This would suggest that each cell centrally controls the delivery of myelin components and every process produces the same amount of myelin. Different oligodendrocyte morphologies would then represent different specialized subtypes of

oligodendrocytes, each subtype fixed to myelinate a particular calibre, i.e., make a particular amount of myelin at the end of every process. In this scenario, the myelinating potential of oligodendrocytes is a fixed, intrinsic property of each cell, that could be specified prior to myelination, and be consequence of each individual oligodendrocyte's inherent program of development. In a complex environment with many types of axons (such as the spinal cord), a "small-calibre axon"-oligodendrocyte, upon contacting and sampling the axonal environment, would only specifically recognize or stabilize contacts with small calibre axons, promoting subsequent ensheathment and myelin formation, and would ignore or actively retract processes that contact large-calibre axons. A slightly different hypothesis is that every OPC/oligodendrocyte is potentially capable of myelinating any competent axon, but upon contacting its first axonal target, the whole cell becomes committed to those types of axons and the myelinating potential of that cell becomes fixed thereafter. Whichever molecular mechanisms would underlie the emergence of such subtypes, whether cell-autonomous or dependent on initial axonal interactions, remain completely unknown in the CNS.

However, an alternative explanation for the different types of oligodendrocyte morphology remains, which does not require central control of myelin biosynthesis. Communication with the target axon could locally regulate each oligodendrocyte process to produce a specific amount of myelin. The complement of myelin sheaths of each cell would then reflect only the influence and constraint of the axons it contacts. The observed tendency of oligodendrocytes to myelinate either large or small diameter axons may simply reflect different timings of axonal development, with different cohorts of the same axons becoming competent for myelination at different times. For instance, the whole cohort of large-diameter axons in a tract may become competent for myelination initially, and tracts containing small diameter axons become competent later with little overlap between the two periods, which has been inferred to happen in mammals (Matthews and Duncan 1971, Butt and Berry 2000).

Thus, the extent to which axons are capable of locally regulating the formation of myelin sheaths in vivo remains unclear. Despite the observed classes of

oligodendrocyte morphologies, oligodendrocyte-lineage cells may still be plastic and able to myelinate any axon that is competent for myelination, irrespective of its caliber, location, neurotransmitter phenotype or other characteristics. The studies describing the heterogeneity of oligodendrocyte morphology and its possible relation with timing of differentiation or axonal calibre are purely correlational; few studies to date address causality. In addition to being able to carefully observe the morphology of individual oligodendrocytes, one must be able to manipulate their axonal targets. If axons locally regulate myelin sheath formation, and oligodendrocytes are plastic in relation to the axons they myelinate, then when artificially challenged with an axonal environment different from what they are normally exposed to during development, they should be able to adapt and myelinate them. For instance, if transplanted into a different region of the CNS, oligodendrocytes should be able to myelinate their new targets; if, alternatively, they represent a fixed subtype of oligodendrocytes, they won't be able to myelinate them.

A hint as to the plasticity of oligodendrocytes and the nature of myelin sheath formation comes from the study of demyelinating diseases such as multiple sclerosis. Following a demyelinating lesion, latent, adult OPCs are capable of differentiating and forming myelin (Franklin and Ffrench-Constant 2008) in what must perforce be an axonal environment drastically different from the developmental situation. Demyelinated axons are much larger and mature than their developmental counterparts were upon initial myelination, and have a distinct state of physiological activity. Adult OPCs can form myelin around them, suggesting that these cells are plastic and can myelinate any axon; however, it could be argued that such adult OPCs represent a specialized, fundamentally different subtype than developmental OPCs, and that this does not represent the general mode of myelin sheath formation. Additionally, remyelinated axons have shorter and thinner myelin sheaths (Franklin and Ffrench-Constant 2008), suggesting that even if these are bona-fide OPCs, the plasticity they show is limited, or the lesioned milieu and demyelinated axons are not capable of recapitulating their developmental signaling.

In a transplantation study in rat, (Fanarraga, Griffiths et al. 1998) isolated optic nerve oligodendrocyte-lineage cells and transplanted them into the spinal cords of *myelin*-

deficient rats, which are deficient for Proteolipid protein and never show any normal compact myelin. The optic nerve is constituted by fairly homogenous small-diameter axons, and optic nerve oligodendrocytes are therefore only typically exposed that narrow range of small axonal calibres. On the other hand, the spinal cord contains a variety of axons of different caliber, including some of the largest axons in the CNS (Hildebrand, Remahl et al. 1993). 10-14 days after transplantation, compact myelin was evident in transversal sections of the spinal cord of the receiving mutant mice, which could not be made by endogenous oligodendrocytes. This indicates that the transplanted cells integrated, differentiated and were able to make myelin sheaths in a vastly different environment from what they usually encounter. The transplanted cells myelinated axons of a very large caliber that they would never encounter in the optic nerve – strongly suggesting that these cells are indeed plastic, and not predetermined to myelinate a subset of axons of a specific caliber. This study, however, could not exclude the hypothesis that already at the OPC stage there may be inherently different subtypes only able to myelinate certain calibers; these may remain undifferentiated in the optic nerve but upon transplantation would contribute to the myelination of very large spinal cord axons. Indeed, around 45% of total transplanted cells had the antigenic phenotype of OPCs. It also remains possible in this paradigm that all OPCs initially have the potential to myelinate any axon, but during contact with its first target, the oligodendrocyte becomes committed to similar axons thereafter.

Although this study challenged oligodendrocyte-lineage cells with a different set of target axons, its readout (transversal sections of the spinal cord) did not allow assessment of the array of myelin sheaths each individual oligodendrocyte made and the size of each sheath, as is the case for the majority of in vivo myelination studies. Essentially, the question remains as to whether the generation, maintenance and growth of myelin sheaths are intrinsically determined in oligodendrocytes, or can be regulated by axons. Recent observations that myelination may be influenced by experience strongly support the latter. For instance, in socially isolated mice, myelin structure and oligodendrocyte transcription (Liu, Dietz et al. 2012), and oligodendrocyte morphology (Makinodan, Rosen et al. 2012) are altered compared to control. Conversely, housing rats in an enriched environment increased the number

of myelinated fibers in the corpus callosum, in parallel with improved performance in a spatial learning task (Zhao, Shi et al. 2012). Training rats in a limb-reaching motor task induced an alteration in the relevant white matter tract associated with the sensorimotor cortex, concomitantly with increased myelin staining (Sampaio-Baptista, Khrapitchev et al. 2013). In humans, piano practice (Bengtsson, Nagy et al. 2005), or juggling (Scholz, Klein et al. 2009), induce microalterations in the relevant white matter tracts that are compatible with changes in myelination. In general, however, it remains to be determined which particular aspect of myelination is influenced, as some of these changes could be explained by de novo myelination, myelin remodelling, changes in the calibre of myelinated fibers, or oligodendrocyte turnover.

In this chapter, I describe strategies in which I challenge the oligodendrocyte-lineage cells with different axonal environments and analyze individual oligodendrocyte morphology in vivo to begin to address two fundamental aspects about the mode of myelin sheath formation:

First, what determines the myelinating capacity (the amount of myelin) of oligodendrocyte-lineage cells? In the rat anterior medullary vellum, oligodendrocytes that myelinate many small axons are estimated to maintain a volume of myelin of around ~600 μm^3, while oligodendrocytes that myelinate few large axons can maintain up to ~30000 μm^3 (Butt, Ibrahim et al. 1998). Is there a maximum, and do oligodendrocytes normally myelinate at full capacity? Can axons regulate that capacity, by modulating the number, length or thickness of the myelin sheaths that each oligodendrocyte makes? Alternatively, is the amount of myelin that each oligodendrocyte makes an inherent property of each cell, specified early on? In the long-term, determining the signaling pathways that regulate the myelinating capacity of oligodendrocytes will contribute, for instance, to the search for repair strategies following demyelinating lesions. Why are myelin sheaths in remyelinated axons thinner and shorter? Do they adequately restore long-term function? In later stages of multiple sclerosis, endogenous remyelination eventually fails, despite the presence of OPCs in the lesions. Can we target developmental signals that regulate the myelinating capacity of oligodendrocyte-lineage cells to maximize remyelination?

Second, do oligodendrocyte-lineage cells centrally coordinate the formation of myelin sheaths and distribute the same myelin synthesis toolkit to the tip of every process? That is, are all myelin sheaths made by an individual oligodendrocyte similar? Occasionally oligodendrocytes myelinate both small and large-calibre axons, but these seem to be a very small minority. Could they be a particular, more plastic subtype of oligodendrocytes? Alternatively, can axons locally control the formation of myelin sheaths in each oligodendrocyte process? That is, can individual oligodendrocytes form myelin sheaths of different size, and myelinate small and large-calibre axons in parallel? If so, the rarity of oligodendrocytes that myelinate large and small axons could simply be due to a very narrow time window in which different types of axons could be simultaneously competent for myelination, as well as be in close proximity.

What is the relevance of finding the answer to these questions? Myelin and white matter alterations have recently been associated with a range of neuropsychiatric disorders, but also with learning and memory in several motor and cognitive tasks (Fields 2008, Zatorre, Fields et al. 2012). In principle, myelin sheath formation and myelinating capacity may be a crucial parameter regulated throughout life and underlying these alterations (Wang and Young 2014). Its dysregulation may directly contribute to a range of disorders. For instance, ErbB4 has been linked to susceptibility to schizophrenia and bipolar disorder. Mice where ErbB4 function is inactivated in oligodendrocytes (Roy, Murtie et al. 2007), and mice raised in social isolation (Makinodan, Rosen et al. 2012) have oligodendrocytes that form fewer and thinner myelin sheaths, leading to a hypomyelinating phenotype and reduced nerve conduction velocity. These mice also exhibit dopaminergic alterations and behavioural changes consistent with a schizophrenic-like phenotype. Elucidating the mechanisms underlying the regulation of sheath formation and oligodendrocyte morphology may help us understand the basis of behavioural and cognitive changes observed not only in a range of conditions, but also in normal aging.

4.2 **Aims**

My general aim is to address whether the myelinating capacity of individual oligodendrocytes in the zebrafish spinal cord can be influenced by their target axons or whether it is a restricted property that is intrinsically determined in oligodendrocytes. To address this, I examined the morphology of individual oligodendrocytes challenged with a different set of target axons to myelinate than they usually encounter: in animals with substantially fewer axonal targets and in animals with supernumerary axonal targets.

In the posterior spinal cord of *kbp* mutants, the number of the initial axonal targets, the reticulospinal axons (including the large-calibre Mauthner axons), is decreased, leading to a drastic 80% reduction in axonal surface available for contact-dependent interactions with oligodendrocyte-lineage cells (see Chapter 3). Interestingly, the number of oligodendrocyte-lineage cells is concomitantly decreased, but only by ~25%. Thus, a potential excess of oligodendrocyte-lineage cells exist in the posterior spinal cord of *kbp* mutants in relation to the amount of target axonal surface. I aimed to determine if this axonal environment could affect the differentiation and morphology of the remaining oligodendrocyte-lineage cells.

I also sought to independently manipulate the axonal environment in the opposite direction, and challenge oligodendrocyte-lineage cells with increased axonal surface to myelinate. I aimed to characterize oligodendrocyte-lineage cells in animals in which the number of initial target axons (reticulospinal axons, and in particular the readily identifiable Mauthner axon) is substantially increased.

These non-invasive manipulations will offer the added advantage over transplantation studies of examining these cells in their endogenous, physiological environment.

4.3 Results

In the posterior spinal cord of *kbp* mutants, many OPCs differentiate into mbp:EGFP+ myelinating oligodendrocytes by 4dpf, but they do so in an environment with a drastic reduction in the amount of target axonal surface. To be able to examine single oligodendrocyte-lineage cells from their OPC stage through to maturation into oligodendrocytes, I generated the transgenic line sox10:KalTA4, where the transcription factor KalTA4 (an optimized version of Gal4 (Distel, Wullimann et al. 2009)) is expressed in oligodendrocyte-lineage cells. By crossing it with the reporter UAS:kaede, the fluorescent protein kaede is expressed in a variegated, mosaic fashion in the cytoplasm of some sox10+ cells. In the spinal cord, in addition to oligodendrocyte-lineage cells, the sox10:KalTA4 line labels a subset of dorsal neurons, radial glia and floor plate cells, which are readily identifiable by morphology and location and were excluded from the analysis. Cells were identified as OPCs if they expressed the fluorescent reporter kaede, resided in their characteristic locations in the spinal cord and if they had multiple branched processes (Figure 4.1 A). If those processes became less branched and terminated in tubular structures (myelin sheaths), I considered those cells as having matured into oligodendrocytes (Figure 4.1 A).

4.3.1 Surviving OPCs don't wait to differentiate

I first wondered whether axons can regulate the timing of differentiation: OPCs could take longer to differentiate in the absence of their reticulospinal axonal targets. As described in Chapter 3, a subset of oligodendrocyte-lineage cells undergoes apoptosis in *kbp* mutant; I excluded that subset from this analysis.

I identified 66 OPCs in 16 WT larvae and 48 OPCs in 10 mutant larvae at 60hpf or 72hpf, and assessed whether they had matured into oligodendrocytes by 96hpf. A similar proportion of all cells identified in WT and mutants transitioned into mature,

myelinating oligodendrocytes by 96hpf – 62/66 WT cells and 46/48 mutant cells (Figure 4.1).

These results indicate that in the absence of a significant number of target axons, surviving OPCs differentiated on time. This suggests that either the exact timing of OPC differentiation is an intrinsically determined feature of each cell, or that the remaining axons are sufficient to provide a timely differentiation cue for the surviving OPCs. In any case, OPCs do not require an exact complement of specific individual axons to differentiate, as the axonal complement is drastically altered in the mutants' spinal cord.

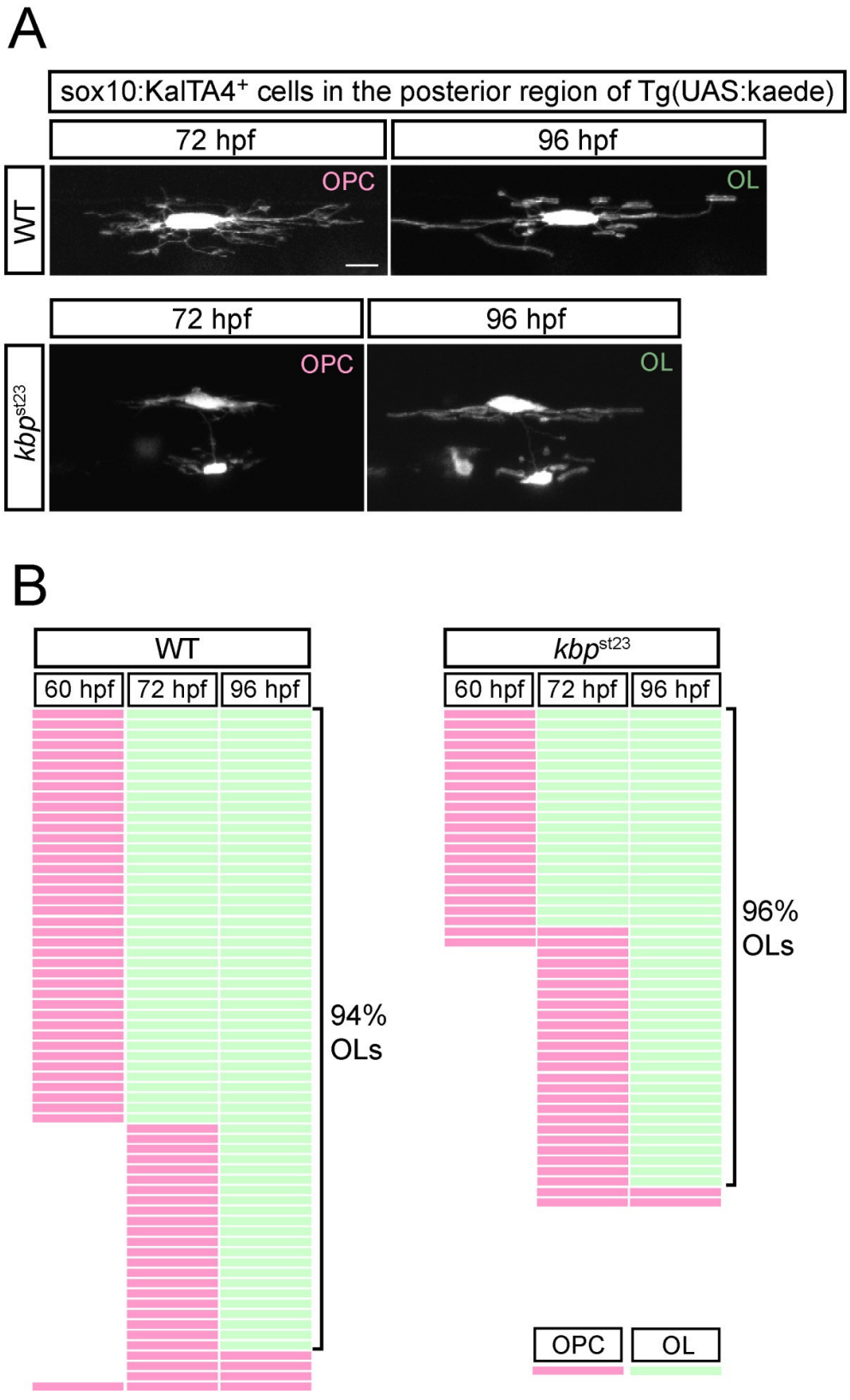
A
sox10:KalTA4+ cells in the posterior region of Tg(UAS:kaede)
72 hpf
96 hpf
WT
OPC
OL
72 hpf
96 hpf
kbpst23
OPC
OL
B
WT
60 hpf
72 hpf
96 hpf
94%
OLs
kbpst23
60 hpf
72 hpf
96 hpf
96%
OLs
OPC
OL

Figure 4.1 – In the posterior spinal cord of *kbp*^{st23} mutants, surviving OPCs do not wait to differentiate

(**A**) Individual oligodendrocyte-lineage cells of Tg(UAS:kaede) larvae at 72-96hpf microinjected with sox10:KalTA4 plasmid at the one-cell stage. Sparse expression of KalTA4 from the plasmid trans-activates expression of the cytoplasmic fluorescent reporter protein kaede in a subset of sox10+ cells. Both in WT (top) and in mutant larvae (bottom), OPCs are readily morphologically distinct from mature oligodendrocytes at 96hpf, which present myelin sheaths. Scalebar: 10 μm.
(**B**) List of all cells identified as OPCs in WT or mutant larvae at either 60hpf or 72hpf and monitored through to 96hpf. Each row represents a cell; a magenta box indicates an OPC morphology (no myelin sheath profiles, ramified processes) and a green box indicates a mature oligodendrocyte morphology (myelin sheath profiles). In both WT and mutant larvae, a similar proportion of OPCs identified at 60 or 72hpf differentiate by 96hpf.

4.3.2 Surplus OPCs don't myelinate incorrect axons

Given the potential excess of surviving oligodendrocyte-lineage cells, I then wondered if the remaining axons could regulate the myelinating capacity of oligodendrocytes as an additional way of matching to the available axonal surface. In the absence of a substantial proportion of their normal axonal targets, OPCs could make less myelin, or alternatively could incorrectly or prematurely myelinate other axons, in different territories than what they usually do in WTs.

I first investigated whether surviving oligodendrocyte-lineage cells in the posterior spinal cord of *kbp* mutants would myelinate their normal targets by 96hpf. To address this, I compared mutant oligodendrocyte morphology with the morphology of oligodendrocytes in WT larvae. I mosaically labeled oligodendrocytes by crossing mbp:Gal4 animals with a Tg(UAS:kaede) reporter. Double transgenic animals express Gal4 in many myelinating oligodendrocytes, which in turn activates expression of the cytoplasmic fluorescent protein kaede in a random subset of mbp+ cells. I imaged sparsely labelled oligodendrocytes at 96hpf (Figure 4.2).

Combined with the previous data set at 96hpf (from Figure 4.1), I assessed the axonal targets of a total of 223 oligodendrocytes from 29 WT larvae and 131 oligodendrocytes from 16 mutant larvae.

In WTs, 114/ 223 oligodendrocytes associated only with Mauthner myelin sheaths. These oligodendrocytes had a very stereotyped location just ventral to the Mauthner axon, and mostly extended just one long and large sheath on the Mauthner axon (example is cell *e* in Figure 4.2). In contrast, in mutant animals, which lack Mauthner axons in the posterior spinal cord, I never observed oligodendrocytes with such morphology (0/ 131)

In WT animals, the remaining ventral oligodendrocytes (71 cells) tended to myelinate numerous small caliber axons in the ventral or medial spinal cord (Figure 4.2, cells a, b and c). Some ventral oligodendrocytes (17/71 ventral cells, 24%) also ensheathed motor axons as they exit the spinal cord in the ventral roots (Figure 4.2,

cell b, red arrowhead). Occasionally, ventral oligodendrocytes ensheathed axons in the dorsal tract of the spinal cord (Figure 4.2, cell b, 4/71 ventral oligodendrocytes). In mutant animals, ventral oligodendrocytes mostly myelinated ventral and medial axons (Figure 4.2, cells f, g and h), and the proportion ensheathing motor axons (Figure 4.2, cell g) is similar to WT: 27/88 ventral cells (31%). Ventral oligodendrocytes in mutant larvae also occasionally ensheathed more dorsal axons (4/88 ventral cells, Figure 4.2, cell f).

Dorsal oligodendrocytes typically ensheathed dorsal or medial axons in WTs (Figure 3.17, cell d) and in mutant animals.

Thus, there is no drastic alteration in the types of axons that are ensheathed by oligodendrocyte-lineage cells when reticulospinal axons are absent. Specifically, in the ventral spinal cord where reticulospinal axons are absent, oligodendrocytes do not prematurely or incorrectly myelinate other axons, such as motor axons, or axons in the more distant dorsal tract. I therefore wondered if oligodendrocyte-lineage cells were making less myelin in response to the greatly decreased target axonal surface.

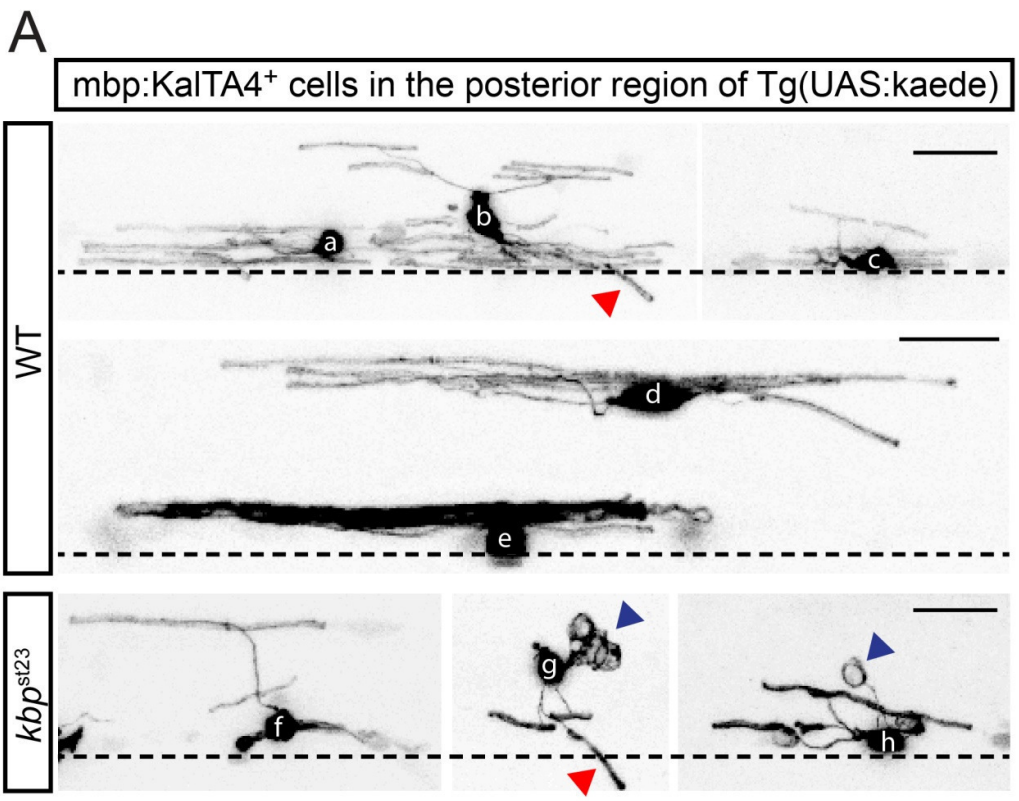

Figure 4.2 – In the posterior spinal cord of *kbp*^{st23} mutants, surviving OPCs do not myelinate incorrect axons or axonal tracts

(**A**) Individual mbp:KalTA4+ mature oligodendrocytes in 4dpf Tg(UAS:kaede) larvae. The dashed line indicates the ventralmost limit of the spinal cord. Red arrowheads point to examples of oligodendrocyte-ensheathed motor axons outwith the spinal cord. Blue arrowheads point to examples of circular profiles resembling ensheathed somas. See text for more details. Scalebars: 20 μm.

4.3.3 Extent of oligodendrocyte myelination is decreased in *kbp* mutants

To investigate whether the extent of myelination of individual oligodendrocytes was affected in the absence of reticulospinal axons, I imaged individual mbp:EGFP-CAAX+ oligodendrocytes at high-resolution (Figure 4.3 A). Injection of mbp:EGFP-CAAX plasmid DNA in newly fertilized eggs results in sparse, stochastic, mosaic expression of the transgene, rather than in all cells of the relevant type. I focused on the morphology of ventral oligodendrocytes, since my target analysis indicated that these are most likely to ensheath reticulospinal axons in WT (Figure 4.2).

I first determined the number of myelin sheaths made by each oligodendrocyte. In the anterior spinal cord, the number of myelin sheaths was variable, and did not reach a statistically significant difference between WT and mutant ventral oligodendrocytes. In the posterior spinal cord, mutant ventral oligodendrocytes made on average 3 myelin sheaths less than WT ventral oligodendrocytes (Figure 4.3 B). This result indicates that oligodendrocytes adapt to the reduced axonal surface by reducing the number of myelin sheaths they make, and suggests that axons can regulate the formation of myelinating processes. Interestingly, when I combined the data for all oligodendrocytes in the spinal cord (ventral and dorsal, indicated in the legend of Figure 4.3), the difference in the posterior region became non-significant statistically, although the trend remained. This may be due to the high variability of sheath number observed per oligodendrocyte (otherwise already well documented (Almeida, Czopka et al. 2011, Chong, Rosenberg et al. 2012)), and a reduced power of this analysis. Alternatively, it may hint that dorsal oligodendrocytes are not quite as affected as ventral oligodendrocytes, highlighting the potential contact-dependence of this regulation, as reticulospinal axons are missing specifically from the ventral spinal cord.

I additionally determined the average length of each myelin sheath made by ventral oligodendrocytes (Figure 4.3 C), as well as the combined total length of myelin sheaths per ventral oligodendrocyte (Figure 4.3 D). Both parameters were significantly reduced in the posterior spinal cord of mutants. This suggests that

oligodendrocytes also adapt to the reduced axonal surface by reducing the length of the myelin sheaths they make, and that axons can locally regulate the growth of myelin sheaths. Surprisingly, however, both parameters were also significantly reduced in the anterior spinal cord. When I combined the data for ventral and dorsal oligodendrocytes (indicated in the legend of Figure 4.3), these differences remained strikingly significant, in both the anterior and posterior spinal cord, indicating that all oligodendrocytes are affected.

This suggests that *kbp* itself, which is globally knocked out, may regulate the growth of myelin sheaths. It is less likely that this phenotype is due to the specific absence of reticulospinal axons, which only affects the posterior region (see Discussion). It will be very interesting to determine whether this reduction in the size of myelin sheaths relates to the function of *kbp* in axons or in oligodendrocyte-lineage cells.

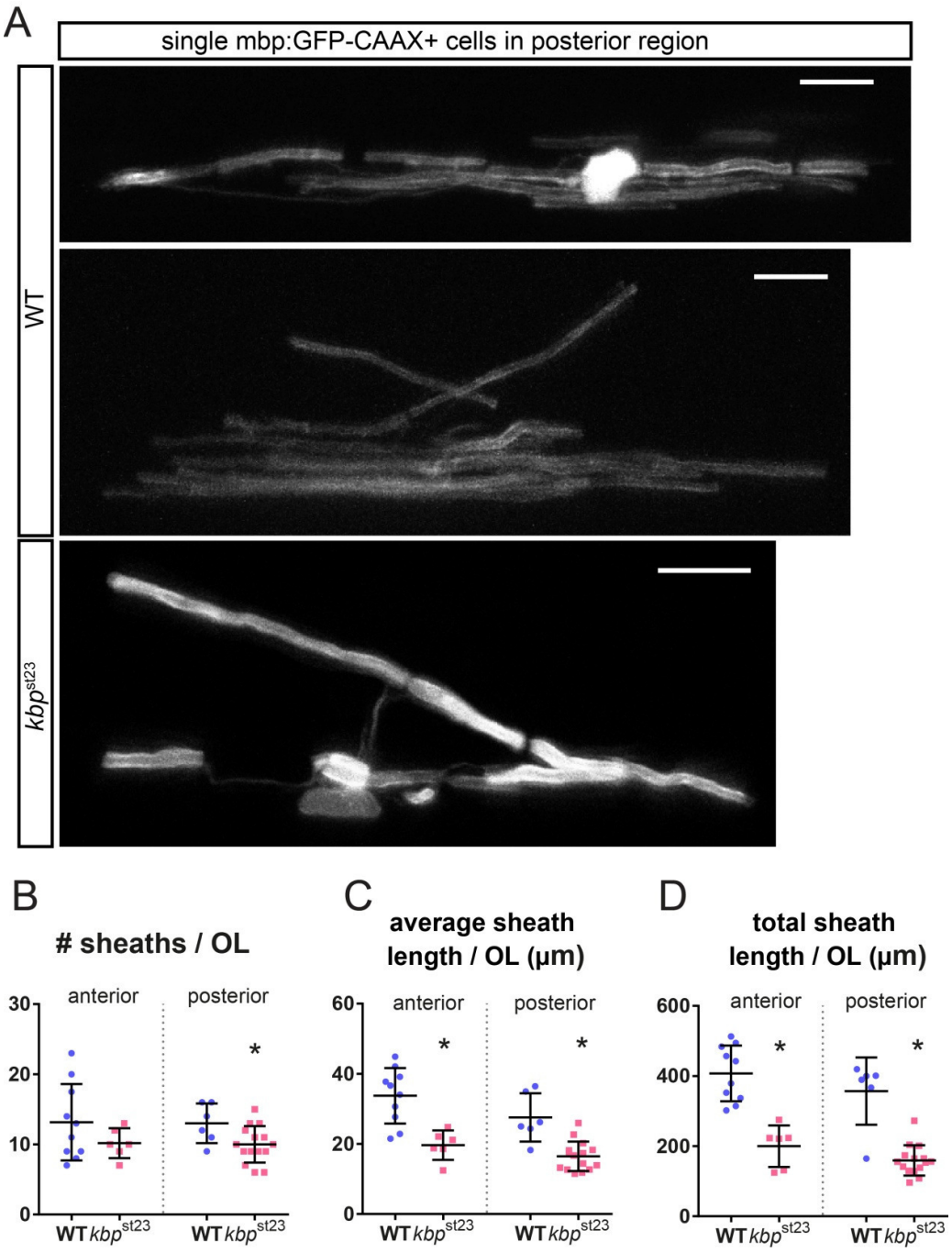
A
single mbp:GFP-CAAX+ cells in posterior region
WT
kbp^st23
B
sheaths / OL
anterior
posterior
30
20
10
0
WT kbp^st23
WT kbp^st23
C
average sheath length / OL (µm)
anterior
posterior
60
40
20
0
WT kbp^st23
WT kbp^st23
D
total sheath length / OL (µm)
anterior
posterior
600
400
200
0
WT kbp^st23
WT kbp^st23

Figure 4.3 – Oligodendrocyte myelinating capacity is reduced in *kbp*^{st23} mutants

(**A**) Single mbp:GFP-CAAX+ oligodendrocytes in the posterior region of 4dpf WT and *kbp* mutant larvae. Note fewer and shorter sheaths in mutant oligodendrocyte. Scalebars: 10 μm.

(**B**) Quantification of myelin sheath number per ventral oligodendrocyte. Error bars represent standard deviation.
Ventral oligodendrocytes:
Anterior: 13±5 (N=10 WT) vs 10±2 sheaths (N=6 mutant), p=0.4063 in t-test
Posterior: 13±3 (N=6 WT) vs 10±3 sheaths (N=15 mutant), p=0.0304 in t-test
All oligodendrocytes (ventral and dorsal):
Anterior: 14±5 (N=18 WT) vs 13±5 sheaths (N=11 mutant), p=0.7517 in t-test
Posterior: 14±3 (N=10 WT) vs 12±4 sheaths (N=17 mutant), p=0.1997 in t-test

(**C**) Quantification of average myelin sheath length per ventral oligodendrocyte. Error bars represent standard deviation.
Ventral oligodendrocytes:
Anterior: 34±8 (N=10 WT) vs 20±4 μm (N=6 mutant), p=0.0013 in t-test
Posterior: 28±7 (N=6 WT) vs 16±4 μm (N=15 mutant), p=0.0002 in t-test
All oligodendrocytes (ventral and dorsal):
Anterior: 32±8 (N=18 WT) vs 20±5 μm (N=11 mutant), p=0.0002 in t-test
Posterior: 28±6 (N=10 WT) vs 16±4 μm (N=17 mutant), p<0.0001 in t-test

(**D**) Quantification of total, combined myelin sheath length per ventral oligodendrocyte. Error bars represent standard deviation.
Ventral oligodendrocytes:
Anterior: 408±80 (N=10 WT) vs 200±59 μm (N=6 mutant), p<0.0001 in t-test
Posterior: 357±96 (N=6 WT) vs 159±43 μm (N=15 mutant), p=0.0007 in Mann-Whitney test
All oligodendrocytes (ventral and dorsal):
Anterior: 406±82 (N=18 WT) vs 261±100 μm (N=11 mutant), p=0.0002 in t-test
Posterior: 381±84 (N=10 WT) vs 182±68 μm (N=17 mutant), p<0.0001 in Mann-Whitney test

4.3.4 Oligodendrocytes incorrectly myelinate neuronal somas in *kbp* mutants

Surprisingly, although I didn't observe incorrectly myelinated axons in the mutant posterior spinal cord, I frequently observed unusual circular profiles at the end of processes of mutant oligodendrocytes (Figure 4.4, blue arrowheads). These circular profiles occurred in addition to normal, tubular looking myelin sheaths. The number of such profiles was variable between cells, sometimes occurring in clusters (Figure 4.4, cell g), or isolated (Figure 4.4, cell h). In my mosaic analysis of mature oligodendrocytes at 96hpf, I observed such profiles in 19/66 oligodendrocytes in mutant larvae (29%), and only in 1/38 oligodendrocytes in WT larvae (3%).

I also identified such profiles in the previous data set of time-coursed mosaic oligodendrocyte-lineage cells (sox10:KalTA4; UAS:kaede). Interestingly, at 72hpf, 5/72 WT oligodendrocytes possessed such profiles, but 3 of these retracted them, as they were not present at 96hpf, totaling 2/72 oligodendrocytes at this time point (3%). In comparison, 9/66 mutant oligodendrocytes exhibited such profiles (14%) at 96hpf, with no cases of retraction.

This suggests that the formation of such unusual profiles occurs at a low level in WT larvae, and is corrected as oligodendrocyte-lineage cells develop; in *kbp* mutants, such profiles are maybe formed more often, or not corrected.

The location and shape of these circular profiles is consistent with the hypothesis that they are cell somas. To exclude the possibility that they were oligodendrocyte somas that aberrantly expressed the reporter fluorescent protein, I analyzed the double transgenic line mbp:EGFP-CAAX; mbp:EGFP, in which both membrane-tethered and cytoplasmic GFP are expressed in all myelinating oligodendrocytes. In this line both the processes and myelin sheaths of every oligodendrocyte are labelled, as well as the cell somas of actual oligodendrocytes (with cytoplasmic GFP). I also readily observed many such profiles in this line (Figure 4.4A), indicating that they represent ensheathments of non-oligodendrocyte lineage cell somas. Both dorsal (Figure 4.4 A, cell a) and ventral oligodendrocytes (Figure 4.4 A, cells b, c and d) bore such circular profiles. These profiles could be made close to the oligodendrocyte cell body (Figure

4.4 A, cell a) or at a distance (Figure 4.4 A, cell b), and were present both in the ventral spinal cord (Figure 4.4 A, cell c) and in more dorsal regions (Figure 4.4 A, cells a and b). Additionally, I occasionally observed incomplete circular profiles, resembling partially ensheathed somas (Figure 4.4 A, cell d).

I quantified the number of such profiles in the anterior and posterior region of WT and mutant spinal cords (Figure 4.4 B). At 4dpf, mutant larvae had significantly more circular profiles than WT in the posterior region. Strikingly, mutant larvae also had more aberrant profiles in the anterior region. This was not a transient phenomenon, as the number of circular profiles remained increased in mutants in the posterior region at 8dpf.

I confirmed the identity of the cells ensheathed in these profiles by analyzing double transgenic lines Tg(glyt2:GFP; sox10:mRFP) and Tg(pax2:GFP; sox10:mRFP). In these lines, cytoplasmic GFP is expressed in a subset of interneurons in the spinal cord (either glycinergic, or expressing the transcription factor pax2), and membrane-tethered RFP labels the membrane of oligodendrocyte-lineage cells. At 3dpf, I readily observed GFP+ neurons partially or totally covered by oligodendrocyte mRFP+ membrane (Figure 4.4 C).

Thus, in *kbp* mutants, oligodendrocyte-lineage cells aberrantly ensheath neuronal somas. The mechanistic basis for this phenotype is likely to relate to the global lack of *kbp* function, in either axons or oligodendrocytes, since it also occurs in the anterior spinal cord, where reticulospinal axons are still present (see Discussion).

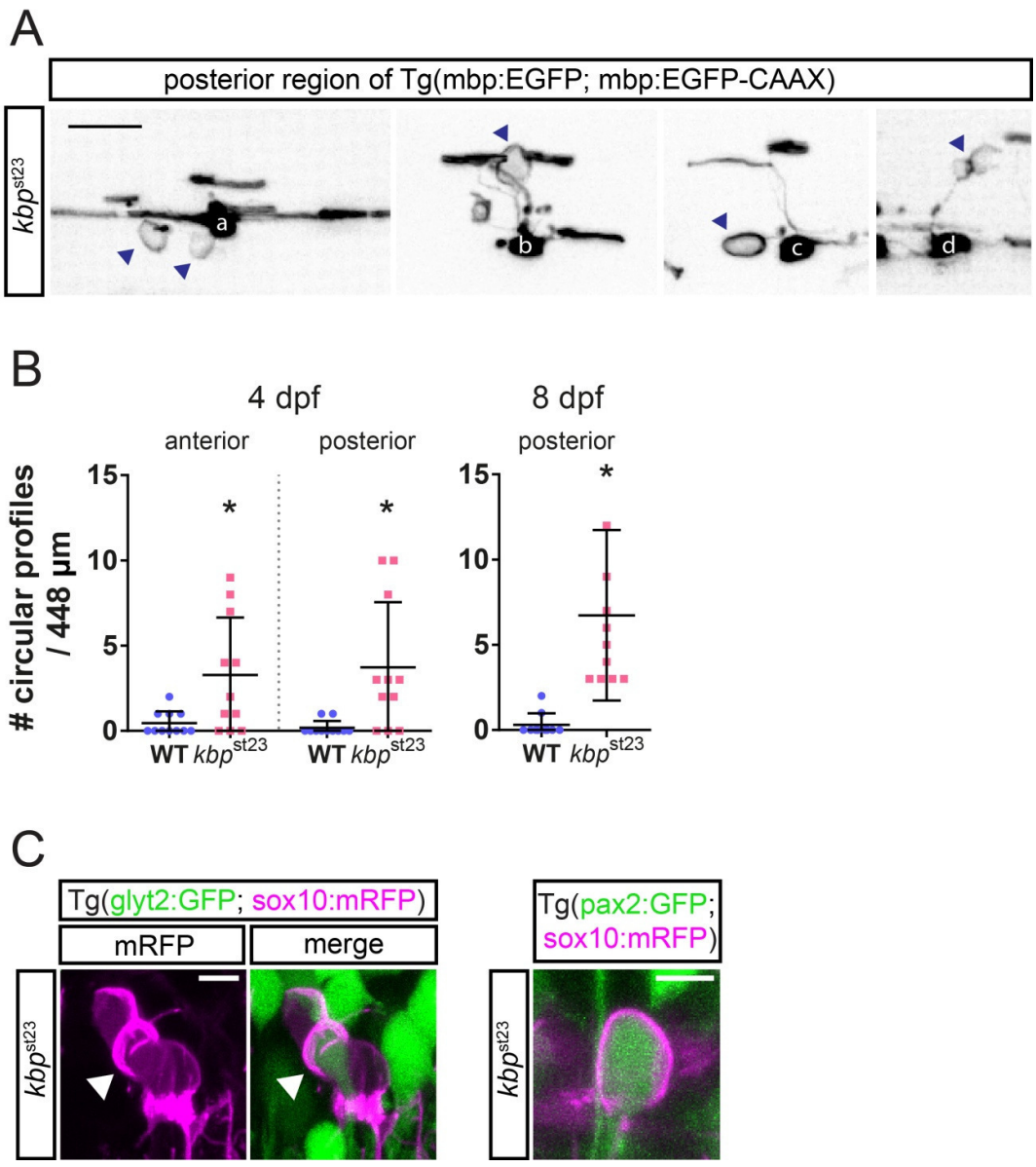

Figure 4.4 – In *kbp*^{st23} mutants, OPCs aberrantly wrap neuron somas.

(**A**) Representative mutant mbp:GFP+ oligodendrocytes (dark cells, labelled with letters) bearing mbp:GFP-CAAX+ circular profiles (blue arrowheads) in the posterior region of 4dpf Tg(mbp:EGFP; mbp:EGFP-CAAX). Scalebars: 20 µm.

(**B**) Number of circular profiles in a 448 µm length of tissue. All p values are from Mann-Whitney tests:

4dpf, anterior: 0.5±0.7 (N=11 WT) vs 3.3±3.4 profiles (N=11 mutant), p=0.0257

4dpf, posterior: 0.2±0.4 (N=11 WT) vs 3.7±3.8 profiles (N=11 mutant), p=0.0022

8dpf, posterior: 0.3±0.7 (N=10 WT) vs 6.7±5.0 profiles (N=11 mutant), p<0.0001

(**C**) Example of Glyt2:GFP+ (left) and Pax2:GFP+ (right) neurons wrapped by sox10:mRFP+ oligodendrocyte membrane in double transgenic larvae Tg(glyt2:GFP; sox10:mRFP) or Tg(pax2a:GFP; sox10:mRFP), at 72hpf. Scalebars: 5 µm

In sum, of the oligodendrocytes that survive and differentiate in the *kbp* mutant, there are variable alterations in morphology in comparison to WT oligodendrocytes.

Some of these alterations occur specifically in the posterior spinal cord where the reticulospinal axons are absent: for instance, ventral oligodendrocytes in that region extend fewer myelin sheaths, suggesting that axons regulate the extension of new myelin sheaths. Ventral oligodendrocytes may be more affected than dorsal oligodendrocytes, which could hint that this regulation occurs locally and requires contact.

Other alterations include the observation that myelin sheaths were shorter, and the combined length of all the sheaths that an individual oligodendrocyte extends is also smaller. This difference occurred both in ventral and dorsal oligodendrocytes. Additionally, I also observed that oligodendrocytes extend myelin sheaths aberrantly around neuronal somas. Strikingly, however, these alterations also occur in the anterior spinal cord, where reticulospinal axons are present. Therefore, these alterations may be due to the global lack of *kbp*. It will be very interesting to determine whether *kbp* functions in oligodendrocytes to promote the growth of myelin sheaths, for instance, or in neurons to prevent the ensheathment of neuronal somas (see Discussion).

The potential role of *kbp* itself in causing these phenotypes precluded concluding whether axons are able to regulate oligodendrocyte myelinating capacity. If axons do directly regulate the growth or localization of myelin sheaths, then a prediction is that providing additional axonal signals might increase oligodendrocyte myelinating capacity, in the opposite direction of the *kbp* manipulation. I therefore sought an experimental way to address this prediction, by increasing the target axonal surface.

4.3.5 Generation of zebrafish with supernumerary Mauthner axons

I sought to provide a "gain-of-function" approach to address whether axons can regulate myelination. I generated animals in which supernumerary Mauthner axons are formed in the spinal cord, in two genetic independent manipulations: temporary knockdown of *notch1a* function and transient overexpression of *hoxb1* genes.

Loss of Notch1a receptor function has been previously described to result in a fairly specific neurogenic phenotype, whereby multiple Mauthner neurons are specified, instead of the typical two (Gray, Moens et al. 2001, Liu, Gray et al. 2003). I sought to temporarily abrogate early Notch1a function by microinjecting an antisense morpholino oligonucleotide into newly fertilized eggs. I found that 500pg of a previously described splice-disrupting Notch1a morpholino (Ma and Jiang 2007) was sufficient to generate larvae with supernumerary Mauthner neurons (Figure 4.5A, "notch1a MO"). I found that the majority of larvae contained supernumerary Mauthner neurons at least on one side of the hindbrain, ranging from 2-7. These supernumerary Mauthner neurons projected very-large diameter axons, similar to the WT larvae, which crossed the midline and grew caudally, throughout the ventral spinal cord.

Importantly, Notch1 function has been implicated in oligodendrocyte development and myelination later during embryonic development (see Chapter 1). Morpholinos interfere with target gene expression only during the first 1-2 days of development, and they become increasingly diluted with each cell division; eventually their effect wears off. I showed that correct *notch1a* transcript is reduced compared to controls at 10hpf, around the time Mauthner neurons are born, but at 72 hpf, when myelination begins, they are already restored to WT levels (Figure 4.5B). Therefore, this manipulation should only transiently abrogate Notch1a function, which precludes any direct effects of the loss of Notch1a function on oligodendrocyte development. To unambiguously exclude this possibility, I sought an additional independent way to increase the number of Mauthner neurons.

Overexpression of *hoxb1* genes, which are important regulators of boundary formation and patterning of the hindbrain (McClintock, Kheirbek et al. 2002, Tumpel, Wiedemann et al. 2009), has previously been described to generate ectopic Mauthner neurons (McClintock, Carlson et al. 2001). When overexpressed ubiquitously in the early embryo, these genes disrupt the identities of the hindbrain in such a way that structures belonging to the 4th hindbrain segment, such as Mauthner neurons, are additionally established elsewhere in the hindbrain (for instance, in the more rostral 2nd segment). I found that injecting 50ng of *hoxb1b* mRNA in newly fertilized eggs generated larvae with ectopic Mauthner neurons that also projected their large-diameter axons contra-laterally in the ventral spinal cord (Figure 4.5A, "hoxb1b mRNA"). Typically, these larvae had one Mauthner neuron on one side of the midline and 2-3 Mauthner neurons on the other side. A subset of larvae with gross morphological abnormalities, as previously described (McClintock, Carlson et al. 2001), were excluded from further analysis.

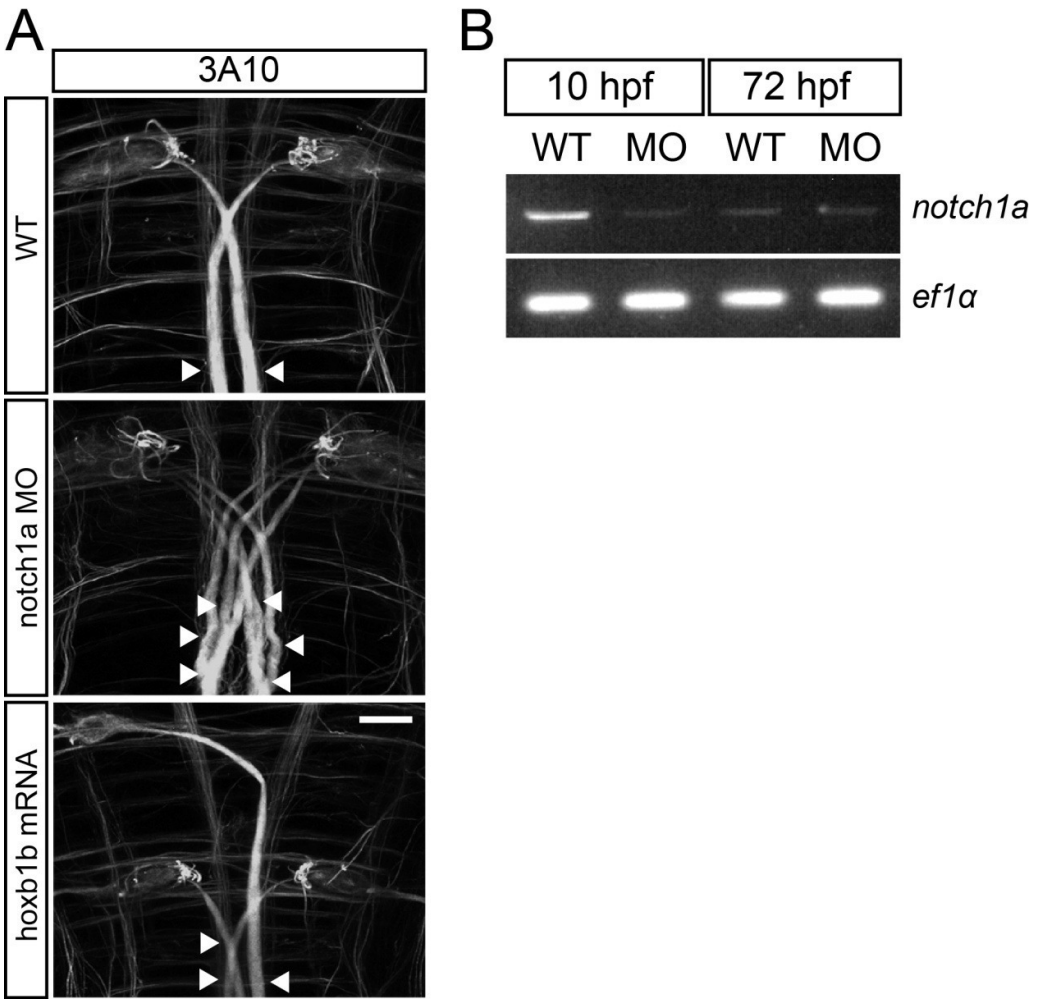

Figure 4.5 – Generation of larvae with supernumerary Mauthner axons

(**A**) Ventral view of the hindbrain of 5dpf 3A10-immunostained larvae. Anterior is top and posterior is towards the bottom. In WT, the two prominently labelled cells are the Mauthner neurons, which project large diameter axons caudally (arrowheads). Larvae injected with *notch1a* MO or *hoxb1b* mRNA have several Mauthner neurons and axons.
(**B**) RT-PCR detecting the correctly spliced form of the notch1a WT transcript (*notch1a*) and *ef1α*, a housekeeping control gene. In notch1a MO-injected larvae, the amount of correctly spliced form is decreased at 10hpf compared with control WT. At 72hpf, the level of correctly spliced form is similar to WT larvae.

4.3.6 Supernumerary axons are normally ensheathed

I next wondered whether the supernumerary Mauthner axons could be recognized by OPCs, and whether OPCs would be able to contact and ensheath them. I injected either *notch1a* morpholino or *hoxb1b* mRNA in newly fertilized eggs of the fluorescent reporter line sox10:mRFP. At 3dpf, the OPC membrane ensheathing the Mauthner axons allowed me to unambiguously identify these axons. Mauthner axons have a stereotyped location in the ventral spinal cord; their axon is several-fold larger than the next largest-diameter axons; additionally, they are continuously ensheathed along their length, without any gaps corresponding to nodes of Ranvier, which is unique in the zebrafish CNS.

In a projection of a lateral view of one half of the spinal cord, only one such Mauthner-surrounding membrane was observed in WT animals (Figure 4.6). In either notch1a MO or hoxb1b mRNA -injected animals, however, several Mauthner-surrounding membranes were clearly visible, indicating that OPCs recognize and ensheath at least some of the supernumerary Mauthner axons. I repeated the injections in newly fertilized eggs of the reporter line mbp:EGFP-CAAX. At 5dpf, similarly, only one continuous Mauthner myelin sheath was visible in each half spinal cord of WT animals, whereas notch1a MO and hoxb1b mRNA-injected animals exhibited several Mauthner-myelin sheaths (Figure 4.6).

These data indicate that at least some supernumerary Mauthner axons are being recognized by OPCs, which are capable of ensheathing them, while undergoing differentiation into mbp:EGFP-CAAX+ oligodendrocytes. This suggests that the supernumerary Mauthner axons likely present the same recognition and adhesion signals that WT Mauthner axons do.

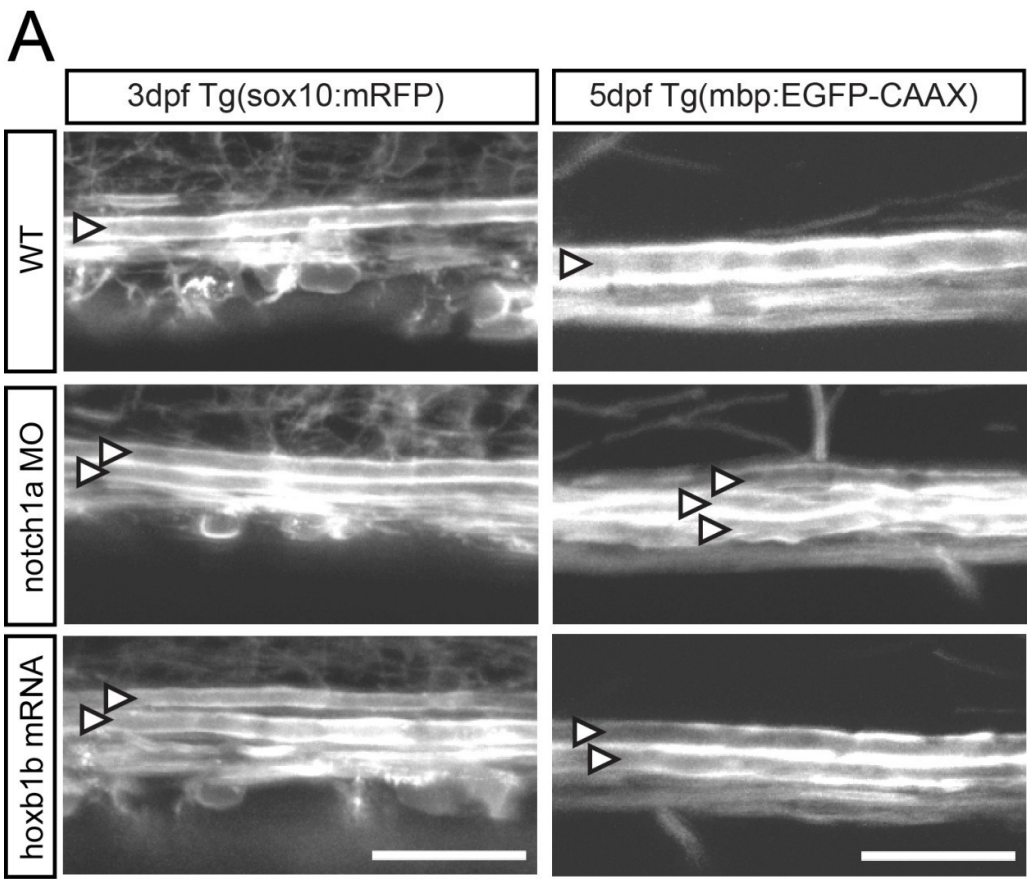

Figure 4.6 - Supernumerary Mauthner axons are ensheathed by myelinating glia

(**A**) Lateral view of one half of the spinal cord of 3dpf Tg(sox10:mRFP) larvae, and of 5dpf Tg(mbp:EGFP-CAAX) larvae. In WT, one Mauthner axon per larvae ensheathed (arrowhead); in larvae with supernumerary Mauthner neurons, additional Mauthner axons are wrapped by OPC- and oligodendrocyte-derived membrane.

4.3.7 Supernumerary Mauthner axons are robustly myelinated

Subsequently to recognition and adhesion between OPCs and oligodendrocytes, different regulatory mechanisms regulate the differentiation into myelinating oligodendrocytes and the formation of myelin sheaths. In the optic nerve, for instance, myelin sheath formation is uncoupled from the expression of myelin genes which mark the onset of differentiation (Colello, Devey et al. 1995). To address whether bona-fide compact, multilamellar myelin was being formed around the supernumerary axons, rather than simply ensheathments by oligodendrocyte-derived membrane, I examined these animals by electron microscopy. In transversal sections of the spinal cord, the Mauthner axon and its lipid and electron-dense myelin sheath are readily identifiable. Only one myelinated Mauthner axon is ever visible on each side of the spinal cord in 9dpf WT animals, whereas many myelinated Mauthner axons are present in notch1a MO and hoxb1b mRNA injected animals (Figure 4.7 A "M"). In all animals examined, I never found very large-diameter axons in the ventral spinal cord that were not myelinated. This indicates that oligodendrocytes do recognize, ensheath and myelinate all of the supernumerary Mauthner axons, which my previous live imaging was unable to unambiguously address, given that the axons themselves were not labelled.

In higher magnification views (Figure 4.7B), the Mauthner myelin sheaths in animals with supernumerary Mauthner axons appear to be bona-fide, compact multi-lamellar sheaths, of comparable thickness to WT Mauthner myelin. In the lower magnification views in Figure 4.7A, the Mauthner myelin sheaths do not always present as compact sheaths apposed to the axon in the entirety of its cross-sectional profile, and at points seems to defasciculate and enlarge or vacuolate. This can be due to sub-optimal fixation, dehydration or embedding during sample processing for electron microscopy (zebrafish are fairly impermeable to liquids, including electron-microscopy fixatives); unfortunately, larvae of such small size are impossible to perfuse. This precluded me from confidently assessing Mauthner axon thickness by determining the number of myelin lamellae or g-ratios (that is, the quotient between

axon diameter and axon+myelin diameter), which is why I don't present these two parameters that are more traditionally used in analyses of myelination.

I next wondered whether the supernumerary Mauthner axons were of a similar cross-sectional size to WT Mauthner axons, and what the net effect of these manipulations was in increasing the total axonal surface. Since axons (including the Mauthner) are of an irregular shape and not circular in cross-sectional profiles in these electron micrographs, I quantified the perimeter of these axons (excluding the myelin sheaths), as this parameter better reflects the axonal surface that is available for potential contact-dependent interactions with OPCs or oligodendrocytes. I found that in animals with up to three Mauthner axons on one side of the spinal cord, the perimeter of each Mauthner axon was not significantly different from WT animals with a single Mauthner axon on one side of the spinal cord (Figure 4.7 C, top graph). This meant that in animals with 2 Mauthner axons on one side of the spinal cord, the total Mauthner axonal surface had essentially doubled, and in animals with three Mauthner axons had essentially tripled (Figure 4.7 C, bottom graph). In animals with 4 or more Mauthner axons, some of the axons were slightly smaller, a reduction that although statistically significant, represents only an average perimeter reduction from 12 to 9 μm. In these animals, the total Mauthner circumference is still significantly increased further than animals with 3 Mauthner axons ($p=0.0384$, t-test), just not quite 4-fold when compared to WT animals with one Mauthner axon.

These results indicate that supernumerary Mauthner axons, which are not normally present in WTs, were capable of providing both the correct adhesion signals and of inducing myelination by oligodendrocytes, which seem to be a plastic population. Interestingly, in the optic nerve, the onset of myelination correlates with the presence of large-diameter axons, even though oligodendrocytes differentiate first in regions with small-diameter axons (Colello, Devey et al. 1995). Similarly, in the zebrafish spinal cord, the large Mauthner axon is the first myelinated. Could supernumerary Mauthner axons be diverting the myelinating capacity of oligodendrocytes from other, smaller nearby axons?

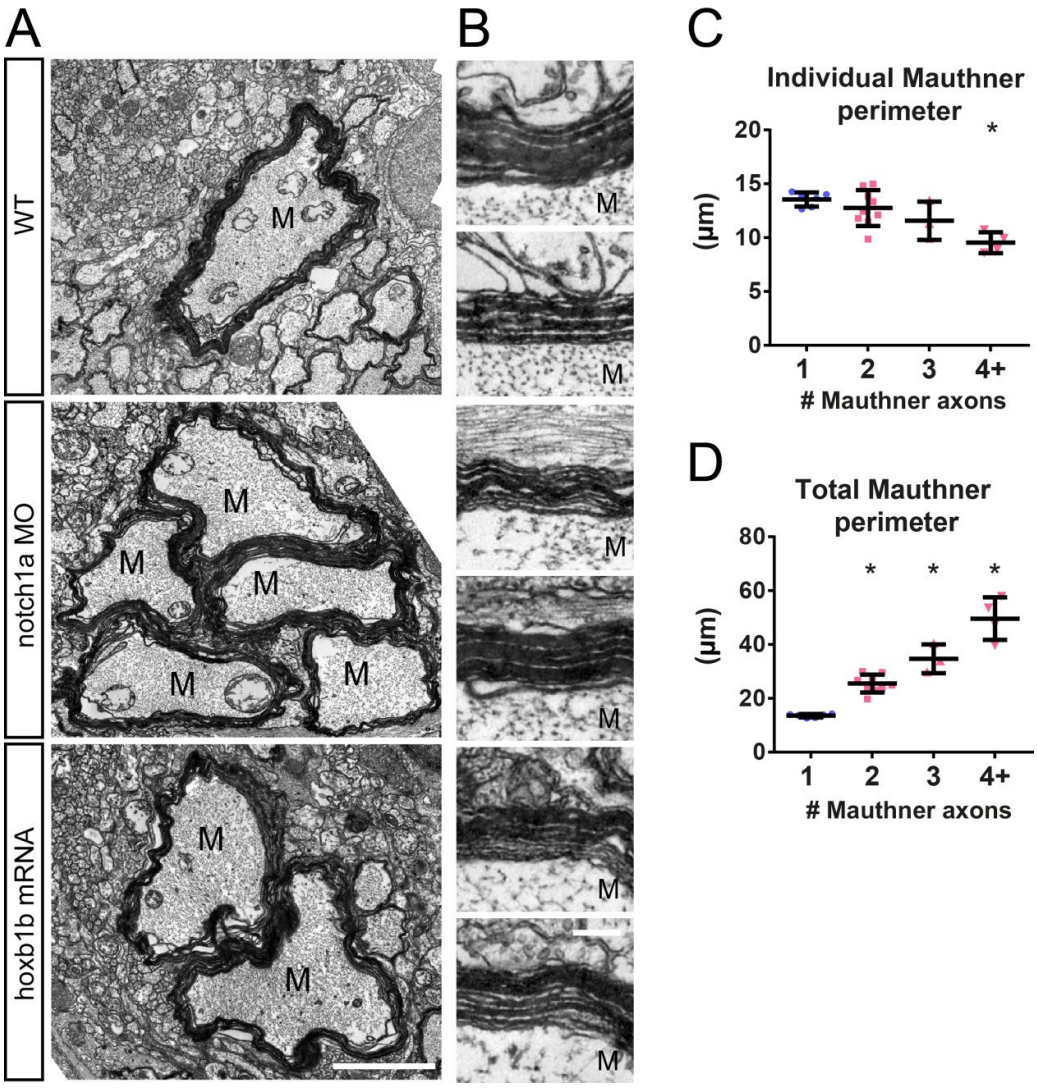
A
B
C
WT
notch1a MO
hoxb1b mRNA
M
Individual Mauthner perimeter
(µm)
20
15
10
5
0
1
2
3
4+
Mauthner axons
*
D
Total Mauthner perimeter
80
60
40
20
0
1
2
3
4+
Mauthner axons
*

Figure 4.7 - Supernumerary Mauthner axons are robustly myelinated.

(A) Electron micrographs of transversal sections of the spinal cord of 9 dpf larvae, focusing on the ventral area. One Mauthner axon (M) is readily identifiable in WT animals, surrounded by black electron-dense myelin. In animals with supernumerary Mauthner neurons, additional Mauthner axons are present in each side of the spinal cord, all of them surrounded by electron-dense myelin.
(**B**) Higher magnification view of the myelin sheath surrounding Mauthner axons (M), in two independent larvae in each condition, showing an apparently similar thickness. notch1a MO examples had 3 and 4 Mauthner axons on that side of the spinal cord. hoxb1b mRNA examples had 2 Mauthner axons on each side of the spinal cord.

(**C**) Quantification of the average perimeter of each individual Mauthner (M-) axon (excluding myelin sheath) in 9 dpf larvae. 1 M-axon category includes only WT M-axons. Error bars represent standard deviation.
1 M-axon: 13.54±0.65 µm (N=6 WT larvae);
2 M-axons: 12.74±1.66 µm (N=9 larvae); p=0.3265 in Mann-Whitney test
3 M-axon: 11.57±1.78 µm (N=3 larvae); p=0.0952 in Mann-Whitney test
4+ M-axon: 9.53±0.98 µm (N=4 larvae); p=0.0095 in Mann-Whitney test

(**D**) Quantification of the total Mauthner perimeter per half spinal cord, according to the number of Mauthner axons per half spinal cord. 1 M-axon category includes only WT M-axons. Error bars represent standard deviation.
1 M-axon: 13.54±0.65 µm (N=6 WT larvae);
2 M-axons: 25.49±3.33 µm (N=9 larvae); p=0.0004 in Mann-Whitney test
3 M-axon: 34.70±5.34 µm (N=3 larvae); p=0.0238 in Mann-Whitney test
4+ M-axon: 49.59±7.90 µm (N=4 larvae); p=0.0095 in Mann-Whitney test

4.3.8 Other ventral large-diameter axons are myelinated normally

To determine if supernumerary Mauthner axons were myelinated at the expense of adjacent axons of smaller diameter, I analyzed the neighbouring ventral spinal cord and counted the number of myelinated axons present (Figure 4.8A), which are mostly other reticulospinal axons. I found that in animals with up to 3 Mauthner axons on each side of the spinal cord, the number of additional myelinated axons was not significantly different from WTs, but that this number decreased slightly in animals with 4 or more Mauthner axons (according to the statistical test used, Figure 4.8 B). I also wondered whether these neighbouring myelinated axons could be of a smaller size in animals with supernumerary Mauthner axons than in WT animals. This could mean that the oligodendrocytes were selecting a smaller cohort of additional ventral axons that would require less myelin. However, the average perimeter of these axons in WT animals was not different from animals with supernumerary Mauthner axons, including those with 4 or more Mauthner axons (according to the statistical test used, Figure 4.8 C). Since their ventral location was also not changed, this indicates that the same cohort of nearby axons also becomes myelinated in animals with supernumerary Mauthner axons. Altogether, these data indicates that in the zebrafish spinal cord, even when tripling the amount of axonal surface that is the initial target for myelination, the oligodendrocyte population will recognize it, adapt to it and myelinate it robustly, without detriment to the myelination of other axons. The ability of the oligodendrocyte population to respond to the challenge in the axonal environment hints that this cell type is very plastic. As I describe in Chapter 3, axons can regulate the size of the oligodendrocyte-lineage population by regulating its proliferation and survival. Therefore, in animals with supernumerary Mauthner axons, the oligodendrocyte population could simply be more numerous. Alternatively, or in addition, supernumerary axons could also regulate the amount of myelin, or number of sheaths, that each individual oligodendrocyte makes. I thus sought to address which of these possibilities underlie the adaptation of oligodendrocytes to supernumerary axons.

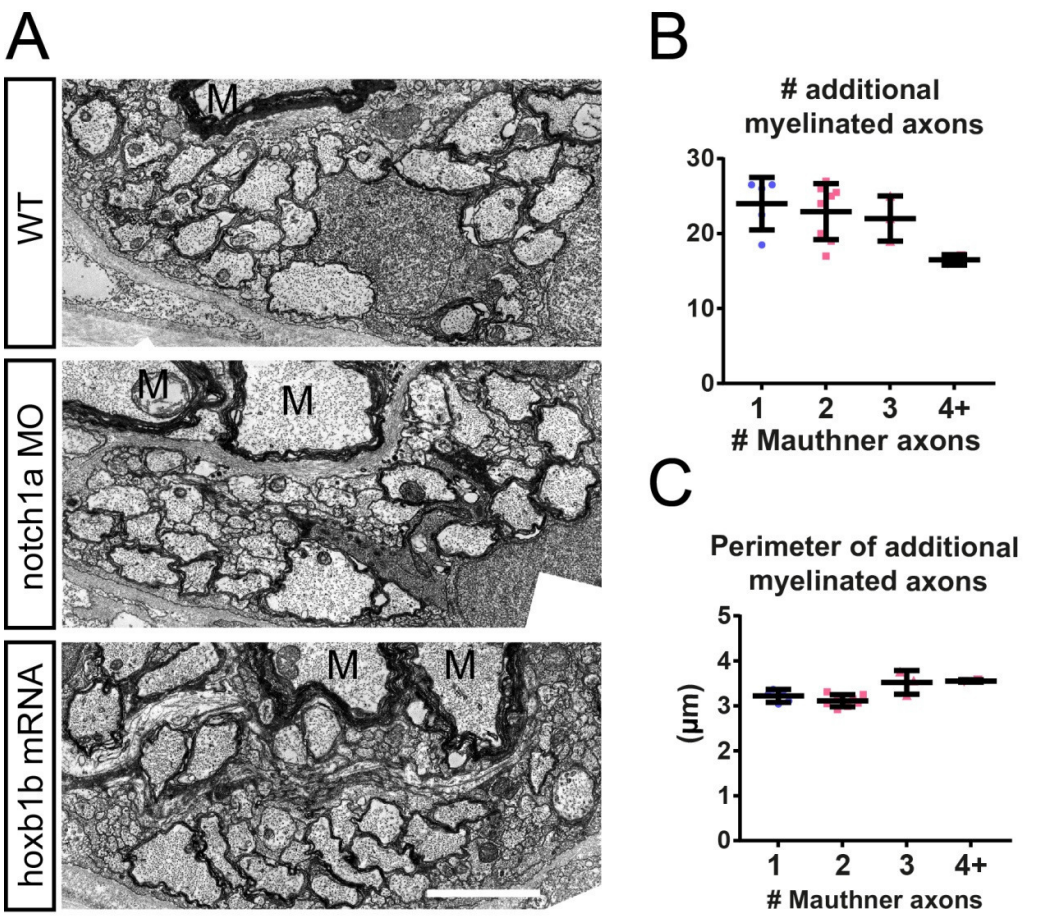

Figure 4.8 - Supernumerary Mauthner axons are not myelinated at the expense of other axons

(**A**) Electron micrographs of transverse sections of the ventral spinal cord of 9dpf larvae. Large myelinated axons other than the Mauthner axon (M) are evident.

(**B**) Quantification of the number of myelinated axons adjacent to the Mauthner axon in the ventral spinal cord. 1 M-axon category includes only WT M-axons. Error bars represent standard deviation.

1 M-axon: 24±4 axons (N=5 WT larvae);

2 M-axons: 23±4 axons (N=8 larvae); p=0.5470 in Mann-Whitney test

3 M-axon: 22±3 axons (N=3 larvae); p=0.3393 in Mann-Whitney test

4+ M-axon: 17±1 axons (N=2 larvae); p=0.0952 in Mann-Whitney test, p=0.0359 in t-test

(**C**) Quantification of the perimeter of additional myelinated axons adjacent to the Mauthner axon(s). 1 M-axon category includes only WT M-axons. Error bars represent standard deviation.

1 M-axon: 3.22±0.14 µm (240 axons from N=5 WT larvae);

2 M-axons: 3.11±0.14 µm (238 axons from N=8 larvae); p=0.222 in Mann-Whitney test

3 M-axon: 3.52±0.26 µm (69 axons from N=3 larvae); p=0.2500 in Mann-Whitney test

4+ M-axon: 3.55±0.03 µm (66 axons from N=2 larvae); p=0.0952 in Mann-Whitney test, p=0.0284 in t-test

4.3.9 Supernumerary axons do not regulate oligodendrocyte number

I wanted to determine whether an increased number of oligodendrocytes could contribute to the myelination of supernumerary Mauthner axons. I injected notch1a MO and hoxb1b mRNA into newly fertilized eggs of the transgenic fluorescent reporter line mbp:EGFP, where cytoplasmic EGFP is expressed in mature oligodendrocytes, which enables counting of oligodendrocyte number (Figure 4.9 A). At 5dpf, over the length of ~5 somites (425μm of the spinal cord), the total number of oligodendrocytes wasn't different between WT animals and animals with supernumerary Mauthner axons (Figure 4.9 B). The size of the dorsal population of oligodendrocytes specifically was also not different from WT, which indicates that in addition to the total number of oligodendrocytes, their dorsal-ventral distribution is not altered, despite the increased number of the ventrally-localized Mauthner axons.

These data indicate that the large-caliber reticulospinal Mauthner axons do not regulate oligodendrocyte distribution or number, in apparent contrast with the results described in Chapter 3. However, this could be a comparatively smaller manipulation, and a small effect on OPC proliferation, which may have occurred at earlier time points, might have gone undetected (see more in Discussion).

In any case, given that the number of oligodendrocytes remains unchanged, to account for the adaptation of oligodendrocytes to the extra axonal surface, it is likely that each individual oligodendrocyte makes more myelin.

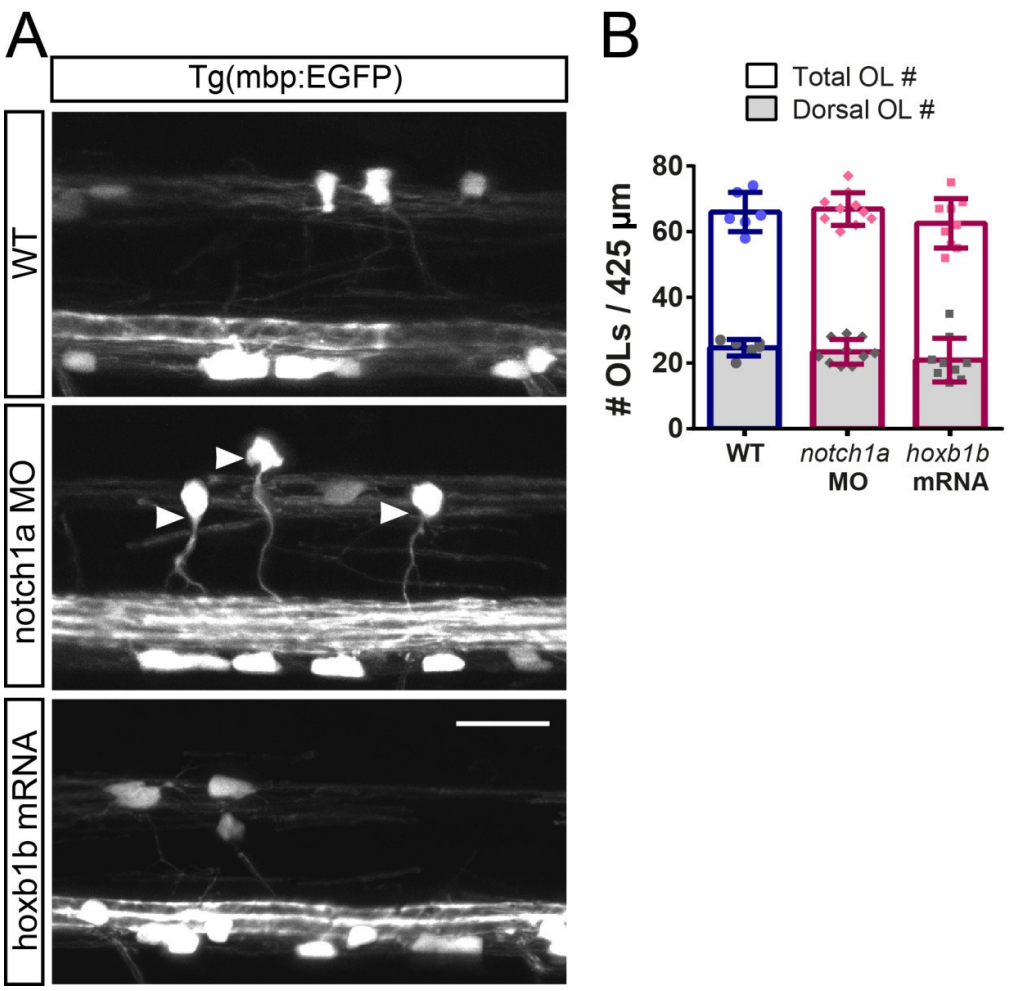

Figure 4.9 – Presence of supernumerary Mauthner axons does not affect oligodendrocyte number or distribution.

(**A**) Lateral view of 5 dpf transgenic Tg(mbp:EGFP) larvae. Similar numbers of oligodendrocytes are apparent in WT larvae and larvae with supernumerary Mauthner axons. Arrowheads point to examples of dorsally located oligodendrocytes which extend processes ventrally to myelinate ventral axons (including Mauthner axons, see Figure 4.12).
(**B**) Quantification of oligodendrocytes per 425µm length of tissue in the midtrunk region of the spinal cord. Error bars represent standard deviation.
Total:
WT: 66±6 oligodendrocytes (N=6); *notch1a MO*: 67±5 oligodendrocytes (N=10), p=0.7495 in t-test; *hoxb1b mRNA*: 63±8 oligodendrocytes (N=9), p=0.3658 in t-test
Dorsal:
WT: 25±3 oligodendrocytes (N=6); *notch1a MO*: 24±4 oligodendrocytes (N=10), p=0.4797 in t-test; *hoxb1b mRNA*: 21±7 oligodendrocytes (N=9), p=0.2123 in t-test

4.3.10 Axons regulate the myelinating potential of individual oligodendrocytes

To investigate whether regulating the number of myelin sheaths and/or their length was the mechanism by which oligodendrocytes adapted to the extra axons, I labeled individual oligodendrocytes in WT larvae or in larvae with supernumerary Mauthner axons by microinjecting a plasmid encoding the transgene mbp:EGFP-CAAX in newly fertilized eggs. This allowed me to identify single EGFP+ oligodendrocytes myelinating the Mauthner axon(s), isolated in a field of view, and analyze their morphology.

In WT animals at 5 dpf, the majority (26/35) of oligodendrocytes that myelinate the Mauthner axons have a very stereotyped position just ventral to the axon and extend only a single large myelin sheath, reminiscent of the association between Schwann cells and peripheral axons (Figure 4.10 A, B). This type of association corresponds to Pio del Rio Hortega's description of "type IV oligodendrocytes". Most of the remainder (7/35) extend just two myelin sheaths, ensheathing one segment of one Mauthner on one side of cord and one segment on the other Mauthner. Very rarely, a WT oligodendrocyte may also ensheath a smaller axon in addition to Mauthner, as discussed previously. Each WT oligodendrocyte that myelinates Mauthner axons covers 151±49 μm of Mauthner axon length.

In larvae with supernumerary Mauthner axons, the majority of oligodendrocytes elaborated 2 or more myelin sheaths, and in contrast to WT oligodendrocytes, those oligodendrocytes myelinating just one segment of Mauthner axons were a minority (Figure 4.10 A, B). In one instance, for example, I observed one oligodendrocyte myelinating seven distinct segments on the supernumerary Mauthner axons (Figure 4.10 A, "notch1a MO"). Additionally, in these larvae, on average, each individual oligodendrocyte covered a significantly longer total length of Mauthner axons in some animals (Figure 4.10 C, 256±67 μm in notch1a MO animals and 185±88 μm in hoxb1b mRNA animals).

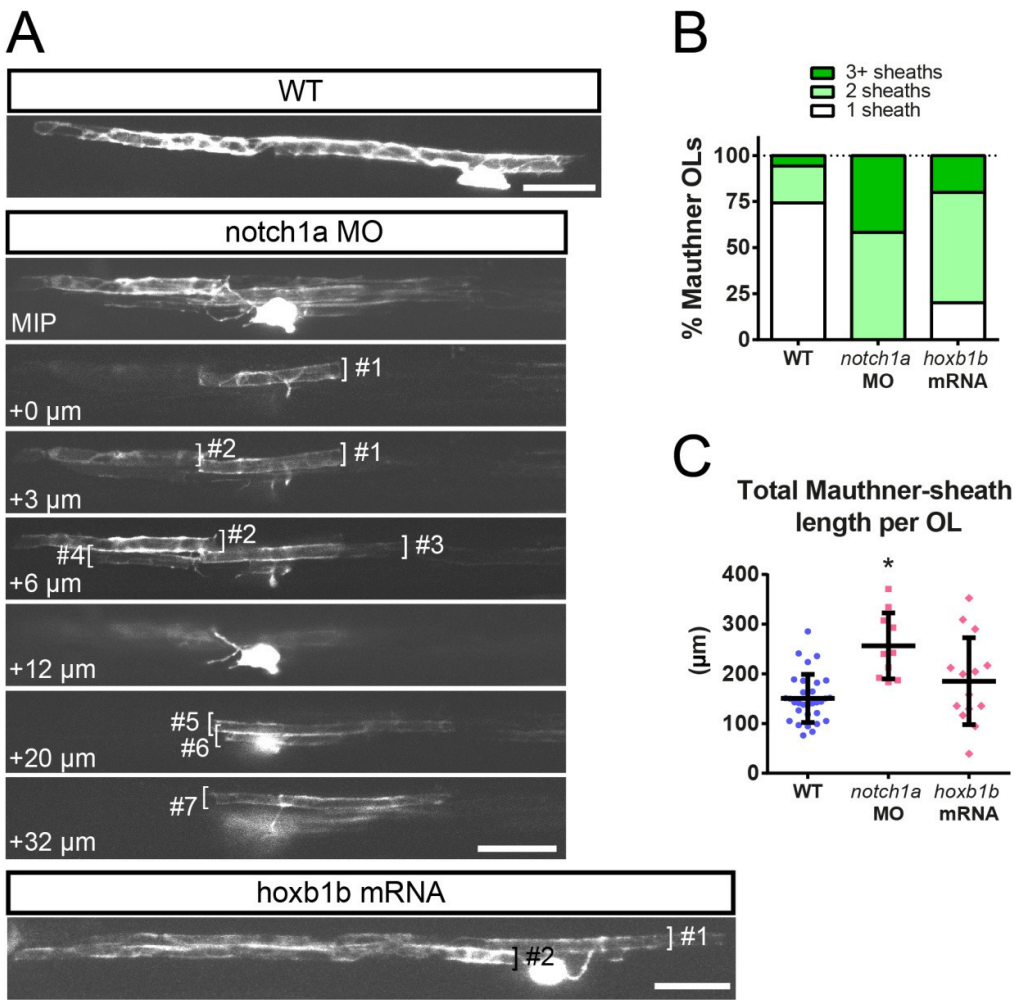

Figure 4.10 – Individual oligodendrocytes myelinate multiple supernumerary Mauthner axons at 5 dpf.

(**A**) Lateral view of single mbp:GFP-CAAX+ oligodendrocytes myelinating Mauthner neurons in 5 dpf larvae. In WT, Mauthner-dedicated oligodendrocytes form one long myelin sheath and lie ventral to the axon. In animals with supernumerary Mauthner axons, Mauthner-associated oligodendrocytes have more than one myelin sheath associated with Mauthner axons. Brackets and numbers label each myelin sheath; MIP = Maximum intensity projection; bottom left corner indicates the depth of each slice in the z-stack.

(**B**) Quantification of the diversity of morphologies of oligodendrocytes that myelinate Mauthner axons, at 5dpf. In WT larvae, the majority of Mauthner-dedicated oligodendrocytes forms one long myelin sheath. In larvae with supernumerary Mauthner neurons, the vast majority of oligodendrocytes myelinating the Mauthner now form 2 or more myelin sheaths. See text for details.

(**C**) Quantification of the total length of myelin sheaths formed along Mauthner axons per oligodendrocyte. Error bars represent standard deviation.

WT: 150.8±48.5 µm (N=31 cells); *notch1a MO*: 256.4±66.5 µm (N=10), p<0.0001 in t-test; *hoxb1b mRNA*: 185.3±87.6 µm (N=14), p=0.0958 in t-test

To investigate whether this was a stable association, I repeated this experiment at 9 dpf, when I had observed normal myelination of extra Mauthner axons by electron microscopy. At this stage, the number of WT oligodendrocytes associated with a single Mauthner myelin sheath was even greater than 5dpf (17/19). In animals with supernumerary Mauthner axons, the number of oligodendrocytes making several myelin sheaths was higher than 5dpf (13/13 in *notch1a* MO, 4/6 in *hoxb1b* mRNA-injected larvae, Figure 4.11B). Therefore, this was not a transient phenotype, and each individual oligodendrocyte maintains more myelin sheaths in the presence of supernumerary axons.

Additionally, each oligodendrocyte that myelinates Mauthner axons covers essentially twice as much axonal length in *notch1a* MO versus WT animals, with a (non-significant) trend towards a longer length in *hoxb1b* mRNA-injected animals (Figure 4.11 C).

I have shown that the total perimeter of Mauthner axons in *notch1a* MO and *hoxb1b* mRNA-injected animals is greatly elevated when compared to WT Mauthner axons. Additionally, the thickness of their myelin sheaths is roughly similar, and other axons are normally myelinated. Collectively, these data indicate that in the presence of supernumerary Mauthner axons, each individual oligodendrocyte makes an increased amount of total myelin.

The individual oligodendrocytes analyzed here presented the stereotyped morphology of Mauthner-dedicated oligodendrocytes described previously in WTs. Mauthner axons have unusual anatomical features: their prominently large axonal calibre, for instance, but also the fact that they are continuously myelinated along their length, without the unmyelinated gaps that are nodes of Ranvier. We never observed these features in any other axons in the zebrafish spinal cord. I therefore considered the hypothesis that these ventral oligodendrocytes represent a specific subtype of Mauthner-dedicated oligodendrocytes. I wondered if other oligodendrocytes in the spinal cord could also be affected by the presence of supernumerary axons.

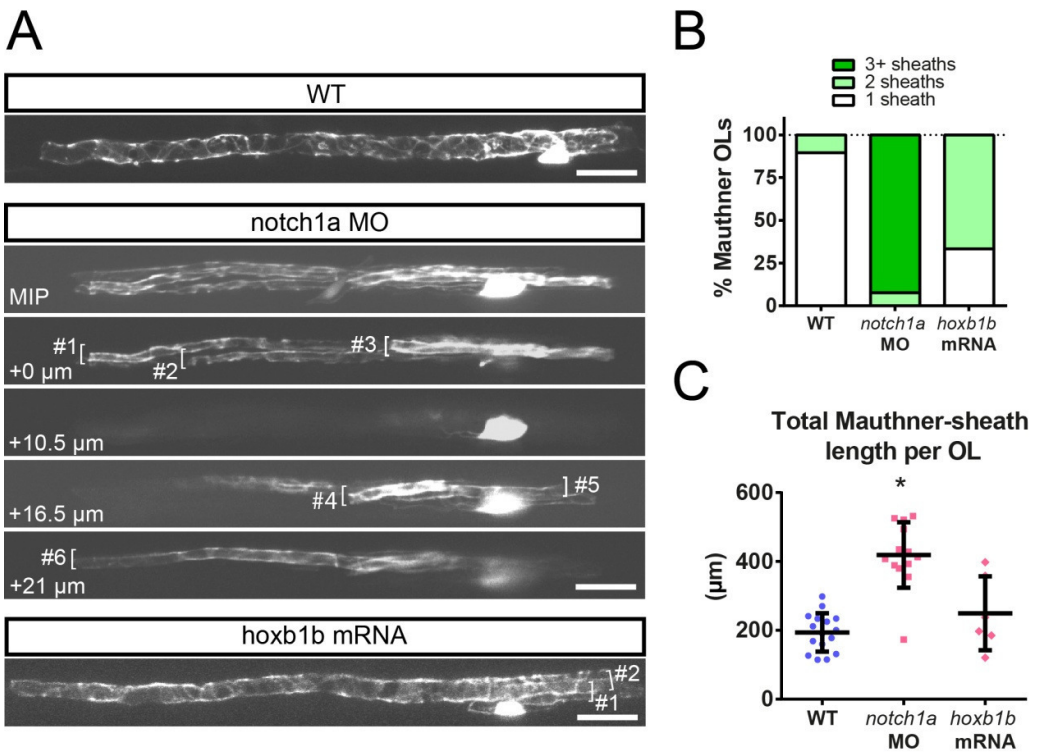

Figure 4.11 - Individual oligodendrocyte myelinating capacity at 9 dpf.

(**A**) Single mbp:EGFP-CAAX+ oligodendrocytes myelinating Mauthner axons in 9 dpf larvae present similar morphologies to 5dpf

(**B**) Quantification of the diversity of morphologies of oligodendrocytes that myelinate Mauthner axons, at 9dpf. 5dpf difference is maintained. See text for details.

(**C**) Total length of myelin sheaths formed along Mauthner axons per oligodendrocyte, at 9dpf. Error bars represent standard deviation.

WT: 193.9±55.7 µm (N=16 cells); *notch1a MO*: 418.8±95.0 µm (N=13), $p<0.0001$ in t-test; *hoxb1b mRNA*: 249.4±107.2 µm (N=6), $p=0.3289$ in Mann-Whitney test.

4.3.11 Axons regulate the localization of oligodendrocyte myelin sheaths

I next investigated whether the myelinating capacity of oligodendrocytes can be regulated only by their normal target axons, or alternatively, whether all oligodendrocytes are plastic and responsive to axonal cues. In other words, can axons regulate the myelinating capacity of any oligodendrocyte? To address this I examined the morphology of other oligodendrocytes in the spinal cord of zebrafish with supernumerary Mauthner axons.

In these animals, I readily observed some dorsal oligodendrocytes that extended processes ventrally and ensheathed large segments of the Mauthner axons, in addition to smaller-diameter axons. In contrast, in WTs, dorsal oligodendrocytes typically myelinate only smaller-diameter dorsal or medial axons (Figure 4.12, and cell *d* in Figure 4.2). Furthermore, I readily observed ventral oligodendrocytes that myelinated the supernumerary Mauthner axons in addition to other small diameter axons (Figure 4.12, arrow). This happened only rarely in WTs. These features were observed at both 5 and 9 dpf, which indicates that this was not a transient phenomenon.

These results indicate that axons are capable of regulating not only the myelinating capacity of those oligodendrocytes that typically associate with them, but can also influence the localization and extension of sheaths belonging to oligodendrocytes located more distally in the spinal cord.

Together, my data suggests that oligodendrocytes are highly plastic in the sense that each individual cell is not destined to myelinate only one particular subtype of axon. When the axonal environment is drastically challenged, they can recognize many diverse axons, adapt, and appropriately myelinate them.

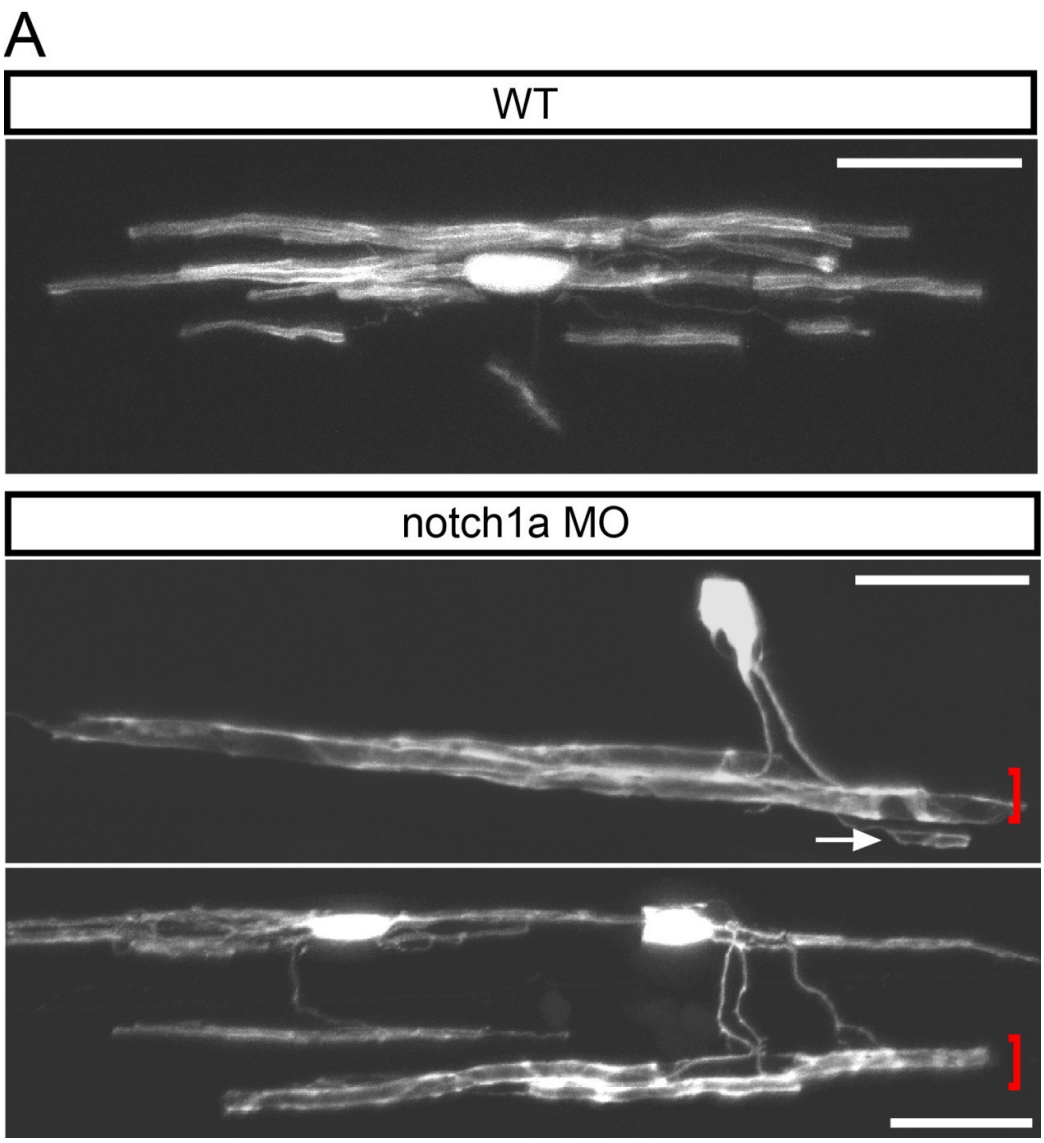

Figure 4.12 - Individual oligodendrocytes readily myelinate supernumerary Mauthner axons and smaller calibre axons.

(**A**) Lateral view of single mbp:EGFP-CAAX+ oligodendrocytes located in the dorsal spinal cord, in 5dpf larvae. In WT, these tend to myelinate smaller diameter axons located in the dorsal spinal cord. In larvae with supernumerary Mauthner axons, many dorsal oligodendrocytes extend processes ventrally to myelinate large segments of the additional Mauthner axons (brackets). Often, this occurs concomitantly with myelination of other smaller dorsal or ventral axons (arrow).

4.4 Discussion

In this Chapter, I investigated whether later stages of the development of oligodendrocyte-lineage cells, such as the timing of terminal differentiation and the extent of myelination could be regulated by axons. I addressed this issue by two approaches, an axonal "loss-of-function", whereby target axonal surface was reduced, and an axonal "gain-of-function", whereby the target axonal surface was increased.

4.4.1 Decreased axonal surface

Following a slight decrease in proliferation and survival of oligodendrocyte-lineage cells, the posterior spinal cord of *kbp* mutants presents with about 75% of the normal number of oligodendrocytes. Strikingly, however, the axonal surface in the ventral spinal cord is reduced to 20% of WT levels. This suggested that oligodendrocyte-lineage cells might exist in excess of their target axonal surface in the posterior spinal cord of mutants, and I proceeded to analyse if this altered axonal environment could affect myelination by those cells.

I first resorted to a mosaic label for OPCs that allowed me to track individual cells as they transition into differentiation (Figure 4.1). *A priori*, one could expect that in the absence of reticulospinal axons, OPCs could simply remain latent, waiting until other axons became competent for myelination. I found that despite the drastically altered axonal environment, OPCs differentiated on schedule, supporting previous in vitro studies of an intrinsic mechanism within OPCs that regulates the number of their divisions and their timing of differentiation (Gao, Apperly et al. 1998, Durand and Raff 2000).

I subsequently determined that oligodendrocyte-lineage cells in the mutant associated with their normal axonal targets (Figure 4.2). Since a large proportion of ventral axonal surface is missing, one could have expected that ventral oligodendrocytes would divert their processes and myelin sheaths towards more distal tracts, such as

the dorsal tract, or towards motor axons. However, the proportion of oligodendrocytes that did this in the mutant was not drastically different from WT.

Given the observations above, if there truly is an excess of oligodendrocyte-lineage cells, then each cell must make less myelin to adapt to the reduced axonal surface. In principle, they could do this in two manners: by elaborating fewer sheaths and/or by making shorter sheaths.

I determined that the number of sheaths made by individual oligodendrocytes was not significantly different in the anterior spinal cords. In the posterior spinal cord, I observed a trend towards fewer sheaths. This was a significant difference in ventral oligodendrocytes in particular (Figure 4.3). Therefore, a small reduction in the number of sheaths contributes to the adaptation of excess oligodendrocytes towards a reduced axonal surface. A small reduction of 3 sheaths on average per oligodendrocyte might be a relevant contribution towards that adaptation, if it occurs in every oligodendrocyte in the region.

In addition, strikingly, I observed that the average length of each myelin sheath was significantly reduced in the posterior spinal cord, as well as the combined length of myelin sheaths per oligodendrocyte. This would imply that a reduced axonal surface could present fewer signals that promote extension of myelin sheaths, thereby regulating the amount of myelin each oligodendrocyte makes. However, even if this is occurring in the posterior spinal cord, it is not the only cause of this phenotype, because I also observed a reduction in sheath length in the anterior region of the spinal cord, where reticulospinal axons are present. There are a number of possible explanations for a reduction in myelin sheath length in the anterior spinal cord:

a) There may be a smaller number of neurons that project potentially smaller axons along the anterior spinal cord, whose outgrowth is also affected by the genetic ablation of *kbp*. Disruption to these axons might have escaped the relatively low-resolution immunohistochemical analysis presented in Figure 3.1 in Chapter 3, but could still contribute to a reduction in target axonal area. A careful high-resolution analysis of electron micrographs of transversal sections of the anterior spinal cord will be essential to investigate this possibility.

b) Alternatively, it is possible that *kbp* function is required in axons for sheath growth. For instance, every axon, including those in the anterior spinal cord, may have actively stopped growing due to the global lack of *kbp*. In addition to its obvious role in reticulospinal axon outgrowth, KBP may generally be required in every axon to promote its basal growth as the animal itself grows. Such an effect would be less obvious than the clear reticulospinal axon disruption. If oligodendrocyte myelin sheaths require signalling from actively growing axons to elongate, then sheaths everywhere in the *kbp* mutant spinal cord would not grow, and remain smaller. Alternatively, KBP could be responsible for transporting a sheath-growth promoting factor along the axon. Testing these hypotheses would require restoring wildtype KBP function solely to axons, which would rescue the phenotype in the anterior region.

c) A third alternative hypothesis is that *kbp* is required in oligodendrocytes for myelin sheath elongation. For instance, KBP could normally promote the transport of components of the growing myelin sheaths along oligodendrocyte processes. *kbp* is disrupted in every cell in mutant larvae, including oligodendrocyte-lineage cells. Therefore, myelin sheaths in the anterior as well as posterior spinal cord would not grow as much as in WT. Testing this hypothesis would require restoring wildtype *kbp* function solely to oligodendrocyte-lineage cells, which would rescue the phenotype in the anterior region.

I will later outline a strategy to address these hypotheses.

I further made the remarkable observation that neuronal somas were ensheathed by oligodendrocyte membrane in the spinal cord of *kbp* mutants (Figure 4.4). These rather unusual ensheathments seemed to occur at a very low level in WT larvae. A search of the literature reveals many reports of ensheathed or myelinated perikarya: in fish (Roberts and Ryan 1976, Kemali and Miralto 1979), amphibians (Rosenbluth 1966, Kemali and Sada 1973), in chicken (Hess 1965), rodents (Blinzinger, Anzil et al. 1972, Hamori, Lakos et al. 1980), cats (Hamori and Silakov 1981), primates (Beal and Cooper 1976, Cooper and Beal 1977, Tigges and Tigges 1980), and humans (Suyeoka 1968, Braak, Braak et al. 1977). Interestingly, some of these report such features following deafferentiation of the areas examined, suggesting that

synaptic input may regulate such aberrant myelination. In any case, it is clear that these represent a rare feature that occurs at a very low level in a wildtype situation, suggesting the existence of mechanisms that ensure it will mostly not happen during development. For instance, somas could display a repulsive cue on their surface, whereas axons could display an attractive signal for oligodendrocyte-lineage cells.

Interestingly, in some instances of WT ensheathed somas, I observed retraction of these profiles between 60-96hpf, suggesting the existence of a correction mechanism. In mutants, however, these profiles were much more frequent, and I never observed any retraction. This suggests that such a correction mechanism is defective in mutants, or that it is not sufficient to cope with an increased number of such profiles.

At first, I thought these profiles could represent one way for oligodendrocyte-lineage cells to adapt to the reduced axonal surface present in the milieu: maybe their processes were diverted towards neuronal somas if they couldn't find enough axonal targets. This would suggest that neuronal somas are not as repulsive to oligodendrocytes as incorrect axons are, since no incorrect axons were myelinated in the posterior spinal cord. It would also suggest that oligodendrocytes have a minimum amount of myelin that they must make, even if it is on unusual structures such as cell bodies.

However, I subsequently observed that such profiles were also more frequent in the anterior spinal cord of *kbp* mutants. Therefore, similarly to the previous phenotype on sheath number per oligodendrocyte, while it remains possible that a decreased axonal surface contributes to the formation of ensheathed cell bodies in the posterior spinal cord, it is likely that the global lack of *kbp* in these mutants plays a role. For instance, KBP itself could be required in neurons to promote transport of an attractive cue to the surface of axons, or alternatively to promote the transport of a repulsive cue to the surface of soma and dendrites. In global *kbp* mutants, oligodendrocytes would be able to ensheath neurons in the anterior and posterior spinal cord that do not appropriately localize such signals. I will later outline a strategy to address the cell autonomy of this phenotype.

What is the fate of these ensheathed neurons? Are they functional? It will be very interesting to determine the molecular pathways that regulate the formation of these profiles, and what ensures they generally do not occur.

Short-term future directions

In the short-term, it will be important to disentangle which phenotypes observed in the *kbp* mutant larvae are due to the decrease in axonal surface, and which are due to an actual loss of *kbp* function. A starting point will be to accurately determine at single-cell resolution which cell types express *kbp* in the anterior and posterior spinal cord. Specifically, it will be important to determine whether oligodendrocyte-lineage cells express *kbp* in situ, since if they do, they too will be affected by the lack of *kbp* function in the global knockout mutant.

Furthermore, I have generated a rescue construct, GFP-2A-KBP, in which I fused the GFP coding sequence to wildtype *kbp* cDNA, with the sequence coding for the short self-breaking peptide 2A inbetween. Expression of this construct results in a 1:1 stoichiometric ratio of GFP (labelling the expressing cell) and of wildtype KBP, as the 2A peptide undergoes a proteolytic cleavage event during translation. I have generated transgenes in which I have placed this construct under the control of the *huC* promoter, which drives its expression in all neurons, and separately also under the control of the *sox10* promoter, which drives its expression in oligodendrocyte-lineage cells. I verified that the sox10:GFP-2A-KBP transgene is expressed in oligodendrocyte-lineage cells, and that the HuC:GFP-2A-KBP transgene is expressed in neurons. Furthermore, I verified that expressing this construct in *kbp* mutant animals rescues the axonal outgrowth of neurons in the posterior lateral line in the PNS, which are also affected in these mutants (Figure 4.13), proving that this construct is functional *in vivo*. I have microinjected these constructs in newly fertilized eggs of a cross between adult $kbp^{st23/+}$ heterozygous animals, which are now being raised as potential founders. These founders will allow me to generate stable transgenic lines in which all of the relevant cells express the transgene.This will allow me to restore wildtype KBP function solely to neurons or solely to oligodendrocyte-lineage cells in *kbp* mutant animals, which will help clarify the nature of the phenotypes I observed in their spinal cord, as I outline below.

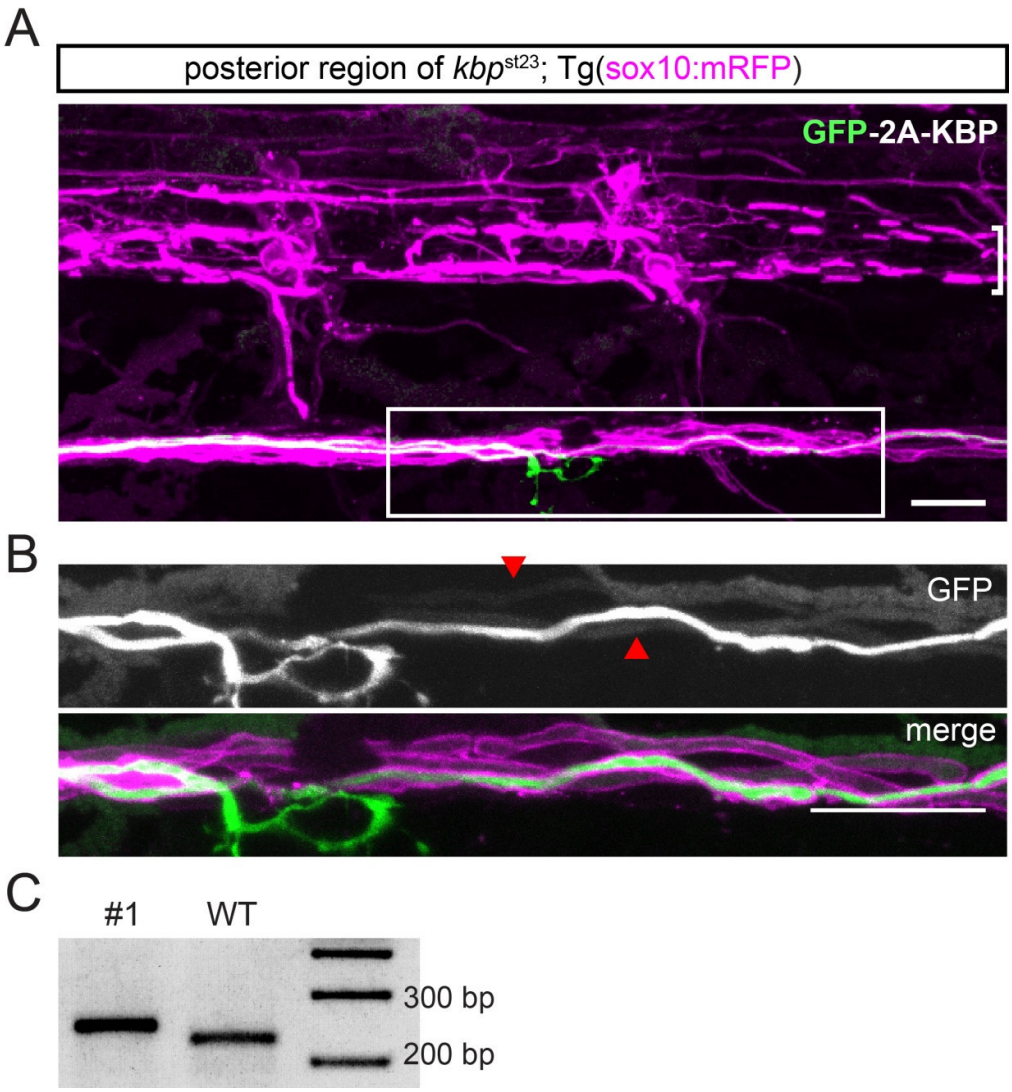

Figure 4.13 – Rescue strategy using GFP-2A-KBP constructs

(A) Posterior spinal cord and posterior lateral line (pLL) of a 5dpf sox10:mRFP *kbp* mutant larva. Brackets indicate the typical disruption to myelination in the ventral spinal cord. Usually, pLL axon outgrowth is more severely disrupted than reticulospinal axon outgrowth and pLL axons and myelin are only detectable in a very anterior region. However, this larva expresses GFP-2A-KBP in some pLL neurons, which rescued their axonal outgrowth and myelination by Schwann cells.
(B) High magnification of the area boxed in A. Four rescued pLL axons grow into the posterior region of the larva (arrowheads indicate three low GFP expressing axons).
(C) Genotyping assay for the larva depicted in A and B ("#1"). *kbp*^{st23} genomic DNA yields a PCR product not cleaved by MaeIII, unlike the WT product, which is cleaved into a lower molecular weight fragment (see Chapter 2).

I observed that some phenotypes affected only the posterior spinal cord of mutants but not the anterior, and therefore could be attributed to a decreased in axon-derived signals – particularly, impaired OPC survival (see Chapter 3). OPC proliferation was also decreased in the posterior spinal cord; however, I didn't specifically measure this parameter in the anterior spinal cord. Even if mature oligodendrocyte number was normal in the anterior spinal cord later on, I cannot formally exclude that OPC proliferation was altered in the anterior spinal cord of mutants. For these phenotypes, the HuC:GFP-2A-KBP transgenic line should provide a rescue experiment – it should restore axonal outgrowth, which should abolish the aforementioned phenotypes only if the reduction in target axonal area is the primary cause of these phenotypes. In this line, oligodendrocytes remain *kbp*$^{-}$. Conversely, the sox10:GFP-2A-KBP should not rescue these phenotypes, since the axonal outgrowth defect should still be present.

Additionally, these rescue transgenic lines will allow me to resolve the cell autonomy of those phenotypes that I observed both in the anterior and posterior spinal cord of *kbp* mutants. If KBP functions in oligodendrocytes to promote sheath extension (for instance, by promoting transport of myelin components), in *kbp* mutants, this transport would be disrupted and sheaths would be smaller throughout the animal. *kbp* mutants crossed into the transgenic line sox10:GFP-2A-KBP will have KBP function restored in their oligodendrocytes, and this phenotype should disappear. Conversely, mutants crossed into the transgenic line HuC:GFP-2A-KBP which have KBP function restored only to neurons should still present with the phenotype.

KBP may function in neurons to localize a signal attractive to OPCs to the axon, directing OPCs away from the soma and dendrites. *kbp* mutant neurons would not localize this signal adequately and OPCs would be able to ensheath somas. *kbp* mutants crossed into the transgenic line HuC:GFP-2A-KBP will have KBP function restored in their neurons, and this "myelinated soma" phenotype should disappear. Conversely, mutants crossed into the transgenic line sox10:GFP-2A-KBP which have KBP function restored only to oligodendrocyte-lineage cells should still present with the phenotype.

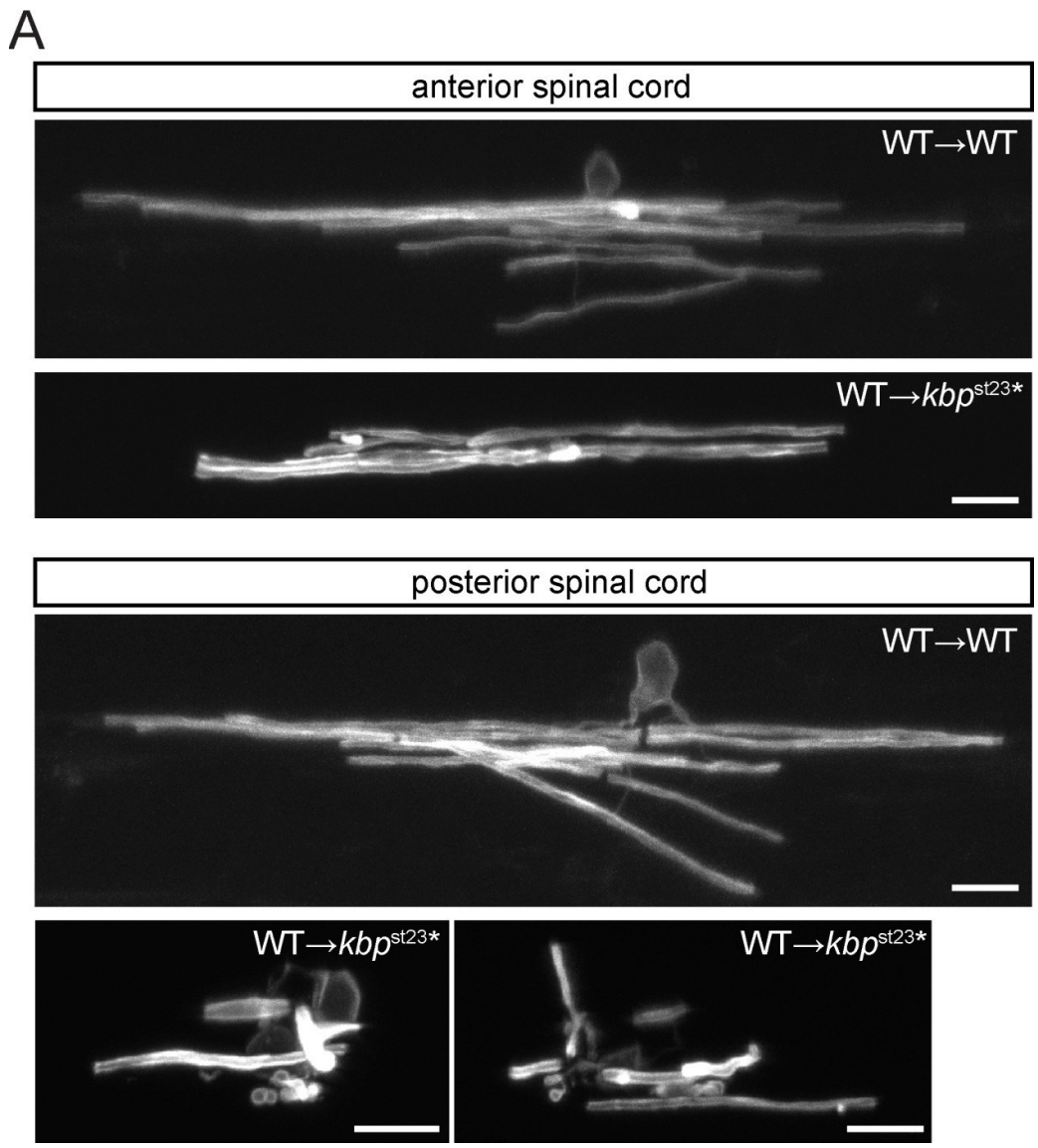

Figure 4.14 – Single mbp:EGFP-CAAX+ oligodendrocytes, example of a blastula-stage transplant experiment

(A) Lateral views of 4 dpf larvae, offspring of *kbp*$^{st23/+}$ incross. These larvae, which include wildtype, heterozygous and *kbp* mutant larva, served as hosts for a transplant experiment in which I transplanted blastula stage cells from a Tg(mbp:EGFP-CAAX) embryo (*kbp*$^{+/+}$). All EGFP-CAAX+ cells originated from the wildtype host. When transplanted into a probable mutant host (*=pending genotyping), oligodendrocytes still elaborate fewer and shorter myelin sheaths, both in the anterior and posterior spinal cord, suggesting a non-cell autonomous role for *kbp* in promoting myelin sheath formation and growth.

Another strategy to address the cell autonomy of these phenotypes is to use blastula stage transplants. In this approach, I transplant uncommitted cells at the blastula stage from a wildtype donor embryo into a mutant host embryo, which results in a chimeric animal with sparse wildtype cells interacting with a majority of mutant cells. For instance, I can analyse the morphology of individual oligodendrocytes from a wildtype mbp:EGFP-CAAX+ donor embryo in an environment composed mostly of mutant neurons and glia in a mutant host embryo that does not carry the transgene Tg(mbp:EGFP-CAAX). Any EGFP-CAAX+ cells are per force oligodendrocytes derived from the wildtype donor and have normal KBP function, whereas most neurons and axons will lack KBP function. Preliminary results from such an experiment indicate that wildtype oligodendrocytes transplanted into a mutant embryo form few and short sheaths (Figure 4.14), suggesting that wildtype levels of KBP in oligodendrocytes are not sufficient to ensure normal sheath length, and that KBP function is required non cell autonomously to promote sheath growth (possibly, in neurons).

Collectively, such findings may provide fairly novel insight into the role of cytoskeleton-associated proteins, such as KBP, in oligodendrocyte biology.

4.4.2 Increased axonal surface

I additionally challenged the oligodendrocyte-lineage cell population by artificially increasing the amount of target axonal surface. I generated animals that instead of one Mauthner axon on each side of the spinal cord presented with 2-7 on each side, in two independent genetic manipulations (Figure 4.5). In both instances, I found that oligodendrocyte-lineage cells recognized, ensheathed and robustly myelinated all of the supernumerary axons (Figure 4.6 and 4.7). It remains formally possible that additional Mauthner axons that did not get myelinated could have remained very small or degenerated, but I did not observe signs of degeneration in electron micrographs. My results show that I could at least triple the Mauthner axonal surface on each side of the spinal cord without detriment to the myelination of nearby axons, at least at 9dpf (Figure 4.8).

I investigated by which mechanism oligodendrocyte-lineage cells adapted to the increased axonal surface. I found that it was not due to an increase in the size of the oligodendrocyte population (Figure 4.9), and instead that it was due to an increase in the myelin production of each individual oligodendrocyte (Figures 4.10 and 4.11). This may at first appear at odds with the results described in Chapter 3, in which the opposite manipulation (removing reticulospinal axons) decreased the number of oligodendrocyte-lineage cells. However, it should be noted that in the *kbp* manipulation, the entirety of reticulospinal axons are missing, leading to an 80% decrease in axonal surface in the ventral spinal cord at 3dpf. Instead, the *notch1a* MO/*hoxb1b* mRNA manipulation only significantly increased the number of Mauthner axons – in fact, the number of neighbouring myelinated axons is not significantly changed in animals injected with *notch1a* MO or *hoxb1b* mRNA at 9dpf (Figure 4.8 B). Therefore, this is likely to represent a comparatively smaller manipulation. The total number of axons in the spinal cord in this manipulation might not be drastically altered; it is the number of the very first targets for myelination that is, which happen to be of a large-calibre. This may mean a very localized increase in axon-derived juxtacrine or paracrine signaling in the ventral spinal cord. An earlier study on mice with twice as many RGC axons in the optic nerve as normal found an increased number of oligodendrocytes, due to an increase in OPC survival and proliferation (Burne, Staple et al. 1996). However, as discussed in Chapter 3, the interpretation of results from that study could have been confounded by technical limitations. Additionally, my manipulation may simply be a qualitatively different manipulation than doubling of total number of axons in the nerve, which may have more significantly increased the amount of secreted factors, for instance. My manipulations, rather than eliciting large changes in oligodendrocyte population size, seem to have deployed a finer means of regulation of the myelinating capacity of the oligodendrocyte population.

Furthermore, in the results described in Chapter 3, the axonal regulation of the oligodendrocyte-lineage cell population size occurs by modulating the proliferation of OPCs and/or survival of OPCs or oligodendrocytes. It is thought that an excess of OPCs competes for limited amounts of pro-survival neurotrophic factors, derived from axons in the milieu, and this roughly matches oligodendrocyte number with

target axonal surface (Barres and Raff 1999). However, as discussed in Chapter 3, no developmental apoptosis of OPCs was observed in the WT zebrafish spinal cord, unlike in other vertebrates. It may be that there is no surplus of OPCs competing for axon-derived survival signals in WT zebrafish larvae, if the number of OPCs generated is already matched to the axonal surface available. Therefore, my manipulation increasing axonal surface and potentially contact-dependent survival signals should not increase the number of such competing OPCs further, as no excess of OPCs exist in the first place that would die. In regards to OPC proliferation, it should be noted that in *kbp* mutants, the observed proliferation effect was small even when removing the entirety of reticulospinal axons. Therefore, increasing only the number of Mauthner axons might have had an even smaller effect which may have gone undetected, as I focused on the number of oligodendrocytes at 5dpf, and did not investigate the number of OPCs.

My results indicate that the typical ventral oligodendrocytes that associate with Mauthner axons are plastic and able to adapt to the axonal environment, since supernumerary Mauthner axons were able to induce these oligodendrocytes to make more and longer myelin sheaths - that is, they greatly increased their myelinating capacity (Figures 4.10 and 4.11). These oligodendrocytes typically maintain only one long myelin sheath on the Mauthner axons, of a large calibre, reminiscent of the oligodendrocyte type IV described by Pio del Rio-Hortega almost 100 years ago (Río-Hortega 1928). However, Mauthner axons are rather unusual axons – in addition to their very large calibre, they do not possess nodes of Ranvier. It is thought that synaptic boutons at axon collaterals serve the purpose of regenerating the Mauthner action potential in other fish species (Funch and Faber 1980, Greeff and Yasargil 1980, Yasargil, Greeff et al. 1982). In cross section, these axon collaterals and synapses interrupt the myelin sheath, resulting in a partially surrounded axon in cross section, another distinctive feature. We have further observed, for instance, that the ends of adjacent Mauthner-associated myelin sheaths often overlap and interdigitate, rather than forming precise internodes flanked by unmyelinated gaps. These rather unique microanatomical features hinted that the ventral subset of oligodendrocytes that myelinate the unique Mauthner axon could be a distinct subtype of oligodendrocytes. A plastic subset, but nonetheless, such

plasticity could be their specific property, rather than a general characteristic of oligodendrocytes. In fact, even in our analyses of WT animals, we very occasionally observe Mauthner-dedicated oligodendrocytes that simultaneously associate with a smaller diameter axon, an arrangement which could be indicative of the plasticity of this subset.

However, I then observed that even dorsal oligodendrocytes, which typically myelinate numerous dorsal or medial small-diameter axons, were also affected in the presence of supernumerary Mauthner neurons (Figure 4.12). Many dorsal oligodendrocytes in these animals were observed to extend processes ventrally and myelinate large segments of the supernumerary Mauthner axons, in addition to smaller-diameter axons. I have not observed such an arrangement in WT animals. This demonstrates that Mauthner axons can also locally induce the ensheathment, synthesis and maintenance of myelin sheaths made by oligodendrocytes that otherwise would not associate with them.

4.4.3 Conclusions

My aim was to address how the morphological diversity of oligodendrocytes arises during development: whether distinct types of morphologies represent distinct intrinsic programs of development within oligodendrocyte-lineage cells, or whether all of these cells are initially plastic, and axons regulate the development of their final morphology. I found that axons can regulate the extent of oligodendrocyte myelination and can also locally promote sheath formation and myelin biosynthesis.

Could these two aspects be related? In principle, the signalling stimulating myelin synthesis could also be responsible for the increase in the extent of myelination of the whole cell. Given that some structural components are locally synthesized from mRNAs, and assuming that delivery of the remaining components from the cell is not rate-limiting in a physiological range, it is possible that the increase in myelination extent is simply the byproduct of the action of the axonal molecules that locally interact with OPC membrane and promote myelin biosynthesis. Which molecules might this be? It is clear that they must act at close-range, likely in a

juxtacrine fashion, presented in the axonal surface. The obvious candidate is Neuregulin-1, as mentioned in Chapter 1; however, it must act in redundancy with other signals, given that its genetic ablation from the CNS does not cause a drastic myelination phenotype (Brinkmann, Agarwal et al. 2008, Perlin, Lush et al. 2011). An elegant in vitro study proposed that neurotransmitter release at axon-OPC synapses plays a major role in stimulating local translation of *mbp* mRNA and myelin synthesis via activation of the Fyn kinase signalling cascade in oligodendrocyte-lineage cells (Wake, Lee et al. 2011). While the identity of the signalling pathways underlying such regulation remains to be directly verified in vivo, our own work has identified a role for synaptic vesicle release in promoting the extension of myelin sheaths during developmental myelination in the zebrafish embryonic spinal cord (Mensch 2014). We have also previously shown that activating Fyn kinase in oligodendrocytes does indeed promote the generation of myelin sheaths in vivo, while downregulating it decreases the number of sheaths generated by oligodendrocytes (Czopka, Ffrench-Constant et al. 2013), so at least that part of the signalling cascade could be correct.

In sum, I have unambiguously demonstrated, in vivo, that axons can regulate the myelinating capacity of oligodendrocytes, which can operate at a larger capacity than they do in a normal situation; and that axons can locally promote sheath formation and myelin biosynthesis, in a process specific manner. These findings raise a number of interesting questions which I will discuss in Chapter 6.

5. Intersectional expression of genes of interest in zebrafish using the split KalTA4 system

Foreword

While investigating the role of axons during oligodendrocyte-lineage cell development and myelination, I sought to live-image OPCs. There is not currently a transgenic line that specifically labels OPCs in the spinal cord. A fragment of the sox10 promoter drives expression in oligodendrocyte-lineage cells, but also in a subset of dorsally-located neurons in the spinal cord, and other neural-crest derived cells outwith the spinal cord. A large portion of the olig2 regulatory sequence drives expression in oligodendrocyte-lineage cells but also in pMN progenitors and terminally differentiated motor neurons. Thus, neither the olig2:GFP transgenic line nor the sox10:mRFP line specifically labels oligodendrocyte-lineage cells in the spinal cord. However, oligodendrocyte-lineage cells are the only subset of cells that specifically express both sox10 and olig2 (motor neurons do not express sox10, and the dorsal sox10+ neurons do not express olig2). Therefore, in the double transgenic line Tg(olig2:GFP; sox10:mRFP), oligodendrocyte-lineage cells, from an OPC stage, are the only double labelled cells, which allowed me to unambiguously identify OPCs. However, since I required two separate channels for the imaging of this line, I was limited in the number of possible combinations with other relevant transgenic lines, which all use green or red fluorescent proteins. I could not, therefore, combine imaging of OPCs with oligodendrocytes, or imaging of OPCs with axons. To attempt to overcome this difficulty, I adapted a strategy of combinatorial expression that would allow me to express a gene-of-interest (GOI), such as GFP, under the control of two different promoters. Although I eventually would not use this tool in my own experiments, the tool works, and may be used in other contexts. I therefore describe here my adaptation of the Drosophila Split Gal4 system for combinatorial expression in zebrafish. I included the description of the relevant experimental procedures in this Chapter.

5.1 Introduction

Ectopic expression of genes-of-interest (GOI) in cells is fundamental for understanding the function of genes and the biology of cells. Driving ectopic expression of a fluorescent protein, for instance, illuminates the target cells' morphology, origin, differentiation and behaviour (Zhang, Campbell et al. 2002). Driving expression of calcium indicators or optogenetic tools permits interrogation or manipulation of the physiological state of the target cell (Fenno, Yizhar et al. 2011). Driving expression of a particular mutant allele of a gene helps elucidate its relevance in the specification, development or function of target cells or tissues (Elliott and Brand 2008). Recently, in an effort to systematically generate mutations in each protein-coding gene of the zebrafish genome, it was determined that over 80% of nonsense or essential splice mutations, representing over 1200 genes, have no obvious morphological or behavioural phenotype within 5dpf(Kettleborough, Busch-Nentwich et al. 2013). Functional data for many of these genes may arise from studies resorting to ectopic expression of their wildtype and mutant forms.

One manner in which to direct GOI expression to a target cell is by fusing the GOI coding sequence to a regulatory element (such as a promoter fragment) known to be expressed in the target cell type. The resulting construct is used to generate transgenic animals and their offspring assessed for fidelity of expression of the GOI, in a pattern similar to that of the endogenous gene.

An alternative manner is to resort to the use of already existing Gal4/UAS transgenic lines. The bipartite Gal4/UAS system is a genetic tool amply used in Drosophila (Elliott and Brand 2008) and in zebrafish (Davison, Akitake et al. 2007, Halpern, Rhee et al. 2008) to drive GOI expression in particular cell types (Figure 5.1 A). A Gal4 driver line expresses the yeast transcription factor Gal4 under the control of a regulatory sequence that drives its expression in a known pattern. It is crossed with a UAS effector line, where an upstream activating sequence (UAS), specifically recognized by Gal4, is cloned upstream of GOI. Directed expression occurs in the double transgenic offspring of crosses between driver and effector lines. An

advantage of this system is that a variety of Gal4 driver lines already exist, targeting expression in different tissues, or targeting expression in a ubiquitous manner but under the temporal control of the heatshock promoter hsp70. Researchers can build a simple UAS effector line with the GOI coding sequence, and combine it with already characterized lines. Similarly, a variety of UAS effector lines already exist. This system provides an enormous versatility of manipulations(Elliott and Brand 2008). For instance, it allows:

a) analysis of a single GOI in different tissues and at different time points;
b) testing gain- or loss-of-function alleles
c) rescue experiments in mutant animals by reconstituting wildtype or downstream effector expression;
d) temporal control over the expression of toxic proteins or functional modulators (such as optogenetic tools).

A striking limitation of both of these approaches, however, is that GOI expression is ultimately under the control of a single promoter, which may not achieve the required specificity. In fact, existing Drosophila or zebrafish Gal4 lines, whether enhancer-trapped or genetically engineered to be driven by a known promoter, rarely confine expression to a single cell type(Suster, Seugnet et al. 2004, Bohm, Welch et al. 2010). This may preclude the analysis of cell autonomous effects of GOI, for instance, or may not enable visualization of a particular cell type with the specificity necessary, if related or nearby cell types also express a reporter protein.

In order to overcome this limitation, ternary systems such as the SplitGal4 system have been developed (Figure 5.1 B)(Luan, Peabody et al. 2006, Pfeiffer, Ngo et al. 2010). This system takes advantage of the modularity of Gal4, and encodes its DNA-binding domain separately from its activation domain, in so called ”hemidrivers”. Each hemidriver is encoded under the control of a different promoter. Therefore, only in those cells in which both promoters are active at the same time will the protein for both hemidrivers be produced. Fusion of each hemidriver to a heterodimerizing leucine-zipper ensures that if and when co-expression happens, the two parts dimerize and reconstitute a functional Gal4. This in turn binds and activates expression from an UAS-sequence.

This allows GOI expression in the intersection of two expression patterns, when a single promoter does not provide enough specificity. It can also be used to temporally control ectopic expression in the target cells by combining a cell-type specific promoter with the heat-shock promoter, hsp70. One other use of the split Gal4 system is to dissect the expression pattern of complex promoters by iterative combinations with more specific enhancers.

Here, I describe an adaptation of the Split Gal4 system for use in zebrafish, which I term Split KalTA4, since I based it on the optimized version of Gal4, KalTA4 (Distel, Wullimann et al. 2009). I provide an example where its use allowed the dissection of a complex expression pattern by restricting reporter expression to subsets of cells.

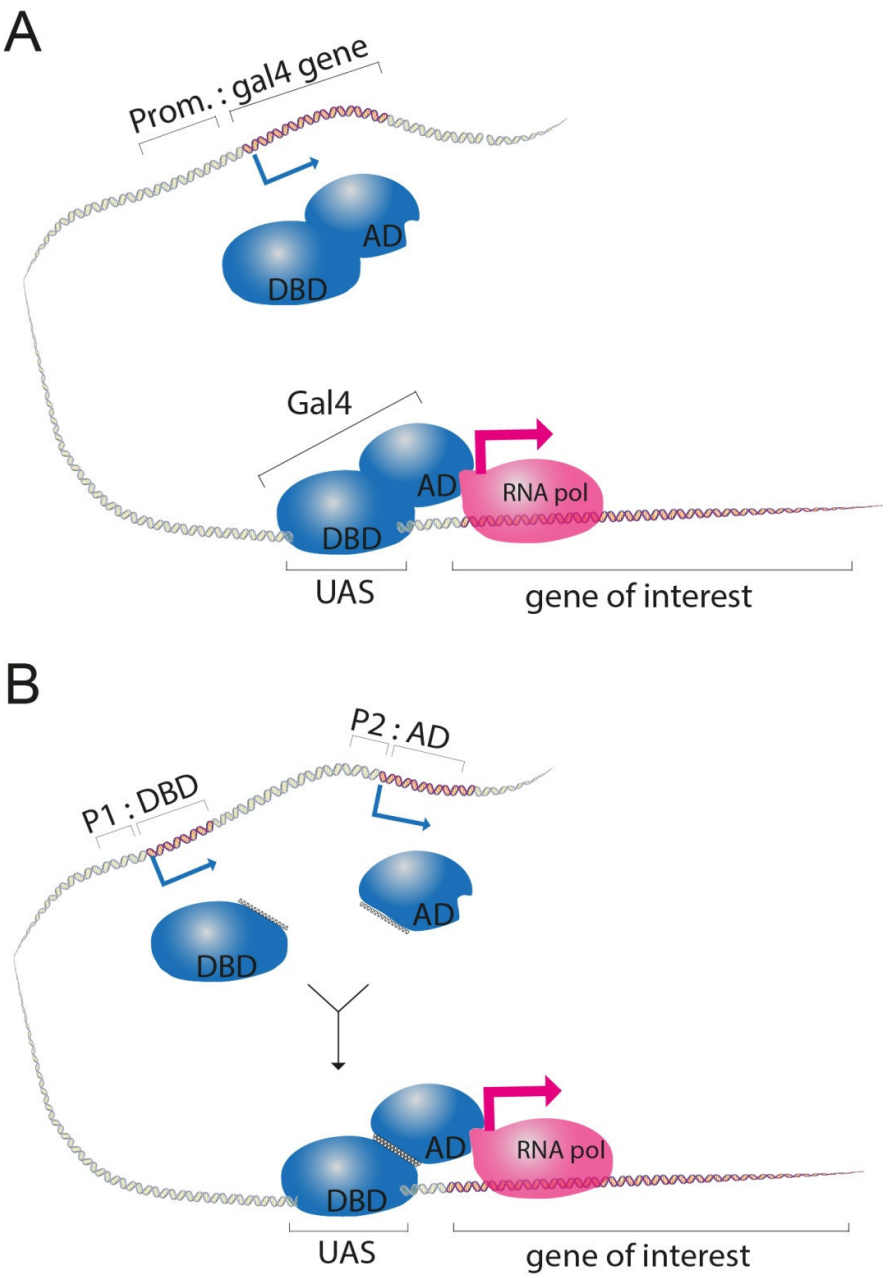

Figure 5.1 – Gal4 vs Split Gal4 system:

(**A**) Gal4 system: the gal4 gene encodes the intact transcription factor including DNA-binding domain (DBD) and the activation domain (AD) in a single ORF, under one promoter (prom). Whole Gal4 protein (blue) binds UAS in another transgene and activates downstream GOI transcription (pink arrow).
(**B**) Split Gal4 system: one transgene encodes Gal4 DBD hemidriver under one promoter (P1) and a separate transgene encodes Gal4 AD hemidriver under a different promoter (P2). When and where both promoters are active, the two domains assemble, due to a heterodimerizing leucine zipper, and reconstitute Gal4 function, activating transcription from UAS and leading to GOI expression.

5.2 Results

5.2.1 Design of Split KalTA4 hemidrivers

In order to generate a conditional expression system in zebrafish where GOI are expressed in the intersection of the expression patterns of two regulatory sequences, I adapted the split Gal4 system developed in Drosophila (Luan, Peabody et al. 2006). In this system, the DNA binding domain (DBD) and the activation domain (AD) of the transcription factor Gal4 are encoded in separate genes ("hemidrivers"), which can be under the control of different promoters. Each domain is not functional on its own, but when co-expressed in the same cell, they reconstitute Gal4 function and activate expression of UAS-driven transgenes. To facilitate heterodimerization and assembly of a functional transcription factor, (Luan, Peabody et al. 2006) fused a heterodimerizing leucine zipper to each hemidriver, and optimized the type of zipper used, as well as its site of fusion and length of the spacer (Figure 5.1C). I designed hemidrivers based on the original sequences, splitting instead KalTA4, a version of Gal4 optimized for zebrafish (Distel, Wullimann et al. 2009). Kalta4 shows a number of optimal modifications compared to Gal4: it includes a strong Kozak sequence; codon usage optimized for zebrafish expression, and instead of the entire VP16 activation domain, (Distel, Wullimann et al. 2009) used attenuated repeats of the VP16 core sequence, TA4. TA4 is similarly potent in transgene activation as VP16 and less toxic. I used the sequence encoding residues 1-147 of KalTA4 for the DBD hemidriver, and encoding residues 154-192 for the TA4 hemidriver. I added the remaining features by extension PCR. In addition to the decaglycine spacer and the heterodimerizing leucine zippers, I changed the original nuclear localization signal sequence of the AD hemidriver to the shorter SV40 nls sequence. I also included the strong Kozak sequence used in KalTA4 in both hemidrivers, and also optimized codon-usage in the remaining features of the hemidrivers for expression in zebrafish (Figure 5.2D). In my constructs, only the plasmids encoding the intact KalTA4 (positive control) included the rabbit beta-globin intron downstream of the coding sequence, which is a modification reported to increase expression originally included in the design of KalTA4. All constructs were verified by Sanger sequencing.

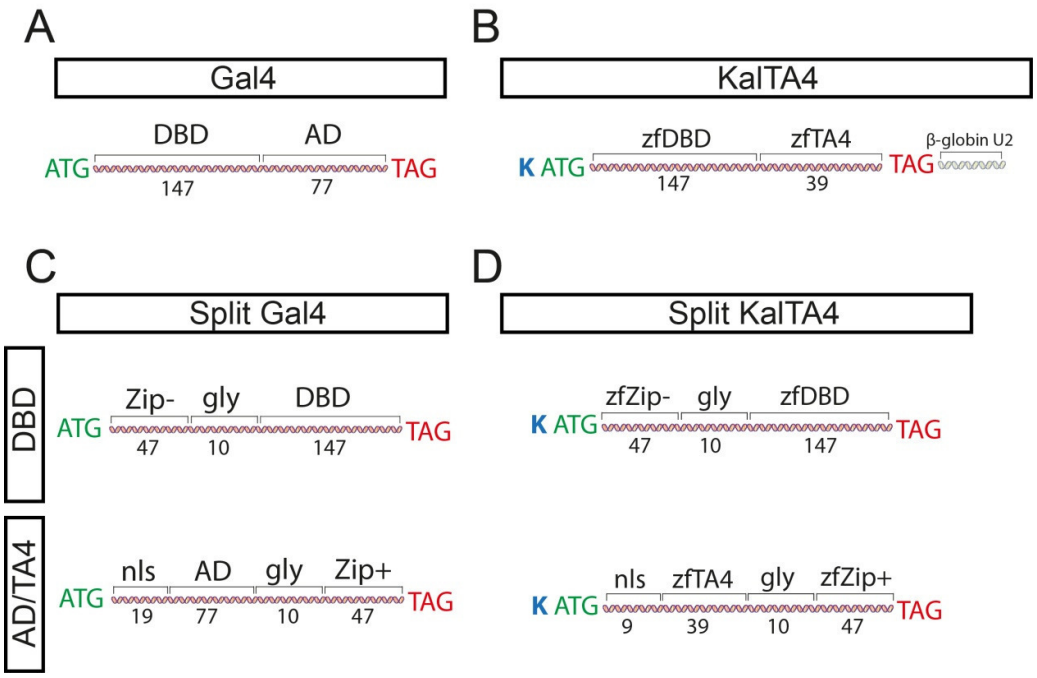

Figure 5.2 – Structure of Gal4, KalTA4, Split Gal4 and Split KalTA4 hemidrivers:

(**A-B**) A single gene encodes Gal4, or KalTA4.
(**C-D**) Two separate genes encode each hemidriver of Split systems.
K: Kozak sequence; ATG: start codon; TAG: stop codon; zf: zebrafish-optimized sequence; Zip+/-: heterodimerizing leucine zipper; nls: nuclear localization signal; gly: 10x glycine linker. Number under each feature indicates size in amino acid residues.

5.2.2 Expression of both hemidrivers is required to transactivate a reporter transgene in vivo

I generated synthetic mRNA of each hemidriver and of intact KalTA4. To test whether split KalTA4 worked as expected, I injected mRNA into Tg(UAS:kaede) fertilized eggs. Injection of mRNA results in ubiquitous expression throughout the early embryo, and the UAS sequence drives expression of the fluorescent protein kaede in this line. When mRNA for each hemidriver is injected alone, no expression of kaede is detected throughout the first days of development (Figure 5.3A; DBD: 0/40 embryos; TA4: 0/60 embryos). When mRNA for both hemidrivers are co-injected, expression of kaede is detected throughout the embryo from at least 24hpf (Figure 5.3B, at 48hpf, 20/31 embryos). Injection of intact KalTA4 mRNA similarly results in activation of kaede expression throughout the embryo (Figure 5.3C, 28/41 embryos). UAS:kaede colony is maintained as a mixture of heterozygous and homozygous animals, thus the subset of non-fluorescent embryos likely does not contain the reporter transgene (similar in the positive control, intact KalTA4).

To determine whether I could genetically target the hemidrivers, I first generated constructs where the coding DNA for each hemidriver is preceded by the histone 2-α promoter, which drives expression in many cell types (Kwan, Fujimoto et al. 2007). Similarly to the mRNA microinjections, only co-injection of h2α:DBD with h2α:TA4 or injection of the intact h2α:KalTA4 resulted in activation of the UAS:kaede reporter (0/20 embryos injected with h2α:DBD; 0/20 embryos injected with h2α:TA4; 29/35 embryos co-injected with h2α:DBD and h2α:TA4; and 23/45 embryos injected with h2α:KalTA4). Thus, recognition of the UAS sequence and activation of downstream gene transcription require the presence of both Split KalTA4 hemidrivers.

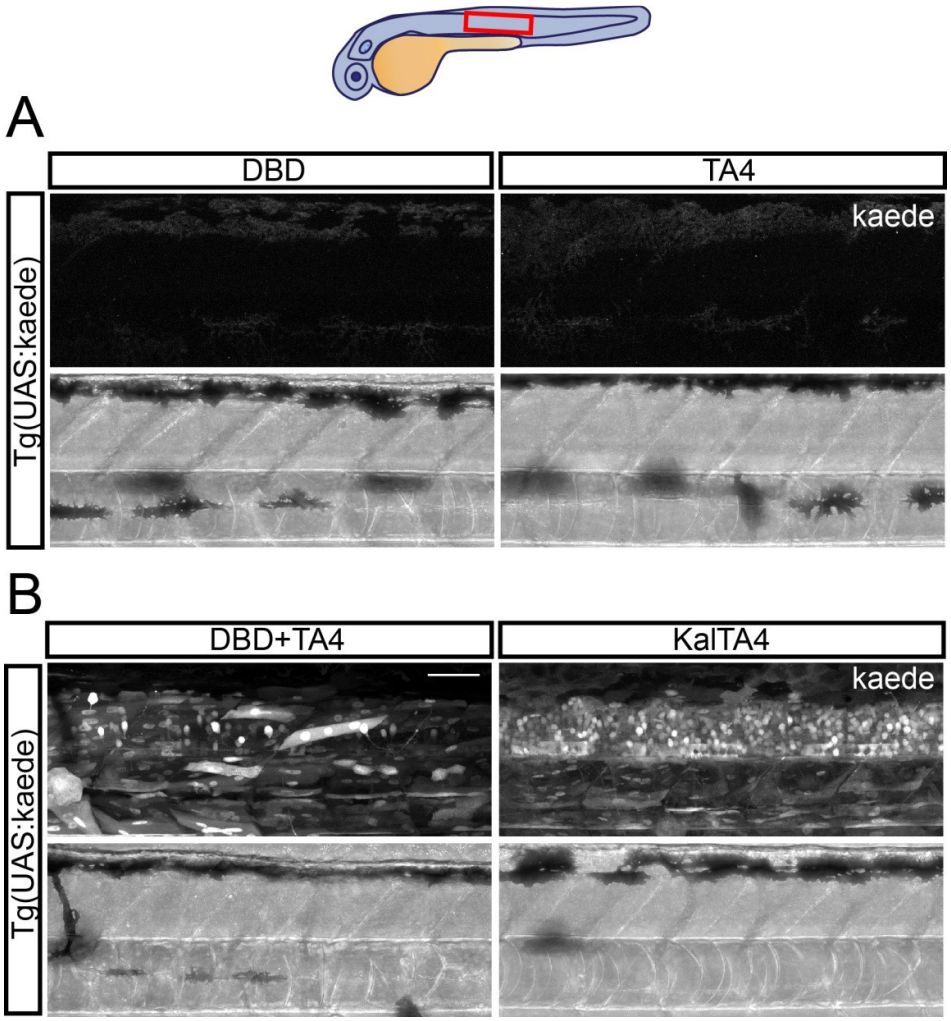

Figure 5.3 –Split KalTA4 hemidriver mRNA expression reconstitutes KalTA4.

(**A**) Injection of DBD or TA4 mRNA alone doesn't activate the reporter UAS:kaede.
(**B**) Injection of both DBD and TA4 mRNA, or intact KalTA4 mRNA is sufficient to transactivate the reporter UAS:kaede.

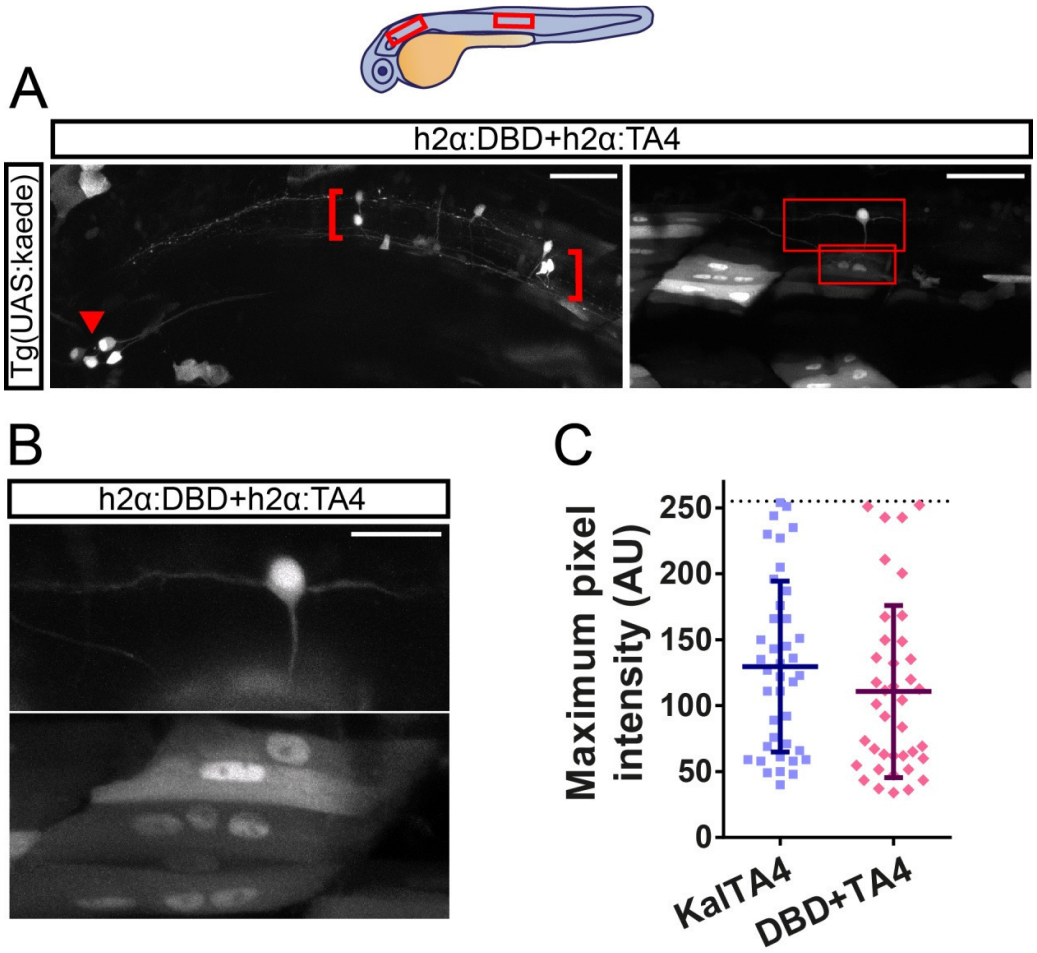

Figure 5.4 – Genetically targeted split KalTA4 hemidrivers activate UAS:kaede in several cell types with similar efficiency to intact KalTA4.

(**A**) Split KalTA4 hemidrivers genetically encoded under the h2α promoter are ubiquitously expressed. Arrowhead points to expression in posterior lateral line (peripheral) neurons, brackets point to spinal cord (central) neurons, boxed areas are displayed at higher magnification in C.
(**B**) Higher magnification of a Commissural Primary Ascending interneuron (top) and several muscle cells (bottom) expressing the reporter transgene.
(**C**) Maximum pixel intensity in arbitrary units of 40 randomly selected cells in larvae injected with h2α:KalTA4 and 39 cells in larvae co-injected with h2α:DBD and h2α:TA4. No significant difference is found (130±65 AU in KalTA4 vs 111±65 AU in DBD+TA4, p=0.1566 in Mann-Whitney test).

5.2.3 Split KalTA4 functions efficienty in many cell types

The use of the quasi-ubiquitous h2α promoter and of DNA constructs (which results in sparser expression than mRNA injections) enabled me to identify by morphology and location the cell types expressing the reporter fluorescent protein kaede. I found that, like intact KalTA4, co-injections of the split KalTA4 hemidrivers resulted in kaede expression in both central and peripheral neurons (Figure 5.4A), muscle cells (Figure 5.4B), skin cells and notochord cells. Thus, the hemidrivers can heterodimerize and transactivate the reporter transgene in many cell types. I then wondered if reconstituted DBD+TA4 activated the reporter transgene with the same efficacy as intact KalTA4. I considered fluorescence intensity as a proxy for the level of UAS:kaede expression and thus transactivation efficiency. The maximum pixel intensity in randomly selected cells expressing kaede driven by split KalTA4 was similar to those in cells where kaede was driven by intact KalTA4 (Figure 5.4C). This suggests that the efficiency of Split KalTA4 transactivation of the transgene is similar to intact KalTA4 in vivo.

5.2.4 Split KalTA4 restricts broad sox10 expression pattern

The *sox10* regulatory region drives expression of reporter genes in several cell types (Dutton, Antonellis et al. 2008). In the Tg(sox10:mRFP) line, a 7.2kbp fragment of the *sox10* promoter drives expression of mRFP in neural crest, in myelinating glial cells and in a subpopulation of dorsal neurons in the embryonic spinal cord. OPCs (Figure 5.5A, asterisk) also co-express the transcription factor Olig2, unlike the sox10+ dorsal neurons (Figure 5.5A, arrowheads). To exclude the possibility that this expression pattern is specific to the Tg(sox10:mRFP) line due to positional effects of its transgene insertion, I generated a different stable transgenic line using the same *sox10* promoter fragment, driving intact KalTA4. When crossed with the reporter UAS:kaede, sox10+ cells are mosaically labelled, allowing imaging of their morphology and unambiguous identification (Figure 5.5B). This confirmed that in the spinal cord, Sox10 is expressed in some dorsal neurons (Figure 5.5B, cell a), mature oligodendrocytes (cell b), OPCs (cell c), and in dorsal root ganglia (not shown). I observed labeling of the same cell types when I co-injected sox10:DBD with sox10:TA4.

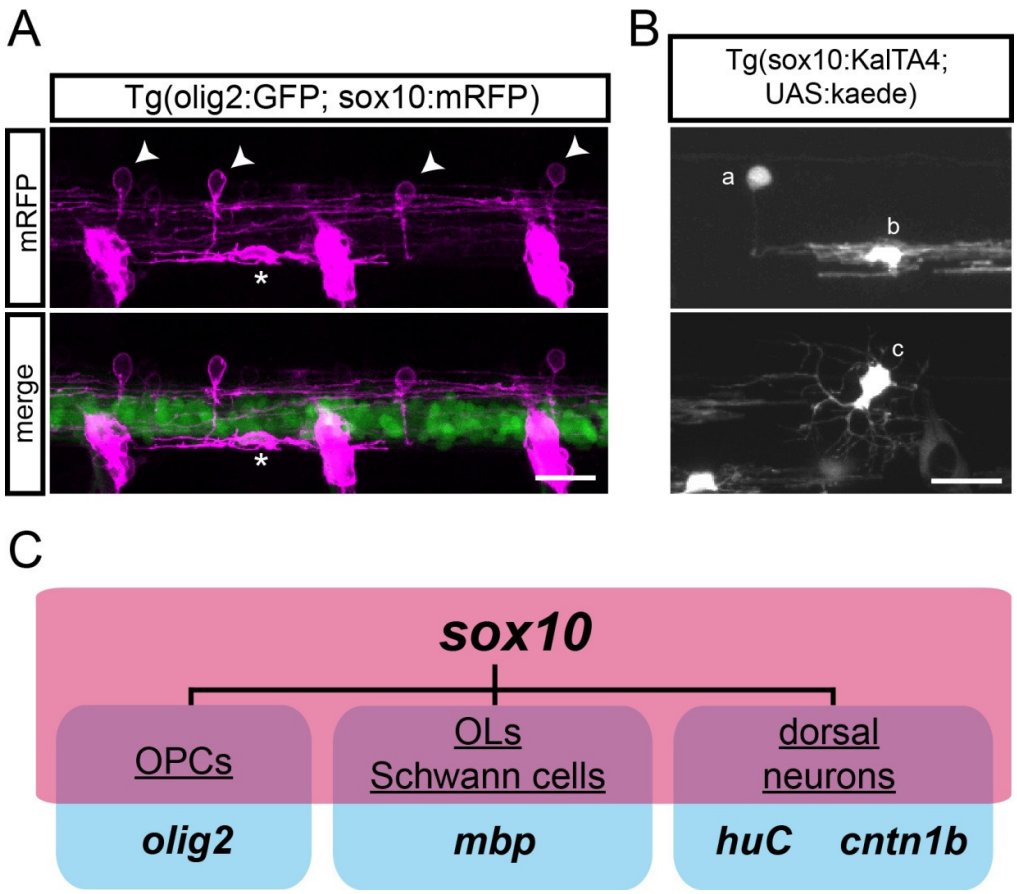

Figure 5.5 – sox10+ cells in the embryonic and larval zebrafish spinal cord.

(**A**) 48hpf Tg(olig2:GFP; sox10:mRFP) embryo, showing sox10:mRFP expression both in dorsal neurons (arrowheads) and in OPCs (asterisk, co-expressing olig2:GFP).
(**B**) 4dpf Tg(sox10:KalTA4; UAS:kaede) larvae, showing *sox10* expression in a neuron (a), mature oligodendrocyte (b) and OPC (c). Scalebars: 20µm.
(**C**) Venn diagram of expression patterns of sox10 and other promoters specific to some of the sox10 component cell types.

I wondered if I could use the split KalTA4 system to restrict expression of the reporter transgene to subtypes of sox10+ cells. Myelinating glial cells (oligodendrocytes in the spinal cord and Schwann cells in the periphery) also express *mbp*. Neurons express HuC (an RNA-binding protein used as a pan-neuronal marker (Park, Kim et al. 2000)). Additionally, many neurons in the zebrafish spinal cord express Contactin1b (Cntn1b) as judged by expression driven by a fragment of its promoter (Czopka, Ffrench-Constant et al. 2013). To label cells only in the intersection of these expression patterns (Figure 5.5C), I first generated hemidriver constructs using fragments of the promoter of the mbp, huC, sox10 and cntn1b genes. I then co-injected different combinations of the hemidrivers.

When I co-injected mbp:DBD and sox10:TA4 hemidrivers in Tg(UAS:kaede; sox10:mRFP) fertilized eggs, I observed kaede expression only myelinating glial cells. I readily observed kaede+ Schwann cells in the posterior lateral line (pLL, Figure 5.6A, top), and in some oligodendrocytes in the spinal cord, but no extensive neuronal expression such as in Tg(sox10:KalTA4) or Tg(sox10:mRFP) animals.

To further dissect the expression pattern of the *sox10* promoter, I co-injected cntn1b:DBD with sox10:TA4 in Tg(UAS:kaede) fertilized eggs. In these larvae, I readily observed labelled neurons, particularly in the dorsal spinal cord (Figure 5.6B), but no myelinating glial cells, confirming that the sox10+ neurons in the dorsal spinal cord also express contactin1b, and that the splitKalTA4 is able to restrict a broad expression pattern to its components. I also co-injected huC:DBD with sox10:TA4 in Tg(UAS:kaede; sox10:mRFP) fertilized eggs. Most labelled cells were neurons, and many of these occupied the dorsal position typical of sox10+ neurons; in addition, they co-localized with mRFP expression in the sox10:mRFP line (Figure 5.6C).

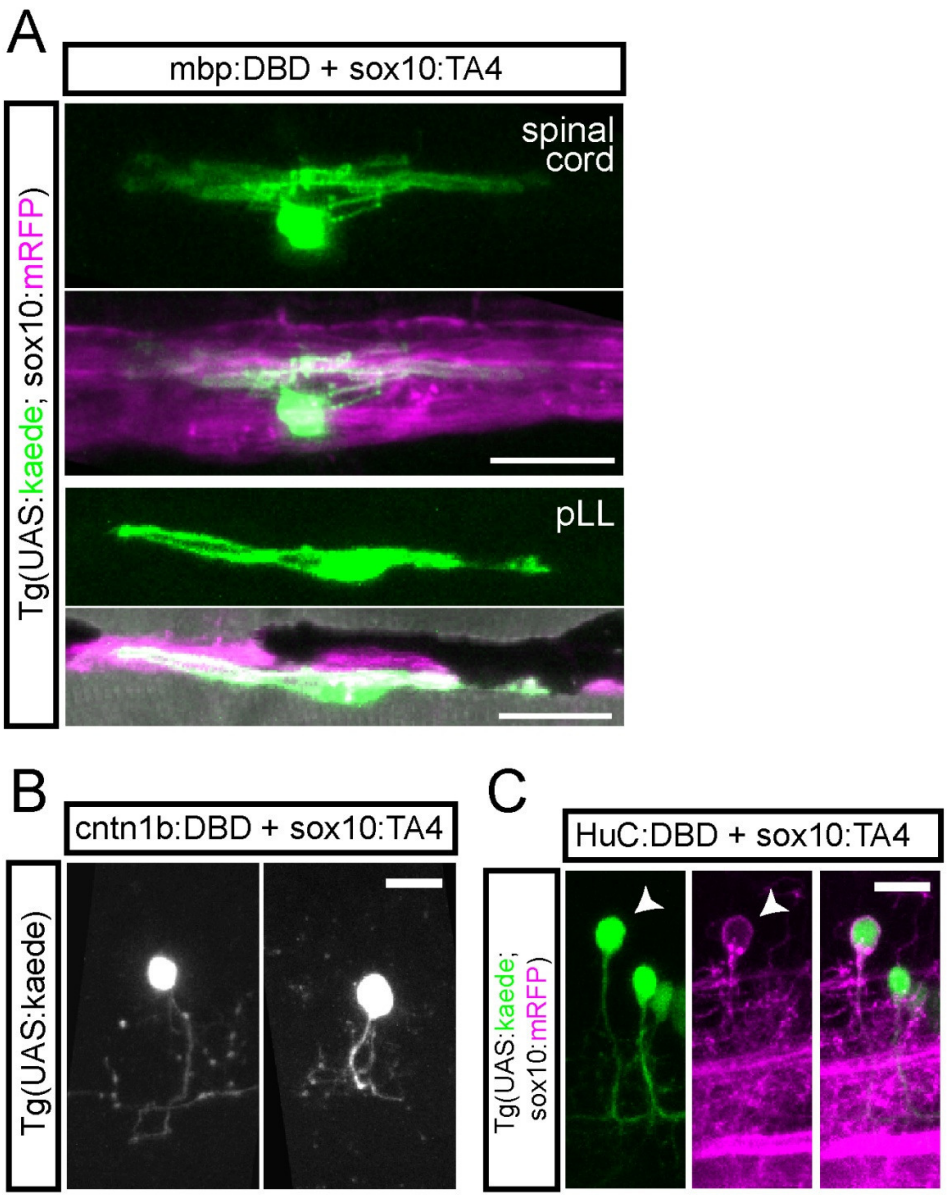

Figure 5.6 – Split KalTA4 restricts sox10 expression pattern in the larval zebrafish.

(**A**) Spinal cord and pLL of 5dpf Tg(UAS:kaede; sox10:mRFP) larvae co-injected with mbp:DBD and sox10:TA4. Schwann cells and oligodendrocytes express the kaede reporter.
(**B**) Dorsal neurons in the spinal cord of 4dpf Tg(UAS:kaede) larvae co-injected with cntn1b:DBD and sox10:TA4.
(**C**) Dorsal neurons in the spinal cord of 3dpf Tg(UAS:kaede; sox10:mRFP) larvae co-injected with HuC:DBD and sox10:TA4. Some sox10:mRFP+ neurons are also labelled by the kaede reporter. Scalebars:10µm

5.3 **Conclusions**

In sum, I have adapted a combinatorial expression system, Split Gal4, for use in the zebrafish, named Split KalTA4. In this ternary system, only cells in the intersection of two expression patterns reconstitute the transcription factor KalTA4. This permits the use of two distinct promoters to drive GOI expression only in the subset of cells in which both promoters are active. I showed that the modifications I inserted in the system work in living zebrafish. These include zebrafish-specific adaptations that were part of the KalTA4 optimization, including a substitution of the entire VP16 activation domain for the minimal activation motif, TA4. The TA4 configuration of the core activation repeats can be replaced with configurations less efficient (TA6) or more efficient (TA2)(Baron, Gossen et al. 1997), providing an additional level of control of the expression of the GOI.

I have also provided a specific example for the use of this system, in which I restricted a broad expression pattern (*sox10*) to its components (*mbp*, *huC* or *cntn1b*). This shows that this system can be used to dissect complex expression patterns.

In the future, full transgenic lines of the hemidrivers will be generated that will permit a more stable, and less mosaic, expression of genes of interest.

5.4 Experimental Procedures

5.4.1 Generation of hemidriver constructs

Dna-binding Domain (dbd) hemidriver:

The original DBD hemidriver consists of a heterodimerizing leucine zipper (Zip) fused to a 10xglycine linker (gly), fused to N-terminus of the Gal4 DBD (residues 1-147; Figure 5.2 C). Residues 1-147 of Gal4 DBD are identical to KalTA4 DBD, therefore the splitKalTA4 DBD hemidriver contains the same residues, with codon usage optimized for zebrafish. I PCR-amplified the DNA binding domain of KalTA4 from pCSKalTA4 (Distel, Wullimann et al. 2009) and added the remaining features by consecutive extension PCRs. These included the leucine zipper, followed by the 10x glycine linker, upstream of the DBD sequence. I also included the strong kozak sequence used in KalTA4. In the last round of PCR I added attB sites and used BP clonase to recombine it with pDONR221 to generate pME-DBD.

TA4 hemidriver:

The original Gal4 or VP16 AD hemidrivers consist of a long nuclear localization signal (nls) from SV40 fused to the N-terminus of the transcription-activation domain of Gal4 or VP16, fused to the N-terminus of a 10x glycine linker, fused to the N-terminus of the heterodimerizing leucine zipper complementary to that of the DBD hemidriver (Figure 5.2 C). To generate my TA4 hemidriver, I amplified the TA4 sequence from pCSKalTA4 (residues 154-192) by PCR and added the remaining features by consecutive extension PCRs. These included a short nuclear localization signal from SV40 upstream of TA4, and a 10x glycine linker and the complementary leucine zipper downstream. I also included the strong kozak sequence used in KalTA4. In the last round of PCR I added attB sites and used BP clonase to recombine it with pDONR221 to generate pME-TA4.

5.4.2 Generation of DBD and TA4 synthetic mRNAs:

The Kozak and coding sequences for DBD and TA4 were PCR-amplified and cloned into pCS2+ digested with BamHI and Klenow-blunted. Constructs were verified by sequencing. Synthetic mRNA was produced by linearizing the templates with NotI and transcribing from the SP6 promoter using SP6 mMessage mMachine (Ambion).

5.4.3 Gateway recombination of split KalTA4 hemidrivers

I recombined 5' entry vectors containing a fragment of the h2α(Kwan, Fujimoto et al. 2007), sox10(Kirby, Takada et al. 2006), mbp(Almeida, Czopka et al. 2011), huC(Park, Kim et al. 2000) or cntn1b(Czopka, Ffrench-Constant et al. 2013) promoters; middle entry vectors pME-DBD, pME-TA4 or pME-KalTA4GI; and 3' entry vectors containing a poly adenylation signal in a LR-recombinase mediated gateway recombination to generate the constructs used in this study. All entry vectors were verified by sequencing and all destination constructs were screened by at least three restriction enzyme digestions.

5.4.4 Microinjection

For synthetic mRNA injections, 100pg of each mRNA in water were microinjected in a volume of 1nL into the yolk of fertilized UAS:kaede eggs (eggs injected with both hemidrivers contained a total amount of 200pg mRNA). Other injections performed as described in Chapter 2.

5.4.5 Imaging

All image acquisition, processing and analysis, including intensity measurements were performed as described in Chapter 2, using a Zeiss LSM710 confocal microscope and the measurement tool in Fiji.

6. Discussion and Conclusions

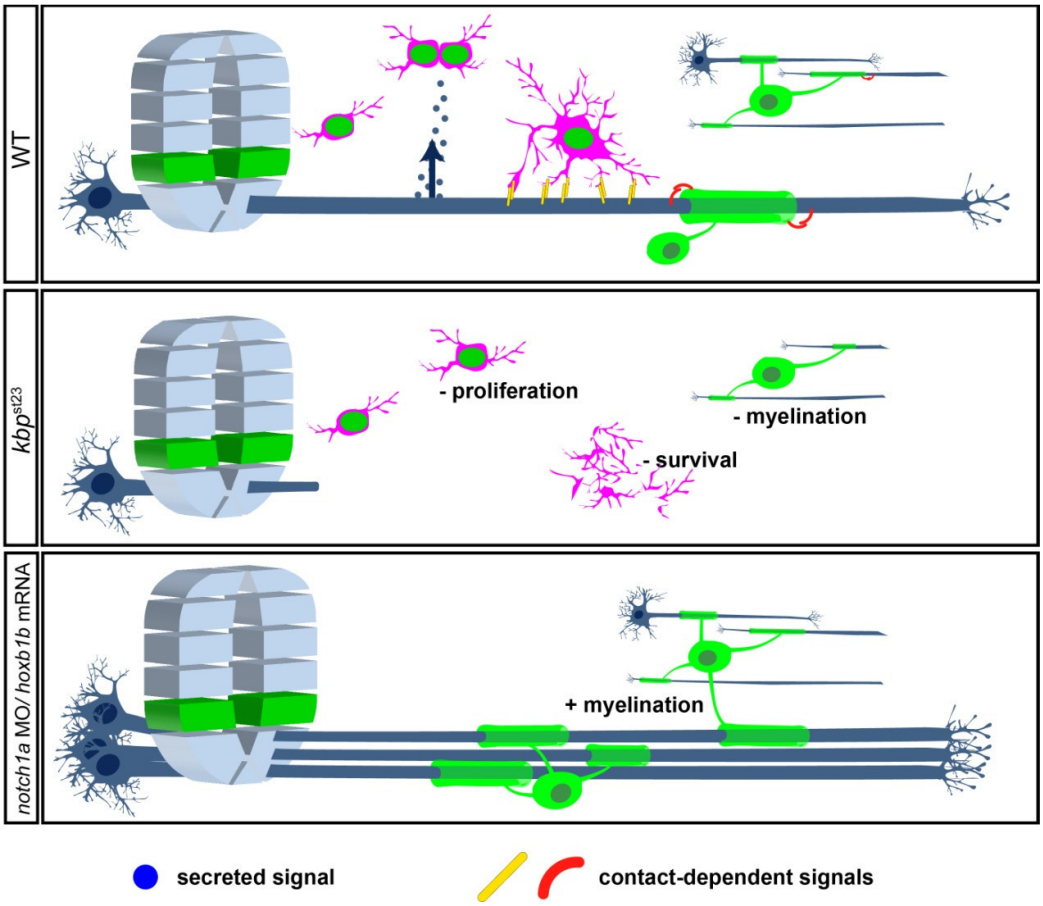

Figure 6.1 – Summary diagram

(**A**) Model of embryonic spinal cord oligodendrocyte development in zebrafish: reticulospinal axons provide a mitogenic secreted signal (arrow) to OPCs, and a contact-dependent survival signal during differentiation. Additionally, axons regulate the formation of myelin sheaths in a contact-dependent manner, modulating their myelinating capacity.
(**B**) In the absence of reticulospinal axons in the posterior spinal cord of *kbp* mutants, the lack of the axon-derived mitogenic and survival signals reduces proliferation and survival, leading to a decreased number of mature oligodendrocytes. Furthermore, the myelinating capacity of other oligodendrocytes is reduced (which could be partly due to the lack of *kbp*).
(**C**) In the presence of supernumerary Mauthner axons, contact-dependent axonal signals locally promote the formation and extension of myelin sheaths made by individual oligodendrocytes, increasing their total myelinating capacity.

In this thesis, I set out to address whether the diversity of myelinated fibers observed in the CNS is a product of axonal regulation. That is, whether axonal signals could regulate any steps of oligodendrocyte-lineage cell development in vivo, from their specification from neural progenitor cells, to their formation of myelin sheaths. The diversity of myelin sheaths observed, for instance in terms of thickness or length, tends to be precisely adjusted to the underlying axon and to optimize its function – which would suggest it is indeed regulated by axon. However, in vitro work had established that oligodendrocyte-lineage cells could essentially develop and form myelin in the absence of axons, even if their presence would stimulate particular aspects of their development to a degree. Could it be that oligodendrocyte-lineage cells do not absolutely require axons for their development, but are still responsive to their influence? Previous studies that attempted to remove axons in an in vivo context suffered from a number of drawbacks – namely, the fact that the paradigms used (transection or enucleation of the optic nerve) are fairly invasive procedures with consequences that could have confounding effects. I set out to readdress this issue in the larval zebrafish spinal cord, which permits manipulation of the axons and live imaging of the behaviour of oligodendrocyte-lineage cells from before they are even specified, until their maturation and myelination. My model presents a series of advantages: I am able to genetically induce alterations in the axonal compartment by manipulating axonal growth, without invasive manipulations, which means that oligodendrocyte-lineage cells never have to deal with the confounding effects of axonal degeneration. I am also able to image very early events in the development of the lineage, namely the specification of OPCs, which in mammals occur before birth. Finally, I am able to live-image the behaviour of these cells, and follow the fate of an OPC and its myelination fate as it matures, in the same individual animal, at several time points. This is in contrast with the static analysis of mammalian models, where different animals need to be sacrificed and tissue fixed at each time point.

I first set out to investigate whether earlier stages of oligodendrocyte-lineage cell development required axons (Chapter 3). I analysed a zebrafish mutant (*kbp*^{st23}) where the outgrowth of the first myelinated axons is disrupted from an early age, but not completely: whereas in WT these axons extend through the entire length of the spinal cord, in the mutants they only extend through the anterior half of the spinal

cord, which looks indistinguishable from WT. This allowed me to have an internal control for the posterior region, where the axonal surface that normally would get myelinated in the ventral spinal cord is 80% reduced. As it turns out, this did not affect the early emergence of OPCs from the pMN domain, nor did it affect the dorsal migration and distribution of a subset of OPCs. This suggests that reticulospinal axons and axonal signals do not regulate OPC specification or migratory capacities. Subsequently, by time lapse imaging, I determined that OPCs throughout the posterior spinal cord proliferated less when ventral axonal surface was absent. This suggests that a (probably secreted) mitogenic signal produced by axons normally promotes OPC proliferation. Furthermore, I found that a subset of ventral oligodendrocyte-lineage cells underwent apoptosis in the absence of ventral target axons, indicating that these axons normally deliver a (probably contact-dependent) survival signal. Interestingly, despite their confounding factors and lack of specific cell type labelling, previous studies manipulating rodent optic nerves had predicted this: cell proliferation was reduced when the optic nerve was cut in WT, but also in *Wld*^{S} mice, whose axons do not immediately degenerate. This means that live axons and their physiological activity or secreted factors were required to provide this mitogenic signal. In contrast, cells underwent apoptosis when the optic nerve of WT animals was cut, but survived in the cut optic nerve of *Wld*^{S} mice, where the disconnected axons are still present. This means that molecules exposed on their surface provide this survival signal to oligodendrocyte-lineage cells. A major candidate for this signal would be Nrg1 type III, a membrane-anchored adhesion molecule whose signalling has shown to be essential for Schwann cell development, and capable of regulating oligodendrocyte development in vitro. However, Nrg1 type III knockout mice and zebrafish do not exhibit impaired CNS myelination, so likely this survival signal is another molecule.

I found that the combination of the proliferation and the survival defects led to a reduction in the number of ventral oligodendrocytes that mature in the ventral spinal cord. This could reflect an evolutionarily incipient mechanism regulating the matching between target axonal surface and oligodendrocyte-membrane, which could be scaled up during evolution as animals and nervous systems became larger.

I then sought to address whether later stages of oligodendrocyte-lineage cell development could also be regulated by axons – namely the timing of differentiation and the extent of myelination. Despite an 80% reduction in ventral axonal surface, mature oligodendrocytes are only reduced by 25%. This suggested that some excess OPCs existed in the spinal cord in relation to the axonal surface even at the time of differentiation. By tracking single cells and following their myelination fate, I found that the same proportion of oligodendrocytes differentiated on schedule in the presence or absence of target axons – suggesting that axons do not regulate the timing of myelination and instead this follows an oligodendrocyte-intrinsic timer, as had been predicted from *in vitro* studies. I found no evidence of prematurely or incorrectly myelinated axons. Instead I found that ventral oligodendrocytes made fewer myelin sheaths, suggesting that axons regulate the formation or stabilization of nascent myelin sheaths, and that ventral oligodendrocytes have a plastic myelinating potential. I additionally found that *kbp* itself may potentially play a role in the growth of myelin sheaths, and in their localization to axons and away from neuronal somas.

In a further challenge to their myelinating capacity, I analysed zebrafish larvae with an excess of very large axons that normally are the first myelinated. I found that oligodendrocyte-lineage cells adapted perfectly to the extra axonal surface, primarily by extending more myelin sheaths and longer sheaths. This further demonstrated that axons can regulate the myelinating capacity of oligodendrocytes, which are plastic, and are not necessarily myelinating at their full capacity in normal situations. Further, I observed that even dorsal oligodendrocytes were affected by this ventral stimulus, and also extended more sheaths ventrally, which they normally do not do. These dorsal oligodendrocytes myelinate their normal small calibre targets in addition to the supernumerary, very large-calibre Mauthner axons. Collectively, these results unambiguously demonstrated that a) local axonal signals can influence the myelinating capacity of oligodendrocyte processes, b) that oligodendrocytes are not predetermined to make the same amount of myelin at the end of every process. The classification of oligodendrocyte morphologies into subtypes very likely reflects that emergence of cohorts of similar axons at distinct times during development, as discussed in Chapter 4, rather than inherently distinct, “fixed”, subtypes of oligodendrocytes.

In sum, the diversity of myelin sheaths and oligodendrocyte morphologies reflects the fact that oligodendrocytes are a plastic cell type that locally responds to axonal signals.

My results open a number of questions which will be interesting to address in the future:

a) When do axon-derived signals act to regulate myelination, at the level of a single OPC? Is there a limited time window during which OPCs can respond to these signals? Early OPCs differentiate and form myelin sheaths more efficiently when transplanted into myelin-free hosts than late OPCs or oligodendrocytes (Gard and Pfeiffer 1989, Warrington, Barbarese et al. 1993, Archer, Cuddon et al. 1997). This indicates that the myelinating capacity of oligodendrocyte-lineage cells is maximal early on and disappears when cells mature into oligodendrocytes. Interestingly, recent work has identified a limited time window of ~5 hours after the formation of the first myelin sheath during which the cell will make all of its myelin sheaths (Czopka, Ffrench-Constant et al. 2013). After this short window, for the remainder of an oligodendrocyte's life, the complement of myelin sheaths they sustain appears fixed. It could be that if such axonal signals are going to have an effect, they must act prior to or during this short period.

b) What happens if there are no such signals? In vivo, if an OPC process is not locally stimulated by contact with an axon, does it eventually retract? Alternatively, could it myelinate an axon or another structure at a low basal rate in the absence of such stimulating signals? If so, which structures do OPCs myelinate? In vitro, in neuron-free cultures, oligodendrocytes are able to myelinate inert structures such as paraformaldehyde-fixed axons (Rosenberg, Kelland et al. 2008) or nano-fibers (Lee, Leach et al. 2012, Li, Ceylan et al. 2014). In vivo, could they myelinate cell bodies, if they are not actively repulsive? Would this at least partly explain the presence of such aberrant profiles in the posterior spinal cord of *kbp* mutants, which lack reticulospinal axons? If oligodendrocytes myelinate at a basal rate, is there a minimum amount of myelin OPCs make?

c) Do the same signals also regulate the formation of myelin sheaths when the adult CNS is regenerating, following a demyelinating lesion? Discovering these signals may help us understand why remyelinated axons have thinner and shorter myelin sheaths, and why remyelination eventually fails. The complex demyelinating microenvironment may inhibit the response of oligodendrocyte-lineage cells to these signals (Piaton, Gould et al. 2010, Boulanger and Messier 2014). Identifying these pathways may open the door for new therapeutical targets for devastating diseases like multiple sclerosis.

d) Are oligodendrocyte-lineage cells generally able to respond to these signals throughout the life of an organism? In the adult optic nerve, de novo differentiation of oligodendrocytes was observed to result in shorter myelin internodes, suggesting that remodelling of myelin occurs throughout life in a healthy CNS (Young, Psachoulia et al. 2013). Could it be that with aging, oligodendrocyte-lineage cells become limited in the magnitude of their response? Could this underlie the white matter alterations that accompany specific motor or cognitive deficits in late life?

e) Finally, are the same signals recapitulated in the adult CNS during experience-driven white matter plasticity? Interestingly, a recent technical tour-de-force established that individual cortical axons are intermittently myelinated, and the length of myelin internodes can vary significantly (Tomassy, Berger et al. 2014), in contrast with the textbook description of regularly spaced nodes of Ranvier. This opens the door for the existence of plastic remodelling and refinement of myelin segments, presumably locally regulated, similarly to the developmental mechanisms I identified here. This remodelling would affect the conduction velocity of the axon and potentially the functional output of the whole circuit. It will be very interesting to determine if the same candidate molecular pathways regulate such a potential plasticity mechanism in the adult, which could provide a framework for understanding the cellular basis of a range of neuropsychiatric diseases.

In sum, my results show that axons can regulate OPC proliferation and oligodendrocyte survival, and importantly, unambiguously demonstrated that axons can locally regulate the myelinating capacity of individual oligodendrocytes in vivo, shedding light on fundamental oligodendrocyte biology.

7. References

Abney, E. R., P. P. Bartlett and M. C. Raff (1981). "Astrocytes, ependymal cells, and oligodendrocytes develop on schedule in dissociated cell cultures of embryonic rat brain." Dev Biol **83**(2): 301-310.

Aggarwal, S., L. Yurlova and M. Simons (2011). "Central nervous system myelin: structure, synthesis and assembly." Trends Cell Biol **21**(10): 585-593.

Aggarwal, S., L. Yurlova, N. Snaidero, C. Reetz, S. Frey, J. Zimmermann, G. Pahler, A. Janshoff, J. Friedrichs, D. J. Muller, C. Goebel and M. Simons (2011). "A size barrier limits protein diffusion at the cell surface to generate lipid-rich myelin-membrane sheets." Dev Cell **21**(3): 445-456.

Ahlgren, S. C., H. Wallace, J. Bishop, C. Neophytou and M. C. Raff (1997). "Effects of thyroid hormone on embryonic oligodendrocyte precursor cell development in vivo and in vitro." Mol Cell Neurosci **9**(5-6): 420-432.

Ainger, K., D. Avossa, F. Morgan, S. J. Hill, C. Barry, E. Barbarese and J. H. Carson (1993). "Transport and localization of exogenous myelin basic protein mRNA microinjected into oligodendrocytes." J Cell Biol **123**(2): 431-441.

Akiyama, M., H. Hasegawa, T. Hongu, M. A. Frohman, A. Harada, H. Sakagami and Y. Kanaho (2014). "Trans-regulation of oligodendrocyte myelination by neurons through small GTPase Arf6-regulated secretion of fibroblast growth factor-2." Nat Commun **5**: 4744.

Almeida, R. G., T. Czopka, C. Ffrench-Constant and D. A. Lyons (2011). "Individual axons regulate the myelinating potential of single oligodendrocytes in vivo." Development **138**(20): 4443-4450.

Almeida, R. G. and D. A. Lyons (2013). "On the resemblance of synapse formation and CNS myelination." Neuroscience.

Alves, M. M., G. Burzynski, J. M. Delalande, J. Osinga, A. van der Goot, A. M. Dolga, E. de Graaff, A. S. Brooks, M. Metzger, U. L. Eisel, I. Shepherd, B. J. Eggen and R. M. Hofstra (2010). "KBP interacts with SCG10, linking Goldberg-Shprintzen syndrome to microtubule dynamics and neuronal differentiation." Hum Mol Genet **19**(18): 3642-3651.

Amlien, I. K. and A. M. Fjell (2014). "Diffusion tensor imaging of white matter degeneration in Alzheimer's disease and mild cognitive impairment." Neuroscience **276C**: 206-215.

Anderson, E. S., C. Bjartmar, G. Westermark and C. Hildebrand (1999). "Molecular heterogeneity of oligodendrocytes in chicken white matter." Glia **27**(1): 15-21.

Arancibia-Carcamo, I. L. and D. Attwell (2014). "The node of Ranvier in CNS pathology." Acta Neuropathol **128**(2): 161-175.

Archer, D. R., P. A. Cuddon, D. Lipsitz and I. D. Duncan (1997). "Myelination of the canine central nervous system by glial cell transplantation: a model for repair of human myelin disease." Nat Med **3**(1): 54-59.

Baas, D., C. Legrand, J. Samarut and F. Flamant (2002). "Persistence of oligodendrocyte precursor cells and altered myelination in optic nerve associated to retina degeneration in mice devoid of all thyroid hormone receptors." Proc Natl Acad Sci U S A **99**(5): 2907-2911.

Bai, Q., M. Sun, D. B. Stolz and E. A. Burton (2011). "Major isoform of zebrafish P0 is a 23.5 kDa myelin glycoprotein expressed in selected white matter tracts of the central nervous system." J Comp Neurol **519**(8): 1580-1596.

Bakiri, Y., R. Karadottir, L. Cossell and D. Attwell (2011). "Morphological and electrical properties of oligodendrocytes in the white matter of the corpus callosum and cerebellum." J Physiol **589**(Pt 3): 559-573.

Baron, U., M. Gossen and H. Bujard (1997). "Tetracycline-controlled transcription in eukaryotes: novel transactivators with graded transactivation potential." Nucleic Acids Res **25**(14): 2723-2729.

Baron, W. and D. Hoekstra (2010). "On the biogenesis of myelin membranes: sorting, trafficking and cell polarity." FEBS Lett **584**(9): 1760-1770.

Barres, B. A., I. K. Hart, H. S. Coles, J. F. Burne, J. T. Voyvodic, W. D. Richardson and M. C. Raff (1992). "Cell death and control of cell survival in the oligodendrocyte lineage." Cell **70**(1): 31-46.

Barres, B. A., M. D. Jacobson, R. Schmid, M. Sendtner and M. C. Raff (1993). "Does oligodendrocyte survival depend on axons?" Curr Biol **3**(8): 489-497.

Barres, B. A., M. A. Lazar and M. C. Raff (1994). "A novel role for thyroid hormone, glucocorticoids and retinoic acid in timing oligodendrocyte development." Development **120**(5): 1097-1108.

Barres, B. A. and M. C. Raff (1993). "Proliferation of oligodendrocyte precursor cells depends on electrical activity in axons." Nature **361**(6409): 258-260.

Barres, B. A. and M. C. Raff (1999). "Axonal control of oligodendrocyte development." J Cell Biol **147**(6): 1123-1128.

Barres, B. A., M. C. Raff, F. Gaese, I. Bartke, G. Dechant and Y. A. Barde (1994). "A crucial role for neurotrophin-3 in oligodendrocyte development." Nature **367**(6461): 371-375.

Barros, C. S., T. Nguyen, K. S. Spencer, A. Nishiyama, H. Colognato and U. Muller (2009). "Beta1 integrins are required for normal CNS myelination and promote AKT-dependent myelin outgrowth." Development **136**(16): 2717-2724.

Bauer, N. G., C. Richter-Landsberg and C. Ffrench-Constant (2009). "Role of the oligodendroglial cytoskeleton in differentiation and myelination." Glia **57**(16): 1691-1705.

Baumann, N. and D. Pham-Dinh (2001). "Biology of oligodendrocyte and myelin in the mammalian central nervous system." Physiol Rev **81**(2): 871-927.

Beal, J. A. and M. H. Cooper (1976). "Myelinated nerve cell bodies in the dorsal horn of the monkey (Saimiri sciureus)." Am J Anat **147**(1): 33-48.

Becker, C. G. and T. Becker (2007). "Growth and pathfinding of regenerating axons in the optic projection of adult fish." J Neurosci Res **85**(12): 2793-2799.

Bengtsson, S. L., Z. Nagy, S. Skare, L. Forsman, H. Forssberg and F. Ullen (2005). "Extensive piano practicing has regionally specific effects on white matter development." Nat Neurosci **8**(9): 1148-1150.

Benninger, Y., H. Colognato, T. Thurnherr, R. J. Franklin, D. P. Leone, S. Atanasoski, K. A. Nave, C. Ffrench-Constant, U. Suter and J. B. Relvas (2006). "Beta1-integrin signaling mediates premyelinating oligodendrocyte survival but is not required for CNS myelination and remyelination." J Neurosci **26**(29): 7665-7673.

Bernhardt, R. R., A. B. Chitnis, L. Lindamer and J. Y. Kuwada (1990). "Identification of spinal neurons in the embryonic and larval zebrafish." J Comp Neurol **302**(3): 603-616.

Bernstein, H. G., J. Steiner and B. Bogerts (2009). "Glial cells in schizophrenia: pathophysiological significance and possible consequences for therapy." Expert Rev Neurother **9**(7): 1059-1071.

Berry, M., M. Ibrahim, J. Carlile, F. Ruge, A. Duncan and A. M. Butt (1995). "Axon-glial relationships in the anterior medullary velum of the adult rat." J Neurocytol **24**(12): 965-983.

Bjartmar, C., C. Hildebrand and K. Loinder (1994). "Morphological heterogeneity of rat oligodendrocytes: electron microscopic studies on serial sections." Glia **11**(3): 235-244.

Blakemore, W. F. (1974). "Pattern of remyelination in the CNS." Nature **249**(457): 577-578.

Blaschuk, K. L., E. E. Frost and C. ffrench-Constant (2000). "The regulation of proliferation and differentiation in oligodendrocyte progenitor cells by alphaV integrins." Development **127**(9): 1961-1969.

Blatch, G. L. and M. Lassle (1999). "The tetratricopeptide repeat: a structural motif mediating protein-protein interactions." Bioessays **21**(11): 932-939.

Blinzinger, K., A. P. Anzil and W. Muller (1972). "Myelinated nerve cell perikaryon in mouse spinal cord." Z Zellforsch Mikrosk Anat **128**(1): 135-138.

Boda, E. and A. Buffo (2014). "Beyond cell replacement: unresolved roles of NG2-expressing progenitors." Front Neurosci **8**: 122.

Bohm, R. A., W. P. Welch, L. K. Goodnight, L. W. Cox, L. G. Henry, T. C. Gunter, H. Bao and B. Zhang (2010). "A genetic mosaic approach for neural circuit mapping in Drosophila." Proc Natl Acad Sci U S A **107**(37): 16378-16383.

Boulanger, J. J. and C. Messier (2014). "From precursors to myelinating oligodendrocytes: contribution of intrinsic and extrinsic factors to white matter plasticity in the adult brain." Neuroscience **269**: 343-366.

Braak, E., H. Braak and H. Strenge (1977). "The fine structure of myelinated nerve cell bodies in the bulbus olfactorius of man." Cell Tissue Res **182**(2): 221-233.

Bradel, E. J. and F. P. Prince (1983). "Cultured neonatal rat oligodendrocytes elaborate myelin membrane in the absence of neurons." J Neurosci Res **9**(4): 381-392.

Brady, S. T. S. G. J. A. R. W. P. D. L. (2012). Basic neurochemistry : principles of molecular, cellular, and medical neurobiology. Amsterdam; Boston, Elsevier Academic Press.

Brinkmann, B. G., A. Agarwal, M. W. Sereda, A. N. Garratt, T. Muller, H. Wende, R. M. Stassart, S. Nawaz, C. Humml, V. Velanac, K. Radyushkin, S. Goebbels, T. M. Fischer, R. J. Franklin, C. Lai, H. Ehrenreich, C. Birchmeier, M. H. Schwab and K. A. Nave (2008). "Neuregulin-1/ErbB signaling serves distinct functions in myelination of the peripheral and central nervous system." Neuron **59**(4): 581-595.

Brooks, A. S., A. M. Bertoli-Avella, G. M. Burzynski, G. J. Breedveld, J. Osinga, L. G. Boven, J. A. Hurst, G. M. Mancini, M. H. Lequin, R. F. de Coo, I. Matera, E. de Graaff, C. Meijers, P. J. Willems, D. Tibboel, B. A. Oostra and R. M. Hofstra (2005). "Homozygous nonsense mutations in KIAA1279 are associated with malformations of the central and enteric nervous systems." Am J Hum Genet **77**(1): 120-126.

Brosamle, C. and M. E. Halpern (2002). "Characterization of myelination in the developing zebrafish." Glia **39**(1): 47-57.

Bujalka, H., M. Koenning, S. Jackson, V. M. Perreau, B. Pope, C. M. Hay, S. Mitew, A. F. Hill, Q. R. Lu, M. Wegner, R. Srinivasan, J. Svaren, M. Willingham, B. A. Barres and B. Emery (2013). "MYRF is a membrane-associated transcription factor that autoproteolytically cleaves to directly activate myelin genes." PLoS Biol **11**(8): e1001625.

Bunge, R. P., M. B. Bunge and M. Bates (1989). "Movements of the Schwann cell nucleus implicate progression of the inner (axon-related) Schwann cell process during myelination." J Cell Biol **109**(1): 273-284.

Burne, J. F., J. K. Staple and M. C. Raff (1996). "Glial cells are increased proportionally in transgenic optic nerves with increased numbers of axons." J Neurosci **16**(6): 2064-2073.

Butt, A. M. and M. Berry (2000). "Oligodendrocytes and the control of myelination in vivo: new insights from the rat anterior medullary velum." J Neurosci Res **59**(4): 477-488.

Butt, A. M., M. Ibrahim and M. Berry (1998). "Axon-myelin sheath relations of oligodendrocyte unit phenotypes in the adult rat anterior medullary velum." J Neurocytol **27**(4): 259-269.

Butt, A. M., M. Ibrahim, F. M. Ruge and M. Berry (1995). "Biochemical subtypes of oligodendrocyte in the anterior medullary velum of the rat as revealed by the monoclonal antibody Rip." Glia **14**(3): 185-197.

Butt, A. M. and S. Kirvell (1996). "Glial cells in transected optic nerves of immature rats. II. An immunohistochemical study." J Neurocytol **25**(6): 381-392.

Buttermore, E. D., C. L. Thaxton and M. A. Bhat (2013). "Organization and maintenance of molecular domains in myelinated axons." J Neurosci Res **91**(5): 603-622.

Buttery, P. C. and C. ffrench-Constant (1999). "Laminin-2/integrin interactions enhance myelin membrane formation by oligodendrocytes." Mol Cell Neurosci **14**(3): 199-212.

Calaora, V., B. Rogister, K. Bismuth, K. Murray, H. Brandt, P. Leprince, M. Marchionni and M. Dubois-Dalcq (2001). "Neuregulin signaling regulates neural precursor growth and the generation of oligodendrocytes in vitro." J Neurosci **21**(13): 4740-4751.

Calver, A. R., A. C. Hall, W. P. Yu, F. S. Walsh, J. K. Heath, C. Betsholtz and W. D. Richardson (1998). "Oligodendrocyte population dynamics and the role of PDGF in vivo." Neuron **20**(5): 869-882.

Camara, J., Z. Wang, C. Nunes-Fonseca, H. C. Friedman, M. Grove, D. L. Sherman, N. H. Komiyama, S. G. Grant, P. J. Brophy, A. Peterson and C. ffrench-Constant (2009). "Integrin-mediated axoglial interactions initiate myelination in the central nervous system." J Cell Biol **185**(4): 699-712.

Campbell, G. R. and D. J. Mahad (2011). "Mitochondria as crucial players in demyelinated axons: lessons from neuropathology and experimental demyelination." Autoimmune Dis **2011**: 262847.

Canoll, P. D., R. Kraemer, K. K. Teng, M. A. Marchionni and J. L. Salzer (1999). "GGF/neuregulin induces a phenotypic reversion of oligodendrocytes." Mol Cell Neurosci **13**(2): 79-94.

Canoll, P. D., J. M. Musacchio, R. Hardy, R. Reynolds, M. A. Marchionni and J. L. Salzer (1996). "GGF/neuregulin is a neuronal signal that promotes the proliferation and survival and inhibits the differentiation of oligodendrocyte progenitors." Neuron **17**(2): 229-243.

Celio, M. R., E. G. Gray and G. M. Yasargil (1979). "Ultrastructure of the Mauthner axon collateral and its synapses in the goldfish spinal cord." J Neurocytol **8**(1): 19-29.

Chomiak, T. and B. Hu (2009). "What is the optimal value of the g-ratio for myelinated fibers in the rat CNS? A theoretical approach." PLoS One **4**(11): e7754.

Chong, S. Y., S. S. Rosenberg, S. P. Fancy, C. Zhao, Y. A. Shen, A. T. Hahn, A. W. McGee, X. Xu, B. Zheng, L. I. Zhang, D. H. Rowitch, R. J. Franklin, Q. R. Lu and J. R. Chan (2012). "Neurite outgrowth inhibitor Nogo-A establishes spatial segregation and extent of oligodendrocyte myelination." Proc Natl Acad Sci U S A **109**(4): 1299-1304.

Chun, S. J., M. N. Rasband, R. L. Sidman, A. A. Habib and T. Vartanian (2003). "Integrin-linked kinase is required for laminin-2-induced oligodendrocyte cell spreading and CNS myelination." J Cell Biol **163**(2): 397-408.

Colak, D., S. J. Ji, B. T. Porse and S. R. Jaffrey (2013). "Regulation of axon guidance by compartmentalized nonsense-mediated mRNA decay." Cell **153**(6): 1252-1265.

Colello, R. J., L. R. Devey, E. Imperato and U. Pott (1995). "The chronology of oligodendrocyte differentiation in the rat optic nerve: evidence for a signaling step initiating myelination in the CNS." J Neurosci **15**(11): 7665-7672.

Colman, D. R., G. Kreibich, A. B. Frey and D. D. Sabatini (1982). "Synthesis and incorporation of myelin polypeptides into CNS myelin." J Cell Biol **95**(2 Pt 1): 598-608.

Colognato, H., W. Baron, V. Avellana-Adalid, J. B. Relvas, A. Baron-Van Evercooren, E. Georges-Labouesse and C. ffrench-Constant (2002). "CNS integrins switch growth factor signalling to promote target-dependent survival." Nat Cell Biol **4**(11): 833-841.

Colognato, H. and C. ffrench-Constant (2004). "Mechanisms of glial development." Curr Opin Neurobiol **14**(1): 37-44.

Colognato, H., J. Galvin, Z. Wang, J. Relucio, T. Nguyen, D. Harrison, P. D. Yurchenco and C. Ffrench-Constant (2007). "Identification of dystroglycan as a second laminin receptor in oligodendrocytes, with a role in myelination." Development **134**(9): 1723-1736.

Cooper, M. H. and J. A. Beal (1977). "Myelinated granule cell bodies in the cerebellum of the monkey (Saimiri sciureus)." Anat Rec **187**(2): 249-255.

Corley, S. M., U. Ladiwala, A. Besson and V. W. Yong (2001). "Astrocytes attenuate oligodendrocyte death in vitro through an alpha(6) integrin-laminin-dependent mechanism." Glia **36**(3): 281-294.

Court, F. A., D. L. Sherman, T. Pratt, E. M. Garry, R. R. Ribchester, D. F. Cottrell, S. M. Fleetwood-Walker and P. J. Brophy (2004). "Restricted growth of Schwann cells lacking Cajal bands slows conduction in myelinated nerves." Nature **431**(7005): 191-195.

Czopka, T., C. Ffrench-Constant and D. A. Lyons (2013). "Individual oligodendrocytes have only a few hours in which to generate new myelin sheaths in vivo." Dev Cell **25**(6): 599-609.

Czopka, T. and D. A. Lyons (2011). "Dissecting mechanisms of myelinated axon formation using zebrafish." Methods Cell Biol **105**: 25-62.

Czopka, T., A. von Holst, C. ffrench-Constant and A. Faissner (2010). "Regulatory mechanisms that mediate tenascin C-dependent inhibition of oligodendrocyte precursor differentiation." J Neurosci **30**(37): 12310-12322.

David, S., R. H. Miller, R. Patel and M. C. Raff (1984). "Effects of neonatal transection on glial cell development in the rat optic nerve: evidence that the oligodendrocyte-type 2 astrocyte cell lineage depends on axons for its survival." J Neurocytol **13**(6): 961-974.

Davis, G. B. and C. A. Parker (1997). Writing the Doctoral Dissertation: A Systematic Approach, Barron's.

Davison, J. M., C. M. Akitake, M. G. Goll, J. M. Rhee, N. Gosse, H. Baier, M. E. Halpern, S. D. Leach and M. J. Parsons (2007). "Transactivation from Gal4-VP16 transgenic insertions for tissue-specific cell labeling and ablation in zebrafish." Dev Biol **304**(2): 811-824.

De Biase, L. M., S. H. Kang, E. G. Baxi, M. Fukaya, M. L. Pucak, M. Mishina, P. A. Calabresi and D. E. Bergles (2011). "NMDA receptor signaling in oligodendrocyte

progenitors is not required for oligodendrogenesis and myelination." J Neurosci **31**(35): 12650-12662.

de Castro, F., A. Bribian and M. C. Ortega (2013). "Regulation of oligodendrocyte precursor migration during development, in adulthood and in pathology." Cell Mol Life Sci **70**(22): 4355-4368.

de Castro, F. and B. Zalc (2013). Chapter 23 - Migration of Myelin-Forming Cells in the CNS. Cellular Migration and Formation of Neuronal Connections. J. L. R. R. Rakic. Oxford, Academic Press**:** 417-429.

De Louw, A. J., W. D. Van De Berg, J. De Vente, C. E. Blanco, A. W. Gavilanes, H. P. Steinbusch, H. W. Steinbusch, J. Troost and J. S. Vles (2002). "Developmental apoptosis in the spinal cord white matter in neonatal rats." Glia **37**(1): 89-91.

De Stefano, N., P. M. Matthews, L. Fu, S. Narayanan, J. Stanley, G. S. Francis, J. P. Antel and D. L. Arnold (1998). "Axonal damage correlates with disability in patients with relapsing-remitting multiple sclerosis. Results of a longitudinal magnetic resonance spectroscopy study." Brain **121 (Pt 8)**: 1469-1477.

Demerens, C., B. Stankoff, M. Logak, P. Anglade, B. Allinquant, F. Couraud, B. Zalc and C. Lubetzki (1996). "Induction of myelination in the central nervous system by electrical activity." Proc Natl Acad Sci U S A **93**(18): 9887-9892.

Distel, M., M. F. Wullimann and R. W. Koster (2009). "Optimized Gal4 genetics for permanent gene expression mapping in zebrafish." Proc Natl Acad Sci U S A **106**(32): 13365-13370.

Drevillon, L., A. Megarbane, B. Demeer, C. Matar, P. Benit, A. Briand-Suleau, V. Bodereau, J. Ghoumid, M. Nasser, X. Decrouy, M. Doco-Fenzy, P. Rustin, D. Gaillard, M. Goossens and I. Giurgea (2013). "KBP-cytoskeleton interactions underlie developmental anomalies in Goldberg-Shprintzen syndrome." Hum Mol Genet **22**(12): 2387-2399.

Dubois-Dalcq, M., T. Behar, L. Hudson and R. A. Lazzarini (1986). "Emergence of three myelin proteins in oligodendrocytes cultured without neurons." J Cell Biol **102**(2): 384-392.

Durand, B. and M. Raff (2000). "A cell-intrinsic timer that operates during oligodendrocyte development." Bioessays **22**(1): 64-71.

Dutton, J. R., A. Antonellis, T. J. Carney, F. S. Rodrigues, W. J. Pavan, A. Ward and R. N. Kelsh (2008). "An evolutionarily conserved intronic region controls the spatiotemporal expression of the transcription factor Sox10." BMC Dev Biol **8**: 105.

Elliott, D. A. and A. H. Brand (2008). "The GAL4 system : a versatile system for the expression of genes." Methods Mol Biol **420**: 79-95.

Emery, B. (2010). "Regulation of oligodendrocyte differentiation and myelination." Science **330**(6005): 779-782.

Emery, B., D. Agalliu, J. D. Cahoy, T. A. Watkins, J. C. Dugas, S. B. Mulinyawe, A. Ibrahim, K. L. Ligon, D. H. Rowitch and B. A. Barres (2009). "Myelin gene regulatory factor is a critical transcriptional regulator required for CNS myelination." Cell **138**(1): 172-185.

Faivre-Sarrailh, C. and J. J. Devaux (2013). "Neuro-glial interactions at the nodes of Ranvier: implication in health and diseases." Front Cell Neurosci **7**: 196.

Fanarraga, M. L., I. R. Griffiths, M. Zhao and I. D. Duncan (1998). "Oligodendrocytes are not inherently programmed to myelinate a specific size of axon." J Comp Neurol **399**(1): 94-100.

Fancy, S. P., J. R. Chan, S. E. Baranzini, R. J. Franklin and D. H. Rowitch (2011). "Myelin regeneration: a recapitulation of development?" Annu Rev Neurosci **34**: 21-43.

Fenno, L., O. Yizhar and K. Deisseroth (2011). "The development and application of optogenetics." Annu Rev Neurosci **34**: 389-412.

Fernandez, P. A., D. G. Tang, L. Cheng, A. Prochiantz, A. W. Mudge and M. C. Raff (2000). "Evidence that axon-derived neuregulin promotes oligodendrocyte survival in the developing rat optic nerve." Neuron **28**(1): 81-90.

Fetcho, J. R. and D. S. Faber (1988). "Identification of motoneurons and interneurons in the spinal network for escapes initiated by the mauthner cell in goldfish." J Neurosci **8**(11): 4192-4213.

Fields, R. D. (2004). "Volume transmission in activity-dependent regulation of myelinating glia." Neurochem Int **45**(4): 503-509.

Fields, R. D. (2005). "Myelination: an overlooked mechanism of synaptic plasticity?" Neuroscientist **11**(6): 528-531.

Fields, R. D. (2008). "White matter in learning, cognition and psychiatric disorders." Trends Neurosci **31**(7): 361-370.

Fields, R. D. (2010). "Neuroscience. Change in the brain's white matter." Science **330**(6005): 768-769.

Fields, R. D. and G. Burnstock (2006). "Purinergic signalling in neuron-glia interactions." Nat Rev Neurosci **7**(6): 423-436.

Flores, A. I., B. S. Mallon, T. Matsui, W. Ogawa, A. Rosenzweig, T. Okamoto and W. B. Macklin (2000). "Akt-mediated survival of oligodendrocytes induced by neuregulins." J Neurosci **20**(20): 7622-7630.

Foran, D. R. and A. C. Peterson (1992). "Myelin acquisition in the central nervous system of the mouse revealed by an MBP-Lac Z transgene." J Neurosci **12**(12): 4890-4897.

Fox, M. A., F. S. Afshari, J. K. Alexander, R. J. Colello and B. Fuss (2006). "Growth conelike sensorimotor structures are characteristic features of postmigratory, premyelinating oligodendrocytes." Glia **53**(5): 563-566.

Franklin, R. J. (2002). "Why does remyelination fail in multiple sclerosis?" Nat Rev Neurosci **3**(9): 705-714.

Franklin, R. J. and C. Ffrench-Constant (2008). "Remyelination in the CNS: from biology to therapy." Nat Rev Neurosci **9**(11): 839-855.

Frost, E., B. W. Kiernan, A. Faissner and C. ffrench-Constant (1996). "Regulation of oligodendrocyte precursor migration by extracellular matrix: evidence for substrate-specific inhibition of migration by tenascin-C." Dev Neurosci **18**(4): 266-273.

Frost, E. E., P. C. Buttery, R. Milner and C. ffrench-Constant (1999). "Integrins mediate a neuronal survival signal for oligodendrocytes." Curr Biol **9**(21): 1251-1254.

Frost, E. E., Z. Zhou, K. Krasnesky and R. C. Armstrong (2009). "Initiation of oligodendrocyte progenitor cell migration by a PDGF-A activated extracellular regulated kinase (ERK) signaling pathway." Neurochem Res **34**(1): 169-181.

Fruttiger, M., A. R. Calver and W. D. Richardson (2000). "Platelet-derived growth factor is constitutively secreted from neuronal cell bodies but not from axons." Curr Biol **10**(20): 1283-1286.

Fruttiger, M., L. Karlsson, A. C. Hall, A. Abramsson, A. R. Calver, H. Bostrom, K. Willetts, C. H. Bertold, J. K. Heath, C. Betsholtz and W. D. Richardson (1999). "Defective oligodendrocyte development and severe hypomyelination in PDGF-A knockout mice." Development **126**(3): 457-467.

Fulcrand, J. and A. Privat (1977). "Neuroglial reactions secondary to Wallerian degeneration in the optic nerve of the postnatal rat: ultrastructural and quantitative study." J Comp Neurol **176**(2): 189-222.

Funch, P. G. and D. S. Faber (1980). "Impulse propagation along a myelinated vertebrate axon lacking nodes of Ranvier." Brain Res **190**(1): 261-267.

Funfschilling, U., L. M. Supplie, D. Mahad, S. Boretius, A. S. Saab, J. Edgar, B. G. Brinkmann, C. M. Kassmann, I. D. Tzvetanova, W. Mobius, F. Diaz, D. Meijer, U. Suter, B. Hamprecht, M. W. Sereda, C. T. Moraes, J. Frahm, S. Goebbels and K.-A. Nave (2012). "Glycolytic oligodendrocytes maintain myelin and long-term axonal integrity." Nature **485**(7399): 517-521.

Fuster, J. M. (2002). "Frontal lobe and cognitive development." J Neurocytol **31**(3-5): 373-385.

Galli, L. and L. Maffei (1988). "Spontaneous impulse activity of rat retinal ganglion cells in prenatal life." Science **242**(4875): 90-91.

Gao, F. B., J. Apperly and M. Raff (1998). "Cell-intrinsic timers and thyroid hormone regulate the probability of cell-cycle withdrawal and differentiation of oligodendrocyte precursor cells." Dev Biol **197**(1): 54-66.

Gao, F. B. and M. Raff (1997). "Cell size control and a cell-intrinsic maturation program in proliferating oligodendrocyte precursor cells." J Cell Biol **138**(6): 1367-1377.

Gao, L. and R. H. Miller (2006). "Specification of optic nerve oligodendrocyte precursors by retinal ganglion cell axons." J Neurosci **26**(29): 7619-7628.

Gard, A. L. and S. E. Pfeiffer (1989). "Oligodendrocyte progenitors isolated directly from developing telencephalon at a specific phenotypic stage: myelinogenic potential in a defined environment." Development **106**(1): 119-132.

Genoud, S., C. Lappe-Siefke, S. Goebbels, F. Radtke, M. Aguet, S. S. Scherer, U. Suter, K. A. Nave and N. Mantei (2002). "Notch1 control of oligodendrocyte differentiation in the spinal cord." J Cell Biol **158**(4): 709-718.

Genoud, S., C. Lappe-Siefke, S. Goebbels, F. Radtke, M. Aguet, S. S. Scherer, U. Suter, K. A. Nave and N. Mantei (2002). "Notch1 control of oligodendrocyte differentiation in the spinal cord." Journal of Cell Biology **158**(4): 709-718.

Gibson, E. M., D. Purger, C. W. Mount, A. K. Goldstein, G. L. Lin, L. S. Wood, I. Inema, S. E. Miller, G. Bieri, J. B. Zuchero, B. A. Barres, P. J. Woo, H. Vogel and M. Monje (2014). "Neuronal activity promotes oligodendrogenesis and adaptive myelination in the mammalian brain." Science **344**(6183): 1252304.

Givogri, M. I., R. M. Costa, V. Schonmann, A. J. Silva, A. T. Campagnoni and E. R. Bongarzone (2002). "Central nervous system myelination in mice with deficient expression of Notch1 receptor." J Neurosci Res **67**(3): 309-320.

Gray, M., C. B. Moens, S. L. Amacher, J. S. Eisen and C. E. Beattie (2001). "Zebrafish deadly seven functions in neurogenesis." Dev Biol **237**(2): 306-323.

Greeff, N. G. and G. M. Yasargil (1980). "Experimental evidence for saltatory propagation of the Mauthner axon impulse in the tench spinal cord." Brain Res **193**(1): 47-57.

Greenwood, K. and A. M. Butt (2003). "Evidence that perinatal and adult NG2-glia are not conventional oligodendrocyte progenitors and do not depend on axons for their survival." Mol Cell Neurosci **23**(4): 544-558.

Griffiths, I., M. Klugmann, T. Anderson, D. Yool, C. Thomson, M. H. Schwab, A. Schneider, F. Zimmermann, M. McCulloch, N. Nadon and K. A. Nave (1998). "Axonal swellings and degeneration in mice lacking the major proteolipid of myelin." Science **280**(5369): 1610-1613.

Gudz, T. I., H. Komuro and W. B. Macklin (2006). "Glutamate stimulates oligodendrocyte progenitor migration mediated via an alphav integrin/myelin proteolipid protein complex." J Neurosci **26**(9): 2458-2466.

Gustavsson, A., M. Svensson, F. Jacobi, C. Allgulander, J. Alonso, E. Beghi, R. Dodel, M. Ekman, C. Faravelli, L. Fratiglioni, B. Gannon, D. H. Jones, P. Jennum, A. Jordanova, L. Jonsson, K. Karampampa, M. Knapp, G. Kobelt, T. Kurth, R. Lieb, M. Linde, C. Ljungcrantz, A. Maercker, B. Melin, M. Moscarelli, A. Musayev, F. Norwood, M. Preisig, M. Pugliatti, J. Rehm, L. Salvador-Carulla, B. Schlehofer, R. Simon, H. C. Steinhausen, L. J. Stovner, J. M. Vallat, P. Van den Bergh, J. van Os, P. Vos, W. Xu, H. U. Wittchen, B. Jonsson, J. Olesen and C. D. Group (2011). "Cost of disorders of the brain in Europe 2010." Eur Neuropsychopharmacol **21**(10): 718-779.

Hale, M. E., M. A. Kheirbek, J. E. Schriefer and V. E. Prince (2004). "Hox gene misexpression and cell-specific lesions reveal functionality of homeotically transformed neurons." J Neurosci **24**(12): 3070-3076.

Halpern, M. E., J. Rhee, M. G. Goll, C. M. Akitake, M. Parsons and S. D. Leach (2008). "Gal4/UAS transgenic tools and their application to zebrafish." Zebrafish **5**(2): 97-110.

Hammerschmidt, M., F. Pelegri, M. C. Mullins, D. A. Kane, F. J. van Eeden, M. Granato, M. Brand, M. Furutani-Seiki, P. Haffter, C. P. Heisenberg, Y. J. Jiang, R. N. Kelsh, J. Odenthal, R. M. Warga and C. Nusslein-Volhard (1996). "dino and mercedes, two genes regulating dorsal development in the zebrafish embryo." Development **123**: 95-102.

Hamori, J., I. Lakos and E. Mezey (1980). "Myelinated dendrites of Purkinje cells in deafferented cerebellar cortex." J Hirnforsch **21**(4): 391-407.

Hamori, J. and V. L. Silakov (1981). "Myelinated perikarya and dendrites in lateral geniculate nucleus of adult cat following chronic cortical deafferentation." J Neurocytol **10**(5): 879-888.

Han, Y., H. Yang, Y. T. Lv, C. Z. Zhu, Y. He, H. H. Tang, Q. Y. Gong, Y. J. Luo, Y. F. Zang and Q. Dong (2009). "Gray matter density and white matter integrity in pianists' brain: a combined structural and diffusion tensor MRI study." Neurosci Lett **459**(1): 3-6.

Hardy, R. J. and V. L. Friedrich, Jr. (1996). "Progressive remodeling of the oligodendrocyte process arbor during myelinogenesis." Dev Neurosci **18**(4): 243-254.

Hartline, D. K. and D. R. Colman (2007). "Rapid conduction and the evolution of giant axons and myelinated fibers." Curr Biol **17**(1): R29-35.

He, L. and Q. R. Lu (2013). "Coordinated control of oligodendrocyte development by extrinsic and intrinsic signaling cues." Neurosci Bull **29**(2): 129-143.

Hess, A. (1965). "Developmental changes in the structure of the synapse on the myelinated cell bodies of the chicken ciliary ganglion." J Cell Biol **25**(3): Suppl:1-19.

Hildebrand, C. and R. Hahn (1978). "Relation between myelin sheath thickness and axon size in spinal cord white matter of some vertebrate species." J Neurol Sci **38**(3): 421-434.

Hildebrand, C., S. Remahl, H. Persson and C. Bjartmar (1993). "Myelinated nerve fibres in the CNS." Prog Neurobiol **40**(3): 319-384.

Hong, W., T. J. Mosca and L. Luo (2012). "Teneurins instruct synaptic partner matching in an olfactory map." Nature **484**(7393): 201-207.

Hornig, J., F. Frob, M. R. Vogl, I. Hermans-Borgmeyer, E. R. Tamm and M. Wegner (2013). "The transcription factors Sox10 and Myrf define an essential regulatory network module in differentiating oligodendrocytes." PLoS Genet **9**(10): e1003907.

Howe, C. L. (2006). "Coated glass and vicryl microfibers as artificial axons." Cells Tissues Organs **183**(4): 180-194.

Hu, Q. D., B. T. Ang, M. Karsak, W. P. Hu, X. Y. Cui, T. Duka, Y. Takeda, W. Chia, N. Sankar, Y. K. Ng, E. A. Ling, T. Maciag, D. Small, R. Trifonova, R. Kopan, H. Okano, M. Nakafuku, S. Chiba, H. Hirai, J. C. Aster, M. Schachner, C. J. Pallen, K. Watanabe and Z. C. Xiao (2003). "F3/contactin acts as a functional ligand for Notch during oligodendrocyte maturation." Cell **115**(2): 163-175.

Hughes, E. G., S. H. Kang, M. Fukaya and D. E. Bergles (2013). "Oligodendrocyte progenitors balance growth with self-repulsion to achieve homeostasis in the adult brain." Nat Neurosci **16**(6): 668-676.

Ibarrola, N., M. Mayer-Proschel, A. Rodriguez-Pena and M. Noble (1996). "Evidence for the existence of at least two timing mechanisms that contribute to oligodendrocyte generation in vitro." Dev Biol **180**(1): 1-21.

Jahn, O., S. Tenzer and H. B. Werner (2009). "Myelin proteomics: molecular anatomy of an insulating sheath." Mol Neurobiol **40**(1): 55-72.

Jarjour, A. A., C. Manitt, S. W. Moore, K. M. Thompson, S. J. Yuh and T. E. Kennedy (2003). "Netrin-1 is a chemorepellent for oligodendrocyte precursor cells in the embryonic spinal cord." J Neurosci **23**(9): 3735-3744.

Jones, K. J., G. Morgan, H. Johnston, V. Tobias, R. A. Ouvrier, I. Wilkinson and K. N. North (2001). "The expanding phenotype of laminin alpha2 chain (merosin) abnormalities: case series and review." J Med Genet **38**(10): 649-657.

Jontes, J. D., J. Buchanan and S. J. Smith (2000). "Growth cone and dendrite dynamics in zebrafish embryos: early events in synaptogenesis imaged in vivo." Nat Neurosci **3**(3): 231-237.

Kachar, B., T. Behar and M. Dubois-Dalcq (1986). "Cell shape and motility of oligodendrocytes cultured without neurons." Cell Tissue Res **244**(1): 27-38.

Kang, S. H., M. Fukaya, J. K. Yang, J. D. Rothstein and D. E. Bergles (2010). "NG2+ CNS glial progenitors remain committed to the oligodendrocyte lineage in postnatal life and following neurodegeneration." Neuron **68**(4): 668-681.

Karadottir, R. and D. Attwell (2007). "Neurotransmitter receptors in the life and death of oligodendrocytes." Neuroscience **145**(4): 1426-1438.

Kemali, M. and A. Miralto (1979). "The habenular nuclei of the elasmobranch "Scyllium stellare": myelinated perikarya." Am J Anat **155**(1): 147-152.

Kemali, M. and E. Sada (1973). "Myelinated cell bodies in the habenular nuclei of the frog." Brain Res **54**: 355-359.

Kettleborough, R. N., E. M. Busch-Nentwich, S. A. Harvey, C. M. Dooley, E. de Bruijn, F. van Eeden, I. Sealy, R. J. White, C. Herd, I. J. Nijman, F. Fenyes, S. Mehroke, C. Scahill, R. Gibbons, N. Wali, S. Carruthers, A. Hall, J. Yen, E. Cuppen and D. L. Stemple (2013). "A

systematic genome-wide analysis of zebrafish protein-coding gene function." Nature **496**(7446): 494-497.

Kidd, G. J., P. E. Hauer and B. D. Trapp (1990). "Axons modulate myelin protein messenger RNA levels during central nervous system myelination in vivo." J Neurosci Res **26**(4): 409-418.

Kimmel, C. B., W. W. Ballard, S. R. Kimmel, B. Ullmann and T. F. Schilling (1995). "Stages of embryonic development of the zebrafish." Dev Dyn **203**(3): 253-310.

Kimmel, C. B., S. L. Powell and W. K. Metcalfe (1982). "Brain neurons which project to the spinal cord in young larvae of the zebrafish." J Comp Neurol **205**(2): 112-127.

Kirby, B. B., N. Takada, A. J. Latimer, J. Shin, T. J. Carney, R. N. Kelsh and B. Appel (2006). "In vivo time-lapse imaging shows dynamic oligodendrocyte progenitor behavior during zebrafish development." Nat Neurosci **9**(12): 1506-1511.

Klugmann, M., M. H. Schwab, A. Puhlhofer, A. Schneider, F. Zimmermann, I. R. Griffiths and K. A. Nave (1997). "Assembly of CNS myelin in the absence of proteolipid protein." Neuron **18**(1): 59-70.

Knobler, R. L., J. G. Stempak and M. Laurencin (1976). "Nonuniformity of the oligodendroglial ensheathment of axons during myelination in the developing rat central nervous system. A serial section electron microscopical study." J Ultrastruct Res **55**(3): 417-432.

Koenning, M., S. Jackson, C. M. Hay, C. Faux, T. J. Kilpatrick, M. Willingham and B. Emery (2012). "Myelin gene regulatory factor is required for maintenance of myelin and mature oligodendrocyte identity in the adult CNS." J Neurosci **32**(36): 12528-12542.

Kucenas, S., H. Snell and B. Appel (2008). "nkx2.2a promotes specification and differentiation of a myelinating subset of oligodendrocyte lineage cells in zebrafish." Neuron Glia Biol **4**(2): 71-81.

Kuspert, M., A. Hammer, M. R. Bosl and M. Wegner (2011). "Olig2 regulates Sox10 expression in oligodendrocyte precursors through an evolutionary conserved distal enhancer." Nucleic Acids Res **39**(4): 1280-1293.

Kwan, K. M., E. Fujimoto, C. Grabher, B. D. Mangum, M. E. Hardy, D. S. Campbell, J. M. Parant, H. J. Yost, J. P. Kanki and C. B. Chien (2007). "The Tol2kit: a multisite gateway-based construction kit for Tol2 transposon transgenesis constructs." Dev Dyn **236**(11): 3088-3099.

Lang, D. M., B. P. Rubin, M. E. Schwab and C. A. Stuermer (1995). "CNS myelin and oligodendrocytes of the Xenopus spinal cord--but not optic nerve--are nonpermissive for axon growth." J Neurosci **15**(1 Pt 1): 99-109.

Lappe-Siefke, C., S. Goebbels, M. Gravel, E. Nicksch, J. Lee, P. E. Braun, I. R. Griffiths and K. A. Nave (2003). "Disruption of Cnp1 uncouples oligodendroglial functions in axonal support and myelination." Nat Genet **33**(3): 366-374.

Laursen, L. S., C. W. Chan and C. ffrench-Constant (2009). "An integrin-contactin complex regulates CNS myelination by differential Fyn phosphorylation." J Neurosci **29**(29): 9174-9185.

Laursen, L. S., C. W. Chan and C. Ffrench-Constant (2011). "Translation of myelin basic protein mRNA in oligodendrocytes is regulated by integrin activation and hnRNP-K." J Cell Biol **192**(5): 797-811.

Lee, J. S., A. Padmanabhan, J. Shin, S. Zhu, F. Guo, J. P. Kanki, J. A. Epstein and A. T. Look (2010). "Oligodendrocyte progenitor cell numbers and migration are regulated by the zebrafish orthologs of the NF1 tumor suppressor gene." Hum Mol Genet **19**(23): 4643-4653.

Lee, K. K., Y. de Repentigny, R. Saulnier, P. Rippstein, W. B. Macklin and R. Kothary (2006). "Dominant-negative beta1 integrin mice have region-specific myelin defects accompanied by alterations in MAPK activity." Glia **53**(8): 836-844.

Lee, S., M. K. Leach, S. A. Redmond, S. Y. Chong, S. H. Mellon, S. J. Tuck, Z. Q. Feng, J. M. Corey and J. R. Chan (2012). "A culture system to study oligodendrocyte myelination processes using engineered nanofibers." Nat Methods **9**(9): 917-922.

Lee, Y., B. M. Morrison, Y. Li, S. Lengacher, M. H. Farah, P. N. Hoffman, Y. Liu, A. Tsingalia, L. Jin, P.-W. Zhang, L. Pellerin, P. J. Magistretti and J. D. Rothstein (2012). "Oligodendroglia metabolically support axons and contribute to neurodegeneration." Nature **487**(7408): 443-448.

Lewis, K. E. and J. S. Eisen (2003). "From cells to circuits: development of the zebrafish spinal cord." Prog Neurobiol **69**(6): 419-449.

Li, H., J. P. de Faria, P. Andrew, J. Nitarska and W. D. Richardson (2011). "Phosphorylation regulates OLIG2 cofactor choice and the motor neuron-oligodendrocyte fate switch." Neuron **69**(5): 918-929.

Li, H., Y. He, W. D. Richardson and P. Casaccia (2009). "Two-tier transcriptional control of oligodendrocyte differentiation." Curr Opin Neurobiol **19**(5): 479-485.

Li, H., Y. Lu, H. K. Smith and W. D. Richardson (2007). "Olig1 and Sox10 interact synergistically to drive myelin basic protein transcription in oligodendrocytes." J Neurosci **27**(52): 14375-14382.

Li, Q., M. Brus-Ramer, J. H. Martin and J. W. McDonald (2010). "Electrical stimulation of the medullary pyramid promotes proliferation and differentiation of oligodendrocyte progenitor cells in the corticospinal tract of the adult rat." Neurosci Lett **479**(2): 128-133.

Li, Y., M. Ceylan, B. Shrestha, H. Wang, Q. R. Lu, R. Asmatulu and L. Yao (2014). "Nanofibers support oligodendrocyte precursor cell growth and function as a neuron-free model for myelination study." Biomacromolecules **15**(1): 319-326.

Ligon, K. L., S. P. Fancy, R. J. Franklin and D. H. Rowitch (2006). "Olig gene function in CNS development and disease." Glia **54**(1): 1-10.

Liu, J., K. Dietz, J. M. DeLoyht, X. Pedre, D. Kelkar, J. Kaur, V. Vialou, M. K. Lobo, D. M. Dietz, E. J. Nestler, J. Dupree and P. Casaccia (2012). "Impaired adult myelination in the prefrontal cortex of socially isolated mice." Nat Neurosci **15**(12): 1621-1623.

Liu, K. S., M. Gray, S. J. Otto, J. R. Fetcho and C. E. Beattie (2003). "Mutations in deadly seven/notch1a reveal developmental plasticity in the escape response circuit." J Neurosci **23**(22): 8159-8166.

Liu, L., V. Korzh, N. V. Balasubramaniyan, M. Ekker and R. Ge (2002). "Platelet-derived growth factor A (pdgf-a) expression during zebrafish embryonic development." Dev Genes Evol **212**(6): 298-301.

Liu, X., R. Bates, D. M. Yin, C. Shen, F. Wang, N. Su, S. A. Kirov, Y. Luo, J. Z. Wang, W. C. Xiong and L. Mei (2011). "Specific regulation of NRG1 isoform expression by neuronal activity." J Neurosci **31**(23): 8491-8501.

Liu, Z., X. Hu, J. Cai, B. Liu, X. Peng, M. Wegner and M. Qiu (2007). "Induction of oligodendrocyte differentiation by Olig2 and Sox10: evidence for reciprocal interactions and dosage-dependent mechanisms." Dev Biol **302**(2): 683-693.

Luan, H., N. C. Peabody, C. R. Vinson and B. H. White (2006). "Refined spatial manipulation of neuronal function by combinatorial restriction of transgene expression." Neuron **52**(3): 425-436.

Lubetzki, C., C. Demerens, P. Anglade, H. Villarroya, A. Frankfurter, V. M. Lee and B. Zalc (1993). "Even in culture, oligodendrocytes myelinate solely axons." Proc Natl Acad Sci U S A **90**(14): 6820-6824.

Ludwin, S. K. (1990). "Oligodendrocyte survival in Wallerian degeneration." Acta Neuropathol **80**(2): 184-191.

Ludwin, S. K. and M. Maitland (1984). "Long-term remyelination fails to reconstitute normal thickness of central myelin sheaths." J Neurol Sci **64**(2): 193-198.

Lyons, D. A., S. G. Naylor, S. Mercurio, C. Dominguez and W. S. Talbot (2008). "KBP is essential for axonal structure, outgrowth and maintenance in zebrafish, providing insight into the cellular basis of Goldberg-Shprintzen syndrome." Development **135**(3): 599-608.

Lyons, D. A., S. G. Naylor, A. Scholze and W. S. Talbot (2009). "Kif1b is essential for mRNA localization in oligodendrocytes and development of myelinated axons." Nat Genet **41**(7): 854-858.

Ma, M. and Y. J. Jiang (2007). "Jagged2a-notch signaling mediates cell fate choice in the zebrafish pronephric duct." PLoS Genet **3**(1): e18.

Macklin, W. B., C. L. Weill and P. L. Deininger (1986). "Expression of myelin proteolipid and basic protein mRNAs in cultured cells." J Neurosci Res **16**(1): 203-217.

Mahad, D., H. Lassmann and D. Turnbull (2008). "Review: Mitochondria and disease progression in multiple sclerosis." Neuropathol Appl Neurobiol **34**(6): 577-589.

Makinodan, M., K. M. Rosen, S. Ito and G. Corfas (2012). "A critical period for social experience-dependent oligodendrocyte maturation and myelination." Science **337**(6100): 1357-1360.

Mangin, J. M., P. Li, J. Scafidi and V. Gallo (2012). "Experience-dependent regulation of NG2 progenitors in the developing barrel cortex." Nat Neurosci **15**(9): 1192-1194.

Mathews, E. S., D. J. Mawdsley, M. Walker, J. H. Hines, M. Pozzoli and B. Appel (2014). "Mutation of 3-hydroxy-3-methylglutaryl CoA synthase I reveals requirements for isoprenoid and cholesterol synthesis in oligodendrocyte migration arrest, axon wrapping, and myelin gene expression." J Neurosci **34**(9): 3402-3412.

Matthews, M. A. and D. Duncan (1971). "A quantitative study of morphological changes accompanying the initiation and progress of myelin production in the dorsal funiculus of the rat spinal cord." J Comp Neurol **142**(1): 1-22.

McClintock, J. M., R. Carlson, D. M. Mann and V. E. Prince (2001). "Consequences of Hox gene duplication in the vertebrates: an investigation of the zebrafish Hox paralogue group 1 genes." Development **128**(13): 2471-2484.

McClintock, J. M., M. A. Kheirbek and V. E. Prince (2002). "Knockdown of duplicated zebrafish hoxb1 genes reveals distinct roles in hindbrain patterning and a novel mechanism of duplicate gene retention." Development **129**(10): 2339-2354.

McDonald, W. I. and T. A. Sears (1970). "The effects of experimental demyelination on conduction in the central nervous system." Brain **93**(3): 583-598.

McLean, D. L., J. Fan, S. Higashijima, M. E. Hale and J. R. Fetcho (2007). "A topographic map of recruitment in spinal cord." Nature **446**(7131): 71-75.

McPhilemy, K., L. S. Mitchell, I. R. Griffiths, S. Morrison, A. W. Deary, I. Sommer and P. G. Kennedy (1990). "Effect of optic nerve transection upon myelin protein gene expression by oligodendrocytes: evidence for axonal influences on gene expression." J Neurocytol **19**(4): 494-503.

Mei, F., H. Wang, S. Liu, J. Niu, L. Wang, Y. He, A. Etxeberria, J. R. Chan and L. Xiao (2013). "Stage-specific deletion of Olig2 conveys opposing functions on differentiation and maturation of oligodendrocytes." J Neurosci **33**(19): 8454-8462.

Mei, L. and W. C. Xiong (2008). "Neuregulin 1 in neural development, synaptic plasticity and schizophrenia." Nat Rev Neurosci **9**(6): 437-452.

Meijer, D. H., M. F. Kane, S. Mehta, H. Liu, E. Harrington, C. M. Taylor, C. D. Stiles and D. H. Rowitch (2012). "Separated at birth? The functional and molecular divergence of OLIG1 and OLIG2." Nat Rev Neurosci **13**(12): 819-831.

Mendelson, B. (1986). "Development of reticulospinal neurons of the zebrafish. I. Time of origin." J Comp Neurol **251**(2): 160-171.

Mendelson, B. (1986). "Development of reticulospinal neurons of the zebrafish. II. Early axonal outgrowth and cell body position." J Comp Neurol **251**(2): 172-184.

Mensch, S. (2014). Investigating axon-oligodendrocyte interactions during myelinated axon formation in vivo.

Metcalfe, W. K., B. Mendelson and C. B. Kimmel (1986). "Segmental homologies among reticulospinal neurons in the hindbrain of the zebrafish larva." J Comp Neurol **251**(2): 147-159.

Michailov, G. V., M. W. Sereda, B. G. Brinkmann, T. M. Fischer, B. Haug, C. Birchmeier, L. Role, C. Lai, M. H. Schwab and K. A. Nave (2004). "Axonal neuregulin-1 regulates myelin sheath thickness." Science **304**(5671): 700-703.

Miller, R. H. (2002). "Regulation of oligodendrocyte development in the vertebrate CNS." Prog Neurobiol **67**(6): 451-467.

Milner, R., G. Edwards, C. Streuli and C. Ffrench-Constant (1996). "A role in migration for the alpha V beta 1 integrin expressed on oligodendrocyte precursors." J Neurosci **16**(22): 7240-7252.

Miron, V. E., A. Boyd, J. W. Zhao, T. J. Yuen, J. M. Ruckh, J. L. Shadrach, P. van Wijngaarden, A. J. Wagers, A. Williams, R. J. Franklin and C. ffrench-Constant (2013). "M2 microglia and macrophages drive oligodendrocyte differentiation during CNS remyelination." Nat Neurosci **16**(9): 1211-1218.

Mitew, S., C. M. Hay, H. Peckham, J. Xiao, M. Koenning and B. Emery (2014). "Mechanisms regulating the development of oligodendrocytes and central nervous system myelin." Neuroscience **276C**: 29-47.

Monk, K. R. and W. S. Talbot (2009). "Genetic dissection of myelinated axons in zebrafish." Curr Opin Neurobiol **19**(5): 486-490.

Morrison, B. M., Y. Lee and J. D. Rothstein (2013). "Oligodendroglia: metabolic supporters of axons." Trends Cell Biol **23**(12): 644-651.

Mudhar, H. S., R. A. Pollock, C. Wang, C. D. Stiles and W. D. Richardson (1993). "PDGF and its receptors in the developing rodent retina and optic nerve." Development **118**(2): 539-552.

Munzel, E., C. G. Becker, T. Becker and A. Williams (2014). "Zebrafish regenerate full thickness optic nerve myelin after demyelination, but this fails with increasing age." Acta Neuropathol Commun **2**(1): 77.

Mutsaers, S. E. and W. M. Carroll (1998). "Focal accumulation of intra-axonal mitochondria in demyelination of the cat optic nerve." Acta Neuropathol **96**(2): 139-143.

Nave, K. A. and B. D. Trapp (2008). "Axon-glial signaling and the glial support of axon function." Annu Rev Neurosci **31**: 535-561.

Noble, M. and K. Murray (1984). "Purified astrocytes promote the in vitro division of a bipotential glial progenitor cell." EMBO J **3**(10): 2243-2247.

Noble, M., K. Murray, P. Stroobant, M. D. Waterfield and P. Riddle (1988). "Platelet-derived growth factor promotes division and motility and inhibits premature differentiation of the oligodendrocyte/type-2 astrocyte progenitor cell." Nature **333**(6173): 560-562.

Nüsslein-Volhard, C. and R. Dahm (2002). Zebrafish: A Practical Approach, Oxford University Press.

O'Rourke, M., R. Gasperini and K. M. Young (2014). "Adult myelination: wrapping up neuronal plasticity." Neural Regen Res **9**(13): 1261-1264.

Pajevic, S., P. J. Basser and R. D. Fields (2014). "Role of myelin plasticity in oscillations and synchrony of neuronal activity." Neuroscience **276**: 135-147.

Paquet, D., R. Bhat, A. Sydow, E. M. Mandelkow, S. Berg, S. Hellberg, J. Falting, M. Distel, R. W. Koster, B. Schmid and C. Haass (2009). "A zebrafish model of tauopathy allows in vivo imaging of neuronal cell death and drug evaluation." J Clin Invest **119**(5): 1382-1395.

Park, H. C. and B. Appel (2003). "Delta-Notch signaling regulates oligodendrocyte specification." Development **130**(16): 3747-3755.

Park, H. C., C. H. Kim, Y. K. Bae, S. Y. Yeo, S. H. Kim, S. K. Hong, J. Shin, K. W. Yoo, M. Hibi, T. Hirano, N. Miki, A. B. Chitnis and T. L. Huh (2000). "Analysis of upstream elements in the HuC promoter leads to the establishment of transgenic zebrafish with fluorescent neurons." Dev Biol **227**(2): 279-293.

Perlin, J. R., M. E. Lush, W. Z. Stephens, T. Piotrowski and W. S. Talbot (2011). "Neuronal Neuregulin 1 type III directs Schwann cell migration." Development **138**(21): 4639-4648.

Pfeiffer, B. D., T. T. Ngo, K. L. Hibbard, C. Murphy, A. Jenett, J. W. Truman and G. M. Rubin (2010). "Refinement of tools for targeted gene expression in Drosophila." Genetics **186**(2): 735-755.

Piaton, G., R. M. Gould and C. Lubetzki (2010). "Axon-oligodendrocyte interactions during developmental myelination, demyelination and repair." J Neurochem **114**(5): 1243-1260.

Picker, A., S. Scholpp, H. Bohli, H. Takeda and M. Brand (2002). "A novel positive transcriptional feedback loop in midbrain-hindbrain boundary development is revealed through analysis of the zebrafish pax2.1 promoter in transgenic lines." Development **129**(13): 3227-3239.

Poliak, S. and E. Peles (2003). "The local differentiation of myelinated axons at nodes of Ranvier." Nat Rev Neurosci **4**(12): 968-980.

Privat, A., J. Valat and J. Fulcrand (1981). "Proliferation of neuroglial cell lines in the degenerating optic nerve of young rats. A radioautographic study." J Neuropathol Exp Neurol **40**(1): 46-60.

Psachoulia, K., F. Jamen, K. M. Young and W. D. Richardson (2009). "Cell cycle dynamics of NG2 cells in the postnatal and ageing brain." Neuron Glia Biol **5**(3-4): 57-67.

Raabe, T. D., S. Suy, A. Welcher and G. H. DeVries (1997). "Effect of neu differentiation factor isoforms on neonatal oligodendrocyte function." J Neurosci Res **50**(5): 755-768.

Raff, M. C., E. R. Abney and J. Fok-Seang (1985). "Reconstitution of a developmental clock in vitro: a critical role for astrocytes in the timing of oligodendrocyte differentiation." Cell **42**(1): 61-69.

Raff, M. C., L. E. Lillien, W. D. Richardson, J. F. Burne and M. D. Noble (1988). "Platelet-derived growth factor from astrocytes drives the clock that times oligodendrocyte development in culture." Nature **333**(6173): 562-565.

Rasminsky, M. and T. A. Sears (1972). "Internodal conduction in undissected demyelinated nerve fibres." J Physiol **227**(2): 323-350.

Reimer, M. M., A. Norris, J. Ohnmacht, R. Patani, Z. Zhong, T. B. Dias, V. Kuscha, A. L. Scott, Y. C. Chen, S. Rozov, S. L. Frazer, C. Wyatt, S. Higashijima, E. E. Patton, P. Panula, S. Chandran, T. Becker and C. G. Becker (2013). "Dopamine from the brain promotes spinal motor neuron generation during development and adult regeneration." Dev Cell **25**(5): 478-491.

Relucio, J., I. D. Tzvetanova, W. Ao, S. Lindquist and H. Colognato (2009). "Laminin alters fyn regulatory mechanisms and promotes oligodendrocyte development." J Neurosci **29**(38): 11794-11806.

Relvas, J. B., A. Setzu, W. Baron, P. C. Buttery, S. E. LaFlamme, R. J. Franklin and C. ffrench-Constant (2001). "Expression of dominant-negative and chimeric subunits reveals an essential role for beta1 integrin during myelination." Curr Biol **11**(13): 1039-1043.

Remahl, S. and C. Hildebrand (1982). "Changing relation between onset of myelination and axon diameter range in developing feline white matter." J Neurol Sci **54**(1): 33-45.

Remahl, S. and C. Hilderbrand (1990). "Relation between axons and oligodendroglial cells during initial myelination. I. The glial unit." J Neurocytol **19**(3): 313-328.

Richardson, W. D., N. Kessaris and N. Pringle (2006). "Oligodendrocyte wars." Nat Rev Neurosci **7**(1): 11-18.

Richardson, W. D., N. Pringle, M. J. Mosley, B. Westermark and M. Dubois-Dalcq (1988). "A role for platelet-derived growth factor in normal gliogenesis in the central nervous system." Cell **53**(2): 309-319.

Richardson, W. D., K. M. Young, R. B. Tripathi and I. McKenzie (2011). "NG2-glia as multipotent neural stem cells: fact or fantasy?" Neuron **70**(4): 661-673.

Richter-Landsberg, C. (2008). "The cytoskeleton in oligodendrocytes. Microtubule dynamics in health and disease." J Mol Neurosci **35**(1): 55-63.

Río-Hortega, P. d. (1928). Tercera aportación al conocimiento morfológico e interpretación funcional de la oligodendroglía. Madrid, Museo Nacional de Ciencias Naturales.

Ritchie, J. M. (1982). "On the relation between fibre diameter and conduction velocity in myelinated nerve fibres." Proc R Soc Lond B Biol Sci **217**(1206): 29-35.

Rivers, L. E., K. M. Young, M. Rizzi, F. Jamen, K. Psachoulia, A. Wade, N. Kessaris and W. D. Richardson (2008). "PDGFRA/NG2 glia generate myelinating oligodendrocytes and piriform projection neurons in adult mice." Nat Neurosci **11**(12): 1392-1401.

Roberts, B. L. and K. P. Ryan (1976). "Myelinated synapse-bearing cell bodies in the central nervous system of Scyliorhinus canicula (L.)." Cell Tissue Res **171**(3): 407-410.

Robu, M. E., J. D. Larson, A. Nasevicius, S. Beiraghi, C. Brenner, S. A. Farber and S. C. Ekker (2007). "p53 activation by knockdown technologies." PLoS Genet **3**(5): e78.

Rome, L. H., P. N. Bullock, F. Chiappelli, M. Cardwell, A. M. Adinolfi and D. Swanson (1986). "Synthesis of a myelin-like membrane by oligodendrocytes in culture." J Neurosci Res **15**(1): 49-65.

Rosenberg, S. S., E. E. Kelland, E. Tokar, A. R. De la Torre and J. R. Chan (2008). "The geometric and spatial constraints of the microenvironment induce oligodendrocyte differentiation." Proc Natl Acad Sci U S A **105**(38): 14662-14667.

Rosenbluth, J. (1966). "Redundant myelin sheaths and other ultrastructural features of the toad cerebellum." J Cell Biol **28**(1): 73-93.

Rowitch, D. H. (2004). "Glial specification in the vertebrate neural tube." Nat Rev Neurosci **5**(5): 409-419.

Rowitch, D. H. and A. R. Kriegstein (2010). "Developmental genetics of vertebrate glial-cell specification." Nature **468**(7321): 214-222.

Roy, K., J. C. Murtie, B. F. El-Khodor, N. Edgar, S. P. Sardi, B. M. Hooks, M. Benoit-Marand, C. Chen, H. Moore, P. O'Donnell, D. Brunner and G. Corfas (2007). "Loss of erbB signaling in oligodendrocytes alters myelin and dopaminergic function, a potential mechanism for neuropsychiatric disorders." Proc Natl Acad Sci U S A **104**(19): 8131-8136.

Rushton, W. A. (1951). "A theory of the effects of fibre size in medullated nerve." J Physiol **115**(1): 101-122.

Saab, A. S., I. D. Tzvetanova and K. A. Nave (2013). "The role of myelin and oligodendrocytes in axonal energy metabolism." Curr Opin Neurobiol **23**(6): 1065-1072.

Salzer, J. L. (2003). "Polarized domains of myelinated axons." Neuron **40**(2): 297-318.

Sampaio-Baptista, C., A. A. Khrapitchev, S. Foxley, T. Schlagheck, J. Scholz, S. Jbabdi, G. C. DeLuca, K. L. Miller, A. Taylor, N. Thomas, J. Kleim, N. R. Sibson, D. Bannerman and H. Johansen-Berg (2013). "Motor skill learning induces changes in white matter microstructure and myelination." J Neurosci **33**(50): 19499-19503.

Scholz, J., M. C. Klein, T. E. Behrens and H. Johansen-Berg (2009). "Training induces changes in white-matter architecture." Nat Neurosci **12**(11): 1370-1371.

Schwab, M. E. and L. Schnell (1989). "Region-specific appearance of myelin constituents in the developing rat spinal cord." J Neurocytol **18**(2): 161-169.

Schweitzer, J., T. Becker, C. G. Becker and M. Schachner (2003). "Expression of protein zero is increased in lesioned axon pathways in the central nervous system of adult zebrafish." Glia **41**(3): 301-317.

Scott, E. K., L. Mason, A. B. Arrenberg, L. Ziv, N. J. Gosse, T. Xiao, N. C. Chi, K. Asakawa, K. Kawakami and H. Baier (2007). "Targeting neural circuitry in zebrafish using GAL4 enhancer trapping." Nat Methods **4**(4): 323-326.

Sefton, A. J. and K. Lam (1984). "Quantitative and morphological studies on developing optic axons in normal and enucleated albino rats." Exp Brain Res **57**(1): 107-117.

Seidl, A. H. (2014). "Regulation of conduction time along axons." Neuroscience **276C**: 126-134.

Sherman, D. L. and P. J. Brophy (2005). "Mechanisms of axon ensheathment and myelin growth." Nat Rev Neurosci **6**(9): 683-690.

Shi, J., A. Marinovich and B. A. Barres (1998). "Purification and characterization of adult oligodendrocyte precursor cells from the rat optic nerve." J Neurosci **18**(12): 4627-4636.

Shin, J., A. Padmanabhan, E. D. de Groh, J. S. Lee, S. Haidar, S. Dahlberg, F. Guo, S. He, M. A. Wolman, M. Granato, N. D. Lawson, S. A. Wolfe, S. H. Kim, L. Solnica-Krezel, J. P. Kanki, K. L. Ligon, J. A. Epstein and A. T. Look (2012). "Zebrafish neurofibromatosis type 1 genes have redundant functions in tumorigenesis and embryonic development." Dis Model Mech **5**(6): 881-894.

Shin, J., H. C. Park, J. M. Topczewska, D. J. Mawdsley and B. Appel (2003). "Neural cell fate analysis in zebrafish using olig2 BAC transgenics." Methods Cell Sci **25**(1-2): 7-14.

Simmons, T. and B. Appel (2012). "Mutation of pescadillo disrupts oligodendrocyte formation in zebrafish." PLoS One **7**(2): e32317.

Simons, M. and J. Trotter (2007). "Wrapping it up: the cell biology of myelination." Curr Opin Neurobiol **17**(5): 533-540.

Small, R. K., P. Riddle and M. Noble (1987). "Evidence for migration of oligodendrocyte--type-2 astrocyte progenitor cells into the developing rat optic nerve." Nature **328**(6126): 155-157.

Smith, K. J., W. F. Blakemore and W. I. McDonald (1979). "Central remyelination restores secure conduction." Nature **280**(5721): 395-396.

Snaidero, N., W. Mobius, T. Czopka, L. H. Hekking, C. Mathisen, D. Verkleij, S. Goebbels, J. Edgar, D. Merkler, D. A. Lyons, K. A. Nave and M. Simons (2014). "Myelin membrane wrapping of CNS axons by PI(3,4,5)P3-dependent polarized growth at the inner tongue." Cell **156**(1-2): 277-290.

Snaidero, N. and M. Simons (2014). "Myelination at a glance." J Cell Sci **127**(Pt 14): 2999-3004.

Snyder, J. L., C. A. Kearns and B. Appel (2012). "Fbxw7 regulates Notch to control specification of neural precursors for oligodendrocyte fate." Neural Dev **7**: 15.

Stolt, C. C., S. Rehberg, M. Ader, P. Lommes, D. Riethmacher, M. Schachner, U. Bartsch and M. Wegner (2002). "Terminal differentiation of myelin-forming oligodendrocytes depends on the transcription factor Sox10." Genes Dev **16**(2): 165-170.

Suster, M. L., L. Seugnet, M. Bate and M. B. Sokolowski (2004). "Refining GAL4-driven transgene expression in Drosophila with a GAL80 enhancer-trap." Genesis **39**(4): 240-245.

Susuki, K., K. J. Chang, D. R. Zollinger, Y. Liu, Y. Ogawa, Y. Eshed-Eisenbach, M. T. Dours-Zimmermann, J. A. Oses-Prieto, A. L. Burlingame, C. I. Seidenbecher, D. R. Zimmermann, T. Oohashi, E. Peles and M. N. Rasband (2013). "Three mechanisms assemble central nervous system nodes of Ranvier." Neuron **78**(3): 469-482.

Suyeoka, O. (1968). "Small myelinated perikarya in the cerebellar granular layer of mammals including man." Experientia **24**(5): 472-473.

Szuchet, S., P. E. Polak and S. H. Yim (1986). "Mature oligodendrocytes cultured in the absence of neurons recapitulate the ontogenic development of myelin membranes." Dev Neurosci **8**(4): 208-221.

Szymczak-Workman, A. L., K. M. Vignali and D. A. Vignali (2012). "Design and construction of 2A peptide-linked multicistronic vectors." Cold Spring Harb Protoc **2012**(2): 199-204.

Szymczak-Workman, A. L., K. M. Vignali and D. A. Vignali (2012). "Generation of 2A-linked multicistronic cassettes by recombinant PCR." Cold Spring Harb Protoc **2012**(2): 251-254.

Takada, N. and B. Appel (2011). "swap70 promotes neural precursor cell cycle exit and oligodendrocyte formation." Mol Cell Neurosci **48**(3): 225-235.

Takada, N., S. Kucenas and B. Appel (2010). "Sox10 is necessary for oligodendrocyte survival following axon wrapping." Glia **58**(8): 996-1006.

Takeichi, M. (2007). "The cadherin superfamily in neuronal connections and interactions." Nat Rev Neurosci **8**(1): 11-20.

Tang, D. G., Y. M. Tokumoto and M. C. Raff (2000). "Long-term culture of purified postnatal oligodendrocyte precursor cells. Evidence for an intrinsic maturation program that plays out over months." J Cell Biol **148**(5): 971-984.

Tauber, H., T. V. Waehneldt and V. Neuhoff (1980). "Myelination in rabbit optic nerves is accelerated by artificial eye opening." Neurosci Lett **16**(3): 235-238.

Temple, S. and M. C. Raff (1986). "Clonal analysis of oligodendrocyte development in culture: evidence for a developmental clock that counts cell divisions." Cell **44**(5): 773-779.

Tigges, M. and J. Tigges (1980). "Distribution and morphology of myelinated perikarya and dendrites in the olfactory bulb of primates." J Neurocytol **9**(6): 825-834.

Tomassy, G. S., D. R. Berger, H. H. Chen, N. Kasthuri, K. J. Hayworth, A. Vercelli, H. S. Seung, J. W. Lichtman and P. Arlotta (2014). "Distinct profiles of myelin distribution along single axons of pyramidal neurons in the neocortex." Science **344**(6181): 319-324.

Trapp, B. D., A. Nishiyama, D. Cheng and W. Macklin (1997). "Differentiation and death of premyelinating oligodendrocytes in developing rodent brain." J Cell Biol **137**(2): 459-468.

Trimmer, P. A. and R. E. Wunderlich (1990). "Changes in astroglial scar formation in rat optic nerve as a function of development." J Comp Neurol **296**(3): 359-378.

Tripathi, R. B., L. E. Rivers, K. M. Young, F. Jamen and W. D. Richardson (2010). "NG2 glia generate new oligodendrocytes but few astrocytes in a murine experimental autoimmune encephalomyelitis model of demyelinating disease." J Neurosci **30**(48): 16383-16390.

Trotter, J., K. Karram and A. Nishiyama (2010). "NG2 cells: Properties, progeny and origin." Brain Res Rev **63**(1-2): 72-82.

Tsai, H. H. and R. H. Miller (2002). "Glial cell migration directed by axon guidance cues." Trends Neurosci **25**(4): 173-175; discussion 175-176.

Tumpel, S., L. M. Wiedemann and R. Krumlauf (2009). "Hox genes and segmentation of the vertebrate hindbrain." Curr Top Dev Biol **88**: 103-137.

Ueda, H., J. M. Levine, R. H. Miller and B. D. Trapp (1999). "Rat optic nerve oligodendrocytes develop in the absence of viable retinal ganglion cell axons." J Cell Biol **146**(6): 1365-1374.

Valat, J., J. Fulcrand and R. Marty (1978). "[Postnatal cellular reactivity of the optic nerve after enucleation in the rat. Quantitative aspects in relation to myelinization]." Acta Anat (Basel) **100**(1): 5-16.

Vartanian, T., G. Corfas, Y. Li, G. D. Fischbach and K. Stefansson (1994). "A role for the acetylcholine receptor-inducing protein ARIA in oligodendrocyte development." Proc Natl Acad Sci U S A **91**(24): 11626-11630.

Vartanian, T., G. Fischbach and R. Miller (1999). "Failure of spinal cord oligodendrocyte development in mice lacking neuregulin." Proc Natl Acad Sci U S A **96**(2): 731-735.

Wake, H., P. R. Lee and R. D. Fields (2011). "Control of local protein synthesis and initial events in myelination by action potentials." Science **333**(6049): 1647-1651.

Wang, S. and K. M. Young (2014). "White matter plasticity in adulthood." Neuroscience **276C**: 148-160.

Wang, S. L., A. D. Sdrulla, G. diSibio, G. Bush, D. Nofziger, C. Hicks, G. Weinmaster and B. A. Barres (1998). "Notch receptor activation inhibits oligodendrocyte differentiation." Neuron **21**(1): 63-75.

Warrington, A. E., E. Barbarese and S. E. Pfeiffer (1993). "Differential myelinogenic capacity of specific developmental stages of the oligodendrocyte lineage upon transplantation into hypomyelinating hosts." J Neurosci Res **34**(1): 1-13.

Watanabe, M., Y. Sakurai, T. Ichinose, Y. Aikawa, M. Kotani and K. Itoh (2006). "Monoclonal antibody Rip specifically recognizes 2',3'-cyclic nucleotide 3'-phosphodiesterase in oligodendrocytes." J Neurosci Res **84**(3): 525-533.

Waxman, S. G. (1980). "Determinants of conduction velocity in myelinated nerve fibers." Muscle Nerve **3**(2): 141-150.

Waxman, S. G. (1997). "Axon-glia interactions: building a smart nerve fiber." Curr Biol **7**(7): R406-410.

Waxman, S. G. (2003). "Current Concepts in Neurology: Membranes, Myelin, and the Pathophysiology of Multiple Sclerosis." Form and Function in the Brain and Spinal Cord: Perspectives of a Neurologist **306**: 109.

Weruaga-Prieto, E., P. Eggli and M. R. Celio (1996). "Topographic variations in rat brain oligodendrocyte morphology elucidated by injection of Lucifer Yellow in fixed tissue slices." J Neurocytol **25**(1): 19-31.

Westerfield, M. (2007). The Zebrafish Book: A Guide for the Laboratory Use of Zebrafish (Danio Rerio), M. Westerfield.

Williams, J. A., A. Barrios, C. Gatchalian, L. Rubin, S. W. Wilson and N. Holder (2000). "Programmed cell death in zebrafish rohon beard neurons is influenced by TrkC1/NT-3 signaling." Dev Biol **226**(2): 220-230.

Wood, P. M. and R. P. Bunge (1986). "Evidence that axons are mitogenic for oligodendrocytes isolated from adult animals." Nature **320**(6064): 756-758.

Wozniak, M. J., M. Melzer, C. Dorner, H. U. Haring and R. Lammers (2005). "The novel protein KBP regulates mitochondria localization by interaction with a kinesin-like protein." BMC Cell Biol **6**: 35.

Wu, L. M., A. Williams, A. Delaney, D. L. Sherman and P. J. Brophy (2012). "Increasing internodal distance in myelinated nerves accelerates nerve conduction to a flat maximum." Curr Biol **22**(20): 1957-1961.

Xin, M., T. Yue, Z. Ma, F. F. Wu, A. Gow and Q. R. Lu (2005). "Myelinogenesis and axonal recognition by oligodendrocytes in brain are uncoupled in Olig1-null mice." J Neurosci **25**(6): 1354-1365.

Yang, Y., R. Lewis and R. H. Miller (2011). "Interactions between oligodendrocyte precursors control the onset of CNS myelination." Dev Biol **350**(1): 127-138.

Yasargil, G. M., N. G. Greeff, H. R. Luescher, K. Akert and C. Sandri (1982). "The structural correlate of saltatory conduction along the Mauthner axon in the tench (Tinca tinca L.): identification of nodal equivalents at the axon collaterals." J Comp Neurol **212**(4): 417-424.

Yeh, H. J., K. G. Ruit, Y. X. Wang, W. C. Parks, W. D. Snider and T. F. Deuel (1991). "PDGF A-chain gene is expressed by mammalian neurons during development and in maturity." Cell **64**(1): 209-216.

Young, K. M., K. Psachoulia, R. B. Tripathi, S. J. Dunn, L. Cossell, D. Attwell, K. Tohyama and W. D. Richardson (2013). "Oligodendrocyte dynamics in the healthy adult CNS: evidence for myelin remodeling." Neuron **77**(5): 873-885.

Yuen, T. J., J. C. Silbereis, A. Griveau, S. M. Chang, R. Daneman, S. P. Fancy, H. Zahed, E. Maltepe and D. H. Rowitch (2014). "Oligodendrocyte-encoded HIF function couples postnatal myelination and white matter angiogenesis." Cell **158**(2): 383-396.

Zalc, B. and R. D. Fields (2000). "Do Action Potentials Regulate Myelination?" Neuroscientist **6**(1): 5-13.

Zatorre, R. J., R. D. Fields and H. Johansen-Berg (2012). "Plasticity in gray and white: neuroimaging changes in brain structure during learning." Nat Neurosci **15**(4): 528-536.

Zeller, N. K., T. N. Behar, M. E. Dubois-Dalcq and R. A. Lazzarini (1985). "The timely expression of myelin basic protein gene in cultured rat brain oligodendrocytes is independent of continuous neuronal influences." J Neurosci **5**(11): 2955-2962.

Zhang, H. and R. H. Miller (1996). "Density-dependent feedback inhibition of oligodendrocyte precursor expansion." J Neurosci **16**(21): 6886-6895.

Zhang, J., R. E. Campbell, A. Y. Ting and R. Y. Tsien (2002). "Creating new fluorescent probes for cell biology." Nat Rev Mol Cell Biol **3**(12): 906-918.

Zhao, Y. Y., X. Y. Shi, X. Qiu, W. Lu, S. Yang, C. Li, L. Chen, L. Zhang, G. H. Cheng and Y. Tang (2012). "Enriched environment increases the myelinated nerve fibers of aged rat corpus callosum." Anat Rec (Hoboken) **295**(6): 999-1005.

Zhou, Q., G. Choi and D. J. Anderson (2001). "The bHLH transcription factor Olig2 promotes oligodendrocyte differentiation in collaboration with Nkx2.2." Neuron **31**(5): 791-807.

Zhu, X., D. E. Bergles and A. Nishiyama (2008). "NG2 cells generate both oligodendrocytes and gray matter astrocytes." Development **135**(1): 145-157.

Zhu, X., R. A. Hill and A. Nishiyama (2008). "NG2 cells generate oligodendrocytes and gray matter astrocytes in the spinal cord." Neuron Glia Biol **4**(1): 19-26.

Zonta, B., S. Tait, S. Melrose, H. Anderson, S. Harroch, J. Higginson, D. L. Sherman and P. J. Brophy (2008). "Glial and neuronal isoforms of Neurofascin have distinct roles in the assembly of nodes of Ranvier in the central nervous system." J Cell Biol **181**(7): 1169-1177.

8. Appendices

Development 138, 4443-4450 (2011) doi:10.1242/dev.071001

Individual axons regulate the myelinating potential of single oligodendrocytes in vivo

Rafael G. Almeida[1,2,*], Tim Czopka[1,2,3,*], Charles ffrench-Constant[2,3] and David A. Lyons[1,2,†]

SUMMARY

The majority of axons in the central nervous system (CNS) are eventually myelinated by oligodendrocytes, but whether the timing and extent of myelination in vivo reflect intrinsic properties of oligodendrocytes, or are regulated by axons, remains undetermined. Here, we use zebrafish to study CNS myelination at single-cell resolution in vivo. We show that the large caliber Mauthner axon is the first to be myelinated (shortly before axons of smaller caliber) and that the presence of supernumerary large caliber Mauthner axons can profoundly affect myelination by single oligodendrocytes. Oligodendrocytes that typically myelinate just one Mauthner axon in wild type can myelinate multiple supernumerary Mauthner axons. Furthermore, oligodendrocytes that exclusively myelinate numerous smaller caliber axons in wild type can readily myelinate small caliber axons in addition to the much larger caliber supernumerary Mauthner axons. These data indicate that single oligodendrocytes can myelinate diverse axons and that their myelinating potential is actively regulated by individual axons.

KEY WORDS: CNS Myelination, In vivo imaging, Oligodendrocyte, Zebrafish

INTRODUCTION

The vast majority of axons in the vertebrate central nervous system are eventually myelinated by oligodendrocytes (Hildebrand et al., 1993), which facilitates rapid saltatory conduction along their length (Bakiri et al., 2011; Waxman and Swadlow, 1977), ensures their long-term viability (Nave, 2010) and contributes to functional regulation of nervous system plasticity (Fields, 2010). Although we know much about the early development of oligodendrocytes (Li et al., 2009; Richardson et al., 2006) and that oligodendrocytes can differentiate and express myelin proteins in the absence of axons in vitro (Barres et al., 1994; Knapp et al., 1987; Nawaz et al., 2009; Temple and Raff, 1986), the key question of whether the timing and extent of myelination in vivo represents intrinsic properties of oligodendrocytes or is regulated by the axons remains unanswered. Although it has been known for nearly 100 years that oligodendrocyte morphology correlates with the caliber of axons that they myelinate, whereby oligodendrocytes usually associate with either a small number of large caliber axons or a larger number of smaller axons (Bunge, 1968; Butt and Berry, 2000; Del Rio-Hortega, 1921; Del Rio-Hortega, 1928; Remahl and Hildebrand, 1990), a causal role for axons in establishing these relationships, although predicted (Ueda et al., 1999), remains to be formally demonstrated.

Here, we use zebrafish, which have recently become established as a powerful model for the study of glial cells and myelinated axons (Brosamle and Halpern, 2002; Buckley et al., 2010; Kazakova et al., 2006; Kirby et al., 2006; Li et al., 2007; Lyons et al., 2009; Monk et al., 2009; Pogoda et al., 2006; Takada and Appel, 2010), to study the role that axons play in regulating CNS myelination in vivo. As is the case in mammals, we show that single oligodendrocytes in zebrafish myelinate either a small number of large caliber axons or a larger number of smaller axons. We identify the very first axon myelinated in the zebrafish CNS as the very large caliber Mauthner axon, and show that increasing the number of Mauthner axons in vivo dramatically regulates myelination by single oligodendrocytes. In the presence of supernumerary Mauthner axons we observe oligodendrocytes that usually myelinate just one Mauthner axon myelinating many Mauthner axons. In addition, we observed oligodendrocytes that usually myelinate only smaller caliber axons readily myelinating both large caliber Mauthner axons as well as axons of much smaller caliber, which happens very rarely in wild types. These results show that oligodendrocytes can myelinate axons of very different size and that individual axons can regulate the myelinating potential and, thus, the morphology of single oligodendrocytes in vivo.

MATERIALS AND METHODS

Zebrafish

We used the following standard zebrafish strains and lines: AB, Golden and Tg(sox10(7.2):mRFP) (Kirby et al., 2006). For this study, we also generated Tg(mbp:EGFP-CAAX) and Tg(mbp:EGFP). All animals were maintained in accordance with UK Home Office guidelines.

Plasmid construction

A 2 kb fragment of *mbp* regulatory sequence (Jung et al., 2010) was amplified from genomic DNA of the AB strain using the following primers that contain att recombination sites (underlined): attB4_mbpF, GGGGACAACTTTGTATAGAAAAGTTGCAGATGCTGAGATGTGACTACTGCAAATGA; attB1R_mbpR, GGGGACTGCTTTTTTGTACAAACTTGGTTGATCTGTTCAGTGGTCTACAGTCTGGA.

Purified PCR products were recombined with pDONRP4-P1R (Invitrogen) using BP clonase (Invitrogen) to generate the 5′ element clone p5E_mbp. Tol2 transgenesis constructs were generated by recombination of the abovementioned and other donor clones, all of which are components of the Tol2kit (Kwan et al., 2007), with pDEST_Tol2_CG2 using LR clonase II Plus (Invitrogen).

[1]Centre for Neuroregeneration, University of Edinburgh, 49 Little France Crescent, Edinburgh EH16 4SB, UK. [2]Centre for Multiple Sclerosis Research, University of Edinburgh, 47-49 Little France Crescent, Edinburgh EH16 4SB, UK. [3]MRC Centre for Regenerative Medicine, University of Edinburgh, 47-49 Little France Crescent, Edinburgh EH16 4SB, UK.

*These authors contributed equally to this work
†Author for correspondence (david.lyons@ed.ac.uk)

Accepted 29 July 2011

DNA injections and generation of transgenic zebrafish

Fertilised eggs were co-injected with 1 nl of a solution containing 10 ng/μl plasmid DNA and 25 ng/μl *tol2* transposase mRNA. Injected fish were analysed as mosaics or grown to adulthood to raise stable transgenic lines.

notch1a morpholino injection

We injected zebrafish embryos with 500 pg of a morpholino directed against a *notch1a*-specific splice junction (Ma and Jiang, 2007) to temporarily abrogate embryonic *notch1a* expression. We carried out RT-PCR to assay *notch1a* mRNA expression levels using the primers 5′-CTTCTGCACTTTCTGGAGATTTAAAGAAG-3′ (Ma and Jiang, 2007) and 5′-CACACGTCTGACCTGTGAAGC-3′.

hoxb1 mRNA injection

We injected zebrafish embryos with 50 pg of *hoxb1* mRNA. The majority of *hoxb1* mRNA-injected animals were morphologically normal and typically had two Mauthner axons on one side of the CNS and one on the contralateral side. A subset of *hoxb1* mRNA-injected animals had morphological abnormalities as have been previously described (Hale et al., 2004), and were therefore excluded from further study.

Immunohistochemistry

Whole-mount antibody labelling was carried out using standard protocols. Anti-3A10 (Developmental Studies Hybridoma Bank) was used at a concentration of 1:200.

Confocal imaging

Embryonic and larval zebrafish were embedded in 1.5% low melting point agarose (Sigma) in embryo medium with tricaine. Imaging was performed at a Zeiss LSM710 confocal microscope. Quantification of cell and myelin sheath number was carried out on confocal *z*-stacks using unbiased stereological methods.

Transmission electron microscopy

Preparation of tissue was as carried out as described previously (Lyons et al., 2008). Microwave stimulation during tissue processing was carried out using a Panasonic microwave with ‘Inverter’ technology. Images were taken with a Phillips CM120 Biotwin. Data analyses were carried out using Adobe Photoshop and ImageJ.

RESULTS

CNS myelination proceeds according to stereotyped gradients in vivo

To define CNS myelination in vivo at single cell resolution, we generated transgenic constructs and stable transgenic lines to drive gene expression in myelinating glial cells of the zebrafish (Fig. 1A; see Fig. S1 in the supplementary material). Time-course analyses of fluorescent reporter lines generated using previously identified regulatory sequences of the myelin basic protein (*mbp*) gene (Jung et al., 2010) showed that the very first axon to be myelinated in the CNS is that of the large Mauthner neuron (Fig. 1B). The Mauthner cell is an individually identifiable reticulospinal neuron; each fish has two Mauthner neurons, one on each side of the midline of rhombomere 4 (Kimmel et al., 1982) and each Mauthner neuron projects a very large caliber axon along a stereotyped path in the ventral spinal cord (Jontes et al., 2000; Kimmel et al., 1982). mbp:EGFP-CAAX (which drives a membrane-tethered variant of EGFP) was first detected along proximal (anterior) parts of the Mauthner axon from about 60 hours post-fertilisation (hpf) and proceeded progressively towards more distal (posterior) parts of the axon over time (Fig. 1B,C). Myelination of axons in more dorsal regions of the spinal cord occurred soon after the appearance of myelination of the ventral Mauthner axon (Fig. 1C). Myelination of these more dorsally located axons also occurred in an anterior to posterior gradient (data not shown). These observations show that myelination occurs according to stereotyped anterior-posterior and ventral-dorsal gradients at the level of axonal tracts and individual axons.

Individual myelinating oligodendrocytes have diverse morphologies in vivo

In order to visualise individual myelinating oligodendrocytes in vivo we injected wild-type embryos with plasmid DNA encoding mbp:EGFP or mbp:EGFP-CAAX and imaged them between 3 and 9 days post-fertilisation (dpf). We observed that the oligodendrocytes that associate with the very large Mauthner axon typically associate only with this axon (Fig. 2A). The vast majority of such cells (103/133) associated with just one Mauthner axon, whereas the remaining cells associated with the Mauthner axon on both sides of the embryonic midline (Fig. 2A). We also found that a very small proportion of wild-type oligodendrocytes (5%, 11/204) were capable of myelinating the Mauthner axon as well as axons of much smaller caliber (Fig. 2B). The position of oligodendrocytes that associate with the Mauthner axons was very stereotyped: the cell bodies always resided in the ventral spinal cord, almost always ventral to the Mauthner axon itself (Fig. 1B,C; Fig. 2A,B).

As expected, the vast majority of oligodendrocytes in the spinal cord extended multiple myelinating processes that associated with numerous axons of relatively small caliber compared with the Mauthner axons. These cells exhibited striking morphological diversity with respect to the number and length of their individual

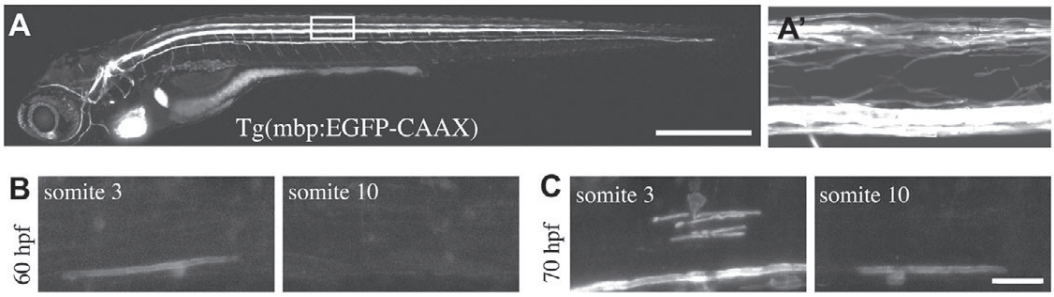

Fig. 1. Transgenic reporters reveal first axon myelinated in vivo in zebrafish CNS. (**A**) Lateral view of a stable Tg(mbp:EGFP-CAAX) zebrafish at 8 dpf. Myelinating glia of the CNS and PNS are labelled, as is the heart, which serves as a marker of transgenesis. (**A′**) Lateral view of the spinal cord (area indicated by box in A). Prominent myelinated tracts myelinated in the dorsal spinal cord and ventral spinal cord are apparent. (**B**) Lateral views of a stable Tg(mbp:EGFP-CAAX) zebrafish at 60 hpf show that the very first axon to be myelinated is the large Mauthner axon in the ventral spinal cord, which is first myelinated in the anterior spinal cord. (**C**) Lateral views of a stable Tg(mbp:EGFP-CAAX) zebrafish at 70 hpf. Myelination of the Mauthner axon has now commenced in the more posterior part of the spinal cord. At this stage, oligodendrocytes have started to myelinate axons in the dorsal spinal cord. Dorsal is up and anterior is to the left in all images. Scale bars: 500 μm in A; 20 μm in C.

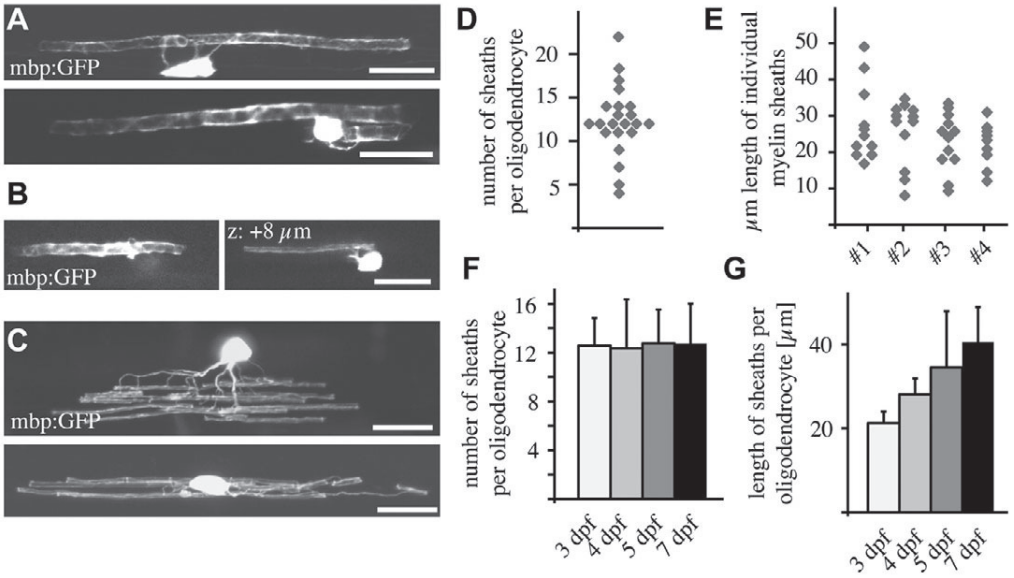

Fig. 2. Single-cell analysis reveals morphological diversity of individual CNS oligodendrocytes. (**A**) Lateral views of single mbp:EGFP-expressing oligodendrocytes associating with one Mauthner axon (top) and both Mauthner axons (bottom). (**B**) Lateral view of a single mbp:EGFP-expressing oligodendrocyte associating with the large Mauthner axon (left) and an axon of much smaller caliber (right). (**C**) Lateral views of single oligodendrocytes associating with multiple axons in the dorsal spinal cord (top) and ventral spinal cord (bottom). (**D**) Myelin sheath number per oligodendrocyte (excluding those that myelinate the Mauthner axons) at 4 dpf. (**E**) Myelin sheath length in four sample oligodendrocytes (that do not associate with the Mauthner axon) at 4 dpf. (**F**) Average myelin sheath number per cell over time. This does not include oligodendrocytes that myelinate the Mauthner axon. (**G**) Average myelin sheath length per cell over time. This does not include oligodendrocytes that myelinate the Mauthner axon. Error bars represent s.d. Scale bars: 10 μm.

myelin sheaths (Fig. 2C-E). At 4 dpf, we found that the majority of such cells (14 of 22) had 11-14 myelinating processes, although process number varied between 4 and 22 (Fig. 2D). Also, the length of individual nascent myelin sheaths per cell was highly variable and ranged from 6 μm to 49 μm (Fig. 2E). The number of myelin sheaths per oligodendrocyte was relatively stable from 3-7 dpf, but average myelin sheath length per cell increased almost twofold over the same time period (Fig. 2F-G).

Supernumerary Mauthner axons are robustly myelinated in vivo

In order to test how individual large caliber axons might regulate CNS myelination, we generated animals with supernumerary Mauthner neurons using two independent genetic manipulations. Previous studies have shown that disruption of *notch1a* causes a mild neurogenic phenotype in zebrafish, characterised in part by the appearance of multiple Mauthner neurons (Gray et al., 2001). Such extra Mauthner neurons are born between 9 and 12 hpf, as in wild type, and extend axons to the posterior spinal cord, as in wild type (Liu et al., 2003). It is important to point out that the birth of these neurons and their axonal growth occurs long before the appearance of oligodendrocytes. Because Notch1 has been associated with oligodendrocyte development and myelination (Genoud et al., 2002; Hu et al., 2003; Park and Appel, 2003; Park et al., 2005; Wang et al., 1998), we sought to only temporarily reduce Notch1a function, and found that injection of 500 pg of a previously published morpholino (Ma and Jiang, 2007) was sufficient to generate animals with supernumerary Mauthner neurons and axons (Fig. 3A,B). The level of *notch1a* mRNA in such morphants is reduced relative to control at 10 hpf (when Mauthner neurons are born) but is indistinguishable from controls by 3 dpf (when extensive myelination commences) (Fig. 3D). In order to have an independent method to generate extra Mauthner axons we injected embryos with *hoxb1* mRNAs (Fig. 3C), which has previously been shown to be capable of generating animals with ectopic Mauthner neurons by duplicating rhombomere 4 identity in the hindbrain (Hale et al., 2004).

Examination of *notch1a* morphants and embryos injected with *hoxb1* mRNA between 3 and 9 dpf using transgenic reporters (sox10:mRFP and mbp:EGFP-CAAX) and transmission electron microscopy showed that normal and supernumerary Mauthner axons were covered by glial membrane and robustly myelinated (Fig. 3; Fig. 4; data not shown). The Mauthner axon, like many axons in situ, is not circular in cross-sectional profile (Fig. 4). We therefore quantified the circumference(s) of Mauthner axon(s) in our analyses, because this variable (in combination with axon length) reflects the axonal surface available for potential interactions with oligodendrocytes. We saw that the summed circumference(s) of all Mauthner axon(s) per hemi-spinal cord increased almost linearly with the number of Mauthner axons present (Fig. 4D). In control animals that have one Mauthner axon on each side of the spinal cord, the average circumference per axon was 13.5±0.8 μm (mean±s.d., n=12) at 9 dpf. In animals with two Mauthner axons on one side of the spinal cord, the combined circumference was approximately doubled (26±3.5 μm, n=11, P<0.0001) and those with three on each side nearly tripled (35±5 μm, n=3, P<0.0001). In animals with even more Mauthner axons, their total circumference increased even further.

In order to test whether myelination of extra Mauthner axons occurred at the expense of other axons, we counted the total number of myelinated axons (excluding the Mauthner axons) in control and experimental ventral spinal cords (Fig. 4E). Control

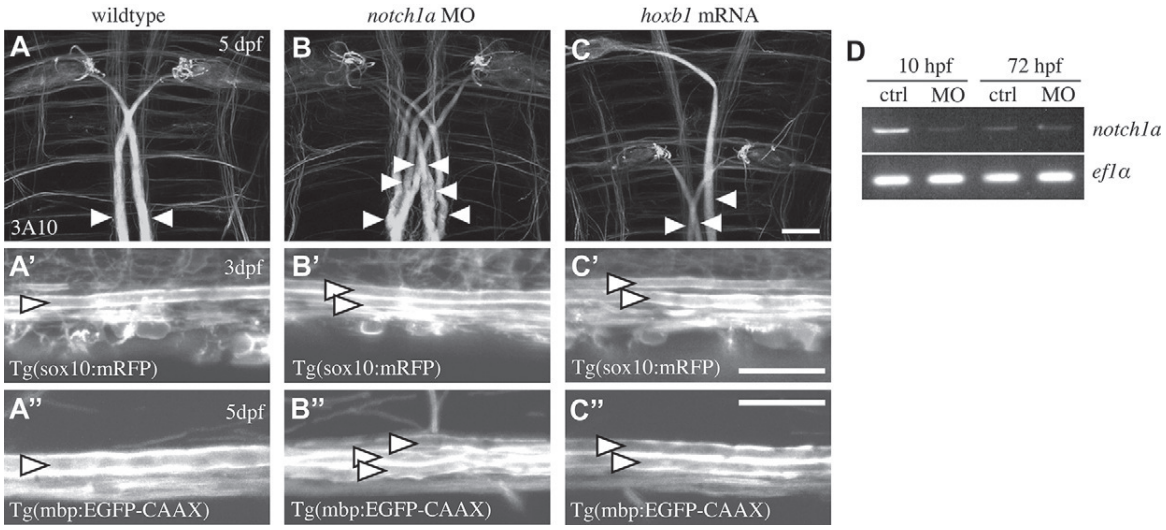

Fig. 3. Supernumerary Mauthner axons are ensheathed by myelinating glia. (**A-C**) Ventral views of the hindbrains of wild-type (A), *notch1a* morphant (B) and *hoxb1* mRNA-injected (C) larvae at 5 dpf labelled with the 3A10 antibody, which recognises neurofilament-associated proteins. Mauthner axons are indicated by arrowheads. Scale bar: 20 μm. (**A′-C″**) Analysis of Tg(sox10:mRFP) (A′-C′) and Tg(mbp:EGFP-CAAX) (A″-C″) shows that wild-type (A′,A″), *notch1a* morphant (B′,B″) and *hoxb1*-injected (C′,C″) Mauthner axons are all ensheathed and myelinated. Arrowheads indicate Mauthner axons. Scale bars: 20 μm. (**D**) RT-PCR analyses show that levels of *notch1a* mRNA are reduced in morpholino (MO)-injected animals relative to controls at 10 hpf but not at 72 hpf.

animals with one Mauthner axon on each side of the spinal cord had an average of 23 additional myelinated axons (±4, *n*=10). In animals with two Mauthner axons on each side of the spinal cord there were 22 additional axons myelinated (±4, *n*=10, *P*=0.58) as was also the case in animals with three Mauthner axons (*n*=3, *P*=0.71). These data show that the presence of even a threefold increase in Mauthner axon circumference does not affect the number of other axons myelinated in the ventral spinal cord. There was, however, a slight decrease in the number of myelinated axons when there were four or more Mauthner axons present in one side of the ventral spinal cord (15±3, *n*=4, *P*=0.0038).

Together, our results show that in two genetically independent manipulations oligodendrocytes can myelinate extra large caliber axons that are not present in their normal wild-type environment and can do so without affecting myelination of other axons. These observations beg the question as to how oligodendrocytes respond to the presence of extra axons and their consequent additional axonal surface area.

Supernumerary Mauthner axons do not regulate myelinating oligodendrocyte number

In order to test whether additional Mauthner axons regulate early stages of oligodendrocyte development, we examined the number and distribution of oligodendrocytes in *notch1* morphants and animals with *hoxb1* mRNA overexpression. We found no significant differences in oligodendrocyte number in the spinal cords of animals with supernumerary Mauthner axons relative to controls over a 425 μm stretch of the spinal cord centred at the mid-trunk level: control animals had an average of 66 mbp:EGFP-expressing oligodendrocytes (±6, *n*=6) at 5 dpf; *notch1a* morphants an average of 67 (±5, *n*=10, *P*=0.72); and *hoxb1* mRNA-injected animals an average of 63 (±8, *n*=9, *P*=0.45) (Fig. 5). Wild-type and supernumerary Mauthner axons are localised to the ventral spinal cord, as are the oligodendrocytes that typically myelinate them (Fig. 1), and given that the Mauthner axon is the first myelinated, we wanted to test the possibility that the distribution of oligodendrocytes within the spinal cord might be affected by the presence of supernumerary Mauthner axons in the ventral spinal cord. We saw, however, that the number of oligodendrocyte cell bodies located specifically in the dorsal spinal cord was almost identical in wild type as in animals with extra Mauthner axons (control: 25±3, *n*=6; *notch1a* morphants: 23±4, *n*=10, *P*=0.31; *hoxb1* mRNA-injected animals: 21±7, *n*=9, *P*=0.21) (Fig. 5D).

Supernumerary Mauthner axons regulate the morphology of single oligodendrocytes

In order to elucidate precisely how supernumerary Mauthner axons regulate single myelinating oligodendrocytes, we injected plasmid DNA encoding mbp:EGFP or mbp:EGFP-CAAX into *notch1a* morphants and into embryos injected with *hoxb1* mRNA. Whereas ~80% of the oligodendrocytes that myelinated the Mauthner axon in wild type associated with only one Mauthner axon, we found no such oligodendrocytes in *notch1a* morphants. Instead, we saw that all oligodendrocytes associated with at least two Mauthner axons (*n*=22) and that the majority of these associated with at least three Mauthner axons (15/22) (Fig. 6). In one case, we saw an oligodendrocyte that associated with seven Mauthner axons (Fig. 6C). In animals injected with *hoxb1* mRNA we also found that the vast majority of oligodendrocytes associated with more than one Mauthner axon (16/21) (Fig. 6). In wild-type animals, the average total length of myelin sheaths along Mauthner axon(s) made by single oligodendrocytes was 150±47 μm, in *notch1a* morphants was 256±57 μm (*P*<0.0001) and in *hoxb1* mRNA-injected animals was 187±85 μm (*P*=0.05) at 5 dpf. By 9 dpf, the average total lengths were 192±53 μm in wild type, 419±95 μm (*P*<0.0001) in *notch1a* morphants and 249±107 μm (*P*=0.09) in *hoxb1* mRNA-injected animals. Together with the fact that the total circumference of supernumerary Mauthner axons far exceeds the circumference

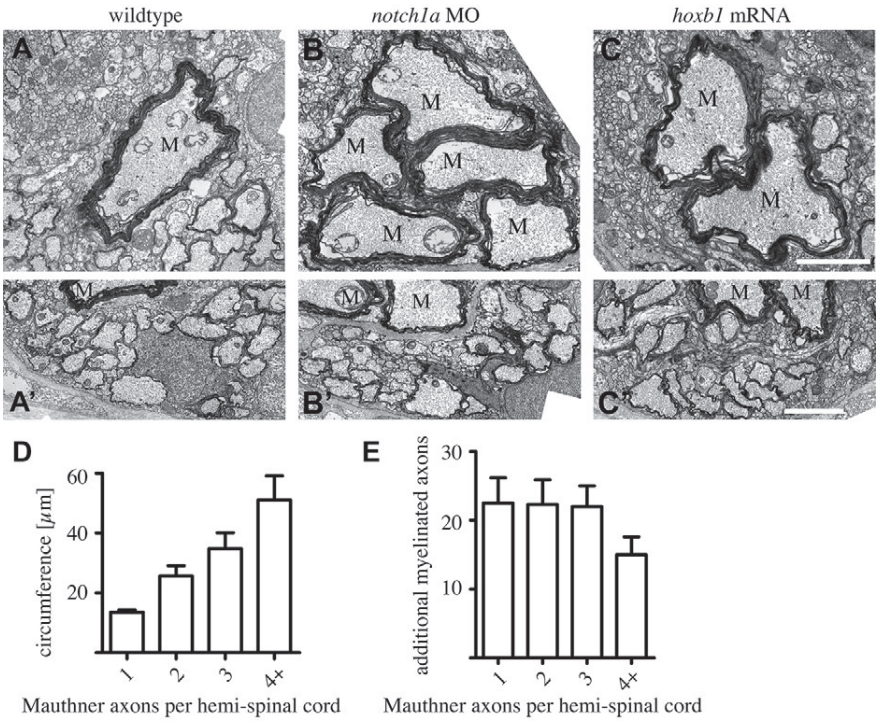

Fig. 4. Supernumerary Mauthner axons are robustly myelinated. (**A-C′**) Transmission electron microscope images of transverse sections through the spinal cord of wild-type (A,A′), *notch1a* morphant (B,B′) and *hoxb1* mRNA-injected (C,C′) zebrafish larvae at 9 dpf shows that all Mauthner axons are robustly myelinated (A-C) and that there is a similar number of axons myelinated in the ventral spinal cord despite the presence of supernumerary Mauthner (M) axons (A′-C′). Scale bars: 2 μm. (**D**) Total circumference of Mauthner axon(s) as a function of the number of Mauthner axons present per hemi-spinal cord. (**E**) Number of myelinated axons, excluding Mauthner axon(s), present in the ventral spinal cord as a function of the number of Mauthner axons present per hemi-spinal cord. Error bars represent s.d.

of individual wild-type Mauthner axons (Fig. 4D), it is clear that individual oligodendrocytes in animals with supernumerary Mauthner axons myelinate a far greater axonal surface area than do wild-type oligodendrocytes.

In addition to identifying oligodendrocytes that myelinated a greater number of Mauthner axons than normal, we observed that oligodendrocytes in the ventral spinal cord can myelinate supernumerary Mauthner axons as well as axons of relatively smaller caliber (data not shown). Remarkably, we also saw oligodendrocytes located in dorsal regions of the spinal cord, which typically only ever myelinate small caliber axons, extend processes to the ventral spinal cord to associate with supernumerary Mauthner axons, and in many cases also myelinate much smaller caliber axons (Fig. 7). This was never observed in wild-type animals but occurred readily in both *notch1* morphants and embryos injected with *hoxb1* mRNA, and at both 5 dpf and 9 dpf, which shows this was a stable association. This dramatic observation shows that individual oligodendrocytes can readily myelinate axons of very different size and that axons profoundly affect the myelination capacity of single oligodendrocytes.

DISCUSSION

Here, we use zebrafish to characterise and manipulate CNS myelination in vivo. Zebrafish are ideally suited to cellular analyses at high resolution owing to their small size, optical transparency, rapid early development, accessibility and relative simplicity compared with mammals, in which the vast majority of studies of myelinated axons have been carried out. By analysing the morphology of single zebrafish oligodendrocytes in vivo using fluorescent transgenes we recapitulate key observations made in mammals nearly 100 years ago by Pio Del Rio-Hortega (Del Rio-Hortega, 1921; Del Rio-Hortega, 1928), which showed that oligodendrocytes typically myelinate either a

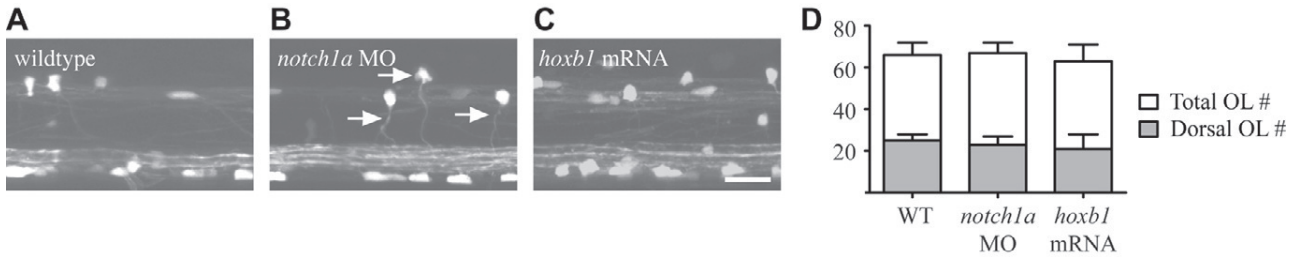

Fig. 5. Presence of supernumerary Mauthner axons does not affect oligodendrocyte number or distribution. (**A-C**) Lateral views of the spinal cords in Tg(mbp:EGFP)-expressing wild-type (A), *notch1a* morphant (B) and *hoxb1* mRNA-injected (C) animals shows that oligodendrocyte number and distribution are not affected by the presence of supernumerary Mauthner axons. Arrows point to oligodendrocytes in the dorsal spinal cord with projections to the ventral spinal cord. Compare with Fig. 7B. Scale bar: 20 μm. (**D**). Total oligodendrocyte number per 425 μm length of tissue in the mid-trunk spinal cord of wild-type, *notch1a* morphant and *hoxb1* mRNA-injected animals and, in grey, the number of oligodendrocytes specifically located in the dorsal domain of the spinal cord. Error bars represent s.d.

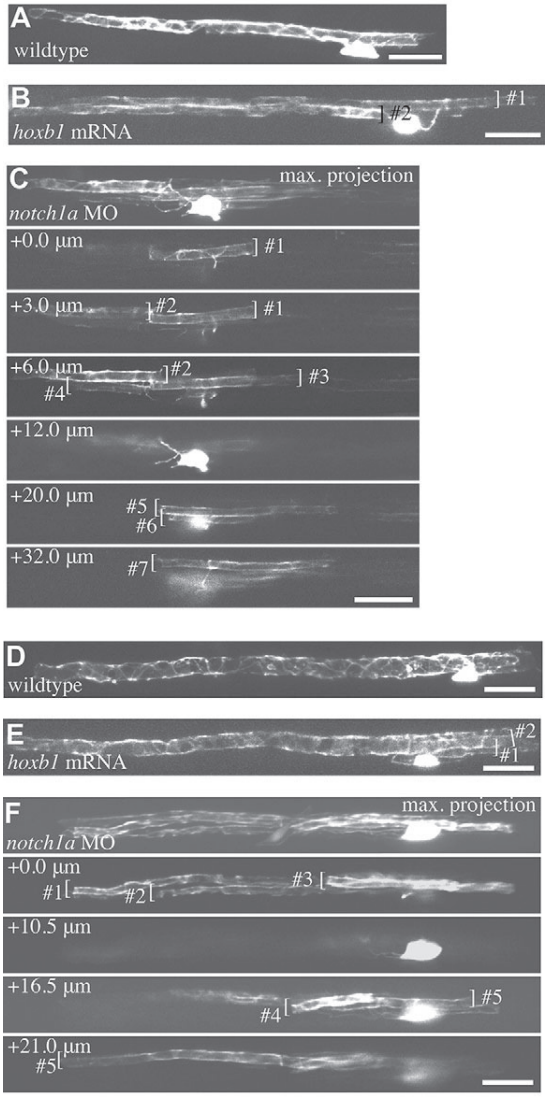

Fig. 6. Individual oligodendrocytes myelinate multiple supernumerary Mauthner axons. (**A-F**) All images are of live single mbp:EGFP-expressing oligodendrocytes in the spinal cord of larvae at 5 dpf (A-C) and 9 dpf (D-F). (A,D) Wild-type oligodendrocytes associated with single Mauthner axons. (B,E) Oligodendrocytes in *hoxb1* mRNA-injected animals with myelin sheaths on two Mauthner axons. (C,F) Oligodendrocytes in *notch1a* morphants that make seven (C) and five (F) myelin sheaths on supernumerary Mauthner axons. Maximum intensity projections and individual confocal *z*-sections are indicated for clarity. Individual myelin sheaths indicated by brackets. Scale bars: 20 µm.

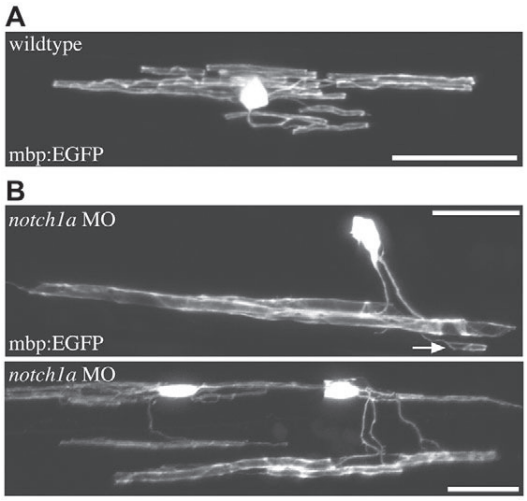

Fig. 7. Individual oligodendrocytes readily myelinate supernumerary Mauthner axons and smaller caliber axons. (**A**) In wild type, oligodendrocytes in the dorsal spinal cord myelinate only small caliber axons. (**B**) Oligodendrocytes in the dorsal spinal cords of animals with supernumerary Mauthner axons can myelinate the large Mauthner axons in the ventral spinal cord in addition to smaller caliber axons (e.g. arrow). Scale bars: 20 µm.

small number of large caliber axons or a larger number of smaller caliber axons in situ. By virtue of being able to visualise myelination from its very onset at single cell resolution in vivo, we identify the large caliber Mauthner axon as the first to be myelinated in the zebrafish CNS, and show that this individual axon is myelinated along a proximal to distal gradient. We make use of two independent genetic manipulations to generate animals that have extra large caliber Mauthner axons and show that these axons can dramatically affect oligodendrocyte behaviour. Our manipulation of large caliber axon number shows that individual oligodendrocytes can readily myelinate axons of vastly different caliber in vivo and that myelination cues are, therefore, independent of axon subtype, a result that was predicted by previous transplantation studies in which oligodendrocytes derived from the optic nerve (which contains primarily small caliber axons) were capable of myelinating axons in the spinal cord (which contains axons of different sizes) (Fanarraga et al., 1998).

Our data that the presence of supernumerary large caliber Mauthner axons does not affect oligodendrocyte number are, at first glance, at odds with a previous study which showed that an increase in optic nerve axon number caused a concomitant increase in oligodendrocyte number (Burne et al., 1996). Indeed, although recent evidence has suggested that cell-cell interactions between neighbouring oligodendrocytes might contribute to regulation of their distribution and number (Kirby et al., 2006), there is extensive evidence from previous studies that axons can regulate oligodendrocyte number by affecting their proliferation and survival (Barres and Raff, 1999). However, it is important to point out that in the study of Burne et al. total axonal number was increased nearly twofold, whereas our manipulation simply increases the number of very large caliber axons during the onset of myelination and has a negligible effect on overall axon number. We do not, therefore, rule out a general role for axons in regulating oligodendrocyte number, but show instead that individual axons can dramatically regulate the myelination potential of single oligodendrocytes.

Although our data indicate that individual axons regulate CNS myelination in vivo, we do not know the identity of the causative axonal signal(s). Previous molecular characterisation has suggested that removal of inhibitory axonal cues is a pre-requisite for CNS myelination. Axons initially express high levels of polysialylated neural cell adhesion molecule (PSA-NCAM) on their surfaces, and myelination commences only when PSA-NCAM levels are reduced (Charles et al., 2000; Fewou et al., 2007; Jakovcevski et

al., 2007; Keirstead et al., 1999). Analyses of the transmembrane protein Lingo1 (Lee et al., 2007; Mi et al., 2005) also suggest that it too might function on axons to inhibit myelination. In the peripheral nervous system (PNS) there is strong evidence that axonal Neuregulin 1 type III serves as an instructive cue for myelination (Michailov et al., 2004; Taveggia et al., 2005). Although Neuregulin 1 type III is not required for CNS myelination in vivo, it can stimulate hypermyelination of CNS axons in vivo (Brinkmann et al., 2008), which indicates that oligodendrocytes can respond to instructive axonal cues. It will be interesting to see whether future studies will identify instructive axonal signals required for CNS myelination.

Our data that single oligodendrocytes faced with supernumerary large caliber Mauthner axons can myelinate a larger axonal surface area than they normally do during development prompts the question of whether there is a maximum amount of axonal surface that any single oligodendrocyte can myelinate. If single oligodendrocytes myelinate close to their maximum capacity, e.g. by adulthood, then unless every oligodendrocyte is replaced following demyelination after injury or disease, incomplete repair might be inevitable. Our demonstration that axon size can regulate oligodendrocyte morphology is also relevant to the remyelination of axons. Given the significant cross-sectional growth of myelinated axons that takes place after the onset of myelination, it is likely that the caliber of any axon demyelinated long after development will be significantly larger than when it was first myelinated. This discrepancy in target caliber might mean that the morphology of remyelinating oligodendrocytes will be different than during development. It is possible that during remyelination more individual oligodendrocytes make fewer myelin sheaths on such larger caliber axons (Blakemore, 1974). If this is indeed the case, remyelination might necessitate the employment of a greater number of oligodendrocytes than are required to myelinate the same complement of axons during development. It is, however, also possible that oligodendrocytes faced with such relatively large caliber axons during remyelination do not regulate their morphology dramatically, but rather extend less myelin around individual axons. This possibility could explain the fact that remyelinated axon profiles are often surrounded by thin myelin (Blakemore, 1974). Future studies of demyelination and remyelination may benefit from high-resolution analyses that can assess precisely how much axonal surface is myelinated or how much myelin is made by individual oligodendrocytes.

In summary, our study shows that individual axons can profoundly regulate the myelinating potential of single oligodendrocytes, which has implications for the formation and regulation of myelinated axons throughout life and for mechanisms that may need to be considered during their repair.

Acknowledgements
We thank Carl Tucker, John Mullins, Patricia Smart and Sebastien Rider for fishroom support; Bruce Appel, Koichi Kawakami, Jiang Yun Jin, Hae-Chul Park and Victoria Prince for sharing reagents; Crerar hotels for free confocal access; and Stephen Mitchell for TEM assistance. Very special thanks to Chi-Bin Chien and the Chien laboratory for the Tol2kit. We are grateful to Thomas Becker, Peter Brophy, Ben Emery, Kelly Monk, Alya Raphael, William Talbot, Anna Williams and members of the Lyons, ffrench-Constant and Brophy laboratories for critical reading of the manuscript.

Funding
This work was supported by a David Phillips Fellowship from the BBSRC, an Innovative grant from the UK MS Society and an International Reintegration Grant to D.A.L., an FCT doctoral studentship to R.G.A. and a Wellcome Trust Programme Grant and UK MS Society Centre award to C.ff.-C. Deposited in PMC for release after 6 months.

Competing interests statement
The authors declare no competing financial interests.

Supplementary material
Supplementary material for this article is available at
http://dev.biologists.org/lookup/suppl/doi:10.1242/dev.071001/-/DC1

References

Bakiri, Y., Karadottir, R., Cossell, L. and Attwell, D. (2011). Morphological and electrical properties of oligodendrocytes in the white matter of the corpus callosum and cerebellum. *J. Physiol.* **589**, 559-573.
Barres, B. A. and Raff, M. C. (1999). Axonal control of oligodendrocyte development. *J. Cell Biol.* **147**, 1123-1128.
Barres, B. A., Lazar, M. A. and Raff, M. C. (1994). A novel role for thyroid hormone, glucocorticoids and retinoic acid in timing oligodendrocyte development. *Development* **120**, 1097-1108.
Blakemore, W. F. (1974). Pattern of remyelination in the CNS. *Nature* **249**, 577-578.
Brinkmann, B. G., Agarwal, A., Sereda, M. W., Garratt, A. N., Muller, T., Wende, H., Stassart, R. M., Nawaz, S., Humml, C., Velanac, V. et al. (2008). Neuregulin-1/ErbB signaling serves distinct functions in myelination of the peripheral and central nervous system. *Neuron* **59**, 581-595.
Brosamle, C. and Halpern, M. E. (2002). Characterization of myelination in the developing zebrafish. *Glia* **39**, 47-57.
Buckley, C. E., Marguerie, A., Roach, A. G., Goldsmith, P., Fleming, A., Alderton, W. K. and Franklin, R. J. (2010). Drug reprofiling using zebrafish identifies novel compounds with potential pro-myelination effects. *Neuropharmacology* **59**, 149-159.
Bunge, R. P. (1968). Glial cells and the central myelin sheath. *Physiol. Rev.* **48**, 197-251.
Burne, J. F., Staple, J. K. and Raff, M. C. (1996). Glial cells are increased proportionally in transgenic optic nerves with increased numbers of axons. *J. Neurosci.* **16**, 2064-2073.
Butt, A. M. and Berry, M. (2000). Oligodendrocytes and the control of myelination in vivo: new insights from the rat anterior medullary velum. *J. Neurosci. Res.* **59**, 477-488.
Charles, P., Hernandez, M. P., Stankoff, B., Aigrot, M. S., Colin, C., Rougon, G., Zalc, B. and Lubetzki, C. (2000). Negative regulation of central nervous system myelination by polysialylated-neural cell adhesion molecule. *Proc. Natl. Acad. Sci. USA* **97**, 7585-7590.
Del Rio-Hortega, P. (1921). Estudios sobre la neuroglia. La glia de escasas radiaciones oligodendroglia. *Bol. Real Soc. Esp. Hist. Nat.* **21**, 63-92.
Del Rio-Hortega, P. (1928). Tercera aportacion al conocimiento morfologico e interpretacion funcional de la oligodendroglia. *Mem. Real Soc. Esp. Hist. Nat.* **14**, 40-122.
Fanarraga, M. L., Griffiths, I. R., Zhao, M. and Duncan, I. D. (1998). Oligodendrocytes are not inherently programmed to myelinate a specific size of axon. *J. Comp. Neurol.* **399**, 94-100.
Fewou, S. N., Ramakrishnan, H., Bussow, H., Gieselmann, V. and Eckhardt, M. (2007). Down-regulation of polysialic acid is required for efficient myelin formation. *J. Biol. Chem.* **282**, 16700-16711.
Fields, R. D. (2010). Neuroscience. Change in the brain's white matter. *Science* **330**, 768-769.
Genoud, S., Lappe-Siefke, C., Goebbels, S., Radtke, F., Aguet, M., Scherer, S. S., Suter, U., Nave, K. A. and Mantei, N. (2002). Notch1 control of oligodendrocyte differentiation in the spinal cord. *J. Cell Biol.* **158**, 709-718.
Gray, M., Moens, C. B., Amacher, S. L., Eisen, J. S. and Beattie, C. E. (2001). Zebrafish deadly seven functions in neurogenesis. *Dev. Biol.* **237**, 306-323.
Hale, M. E., Kheirbek, M. A., Schriefer, J. E. and Prince, V. E. (2004). Hox gene misexpression and cell-specific lesions reveal functionality of homeotically transformed neurons. *J. Neurosci.* **24**, 3070-3076.
Hildebrand, C., Remahl, S., Persson, H. and Bjartmar, C. (1993). Myelinated nerve fibres in the CNS. *Prog. Neurobiol.* **40**, 319-384.
Hu, Q. D., Ang, B. T., Karsak, M., Hu, W. P., Cui, X. Y., Duka, T., Takeda, Y., Chia, W., Sankar, N., Ng, Y. K. et al. (2003). F3/contactin acts as a functional ligand for Notch during oligodendrocyte maturation. *Cell* **115**, 163-175.
Jakovcevski, I., Mo, Z. and Zecevic, N. (2007). Down-regulation of the axonal polysialic acid-neural cell adhesion molecule expression coincides with the onset of myelination in the human fetal forebrain. *Neuroscience* **149**, 328-337.
Jontes, J. D., Buchanan, J. and Smith, S. J. (2000). Growth cone and dendrite dynamics in zebrafish embryos: early events in synaptogenesis imaged in vivo. *Nat. Neurosci.* **3**, 231-237.
Jung, S. H., Kim, S., Chung, A. Y., Kim, H. T., So, J. H., Ryu, J., Park, H. C. and Kim, C. H. (2010). Visualization of myelination in GFP-transgenic zebrafish. *Dev. Dyn.* **239**, 592-597.
Kazakova, N., Li, H., Mora, A., Jessen, K. R., Mirsky, R., Richardson, W. D. and Smith, H. K. (2006). A screen for mutations in zebrafish that affect myelin gene expression in Schwann cells and oligodendrocytes. *Dev. Biol.* **297**, 1-13.

Keirstead, H. S., Ben-Hur, T., Rogister, B., O'Leary, M. T., Dubois-Dalcq, M. and Blakemore, W. F. (1999). Polysialylated neural cell adhesion molecule-positive CNS precursors generate both oligodendrocytes and Schwann cells to remyelinate the CNS after transplantation. *J. Neurosci.* **19**, 7529-7536.
Kimmel, C. B., Powell, S. L. and Metcalfe, W. K. (1982). Brain neurons which project to the spinal cord in young larvae of the zebrafish. *J. Comp. Neurol.* **205**, 112-127.
Kirby, B. B., Takada, N., Latimer, A. J., Shin, J., Carney, T. J., Kelsh, R. N. and Appel, B. (2006). In vivo time-lapse imaging shows dynamic oligodendrocyte progenitor behavior during zebrafish development. *Nat. Neurosci.* **9**, 1506-1511.
Knapp, P. E., Bartlett, W. P. and Skoff, R. P. (1987). Cultured oligodendrocytes mimic in vivo phenotypic characteristics: cell shape, expression of myelin-specific antigens, and membrane production. *Dev. Biol.* **120**, 356-365.
Kwan, K. M., Fujimoto, E., Grabher, C., Mangum, B. D., Hardy, M. E., Campbell, D. S., Parant, J. M., Yost, H. J., Kanki, J. P. and Chien, C. B. (2007). The Tol2kit: a multisite gateway-based construction kit for Tol2 transposon transgenesis constructs. *Dev. Dyn.* **236**, 3088-3099.
Lee, X., Yang, Z., Shao, Z., Rosenberg, S. S., Levesque, M., Pepinsky, R. B., Qiu, M., Miller, R. H., Chan, J. R. and Mi, S. (2007). NGF regulates the expression of axonal LINGO-1 to inhibit oligodendrocyte differentiation and myelination. *J. Neurosci.* **27**, 220-225.
Li, H., Lu, Y., Smith, H. K. and Richardson, W. D. (2007). Olig1 and Sox10 interact synergistically to drive myelin basic protein transcription in oligodendrocytes. *J. Neurosci.* **27**, 14375-14382.
Li, H., He, Y., Richardson, W. D. and Casaccia, P. (2009). Two-tier transcriptional control of oligodendrocyte differentiation. *Curr. Opin. Neurobiol.* **19**, 479-485.
Liu, K. S., Gray, M., Otto, S. J., Fetcho, J. R. and Beattie, C. E. (2003). Mutations in deadly seven/notch1a reveal developmental plasticity in the escape response circuit. *J. Neurosci.* **23**, 8159-8166.
Lyons, D. A., Naylor, S. G., Mercurio, S., Dominguez, C. and Talbot, W. S. (2008). KBP is essential for axonal structure, outgrowth and maintenance in zebrafish, providing insight into the cellular basis of Goldberg-Shprintzen syndrome. *Development* **135**, 599-608.
Lyons, D. A., Naylor, S. G., Scholze, A. and Talbot, W. S. (2009). Kif1b is essential for mRNA localization in oligodendrocytes and development of myelinated axons. *Nat. Genet.* **41**, 854-858.
Ma, M. and Jiang, Y. J. (2007). Jagged2a-notch signaling mediates cell fate choice in the zebrafish pronephric duct. *PLoS Genet.* **3**, e18.
Mi, S., Miller, R. H., Lee, X., Scott, M. L., Shulag-Morskaya, S., Shao, Z., Chang, J., Thill, G., Levesque, M., Zhang, M. et al. (2005). LINGO-1 negatively regulates myelination by oligodendrocytes. *Nat. Neurosci.* **8**, 745-751.
Michailov, G. V., Sereda, M. W., Brinkmann, B. G., Fischer, T. M., Haug, B., Birchmeier, C., Role, L., Lai, C., Schwab, M. H. and Nave, K. A. (2004). Axonal neuregulin-1 regulates myelin sheath thickness. *Science* **304**, 700-703.
Monk, K. R., Naylor, S. G., Glenn, T. D., Mercurio, S., Perlin, J. R., Dominguez, C., Moens, C. B. and Talbot, W. S. (2009). A G protein-coupled receptor is essential for Schwann cells to initiate myelination. *Science* **325**, 1402-1405.
Nave, K. A. (2010). Myelination and support of axonal integrity by glia. *Nature* **468**, 244-252.
Nawaz, S., Kippert, A., Saab, A. S., Werner, H. B., Lang, T., Nave, K. A. and Simons, M. (2009). Phosphatidylinositol 4,5-bisphosphate-dependent interaction of myelin basic protein with the plasma membrane in oligodendroglial cells and its rapid perturbation by elevated calcium. *J. Neurosci.* **29**, 4794-4807.
Park, H. C. and Appel, B. (2003). Delta-Notch signaling regulates oligodendrocyte specification. *Development* **130**, 3747-3755.
Park, H. C., Boyce, J., Shin, J. and Appel, B. (2005). Oligodendrocyte specification in zebrafish requires notch-regulated cyclin-dependent kinase inhibitor function. *J. Neurosci.* **25**, 6836-6844.
Pogoda, H. M., Sternheim, N., Lyons, D. A., Diamond, B., Hawkins, T. A., Woods, I. G., Bhatt, D. H., Franzini-Armstrong, C., Dominguez, C., Arana, N. et al. (2006). A genetic screen identifies genes essential for development of myelinated axons in zebrafish. *Dev. Biol.* **298**, 118-131.
Remahl, S. and Hildebrand, C. (1990). Relation between axons and oligodendroglial cells during initial myelination I. The glial unit. *J. Neurocytol.* **19**, 313-328.
Richardson, W. D., Kessaris, N. and Pringle, N. (2006). Oligodendrocyte wars. *Nat. Rev. Neurosci.* **7**, 11-18.
Takada, N. and Appel, B. (2010). Identification of genes expressed by zebrafish oligodendrocytes using a differential microarray screen. *Dev. Dyn.* **239**, 2041-2047.
Taveggia, C., Zanazzi, G., Petrylak, A., Yano, H., Rosenbluth, J., Einheber, S., Xu, X., Esper, R. M., Loeb, J. A., Shrager, P. et al. (2005). Neuregulin-1 type III determines the ensheathment fate of axons. *Neuron* **47**, 681-694.
Temple, S. and Raff, M. C. (1986). Clonal analysis of oligodendrocyte development in culture: evidence for a developmental clock that counts cell divisions. *Cell* **44**, 773-779.
Ueda, H., Levine, J. M., Miller, R. H. and Trapp, B. D. (1999). Rat optic nerve oligodendrocytes develop in the absence of viable retinal ganglion cell axons. *J. Cell Biol.* **146**, 1365-1374.
Wang, S., Sdrulla, A. D., diSibio, G., Bush, G., Nofziger, D., Hicks, C., Weinmaster, G. and Barres, B. A. (1998). Notch receptor activation inhibits oligodendrocyte differentiation. *Neuron* **21**, 63-75.
Waxman, S. G. and Swadlow, H. A. (1977). The conduction properties of axons in central white matter. *Prog. Neurobiol.* **8**, 297-324.

Neuroscience 276 (2014) 98–108

REVIEW

ON THE RESEMBLANCE OF SYNAPSE FORMATION AND CNS MYELINATION

R. G. ALMEIDA AND D. A. LYONS *

Centre for Neuroregeneration, University of Edinburgh, Edinburgh EH16 4SB, UK

MS Society Centre for Translational Research, University of Edinburgh, Edinburgh EH16 4SB, UK

Euan MacDonald Centre for Motor Neurone Disease Research, University of Edinburgh, Edinburgh EH16 4SB, UK

Abstract—The myelination of axons in the central nervous system (CNS) is essential for nervous system formation, function and health. CNS myelination continues well into adulthood, but not all axons become myelinated. Unlike the peripheral nervous system, where we know of numerous axon–glial signals required for myelination, we have a poor understanding of the nature or identity of such molecules that regulate which axons are myelinated in the CNS. Recent studies have started to elucidate cell behavior during myelination *in vivo* and indicate that the choice of which axons are myelinated is made prior to myelin sheath generation. Here we propose that interactions between axons and the exploratory processes of oligodendrocyte precursor cells (OPCs) lead to myelination and may be similar to those between dendrites and axons that prefigure and lead to synapse formation. Indeed axons and OPCs form synapses with striking resemblance to those of neurons, suggesting a similar mode of formation. We discuss families of molecules with specific functions at different stages of synapse formation and address studies that implicate the same factors during axon–OPC synapse formation and myelination. We also address the possibility that the function of such synapses might directly regulate the myelinating behavior of oligodendrocyte processes *in vivo*. In the future it may be of benefit to consider these similarities when taking a candidate-based approach to dissect mechanisms of CNS myelination.

***This article is part of a Special Issue entitled: The CNS White Matter*.**

Key words: oligodendrocyte, oligodendrocyte precursor cell, axon, dendrite, synapse.

*Correspondence to: D. A. Lyons, Centre for Neuroregeneration, University of Edinburgh, Edinburgh EH16 4SB, UK. Tel: +44-1312427986.

E-mail addresses: rafael.g.almeida@ed.ac.uk (R. G. Almeida), david.lyons@ed.ac.uk (D. A. Lyons).

Abbreviations: cdh, cadherin; DRG, dorsal root ganglia; EGF, epidermal growth factor; mRNA, messenger RNA; Necl, Nectin-like molecule; NMDAR, *N*-methyl-D-aspartate receptor; OL, oligodendrocyte; OPC, oligodendrocyte precursor cell; PNS, peripheral nervous system; ten, teneurins.

Contents

INTRODUCTION

Myelination of axons in the central nervous system (CNS, brain and spinal cord) by oligodendrocytes (OLs) facilitates rapid impulse conduction and provides metabolic and trophic support to the axons (Sherman and Brophy, 2005; Nave, 2010a,b; Fünfschilling et al., 2012; Lee et al., 2012b). It is an ongoing process that starts around birth and continues at least into the fourth decade in humans (Miller et al., 2012, see Wang and Young, this issue). Myelination of specific axons and axonal tracts is highly regulated throughout life. During early development certain axonal tracts are myelinated ahead of others and this is true in all species studied (Remahl and Hildebrand, 1982; Schreyer and Jones, 1982; Schwab and Schnell, 1989; Baumann and Pham-Dinh, 2001; Almeida et al., 2011). Furthermore, myelination of specific brain areas can be regulated by social experience (Liu et al., 2012; Makinodan et al., 2012) and activity-dependent myelination of specific axons or specific axonal tracts may represent an important form of nervous system plasticity (Zatorre et al., 2012). Remarkably, our knowledge of the key molecules that control the initiation of myelination and may be responsible for temporal and spatial regulation of myelination in the CNS remains incomplete.

Myelin in the peripheral nervous system (PNS) has a similar structure and fulfills similar functions as CNS

0306-4522/13 $36.00
http://dx.doi.org/10.1016/j.neuroscience.2013.08.062

myelin, yet surprisingly there are fundamental differences in its formation, best underscored by the fact that crucial molecular regulators of axon–Schwann cell interactions are by and large not required for axon–OL interactions e.g. (Brinkmann et al., 2008; Monk et al., 2009). Furthermore, the cell–cell interactions that lead to myelination of peripheral nerves by Schwann cells are quite distinct from those in the CNS. Schwann cells require axons for almost all stages of their early development, including myelination *in vitro* and *in vivo* (Jessen and Mirsky, 2005). In contrast, OLs can develop and differentiate in cell culture in the absence of axons (Knapp et al., 1987) and can myelinate inert structures including paraformaldehyde-fixed axons (Rosenberg et al., 2008) and polystyrene nanofibers (Lee et al., 2012a). Schwann cells myelinate only one segment of one axon along a nerve that they are in close proximity to throughout their entire development, whereas OLs typically make many myelin sheaths on many different axons in territories that their myelinating processes first explore following the end of the cell's migration. The molecular and cellular mechanisms of PNS myelination have been reviewed extensively elsewhere (Jessen and Mirsky, 2005; Pereira et al., 2012) and we will focus here on the less understood regulation of CNS myelination.

Whether to ensure normal development or to fine-tune specific nervous system function, it is clear that the myelination of CNS axons *in vivo* requires intimate communication between the axons themselves and the OLs that myelinate them (Emery, 2010a; Simons and Lyons, 2013). To date, we have learned much about the early development of axons (Chao et al., 2009; Tojima et al., 2011; Jung et al., 2012) and of the early stages of OL development (Richardson et al., 2006, 2011; Li et al., 2009; Emery, 2010b). However, we know much less about the interactions between axons and oligodendrocyte precursor cells (OPCs) and later interactions between axons and OLs that regulate CNS myelination *in vivo*. A number of ligands and receptors have been implicated in OPC to OL differentiation and myelination, including Jagged, Contactin1 and Notch (Wang et al., 1998; Genoud et al., 2002; Hu et al., 2003), Neuregulin1–ErbB (Brinkmann et al., 2008; Taveggia et al., 2008; Makinodan et al., 2012), Wnt (Fancy et al., 2009), Lingo (Mi et al., 2004, 2005; Lee et al., 2007), Gpr17 (Chen et al., 2009, reviewed in He and Lu, 2013). Axon–OL signals regulating the thickness of CNS myelin sheaths have also been identified, including Neuregulin1–ErbB (Brinkmann et al., 2008; Makinodan et al., 2012) and Fibroblast Growth Factor Receptor (FGFR) signaling (Furusho et al., 2012). However, we know of essentially no signals between axons and OPCs or OLs that are absolutely required for CNS myelination *in vivo*. Here we will review recent data that are starting to elucidate interactions between axons and cells of the oligodendrocyte lineage during myelination *in vivo* and speculate on the similarities between such interactions and axon–dendrite interactions during synapse formation. We also speculate on how the principles of the molecular regulation of synapse formation might be repurposed to coordinate the initiation events of CNS myelination *in vivo*.

BEFORE MYELINATION: OPC–OPC INTERACTIONS CAN REGULATE OL NUMBER AND DENSITY

OPCs are specified in discrete progenitor cell domains throughout the CNS (Richardson et al., 2006) from where they undergo extensive cell migration and proliferation toward specific axonal tracts. Upon reaching axonal tracts, the number and distribution of OPCs are regulated ahead of myelination and this is thought to involve axon–OPC interactions (Barres and Raff, 1999), and also, as recent studies indicate, OPC–OPC interactions (Kirby et al., 2006; Hughes et al., 2013). Elegant time-lapse imaging of OPC behavior in the zebrafish spinal cord shows that post-migratory OPCs extend exploratory processes over a wide territory. When the processes of neighboring OPCs come into contact, they withdraw, suggesting repulsive cell–cell interactions. When individual or small numbers of OPCs are ablated, neighboring OPCs either proliferate and/or migrate to colonize the vacated territory. Subsequently, they again extend exploratory processes that collapse upon meeting those of neighboring cells (Kirby et al., 2006). A more recent study documented similar behavior of OPCs in the adult mouse brain (Hughes et al., 2013), suggesting that this tiling mechanism is retained throughout life. The molecular basis of this mechanism, which regulates OPC number and distribution, is not known. Lessons may be learned from considering similar events in neurons. In the visual system of *Drosophila*, separate studies showed that homophilic interactions between immunoglobulin superfamily members (Dscam2 and Turtle) mediate tiling between neighboring neurons of the same class (Millard et al., 2007; Ferguson et al., 2009). It would be interesting to investigate whether such molecules or principles of repulsive homophilic interactions regulate the tiling behavior of an altogether different cell type, the OPC.

AT THE ONSET OF MYELINATION: RAPID TRANSITION OF OPC TO OL

Following establishment of their number and distribution in the vicinity of axons, many OPCs differentiate into myelinating OLs. Several transcription factors responsible for driving OPC to OL differentiation have been identified (Emery, 2010b), but our understanding of how OPCs or OLs select which axons in their territory to myelinate and which to avoid is incomplete. Many areas of the CNS and many axonal tracts contain functionally distinct axons, some of which are myelinated and some which are not (Leenen et al., 1985). Furthermore, neighboring axons in axonal tracts may develop at different times and be at distinct maturation states, even if they are all eventually myelinated. To understand how OPCs transition to

myelinating OLs *in vivo*, Czopka et al. recently carried out time-lapse imaging of cell behavior during myelination of the larval zebrafish spinal cord (Czopka et al., 2013). This work showed that each individual cell, irrespective of its location in the spinal cord or its precise time of differentiation, generated its final new myelin sheath on average just 5 h after generating its first myelin sheath. Long-term imaging showed that mature OLs never generated a new myelin sheath, suggesting that OLs have only a few hours in which to generate all of their myelin sheaths. This mirrors a previous *in vitro* study of rodent co-cultures in which mammalian OLs also make their myelin sheaths in a short period: about 12 h (Watkins et al., 2008). One possible mechanism to regulate which axons are myelinated and which are not would be to generate nascent myelin sheaths around numerous axons indiscriminately and later prune away the sheaths made on the incorrect axons. However, about 75% of all nascent myelin sheaths made by a single OL were maintained long term and about 25% retracted within two days, even at a time point when most axons (>90%) in the embryonic zebrafish spinal cord remain unmyelinated (Czopka et al., 2013; Liu et al., 2013). This indicates that OLs are accurate when ensheathing axons, rather than doing so in a purely stochastic manner. Therefore, the mechanisms and events that regulate axon choice during myelination must occur prior to sheath formation. At that earlier point, the processes of OPCs have a distinct growth cone-like morphology as observed in live imaging studies in zebrafish and characterized in rodents (Fox et al., 2006; Czopka et al., 2013). Here, we explore the hypothesis that the decisions that regulate the myelination fate of specific axons are mediated by interactions between those axons and the exploratory processes of OPCs; and that these interactions may resemble the formation of nascent synapses between axons and dendrites.

In this review, we will refer to cells with exploratory processes but no nascent myelin sheaths as OPCs (often referred to as NG2 cells due to their expression of the cell surface proteoglycan NG2), and to cells that have already made their first myelin sheath as OLs.

SIMILARITIES BETWEEN AXON–OPC INTERACTIONS DURING MYELINATION AND AXON–DENDRITE INTERACTIONS DURING SYNAPSE FORMATION

The exploratory processes of post-migratory OPCs engage their targets in a local and restricted territory. Therefore, we believe it is informative to compare the behavior of OPC processes interacting with target axons with that of prospective dendrites interacting with axons just prior to synapse formation.

Multiple studies have elucidated the initial stages of synaptogenesis. Dynamic dendritic filopodia, the precursors of dendritic spines, initially contact growing axons (Dailey and Smith, 1996; Jontes and Smith, 2000; Shen and Cowan, 2010; Shen and Scheiffele, 2010). Live imaging of the zebrafish embryonic spinal cord, for instance, has identified such filopodia in individual motor neurons which contact the growing Mauthner axon, a large-diameter projection axon that innervates them *en passant* (Jontes et al., 2000). Such brief, transient interactions can induce pre- and postsynaptic differentiations. Interestingly, some postsynaptic transmembrane molecules such as neuroligin (Scheiffele et al., 2000), EphB (Kayser et al., 2008), SynCAM (Biederer, 2002) and Netrin-G ligand (Kim et al., 2006), can trigger presynaptic membrane specializations in adjacent neurons, even when expressed in non-neuronal cells in culture, revealing their role as synaptic organizers. The formation of pre- and postsynaptic complexes can stabilize the interaction, promoting synapse maturation (Jontes and Smith, 2000). Strengthening of nascent synapses stabilizes axon growth (Meyer and Smith, 2006) and the dynamic filopodia, which mature into dendritic spines (Niell et al., 2004) (Fig. 1A). A mature synapse is identifiable by the rigid parallel apposition of the pre and postsynaptic membranes. On the presynaptic side, neurotransmitter-filled vesicles cluster, dock to the membrane, fuse and release neurotransmitter across the synaptic cleft. On the postsynaptic side, an electron-dense postsynaptic density is often found which corresponds to the accumulation of cell-adhesion molecules, neurotransmitter receptors, ion channels, scaffolding proteins and signaling molecules (Emes and Grant, 2012).

Intriguingly, synapses between axons and OPCs, bearing striking resemblance to classical neuronal synapses, have been documented in the CNS. They have been documented electrophysiologically by patching OPCs (NG2 cells) in the juvenile and adult optic nerve and in organotypic slices. Excitatory postsynaptic currents in these cells were detected in response to both spontaneous and evoked firing of glutamatergic axons in the corpus callosum (Kukley et al., 2007; Ziskin et al., 2007), including during remyelination (Etxeberria et al., 2010), optic nerve (Kukley et al., 2007), cerebellum (Lin et al., 2005; Káradóttir et al., 2008), barrel cortex (Li et al., 2012), auditory pathway (Müller et al., 2009) and hippocampus (Bergles et al., 2000; Haberlandt et al., 2011), as well as firing of GABAergic axons in the hippocampus (Lin and Bergles, 2003; Jabs et al., 2005). Several lines of evidence indicate that postsynaptic currents in OPCs result from direct synapses with axons, in response to action potentials, reviewed comprehensively in (Bergles et al., 2010). A variety of neurotransmitter receptors are known to be expressed by OPCs and OLs (Karadottir and Attwell, 2007), which are well poised to directly mediate such transmission. Pharmacological inhibition of AMPA receptors suggests that they are the major contributors to OPC postsynaptic currents in response to glutamatergic synapses (Bergles et al., 2010). Axon–OPC synapses have also been identified in electron micrographs using the same morphological criteria as for classical synapses, including presynaptic

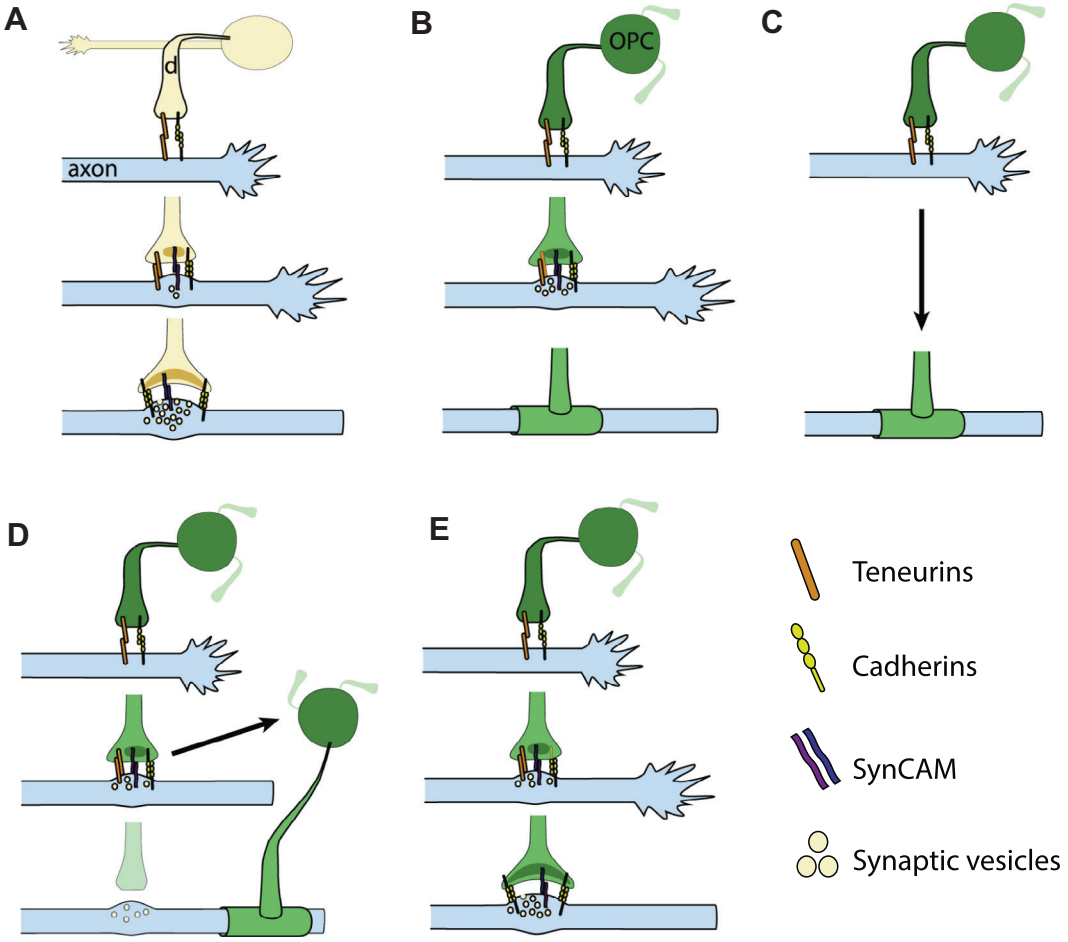

Fig. 1. Models of cell–cell interactions during synapse formation and myelination in the CNS. (A) A neuron (yellow) extends an exploratory dendrite (d) expressing matchmaker molecules (e.g. teneurins/cadherins) toward a target axon (blue). Because the target axon expresses the same molecules, the initial homophilic interactions are strengthened and synaptic organizers (e.g. SynCAM) induce pre and postsynaptic differentiation. (B) An OPC (green) extends an exploratory process toward a target axon. Because the OPC process and axon express similar matchmaker molecules this leads to the formation of an axon–OPC synapse, which matures into a myelin sheath. (C) An OPC (green) extends an exploratory process toward a target axon. Because the OPC process and axon express similar matchmaker molecules this leads to the formation of a myelin sheath. (D) An OPC (green) extends an exploratory process toward a target axon. Because the OPC process and axon express similar matchmaker molecules this leads to the formation of an axon–OPC synapse, which signals to other OPCs/OLs to myelinate the target axon. (E) An OPC (green) extends an exploratory process toward a target axon. Because the OPC process and axon express similar matchmaker molecules this leads to the formation of an axon–OPC synapse, which performs functions unrelated to myelination.

accumulation of vesicles, electron-dense material in the synaptic cleft and recently, the existence of a postsynaptic density in the OPC membrane (Haberlandt et al., 2011). In addition, markers for pre and postsynaptic specializations such as GAD65 (Lin and Bergles, 2003), VGlut1 (Ziskin et al., 2007), GRIP (Stegmüller et al., 2003) and synaptophysin (Kukley et al., 2007) have been shown to localize in puncta where axons are closely apposed to OPC processes. Importantly, the existence of axon–OPC synapses has been confirmed *in vivo* (Bergles et al., 2000), but their functions are not yet known. Recently, in addition to calcium-permeable AMPA receptors (Zonouzi et al., 2011), the presence of functional voltage-gated calcium channels in OPCs was confirmed (Haberlandt et al., 2011). These proteins may enable calcium entry following axon–OPC synapse activity and subsequent activation of intracellular signaling cascades. In fact, small calcium increases were detected in OPC somas directly following tetanic stimulation of GABAergic interneurons or glutamatergic CA3 hippocampal neurons (Haberlandt et al., 2011). At more physiological firing rates, the calcium increases may be restricted to the OPC processes and not reach the soma (Chan et al., 2013). These findings provide evidence of a physiological substrate by which the axon–OPC synapse may regulate OPC process behavior via calcium signaling, in similar ways to which the activation of postsynaptic calcium signaling can regulate dendrite behavior (Kennedy et al., 2005; Flavell and Greenberg, 2008; Greer and Greenberg, 2008). Intriguingly local calcium transients in OPC processes have also recently been implicated in the direct regulation of myelination *in vitro*, which we discuss below (Wake et al., 2011).

The resemblance of axon–OPC synapses to classical axon–dendrite synapses implies a similar mode of formation. It suggests that the same molecular adhesion

mechanisms that ensure specific contacts between an axon and its correct postsynaptic dendritic target may also ensure target matching in axon–OPC interactions (Fig. 1A–E, top panels). Given the recent evidence that this axonal selection occurs prior to myelin sheath formation, we suggest that during the period when OPCs are extending exploratory processes and contacting axons, they are doing so in an analogous way to how dendritic filopodia interact with target axons. In classical synapses, a plethora of mechanisms may guide target matching (extensively reviewed in (Sanes and Yamagata, 2009; Margeta and Shen, 2010; Shen and Scheiffele, 2010; Williams et al., 2010). One mechanism that can confer almost single-cell specificity is chemoaffinity, i.e. the molecular recognition of specific markers in targets (Zipursky and Sanes, 2010). Several molecules have been implicated in promoting regional or local specificity between axons and their targets, such as EphA and EphrinA (Cheng et al., 1995; Feldheim et al., 2000), Dscam and Sidekick (Yamagata and Sanes, 2008; Cvetkovska et al., 2013), and Capricious (Shinza-Kameda et al., 2006; Kurusu et al., 2008), among others. More recently, Cadherins (Osterhout et al., 2011; Williams et al., 2011) and Teneurins (Hong et al., 2012; Mosca et al., 2012) have been demonstrated to be crucial in the matching of individual axons with their specific dendritic targets at the level of individual synapses.

During synaptogenesis, after such matchmaking molecules (e.g. cadherins and teneurins) drive the correct axon–dendrite pairing, the initial contact must be stabilized, through the recruitment of pre- and postsynaptic protein complexes. Adhesion molecules such as Neurexin–Neuroligin (Krueger et al., 2012) Netrin-G ligands (Woo et al., 2009), SynCAMs (Biederer, 2002) and Cadherins (Arikkath and Reichardt, 2008; Rebsam and Mason, 2011), are examples of synaptic organizers that play essential roles in the maturation of the presynaptic release machinery and postsynaptic signaling apparatus.

Here we would like to ask: can the same matchmaking molecules regulate interactions between specific axons and OPC processes? Can synaptic organizers also stabilize the axon–OPC synapse? Can axon–OPC synapses mature into myelin sheaths or are such synapses an alternative differentiated state to a myelin sheath?

We will address the first two of these questions by discussing recent evidence for the roles of synaptic matchmakers (teneurins and cadherins) and organizers (SynCAMs and Neurexins) during myelination.

SYNAPTIC MATCHMAKERS

Teneurins

Teneurins (*ten*) are transmembrane glycoproteins containing epidermal growth factor (EGF)-like repeats followed by a globular domain in their C-terminal extracellular domain, and an N-terminal cytoplasmic domain that can undergo cleavage and translocate to the nucleus to regulate gene expression (Tucker et al., 2007). This phylogenetically conserved family is present both in invertebrates and vertebrates, which strongly express all four of their teneurins in the nervous system (Tucker and Chiquet-Ehrismann, 2006).

In *Drosophila*, ten-a and ten-m have recently been shown to mediate direct target choice through homophillic interactions both in olfactory neuron synapses (Hong et al., 2012) and at the neuromuscular junction (Mosca et al., 2012). In addition to their putative role as transcriptional regulators, teneurins also regulate the cytoskeleton through alpha-spectrin (Mosca et al., 2012), which suggests a structural role in organizing the synapse.

Teneurins may also determine which axons in a milieu an OPC contacts prior to myelination. Global disruption of ten-4 has been shown to abolish the myelination of some axons in the CNS of mice (Suzuki et al., 2012). Suzuki et al. show that this is likely due to the loss of ten-4 function in OPCs, which fail to differentiate. Precisely when ten-4 functions in a single OPC during transition to myelination remains unclear. It is tempting to speculate that ten-4 is also expressed on axons destined to be myelinated and that loss of ten-4 homophillic interactions between axons and OPCs might disrupt the initial adhesion, with the secondary consequence of preventing OPC differentiation and myelination. Further studies that manipulate ten-4 function while visualizing the dynamics of OPC process extension and axonal contact would test whether such a mechanism underlies the role for this class of proteins in axon–OPC interactions and myelination.

Cadherins

The cadherin (*cdh*) superfamily of adhesion proteins has been implicated in many aspects of synapse formation and function. Classical cadherins contain an extracellular calcium-binding domain that mediates mostly homophilic interactions, a single transmembrane domain and a cytoplasmic domain that binds several proteins, most notably catenins. This latter intracellular interaction permits the adhesion complex to signal to several pathways and regulate the actin cytoskeleton. Multiple cadherins are expressed in the nervous system, with remarkable spatial and developmental regulation (Takeichi, 2007; Arikkath and Reichardt, 2008).

Recently, Osterhout et al. demonstrated that classical cadherins likely mediate specific recognition of targets in the mammalian visual system: cdh3-expressing retinal ganglion cells synapse specifically with cdh6-expressing retinorecipient target nuclei, a specificity that is lost in cdh6 knockout (Osterhout et al., 2011). Also, Williams et al. showed that cdh9 homophilic interactions match dentate gyrus axons to CA3 pyramidal dendrites at the level of the individual synapse (Williams et al., 2011). Given the diversity of cadherins expressed in the nervous system, sometimes in a single neuron, the concept of a ‘cadherin’ code, possibly combinatorial, has been suggested to explain synaptic matchmaking in the developing CNS (Rebsam and Mason, 2011).

Interestingly, N-cadherin was shown to be expressed in OPCs and OLs *in vitro*, and to localize to the major processes originating from the soma (Payne et al., 1996). It was also shown to increase OPC adhesion *in vitro* (Schnadelbach et al., 2000), and in experiments where OPCs are co-cultured with dorsal root ganglia neurons and N-cadherin function is blocked, OPCs made fewer contacts with axons. In organotypic rat cerebellar slice cultures treated in the same way, myelinated axon number is reduced, despite the timely differentiation of OLs (Schnadelbach, 2001). This suggests that cadherins might mediate the initial interaction and recognition between OPCs and axons, but the potential role(s) of this large group of diverse molecules in CNS myelination remain to be fully tested *in vivo*.

That synaptic matchmakers such as teneurins and cadherins are expressed in OPCs and function in myelination reveals an intriguing parallel to axon–dendrite synapse formation. It hints that the initial adhesion of an OPC process to an axon might require the same type of homophilic interactions that a nascent synapse does (Fig. 1B–E, top panel). Some of the additional families of molecules proposed to guide target matching (e.g. DSCAM in invertebrates and Protocadherins in vertebrates), are encoded in large, complex genomic loci with alternative promoters, and messenger RNA (mRNA) that undergoes extensive alternative splicing to generate many isoforms with different extracellular domains. Each cell expresses a complement of isoforms that is apparently stochastic (Zipursky and Sanes, 2010), and this creates enough variety for a combinatorial code to specifically label almost every individual cell. In this way, the remarkable precision and specificity of connection between individual axons and individual dendrites can be achieved. In contrast, axon–OPC interactions may require less elaborate specificity. OPCs are more promiscuous – OLs that typically only myelinate small-diameter axons can readily myelinate large-diameter axons, for instance, following transplantation from the optic nerve into the spinal cord (Fanarraga et al., 1998) or when supernumerary large-diameter axons are introduced in the ventral spinal cord (Almeida et al., 2011). This indicates that individual OLs are capable of myelinating any competent axon, and in turn that specific axons do not need to be myelinated by a particular subtype of OL. Thus, matchmaking prior to myelination more likely involves a simple 'yes', 'no', or 'not yet' decision. Therefore, it is more likely that a smaller number of molecules and a ''simpler'' family of adhesion molecules are required. Interestingly, in a microarray-based transcriptome analysis of acutely dissociated neurons and glia in the CNS, transcripts of *dscam* and *dscamL1* (mRNAs with few alternatively spliced isoforms in vertebrates), several individual *pcdh*s, *ephA*/*ephrinA* and *ephB*/*ephrinB* genes were found to be expressed in OPCs at a similar or higher level than neurons. Moreover, expression of some of these genes is downregulated as OPCs mature into myelinating OLs – *pcdh20*, which is encoded in a simple locus distinct from clustered protocadherins, is downregulated about 50-fold, *ephA5* about 11-fold, *ephrinB2* about 8.5-fold and *dscam* eightfold (Cahoy et al., 2008). This further suggests that even in a CNS interaction involving different cell types (neurons and OPCs), the same molecular toolkit may be recurrently used to ensure target selection conducive to the appropriate connection.

SYNAPSE ORGANIZERS

SynCAMs

SynCAMs, or Nectin-like molecules (*Necl*) belong to the immunoglobulin superfamily of cell-adhesion molecules and are highly expressed in the vertebrate brain, where they assemble across the synaptic cleft both homo- and heterophilically. Co-expression of SynCAM1 and glutamate receptors in HEK293 cells is sufficient to trigger the formation of an active synapse with co-cultured hippocampal neurons (Biederer, 2002; Sara, 2005). In agreement with a central role in organizing the synapse, the cytosolic tail of SynCAM is predicted to interact with PDZ domain-containing proteins such as postsynaptic scaffolds, and with 4.1 family proteins which assemble the actin cytoskeleton (Biederer, 2006). Indeed, SynCAM disruption affects synaptic maintenance and plasticity (Robbins et al., 2010).

Interestingly, SynCAM1 (Necl2) was found to be expressed in OPCs in the perinatal mouse brain (Galuska et al., 2010), where it is a target of polysialylation, a modification that drastically modulates its functional interactions. Another polysialylated but axonal cell-adhesion molecule, NCAM, needs to be downregulated in the surface of maturing axons in order for myelination to proceed (Charles et al., 2000; Fewou et al., 2007; Jakovcevski et al., 2007). Polysialylation of SynCAM1 may serve a similar function to Polysialylated Neural Cell Adhesion Molecule (PSA–NCAM) in axons, and control the precise timing of myelination of specific axons.

SynCAM2 (Necl3) and SynCAM3 (Necl1) are instead expressed in neurons in the rodent CNS, where they can accumulate at contact sites between axons and OLs (Pellissier et al., 2007). Interestingly, knockout mice for SynCAM3 show normal neuronal and glial development, but a delay in myelination of the optic nerve and spinal cord (Park et al., 2008). SynCAM4 (Necl4) is expressed in neurons and myelinating glia of both CNS (Zhu et al., 2013) and PNS (Spiegel et al., 2007). It has been shown to regulate myelination *in vitro* (Maurel et al., 2007; Spiegel et al., 2007), and recently, examination of SynCAM4 knockout mice determined that in its absence, Schwann cells myelinate with a slight delay and generate many myelin sheaths with multiple abnormalities (Golan et al., 2013). Altogether, these results suggest a role for the SynCAM family of adhesion molecules in mediating axonal-glial adhesion and the timing of myelination. Given that OPCs express several glutamate receptors, it is possible that the localization of SynCAMs and such receptors is sufficient to drive formation of a minimal axon–OPC synapse.

Contactin-associated protein Caspr

In addition, molecules related to synaptic organizers are known to function during the formation of myelin sheaths. Caspr, for example, is a homolog of *Drosophila* Neurexin IV, a member of a well-established group of molecules that organize the synapse. Presynaptic neurexins are transmembrane proteins whose extracellular domain (containing EGF and LaminG repeats) mediates binding to postsynaptic neuroligins. This heterophilic interaction results in bi-directional signaling – neurexins can induce postsynaptic differentiation by clustering of neurotransmitter receptors and intracellular scaffolds, and they also interact with the presynaptic actin cytoskeleton and may modulate synaptic vesicle recycling (Krueger et al., 2012).

Caspr is initially localized along the axon, but as soon as the axon is contacted by an OPC process Caspr becomes clustered (Soetaert and Lyons, unpublished observation). Moreover, Caspr also forms a complex with axonal contactin1 and glial neurofascin155 at the tips of growing myelin sheaths (Zonta et al., 2008). This complex of proteins maintains tight contact between the myelin sheath and the underlying axon. The intracellular domain of Caspr, as that of neurexins, interacts with the 4.1 protein family, which mediates adhesion to the axon cytoskeleton, stabilizing the axon–glial contact (Gollan et al., 2002). Interestingly, disruption of this complex by deletion of glial neurofascin155 delays CNS myelination (Zonta et al., 2008). Although Caspr is not ultimately necessary for myelin sheath formation (Bhat et al., 2001; Gollan et al., 2003), it would be interesting to test whether its disruption delayed myelination to the same extent as that of neurofascin155, which would indicate a role for this specific axon–OL molecular interaction in regulating the precise timing of CNS myelination.

In addition to the aforementioned families of synaptic organizers, many other canonical postsynaptic constituents are found to be expressed in OPCs. Transcripts of the scaffold proteins of the Discs large homolog family (of which Dlg4/PSD-95 is the major scaffold of excitatory synapses), the scaffold proteins Shank3 and Gephyrin (the main scaffold protein of inhibitory synapses), ADAM22, a known PSD-95 interactor, calcium/calmodulin-dependent protein kinase II (highly enriched in neuronal synapses), among others, are all expressed in OPCs (Cahoy et al., 2008), as reported for synaptic matchmakers. It would be interesting to test the functional significance of their presence, e.g. by conditional deletion in OPCs *in vivo*.

CAN AN AXON–OPC SYNAPSE TURN INTO A MYELIN SHEATH?

Synaptic activity has been shown to regulate numerous stages of synapse formation, morphology, maintenance and function and the molecular basis of these roles is beginning to be elucidated (Cohen and Greenberg, 2008; Greer and Greenberg, 2008; West and Greenberg, 2011). Neuronal activity has also long been proposed to regulate myelination (Zalc and Fields, 2000; Fields, 2005, 2010), but how this might occur, particularly *in vivo*, has remained quite unclear. A recent *in vitro* study has suggested that communication via the axon–OPC/OL synapse directly regulates the myelinating capacity of the synapse-bearing process (Wake et al., 2011).

In an OPC–dorsal root ganglia (DRG) co-culture system, Wake et al. found that electrode-stimulation of DRGs causes vesicle release from axons resulting in calcium spikes in OPCs. When this stimulus-evoked axonal vesicle release was inhibited pharmacologically, OLs later made fewer myelin sheaths, despite differentiating normally (Wake et al., 2011). Wake et al. further demonstrated that the local translation of the major myelin protein, MBP, in OL processes is enhanced by axonal stimulation, and that this is blocked by inhibition of *N*-methyl-D-aspartate receptor (NMDAR) or metabotropic glutamate receptor signaling. However, knockout of the obligate NR1 subunit of NMDARs specifically in the oligodendrocyte lineage does not affect myelination *in vivo* (De Biase et al., 2011; Guo et al., 2012), implying that alternative signals may be required *in vivo*. It is important to note that Wake et al. did not actually assess myelination status in their *in vitro* system following inhibition of glutamate receptor signaling – they focused only on its role in promoting mbp mRNA translation (Wake et al., 2011). Interestingly, if mbp mRNA transport to distal OPC processes is disrupted *in vivo* (by mutation of the kinesin motor protein essential for its localization) the majority of myelin sheaths are still made (Lyons et al., 2009). This suggests that local mbp mRNA translation may not be strictly required for the formation of a myelin sheath, but that activity-dependent regulation of local translation (mediated through glutamate receptor signaling) might fine-tune the timing or extent of myelination along particular axons, perhaps in specific brain areas, or later in life.

Such a mechanism would rely on the maintenance and function of axon–OPC synapses through differentiation of OPCs into OLs and formation of myelin sheaths. However, although it appears that at early postnatal stages essentially all OPCs have synaptic input (Kukley et al., 2008; Ge et al., 2009), as soon as these cells start differentiating into NG2-PLP+ cells and acquiring a myelinating morphology, the size of the currents and the expression of the operant neurotransmitter receptors become reduced (De Biase et al., 2010; Kukley et al., 2010). After a demyelinating injury, newly born OPCs also receive synaptic input from unmyelinated glutamatergic axons, and as these OPCs differentiate and the axons get remyelinated, synaptic connectivity is lost (Etxeberria et al., 2010). Given the short period of myelin sheath formation by individual cells *in vivo*, it remains unclear whether such synapses are actually restricted to the OPC stage as we have defined it here, or whether they also exist during the brief time in which OLs generate their myelin sheaths. To elucidate the relationship between such synapses and myelination *in vivo*, one would need to

visualize individual axon–OPC synapses *in vivo* and track their fate over time to determine whether they can transform into myelin sheaths.

Such imaging-based approaches would help to address multiple outstanding questions: are transient axon–OPC synapses formed along the length of all axons, only the specific axons destined for myelination, or axons fated to remain unmyelinated? Could selective strengthening of axon–OPC synapses prefigure the formation of individual myelin sheaths? If such synapses directly transform into myelin sheaths (Fig. 1B), the underlying molecular mechanisms of synapse formation may indeed decide which specific axons get myelinated at a particular time. It also remains possible that after the initial synaptogenic-like interaction between an axon and an OPC process, myelin sheaths form without ever resembling synapses (Fig. 1C). Alternatively, synapses may not directly transform into sheaths but may still play a role in regulating myelination by monitoring the functional state of axons and recruiting other OPCs or OLs to form the myelin sheath(s) (Fig. 1D). Axon–OPC synapses may be a differentiated structure that cannot transform into a myelin sheath and which does not regulate myelination at all (Fig. 1E). Instead, axon–OPC synapses may perform other tasks unrelated to myelination, but which are essential for healthy nervous system function, plasticity, and perhaps repair. Some suggested roles include process motility, migration, tract fasciculation, monitoring the health state of neurons and release of neurotrophic molecules – these are outside the scope of this review and have been excellently reviewed elsewhere (Gallo et al., 2008; Mangin and Gallo, 2011; Sakry et al., 2011).

CONCLUSION

We suggest that the early events of axon–dendritic interactions mirror the early events of axon–OL interactions that prefigure myelination. We propose that some of the same molecular machinery that regulates the initial specificity of axon–dendrite interactions is important for regulating specific axon–OPC interactions. Mechanisms that strengthen axon–dendrite interactions may do the same at axon–OPC synapses, and such synapses may play a role in the transformation of an exploratory process into a myelin sheath. Our knowledge of the molecular regulators of CNS myelination is currently poor. We propose that a candidate-based approach to elucidating the genetic basis of CNS myelination might include consideration of the mechanisms and molecules discussed here.

REFERENCES

Almeida RG, Czopka T, Ffrench-Constant C, Lyons DA (2011) Individual axons regulate the myelinating potential of single oligodendrocytes in vivo. Development 138:4443–4450.

Arikkath J, Reichardt LF (2008) Cadherins and catenins at synapses: roles in synaptogenesis and synaptic plasticity. Trends Neurosci 31:487–494.

Barres BA, Raff MC (1999) Axonal control of oligodendrocyte development. J Cell Biol 147:1123–1128.

Baumann N, Pham-Dinh D (2001) Biology of oligodendrocyte and myelin in the mammalian central nervous system. Physiol Rev 81:871–927.

Bergles DE, Jabs R, Steinhäuser C (2010) Neuron-glia synapses in the brain. Brain Res Rev 63:130–137.

Bergles DE, Roberts JD, Somogyi P, Jahr CE (2000) Glutamatergic synapses on oligodendrocyte precursor cells in the hippocampus. Nature 405:187–191.

Bhat MA, Rios JC, Lu Y, Garcia-Fresco GP, Ching W, St. Martin M, Li J, Einheber S, Chesler M, Rosenbluth J, Salzer JL, Bellen HJ (2001) Axon–glia interactions and the domain organization of myelinated axons requires neurexin IV/Caspr/Paranodin. Neuron 30:369–383.

Biederer T (2002) SynCAM, a synaptic adhesion molecule that drives synapse assembly. Science 297:1525–1531.

Biederer T (2006) Bioinformatic characterization of the SynCAM family of immunoglobulin-like domain-containing adhesion molecules. Genomics 87:139–150.

Brinkmann BG, Agarwal A, Sereda MW, Garratt AN, Muller T, Wende H, Stassart RM, Nawaz S, Humml C, Velanac V, Radyushkin K, Goebbels S, Fischer TM, Franklin RJ, Lai C, Ehrenreich H, Birchmeier C, Schwab MH, Nave KA (2008) Neuregulin-1/ErbB signaling serves distinct functions in myelination of the peripheral and central nervous system. Neuron 59:581–595.

Cahoy JD, Emery B, Kaushal A, Foo LC, Zamanian JL, Christopherson KS, Xing Y, Lubischer JL, Krieg PA, Krupenko SA, Thompson WJ, Barres BA (2008) A transcriptome database for astrocytes, neurons, and oligodendrocytes: a new resource for understanding brain development and function. J Neurosci 28:264–278.

Chan C-F, Kuo T-W, Weng J-Y, Lin Y-C, Chen T-Y, Cheng J-K, Lien C-C (2013) Ba^{2+}- and bupivacaine-sensitive background K^{+} conductances mediate rapid EPSP attenuation in oligodendrocyte precursor cells. J Physiol. http://dx.doi.org/10.1113/jphysiol.2013.257113.

Chao DL, Ma L, Shen K (2009) Transient cell–cell interactions in neural circuit formation. Nat Rev Neurosci 10:262–271.

Charles P, Hernandez MP, Stankoff B, Aigrot MS, Colin C, Rougon G, Zalc B, Lubetzki C (2000) Negative regulation of central nervous system myelination by polysialylated-neural cell adhesion molecule. Proc Nat Acad Sci USA 97:7585–7590.

Chen Y, Wu H, Wang S, Koito H, Li J, Ye F, Hoang J, Escobar SS, Gow A, Arnett HA, Trapp BD, Karandikar NJ, Hsieh J, Lu QR (2009) The oligodendrocyte-specific G protein-coupled receptor GPR17 is a cell-intrinsic timer of myelination. Nat Neurosci 12:1398–1406.

Cheng HJ, Nakamoto M, Bergemann AD, Flanagan JG (1995) Complementary gradients in expression and binding of ELF-1 and Mek4 in development of the topographic retinotectal projection map. Cell 82:371–381.

Cohen S, Greenberg ME (2008) Communication between the synapse and the nucleus in neuronal development, plasticity, and disease. Annu Rev Cell Dev Biol 24:183–209.

Cvetkovska V, Hibbert AD, Emran F, Chen BE (2013) Overexpression of Down syndrome cell adhesion molecule impairs precise synaptic targeting. Nat Neurosci 16:677–682.

Czopka T, Ffrench-Constant C, Lyons DA (2013) Individual oligodendrocytes have only a few hours in which to generate new myelin sheaths in vivo. Dev Cell 25:599–609.

Dailey ME, Smith SJ (1996) The dynamics of dendritic structure in developing hippocampal slices. J Neurosci 16:2983–2994.

De Biase LM, Kang SH, Baxi EG, Fukaya M, Pucak ML, Mishina M, Calabresi PA, Bergles DE (2011) NMDA receptor signaling in oligodendrocyte progenitors is not required for oligodendrogenesis and myelination. J Neurosci 31:12650–12662.

De Biase LM, Nishiyama A, Bergles DE (2010) Excitability and synaptic communication within the oligodendrocyte lineage. J Neurosci 30:3600–3611.

Emery B (2010a) Regulation of oligodendrocyte differentiation and myelination. Science 330:779–782.
Emery B (2010b) Transcriptional and post-transcriptional control of CNS myelination. Curr Opin Neurobiol 20:601–607.
Emes RD, Grant SGN (2012) Evolution of synapse complexity and diversity. Annu Rev Neurosci 35:111–131.
Etxeberria A, Mangin J-M, Aguirre A, Gallo V (2010) Adult-born SVZ progenitors receive transient synapses during remyelination in corpus callosum. Nat Neurosci 13:287–289.
Fanarraga ML, Griffiths IR, Zhao M, Duncan ID (1998) Oligodendrocytes are not inherently programmed to myelinate a specific size of axon. J Comp Neurol 399:94–100.
Fancy SPJ, Baranzini SE, Zhao C, Yuk D-I, Irvine K-A, Kaing S, Sanai N, Franklin RJM, Rowitch DH (2009) Dysregulation of the Wnt pathway inhibits timely myelination and remyelination in the mammalian CNS. Genes Dev 23:1571–1585.
Feldheim DA, Kim YI, Bergemann AD, Frisén J, Barbacid M, Flanagan JG (2000) Genetic analysis of ephrin-A2 and ephrin-A5 shows their requirement in multiple aspects of retinocollicular mapping. Neuron 25:563–574.
Ferguson K, Long H, Cameron S, Chang W-T, Rao Y (2009) The conserved Ig superfamily member Turtle mediates axonal tiling in *Drosophila*. J Neurosci 29:14151–14159.
Fewou SN, Ramakrishnan H, Bussow H, Gieselmann V, Eckhardt M (2007) Down-regulation of polysialic acid is required for efficient myelin formation. J Biol Chem 282:16700–16711.
Fields RD (2005) Myelination: an overlooked mechanism of synaptic plasticity? Neuroscientist 11:528–531.
Fields RD (2010) Neuroscience. Change in the brain's white matter. Science 330:768–769.
Flavell SW, Greenberg ME (2008) Signaling mechanisms linking neuronal activity to gene expression and plasticity of the nervous system. Annu Rev Neurosci 31:563–590.
Fox MA, Afshari FS, Alexander JK, Colello RJ, Fuss B (2006) Growth conelike sensorimotor structures are characteristic features of postmigratory, premyelinating oligodendrocytes. Glia 53:563–566.
Furusho M, Dupree JL, Nave KA, Bansal R (2012) Fibroblast growth factor receptor signaling in oligodendrocytes regulates myelin sheath thickness. J Neurosci 32:6631–6641.
Fünfschilling U, Supplie LM, Mahad D, Boretius S, Saab AS, Edgar J, Brinkmann BG, Kassmann CM, Tzvetanova ID, Möbius W, Diaz F, Meijer D, Suter U, Hamprecht B, Sereda MW, Moraes CT, Frahm J, Goebbels S, Nave K-A (2012) Glycolytic oligodendrocytes maintain myelin and long-term axonal integrity. Nature 485:517–521.
Gallo V, Mangin JM, Kukley M, Dietrich D (2008) Synapses on NG2-expressing progenitors in the brain: multiple functions? J Physiol 586:3767–3781.
Galuska SP, Rollenhagen M, Kaup M, Eggers K, Oltmann-Norden I, Schiff M, Hartmann M, Weinhold B, Hildebrandt H, Geyer R, Mühlenhoff M, Geyer H (2010) Synaptic cell adhesion molecule SynCAM 1 is a target for polysialylation in postnatal mouse brain. PNAS 107:10250–10255.
Ge W-P, Zhou W, Luo Q, Jan LY, Jan Y-N (2009) Dividing glial cells maintain differentiated properties including complex morphology and functional synapses. PNAS 106:328–333.
Genoud S, Lappe-Siefke C, Goebbels S, Radtke F, Aguet M, Scherer SS, Suter U, Nave KA, Mantei N (2002) Notch1 control of oligodendrocyte differentiation in the spinal cord. J Cell Biol 158:709–718.
Golan N, Kartvelishvily E, Spiegel I, Salomon D, Sabanay H, Rechav K, Vainshtein A, Frechter S, Maik-Rachline G, Eshed-Eisenbach Y, Momoi T, Peles E (2013) Genetic deletion of Cadm4 results in myelin abnormalities resembling charcot-marie-tooth neuropathy. J Neurosci 33:10950–10961.
Gollan L, Sabanay H, Poliak S, Berglund EO, Ranscht B, Peles E (2002) Retention of a cell adhesion complex at the paranodal junction requires the cytoplasmic region of Caspr. J Cell Biol 157:1247–1256.
Gollan L, Salomon D, Salzer JL, Peles E (2003) Caspr regulates the processing of contactin and inhibits its binding to neurofascin. J Cell Biol 163:1213–1218.
Greer PL, Greenberg ME (2008) From synapse to nucleus: calcium-dependent gene transcription in the control of synapse development and function. Neuron 59:846–860.
Guo F, Maeda Y, Ko EM, Delgado M, Horiuchi M, Soulika A, Miers L, Burns T, Itoh T, Shen H, Lee E, Sohn J, Pleasure D (2012) Disruption of NMDA receptors in oligodendroglial lineage cells does not alter their susceptibility to experimental autoimmune encephalomyelitis or their normal development. J Neurosci 32:639–645.
Haberlandt C, Derouiche A, Wyczynski A, Haseleu J, Pohle J, Karram K, Trotter J, Seifert G, Frotscher M, Steinhäuser C, Jabs R (2011) Gray matter NG2 cells display multiple Ca^{2+}-signaling pathways and highly motile processes. PLoS One 6:e17575.
He L, Lu QR (2013) Coordinated control of oligodendrocyte development by extrinsic and intrinsic signaling cues. Neurosci Bull 29:129–143.
Hong W, Mosca TJ, Luo L (2012) Teneurins instruct synaptic partner matching in an olfactory map. Nature 484:201–207.
Hu QD, Ang BT, Karsak M, Hu WP, Cui XY, Duka T, Takeda Y, Chia W, Sankar N, Ng YK, Ling EA, Maciag T, Small D, Trifonova R, Kopan R, Okano H, Nakafuku M, Chiba S, Hirai H, Aster JC, Schachner M, Pallen CJ, Watanabe K, Xiao ZC (2003) F3/contactin acts as a functional ligand for Notch during oligodendrocyte maturation. Cell 115:163–175.
Hughes EG, Kang SH, Fukaya M, Bergles DE (2013) Oligodendrocyte progenitors balance growth with self-repulsion to achieve homeostasis in the adult brain. Nat Neurosci:1–11.
Jabs R, Pivneva T, Hüttmann K, Wyczynski A, Nolte C, Kettenmann H, Steinhäuser C (2005) Synaptic transmission onto hippocampal glial cells with hGFAP promoter activity. J Cell Sci 118:3791–3803.
Jakovcevski I, Mo Z, Zecevic N (2007) Down-regulation of the axonal polysialic acid-neural cell adhesion molecule expression coincides with the onset of myelination in the human fetal forebrain. Neuroscience 149:328–337.
Jessen KR, Mirsky R (2005) The origin and development of glial cells in peripheral nerves. Nat Rev Neurosci 6:671–682.
Jontes JD, Buchanan J, Smith SJ (2000) Growth cone and dendrite dynamics in zebrafish embryos: early events in synaptogenesis imaged in vivo. Nat Neurosci 3:231–237.
Jontes JD, Smith SJ (2000) Filopodia, spines, and the generation of synaptic diversity. Neuron 27:11–14.
Jung H, Yoon BC, Holt CE (2012) Axonal mRNA localization and local protein synthesis in nervous system assembly, maintenance and repair. Nat Rev Neurosci 13:308–324.
Karadottir R, Attwell D (2007) Neurotransmitter receptors in the life and death of oligodendrocytes. Neuroscience 145:1426–1438.
Kayser MS, Nolt MJ, Dalva MB (2008) EphB receptors couple dendritic filopodia motility to synapse formation. Neuron 59:56–69.
Káradóttir R, Hamilton NB, Bakiri Y, Attwell D (2008) Spiking and nonspiking classes of oligodendrocyte precursor glia in CNS white matter. Nat Neurosci 11:450–456.
Kennedy MB, Beale HC, Carlisle HJ, Washburn LR (2005) Integration of biochemical signalling in spines. Nat Rev Neurosci 6:423–434.
Kim S, Burette A, Chung HS, Kwon S-K, Woo J, Lee HW, Kim K, Kim H, Weinberg RJ, Kim E (2006) NGL family PSD-95–interacting adhesion molecules regulate excitatory synapse formation. Nat Neurosci 9:1294–1301.
Kirby BB, Takada N, Latimer AJ, Shin J, Carney TJ, Kelsh RN, Appel B (2006) In vivo time-lapse imaging shows dynamic oligodendrocyte progenitor behavior during zebrafish development. Nat Neurosci 9:1506–1511.
Knapp PE, Bartlett WP, Skoff RP (1987) Cultured oligodendrocytes mimic in vivo phenotypic characteristics: cell shape, expression of myelin-specific antigens, and membrane production. Dev Biol 120:356–365.

Krueger DD, Tuffy LP, Papadopoulos T, Brose N (2012) The role of neurexins and neuroligins in the formation, maturation, and function of vertebrate synapses. Curr Opin Neurobiol 22:412–422.
Kukley M, Capetillo-Zarate E, Dietrich D (2007) Vesicular glutamate release from axons in white matter. Nat Neurosci 10:311–320.
Kukley M, Kiladze M, Tognatta R, Hans M, Swandulla D, Schramm J, Dietrich D (2008) Glial cells are born with synapses. FASEB J 22:2957–2969.
Kukley M, Nishiyama A, Dietrich D (2010) The fate of synaptic input to NG2 glial cells: neurons specifically downregulate transmitter release onto differentiating oligodendroglial cells. J Neurosci 30:8320–8331.
Kurusu M, Cording A, Taniguchi M, Menon K, Suzuki E, Zinn K (2008) A screen of cell-surface molecules identifies leucine-rich repeat proteins as key mediators of synaptic target selection. Neuron 59:972–985.
Lee S, Leach MK, Redmond SA, Chong SYC, Mellon SH, Tuck SJ, Feng Z-Q, Corey JM, Chan JR (2012a) A culture system to study oligodendrocyte myelination processes using engineered nanofibers. Nat Methods 9:917–922.
Lee X, Yang Z, Shao Z, Rosenberg SS, Levesque M, Pepinsky RB, Qiu M, Miller RH, Chan JR, Mi S (2007) NGF regulates the expression of axonal LINGO-1 to inhibit oligodendrocyte differentiation and myelination. J Neurosci 27:220–225.
Lee Y, Morrison BM, Li Y, Lengacher S, Farah MH, Hoffman PN, Liu Y, Tsingalia A, Jin L, Zhang P-W, Pellerin L, Magistretti PJ, Rothstein JD (2012b) Oligodendroglia metabolically support axons and contribute to neurodegeneration. Nature 487:443–448.
Leenen LP, Meek J, Posthuma PR, Nieuwenhuys R (1985) A detailed morphometrical analysis of the pyramidal tract of the rat. Brain Res 359:65–80.
Li H, He Y, Richardson WD, Casaccia P (2009) Two-tier transcriptional control of oligodendrocyte differentiation. Curr Opin Neurobiol 19:479–485.
Li P, Scafidi J, Mangin J-M, Gallo V (2012) Experience-dependent regulation of NG2 progenitors in the developing barrel cortex. Nat Neurosci:1–5.
Lin S-C, Bergles DE (2003) Synaptic signaling between GABAergic interneurons and oligodendrocyte precursor cells in the hippocampus. Nat Neurosci 7:24–32.
Lin S-C, Huck JHJ, Roberts JDB, Macklin WB, Somogyi P, Bergles DE (2005) Climbing fiber innervation of NG2-expressing glia in the mammalian cerebellum. Neuron 46:773–785.
Liu J, Dietz K, DeLoyht JM, Pedre X, Kelkar D, Kaur J, Vialou V, Lobo MK, Dietz DM, Nestler EJ, Dupree J, Casaccia P (2012) Impaired adult myelination in the prefrontal cortex of socially isolated mice. Nat Neurosci 15:1621–1623.
Liu P, Du J-L, He C (2013) Developmental pruning of early-stage myelin segments during CNS myelination in vivo. Cell Res:1–3.
Lyons DA, Naylor SG, Scholze A, Talbot WS (2009) Kif1b is essential for mRNA localization in oligodendrocytes and development of myelinated axons. Nat Genet 41:854–858.
Makinodan M, Rosen KM, Ito S, Corfas G (2012) A critical period for social experience-dependent oligodendrocyte maturation and myelination. Science 337:1357–1360.
Mangin J-M, Gallo V (2011) The curious case of NG2 cells: transient trend or game changer? ASN Neuro 3:37–49.
Margeta MA, Shen K (2010) Molecular mechanisms of synaptic specificity. Mol Cell Neurosci 43:261–267.
Maurel P, Einheber S, Galinska J, Thaker P, Lam I, Rubin MB, Scherer SS, Murakami Y, Gutmann DH, Salzer JL (2007) Nectin-like proteins mediate axon Schwann cell interactions along the internode and are essential for myelination. J Cell Biol 178:861–874.
Meyer MP, Smith SJ (2006) Evidence from in vivo imaging that synaptogenesis guides the growth and branching of axonal arbors by two distinct mechanisms. J Neurosci 26:3604–3614.
Mi S, Lee X, Shao Z, Thill G, Ji B, Relton J, Levesque M, Allaire N, Perrin S, Sands B, Crowell T, Cate RL, McCoy JM, Pepinsky RB (2004) LINGO-1 is a component of the Nogo-66 receptor/p75 signaling complex. Nat Neurosci 7:221–228.
Mi S, Miller RH, Lee X, Scott ML, Shulag-Morskaya S, Shao Z, Chang J, Thill G, Levesque M, Zhang M, Hession C, Sah D, Trapp B, He Z, Jung V, McCoy JM, Pepinsky RB (2005) LINGO-1 negatively regulates myelination by oligodendrocytes. Nat Neurosci 8:745–751.
Millard SS, Flanagan JJ, Pappu KS, Wu W, Zipursky SL (2007) Dscam2 mediates axonal tiling in the *Drosophila* visual system. Nature 447:720–724.
Miller DJ, Duka T, Stimpson CD, Schapiro SJ, Baze WB, McArthur MJ, Fobbs AJ, Sousa AMM, Sestan N, Wildman DE, Lipovich L, Kuzawa CW, Hof PR, Sherwood CC (2012) Prolonged myelination in human neocortical evolution. PNAS 109:16480–16485.
Monk KR, Naylor SG, Glenn TD, Mercurio S, Perlin JR, Dominguez C, Moens CB, Talbot WS (2009) A G protein-coupled receptor is essential for Schwann cells to initiate myelination. Science 325:1402–1405.
Mosca TJ, Hong W, Dani VS, Favaloro V, Luo L (2012) Trans-synaptic Teneurin signalling in neuromuscular synapse organization and target choice. Nature 484:237–241.
Müller J, Reyes-Haro D, Pivneva T, Nolte C, Schaette R, Lübke J, Kettenmann H (2009) The principal neurons of the medial nucleus of the trapezoid body and NG2(+) glial cells receive coordinated excitatory synaptic input. J Gen Physiol 134:115–127.
Nave K-A (2010a) Myelination and the trophic support of long axons. Nat Rev Neurosci 11:275–283.
Nave KA (2010b) Myelination and support of axonal integrity by glia. Nature 468:244–252.
Niell CM, Meyer MP, Smith SJ (2004) In vivo imaging of synapse formation on a growing dendritic arbor. Nat Neurosci 7:254–260.
Osterhout JA, Josten N, Yamada J, Pan F, Wu S-W, Nguyen PL, Panagiotakos G, Inoue YU, Egusa SF, Volgyi B, Inoue T, Bloomfield SA, Barres BA, Berson DM, Feldheim DA, Huberman AD (2011) Cadherin-6 mediates axon-target matching in a non-image-forming visual circuit. Neuron 71:632–639.
Park J, Liu B, Chen T, Li H, Hu X, Gao J, Zhu Y, Zhu Q, Qiang B, Yuan J, Peng X, Qiu M (2008) Disruption of Nectin-like 1 cell adhesion molecule leads to delayed axonal myelination in the CNS. J Neurosci 28:12815–12819.
Payne HR, Hemperly JJ, Lemmon V (1996) N-cadherin expression and function in cultured oligodendrocytes. Brain Res Dev Brain Res 97:9–15.
Pellissier F, Gerber A, Bauer C, Ballivet M, Ossipow V (2007) The adhesion molecule Necl-3/SynCAM-2 localizes to myelinated axons, binds to oligodendrocytes and promotes cell adhesion. BMC Neurosci 8:90.
Pereira JA, Lebrun-Julien F, Suter U (2012) Molecular mechanisms regulating myelination in the peripheral nervous system. Trends Neurosci 35:123–134.
Rebsam A, Mason CA (2011) Cadherins as matchmakers. Neuron 71:566–568.
Remahl S, Hildebrand C (1982) Changing relation between onset of myelination and axon diameter range in developing feline white matter. J Neurol Sci 54:33–45.
Richardson WD, Kessaris N, Pringle N (2006) Oligodendrocyte wars. Nat Rev Neurosci 7:11–18.
Richardson WD, Young KM, Tripathi RB, McKenzie I (2011) NG2-glia as multipotent neural stem cells: fact or fantasy? Neuron 70:661–673.
Robbins EM, Krupp AJ, de Arce KP, Ghosh AK, Fogel AI, Boucard A, Südhof TC, Stein V, Biederer T (2010) SynCAM 1 adhesion dynamically regulates synapse number and impacts plasticity and learning. Neuron 68:894–906.
Rosenberg SS, Kelland EE, Tokar E, De La Torre AR, Chan JR (2008) The geometric and spatial constraints of the microenvironment induce oligodendrocyte differentiation. Proc Nat Acad Sci 105:14662–14667.

Sakry D, Karram K, Trotter J (2011) Synapses between NG2 glia and neurons. J Anat 219:2–7.
Sanes JR, Yamagata M (2009) Many paths to synaptic specificity. Annu Rev Cell Dev Biol 25:161–195.
Sara Y (2005) Selective capability of SynCAM and neuroligin for functional synapse assembly. J Neurosci 25:260–270.
Scheiffele P, Fan J, Choih J, Fetter R, Serafini T (2000) Neuroligin expressed in nonneuronal cells triggers presynaptic development in contacting axons. Cell 101:657–669.
Schnadelbach O (2001) N-cadherin is involved in axon-oligodendrocyte contact and myelination. Mol Cell Neurosci 17:1084–1093.
Schnadelbach O, Blaschuk OW, Symonds M, Gour BJ, Doherty P, Fawcett JW (2000) N-cadherin influences migration of oligodendrocytes on astrocyte monolayers. Mol Cell Neurosci 15:288–302.
Schreyer DJ, Jones EG (1982) Growth and target finding by axons of the corticospinal tract in prenatal and postnatal rats. Neuroscience 7:1837–1853.
Schwab ME, Schnell L (1989) Region-specific appearance of myelin constituents in the developing rat spinal cord. J Neurocytol 18:161–169.
Shen K, Cowan CW (2010) Guidance molecules in synapse formation and plasticity. Cold Spring Harb Perspect Biol 2:a001842.
Shen K, Scheiffele P (2010) Genetics and cell biology of building specific synaptic connectivity. Annu Rev Neurosci 33:473–507.
Sherman DL, Brophy PJ (2005) Mechanisms of axon ensheathment and myelin growth. Nat Rev Neurosci 6:683–690.
Shinza-Kameda M, Takasu E, Sakurai K, Hayashi S, Nose A (2006) Regulation of layer-specific targeting by reciprocal expression of a cell adhesion molecule, capricious. Neuron 49:205–213.
Simons M, Lyons DA (2013) Axonal selection and myelin sheath generation in the central nervous system. Curr Opin Cell Biol 25:512–519.
Spiegel I, Adamsky K, Eshed Y, Milo R, Sabanay H, Sarig-Nadir O, Horresh I, Scherer SS, Rasband MN, Peles E (2007) A central role for Necl4 (SynCAM4) in Schwann cell–axon interaction and myelination. Nat Neurosci 10:861–869.
Stegmüller J, Werner H, Nave K-A, Trotter J (2003) The proteoglycan NG2 is complexed with alpha-amino-3-hydroxy-5-methyl-4-isoxazolepropionic acid (AMPA) receptors by the PDZ glutamate receptor interaction protein (GRIP) in glial progenitor cells. Implications for glial-neuronal signaling. J Biol Chem 278:3590–3598.
Suzuki N, Fukushi M, Kosaki K, Doyle AD, de Vega S, Yoshizaki K, Akazawa C, Arikawa-Hirasawa E, Yamada Y (2012) Teneurin-4 Is a novel regulator of oligodendrocyte differentiation and myelination of small-diameter axons in the CNS. J Neurosci 32:11586–11599.
Takeichi M (2007) The cadherin superfamily in neuronal connections and interactions. Nat Rev Neurosci 8:11–20.
Taveggia C, Thaker P, Petrylak A, Caporaso GL, Toews A, Falls DL, Einheber S, Salzer JL (2008) Type III neuregulin-1 promotes oligodendrocyte myelination. Glia 56:284–293.
Tojima T, Hines JH, Henley JR, Kamiguchi H (2011) Second messengers and membrane trafficking direct and organize growth cone steering. Nat Rev Neurosci 12:191–203.
Tucker RP, Chiquet-Ehrismann R (2006) Teneurins: a conserved family of transmembrane proteins involved in intercellular signaling during development. Dev Biol 290:237–245.
Tucker RP, Kenzelmann D, Trzebiatowska A, Chiquet-Ehrismann R (2007) Teneurins: transmembrane proteins with fundamental roles in development. Int J Biochem Cell Biol 39:292–297.
Wake H, Lee PR, Fields RD (2011) Control of local protein synthesis and initial events in myelination by action potentials. Science 333:1647–1651.
Wang S, Sdrulla AD, diSibio G, Bush G, Nofziger D, Hicks C, Weinmaster G, Barres BA (1998) Notch receptor activation inhibits oligodendrocyte differentiation. Neuron 21:63–75.
Watkins TA, Emery B, Mulinyawe S, Barres BA (2008) Distinct stages of myelination regulated by gamma-secretase and astrocytes in a rapidly myelinating CNS coculture system. Neuron 60:555–569.
West AE, Greenberg ME (2011) Neuronal activity-regulated gene transcription in synapse development and cognitive function. Cold Spring Harb Perspect Biol 3.
Williams ME, de Wit J, Ghosh A (2010) Molecular mechanisms of synaptic specificity in developing neural circuits. Neuron 68:9–18.
Williams ME, Wilke SA, Daggett A, Davis E, Otto S, Ravi D, Ripley B, Bushong EA, Ellisman MH, Klein G, Ghosh A (2011) Cadherin-9 regulates synapse-specific differentiation in the developing hippocampus. Neuron 71:640–655.
Woo J, Kwon S-K, Choi S, Kim S, Lee J-R, Dunah AW, Sheng M, Kim E (2009) Trans-synaptic adhesion between NGL-3 and LAR regulates the formation of excitatory synapses. Nat Neurosci 12:428–437.
Yamagata M, Sanes JR (2008) Dscam and Sidekick proteins direct lamina-specific synaptic connections in vertebrate retina. Nature 451:465–469.
Zalc B, Fields RD (2000) Do action potentials regulate myelination? Neuroscientist 6:5–13.
Zatorre RJ, Fields RD, Johansen-Berg H (2012) Plasticity in gray and white: neuroimaging changes in brain structure during learning. Nat Neurosci 15:528–536.
Zhu Y, Li H, Li K, Zhao X, An T, Hu X, Park J, Huang H, Bin Y, Qiang B, Yuan J, Peng X, Qiu M (2013) Necl-4/SynCAM-4 is expressed in myelinating oligodendrocytes but not required for axonal myelination. PLoS One 8:e64264.
Zipursky SL, Sanes JR (2010) Chemoaffinity revisited: dscams, protocadherins, and neural circuit assembly. Cell 143:343–353.
Ziskin JL, Nishiyama A, Rubio M, Fukaya M, Bergles DE (2007) Vesicular release of glutamate from unmyelinated axons in white matter. Nat Neurosci 10:321–330.
Zonouzi M, Renzi M, Farrant M, Cull-Candy SG (2011) Bidirectional plasticity of calcium-permeable AMPA receptors in oligodendrocyte lineage cells. Nat Neurosci 14:1430–1438.
Zonta B, Tait S, Melrose S, Anderson H, Harroch S, Higginson J, Sherman DL, Brophy PJ (2008) Glial and neuronal isoforms of Neurofascin have distinct roles in the assembly of nodes of Ranvier in the central nervous system. J Cell Biol 181:1169–1177.

(Accepted 29 August 2013)
(Available online 12 September 2013)